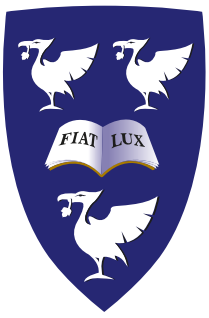

UNIVERSITY OF LIVERPOOL

An Investigation of the Neural Basis of Texture Processing during Active Touch

Thesis submitted in accordance with the requirements of the University of Liverpool for the degree of Doctor in Philosophy by Jessica Henderson

March 2023

Contents

Declaration

No part of this work was submitted in support of any other applications for degree or qualification at this or any other university or institute of learning.

Preface

This thesis is submitted in fulfilment of the conditions for a PhD by published papers. In accordance with the guidelines and regulations of the University of Liverpool, the experimental chapters (Chapters 4–7) are composed of published or currently under review journal articles, of which I am the first author. Specific details regarding the contribution of authors are given at the beginning of each chapter, as required.

Publications relating to the work presented in this thesis:

Henderson, J., Mari, T., Hewitt, D., Newton-Fenner, A., Giesbrecht, T., Marshall, A., Stancák, A., & Fallon, N. (Under Review). The neural correlates of texture perception: A systematic review and activation likelihood estimation meta-analysis of functional magnetic resonance imaging studies. *Brain and Behavior*.

Henderson, J., Mari, T., Hopkinson, A., Byrne, A., Hewitt, D., Newton-Fenner, A., Giesbrecht, T., Marshall, A., Stancak, A., & Fallon, N. (2022). Neural correlates of texture perception during active touch. *Behavioural Brain Research*, 429 (April), 113908. https://doi.org/10.1016/j.bbr.2022.113908

Henderson, J., Mari, T., Hewitt, D., Newton-Fenner, A., Hopkinson, A., Giesbrecht, T., Marshall, A., Stancák, A., & Fallon, N. (Under Review). Tactile estimation of hedonic and sensory properties during active touch: an electroencephalography study. *European Journal of Neuroscience*.

Henderson, J., Mari, T., Hopkinson, A., Hewitt, D., Newton-Fenner, A., Giesbrecht, T., Marshall, A., Stancák, A., & Fallon, N. (2023). Neural correlates of perceptual texture change during active touch. *Frontiers in Neuroscience*, 17, 921. https://doi.org/10.3389/FNINS.2023.1197113

List of other publications completed during this PhD but not directly related to this thesis:

Newton-Fenner, A., Hewitt, D., **Henderson, J.**, Roberts, H., Mari, T., Gu, Y., Gorelkina, O., Giesbrecht, T., Fallon, N., Roberts, C., & Stancak, A. (In Press). Economic value in the Brain: A Meta-Analysis of Willingness-to-pay using the Becker-DeGroot-Marschak Auction. *PLoS ONE*.

Newton-Fenner, A., Hewitt, D., **Henderson, J.**, Fallon, N., Gu, Y., Gorelkina, O., Giesbrecht, T., & Stancak, A. (2023). A Comparison of reward processing during Becker–DeGroot–Marschak and Vickrey auctions: an ERP study. *Psychophysiology*, e14313. https://doi.org/10.1111/PSYP.14313

Mari, T., Asgard, O., **Henderson, J.**, Hewitt, D., Brown, C., Stancak, A., & Fallon, N. (2023). External validation of binary machine learning models for pain intensity perception classification from EEG in healthy individuals. *Scientific Reports*, *13*(1), 242. https://doi.org/10.1038/s41598-022-27298-1

Hewitt, D., Byrne, A., **Henderson, J.**, Wilford, K., Chawla, R., Sharma, M. L., Frank, B., Fallon, N., Brown, C., & Stancak, A. (2022). Pulse Intensity Effects of Burst and Tonic Spinal Cord Stimulation on Neural Responses to Brushing in Patients With Neuropathic Pain. Neuromodulation*: Journal of the International Neuromodulation Society.* https://doi.org/10.1016/J.NEUROM.2022.11.001

Hewitt, D., Newton-Fenner, A., **Henderson, J.**, Fallon, N. B., Brown, C., & Stancak, A. (2022). Intensity-dependent modulation of cortical somatosensory processing during external, low-frequency peripheral nerve stimulation in humans. *Journal of Neurophysiology*, *127*(6), 1629–1641. https://doi.org/10.1152/JN.00511.2021

Newton-Fenner, A., Tyson-Carr, J., Roberts, H., **Henderson, J.**, Hewitt, D., Byrne, A., Fallon, N., Gu, Y., Gorelkina, O., Xie, Y., Pantelous, A., Giesbrecht, T., & Stancak, A. (2022). Bid outcome processing in Vickrey auctions: An ERP study. *Psychophysiology*, *59*(12), e14125. https://doi.org/10.1111/PSYP.14125

Byrne, A., Hewitt, D., **Henderson, J.**, Newton-Fenner, A., Roberts, H., Tyson-Carr, J., Fallon, N., Giesbrecht, T., & Stancak, A. (2022). Investigating the effect of losses and gains on effortful engagement during an incentivized Go/NoGo task through anticipatory cortical oscillatory changes. *Psychophysiology*, *59*(5), e13897. https://doi.org/10.1111/PSYP.13897

Mari, T., **Henderson, J.**, Maden, M., Nevitt, S., Duarte, R., & Fallon, N. (2022). Systematic Review of the Effectiveness of Machine Learning Algorithms for Classifying Pain Intensity, Phenotype or Treatment Outcomes Using Electroencephalogram Data. *The Journal of Pain*, *23*(3), 349–369. https://doi.org/10.1016/J.JPAIN.2021.07.011

Hewitt, D., Byrne, A., **Henderson, J.**, Newton-Fenner, A., Tyson-Carr, J., Fallon, N., Brown, C., & Stancak, A. (2021). Inhibition of cortical somatosensory processing during and after low frequency peripheral nerve stimulation in humans. *Clinical Neurophysiology*, *132*(7), 1481–1495. https://doi.org/10.1016/J.CLINPH.2021.03.024

Byrne, A., Hewitt, D., **Henderson, J.**, Newton-Fenner, A., Roberts, H., Tyson-Carr, J., Giesbrecht, T., & Stancak, A. (In Prep). Changes in anticipatory ERD during an effortful task when incentivised with a gain or loss.

Mari, T., **Henderson, J.**, Ali, H., Hewitt, D., Brown, C., Stancak, A., & Fallon, N. (In Prep). Cross- and within-subject external validation of machine learning and EEG for pain intensity prediction in health individuals.

Acknowledgements

Firstly, I wish to thank my supervisor, Dr Nick Fallon, for his expertise, patience and for being a constant source of encouragement. I feel incredibly fortunate to have had such a dedicated supervisor. I am also grateful to Dr Andrej Stancak, Dr Timo Giesbrecht, Dr Andrew Hopkinson, and Professor Alan Marshall, for their guidance and feedback. Together, their contributions have been instrumental in shaping my research.

I would like to thank every member of my lab group, with a special mention to Alice Newton-Fenner, Danielle Hewitt, Tyler Mari, and Adam Byrne. Their technical assistance, proofreading, and feedback have been crucial during this PhD, and their friendship has made the whole experience more enjoyable and memorable.

I extend my thanks to Unilever and EPSRC for funding this project and I recognise all the time and effort generously volunteered by participants. Without their contribution, this work would not have been possible.

I am grateful to my partner Dan who has provided an endless supply of positivity, encouragement, and bad jokes. This PhD would have been much harder without you by my side.

Finally, I am thankful to my family, for their unwavering support and for always telling me that I can do anything I set my mind to.

Thank you all for being part of my academic journey.

List of abbreviations

In alphabetical order:

ALE	Activation-likelihood estimation
ANCOVA	Analysis of covariance
ANOVA	Analysis of variance
BOLD	Blood-oxygen-level-dependent
CBMA	Coordinate-based meta-analyses
CT	C-tactile
DCML	dorsal column-medial lemniscal
DLPFC	Dorsolateral prefrontal cortex
ECG	Electrocardiographic
EEG	Electroencephalography
EOG	Electrooculographic
ERD	Event-related desynchronisation
ERP	Event-related potentials
ERS	Event-related synchronisation
ERSP	Event-related spectral perturbation
FDR	False discovery rate
FWE	Family-wise error
fMRI	functional magnetic resonance imaging
GABA	Gamma-aminobutyric acid
GLM	General linear model
HTMR	High-threshold mechanoreceptor
IBMA	Image-based meta-analyses
IPL	Inferior parietal lobule
IQR	Interquartile range
LTMR	Low-threshold mechanoreceptor
MA	Modelled activation
MAD	Median absolute deviation
MEG	Magnetoencephalography
MI	Primary motor cortex

MMN	Mismatch negativity
MNI	Montreal Neurologic Institute
MRI	Magnetic resonance imaging
OFC	Orbitofrontal cortex
PCA	Principal component analysis
PET	Positron emission tomography
PI	Posterior insula
PMd	Dorsal premotor cortex
PMv	Ventral premotor cortex
PPC	Posterior parietal cortex
PRISMA	Preferred Reporting Items for Systematic Review and Meta-Analysis
PSD	Power spectral distribution
RA	Rapidly adapting
RBP	Relative band power
RF	Radio frequency
RFT	Random field theory
ROI	Region of interest
SA	Slowly adapting
SEP	Somatosensory evoked potentials
SI	Primary somatosensory cortex
SII	Secondary somatosensory cortex
SLA	Stereolithography
SMA	Supplementary motor area
SMG	Supramarginal gyrus
SPL	Superior parietal lobule
SPM	Statistical parametric mapping
SS-EP	Steady-state evoked potentials
VAS	Visual analogue scale
VPL	Ventral posterior nucleus

List of figures

List of tables

Abstract

Jessica Henderson, Investigating the Neural Basis of Texture Processing during Active Touch

Humans typically explore their haptic environments with the glabrous skin on their hands through dynamic interactions with surfaces, termed active touch. The somatosensory input transduced by low-threshold mechanoreceptors facilitates discrimination of tactile stimuli and informs decision making to subsequently guide behaviour and decision-making. However, research considering the neural correlates of texture processing has primarily employed passive stimulation devices due to difficulties in time-locking signals to behaviour during active exploration, which lacks ecological validity. Consequently, the neural correlates of texture processing during active touch were previously not well understood. This thesis utilised a novel approach to investigate the modulation of neural oscillatory activity in relevant frequency bands during active exploration of textured surfaces, which was enabled by combining electroencephalography and novel force plate technology.

The findings of this thesis demonstrate cortical activation across sensorimotor brain regions in response to texture processing during active touch. Further, sensorimotor cortex activation was modulated by texture during active touch in the three electroencephalography experimental chapters. Increased alpha-band event-related desynchronisation was observed for rough textures and increased beta-band event-related desynchronisation for smooth and soft textures. These findings may reflect distinct cortical responses to different peripheral tactile coding mechanisms during active touch. Furthermore, alpha-band sensorimotor power was found to be modulated by texture change during complex ongoing tactile exploration which may represent an important mechanism for change detection in humans. Other findings point towards the role of higher-order regions in texture processing and estimation of tactile

surface properties. The estimation of hedonic preference modulated event-related desynchronisation in frontal, temporoparietal, and occipital brain regions. Further, meta-analysis of functional magnetic resonance imaging studies revealed that texture-specific processing elicits activation in secondary somatosensory regions, which may encode higher-order aspects of tactile processing.

For the first time, the novel fusion of force plate and electroencephalography data developed in this thesis allowed for the accurate investigation of the neural correlates of texture processing during active touch. Furthermore, tactile estimation and detection of texture change were found to modulate oscillatory brain responses, demonstrating new targets for future research. Overall, this thesis provides new and unique insights into the neural basis of texture processing in humans.

Chapter 1
General introduction

The somatosensory system allows for the perception of the body and the environment, and is responsive to several types of stimuli, including pressure, vibration, temperature, and position of the joints and muscles (Bear et al., 2020). The sense of touch refers to the perception of tactile stimuli though cutaneous mechanoreceptors in the skin and joints. Touch is broadly divided into two main types, discriminative and affective touch (McGlone et al., 2014). Discriminative touch allows humans to detect, discriminate, and identify external stimuli, which enables fast decision making to guide subsequent behaviour (McGlone et al., 2014), whilst affective touch is thought to facilitate emotional and social bonds between humans (Hertenstein et al., 2006; McGlone & Walker, 2020; Morrison et al., 2010). Discriminative and affective touch are thought to be encoded by different nerve fibres, with discriminative touch mediated by fast Aβ fibres and affective touch facilitated by slow C-tactile (CT) fibres.

1.1 Discriminative touch

From the start of life humans engage in tactile perception, first by manipulating objects with their mouth (Essick & Trulsson, 2009), then as we age haptic attention shifts from the mouth to the hands (Rochat & Senders, 1991). Discriminative touch provides information about surface properties, such as texture or shape, and builds a representation of objects and hand movements (Ryan et al., 2021). Discriminative touch is linked with motor control, whereby voluntary movements are made to obtain information about tactile properties, which also guides subsequent behaviour, particularly during object handling and exploratory procedures. As a result, the speed of transduction, transmission and central processing are incredibly important (McGlone et al., 2014). To quickly discriminate external tactile stimuli, cutaneous

mechanoreceptors in the skin and joints transduce incoming information, which is then conducted by large myelinated cutaneous Aβ afferents with a fast conduction velocity.

1.2 Active and passive touch

Active and passive touch are distinct modes of touch (Gibson, 1962). Active touch employs voluntary movements, to explore the environment to gather information about surface properties and objects. For this reason, active touch is associated with discrimination of external stimuli. On the other hand, passive touch refers to sensory input that is generated by an external agent. In the lab setting, passive touch is used to stimulate a section of skin, whilst controlling for stimuli properties such as force, which can be delivered to the hand or fingers under discrimination paradigms (Aviles et al., 2010; Essick et al., 2010; McGlone et al., 2012; Weber et al., 2013). This can be dynamic, which implies movement between the surface and the skin, or static, where there is no movement (Chapman, 2008).

1.2.1 Active touch

Gibson (1962) first defined the term "active touch" as the touching we perform when we explore our environments, whereby the impression on the skin is brought about by the perceiver themselves. Active touch is a complex goal-oriented behaviour that combines both cutaneous and proprioceptive input to derive information about the properties of surfaces and objects as they are explored (Bajcsy, 1988; Lederman & Klatzky, 2009).

Specialised touch organs are used in active tactile exploration; in humans and other primates, this is typically the hand (Jones & Lederman, 2006). The hand has a high density of cutaneous and subcutaneous mechanoreceptors that transduce incoming tactile information (Johansson & Vallbo, 1979). The human hand also has a large cortical representation in the primary somatosensory cortex (SI), as well as the primary motor cortex (MI; Penfield et al.,

1937). Taken together, this means that the hand has high sensory acuity while also being able to perform complex individual movements of the digits.

There has been much debate as to whether active and passive touch are perceptually equivalent (Chapman, 2008). Studies suggesting that tactile perception is greater during active touch have investigated perception of Braille, simulated shapes, object shapes, and vibrotactile stimuli (Heller, 1984, 1986; Heller et al., 1990; Smith et al., 2009; Voisin et al., 2002). Though, no difference in perceptual abilities was observed when contrasting active and passive touch during roughness magnitude estimations (Friedman et al., 2008; Lamb, 1983; Lederman, 1981; Yoshioka et al., 2011).

While some argue that perceptual performance during active and passive touch are comparable, it has been found that this is only true when conditions are suitably matched. Chapman (1994) found that perceptual performance was comparable between 30 seconds of passive touch and five seconds of active touch, suggesting that active touch is the most efficient mode. Importantly, active touch is representative of how humans explore their natural environments. This mode of touch allows us to orient digits to optimise skin object contact (Xu et al., 2021b), whilst movement speed can be modulated at critical times during exploration (Morley et al., 1983; Smith et al., 2002a), and force can be varied between and during explorations. Therefore, results from passive touch paradigms may not be representative of the processing that is involved during active touch (Iwamura, 2009).

1.2.2 Haptic exploration

It is generally acknowledged that tactile perception is better with dynamic stimuli especially for fine textures. During haptic exploration, humans use a wide range of relatively stereotyped movements, referred to as exploratory procedures, to optimise and seek specific sensory information (Figure 1.1; Lederman & Klatzky, 1987). The patterns of movements

used by humans differ based on the information the individual is trying to gain, for example, perception of texture uses lateral motion, which manifests as sideways movement between the skin and object surface. Roughness estimates have been found to be modulated by force exerted, suggesting that the way we perform haptic exploration changes the way we perceive surface and object properties (Lederman & Taylor, 1972; Tanaka et al., 2014). Ultimately, haptic exploration allows humans to modify their exploratory patterns according to the features they are trying to detect, thus optimising sensory feedback.

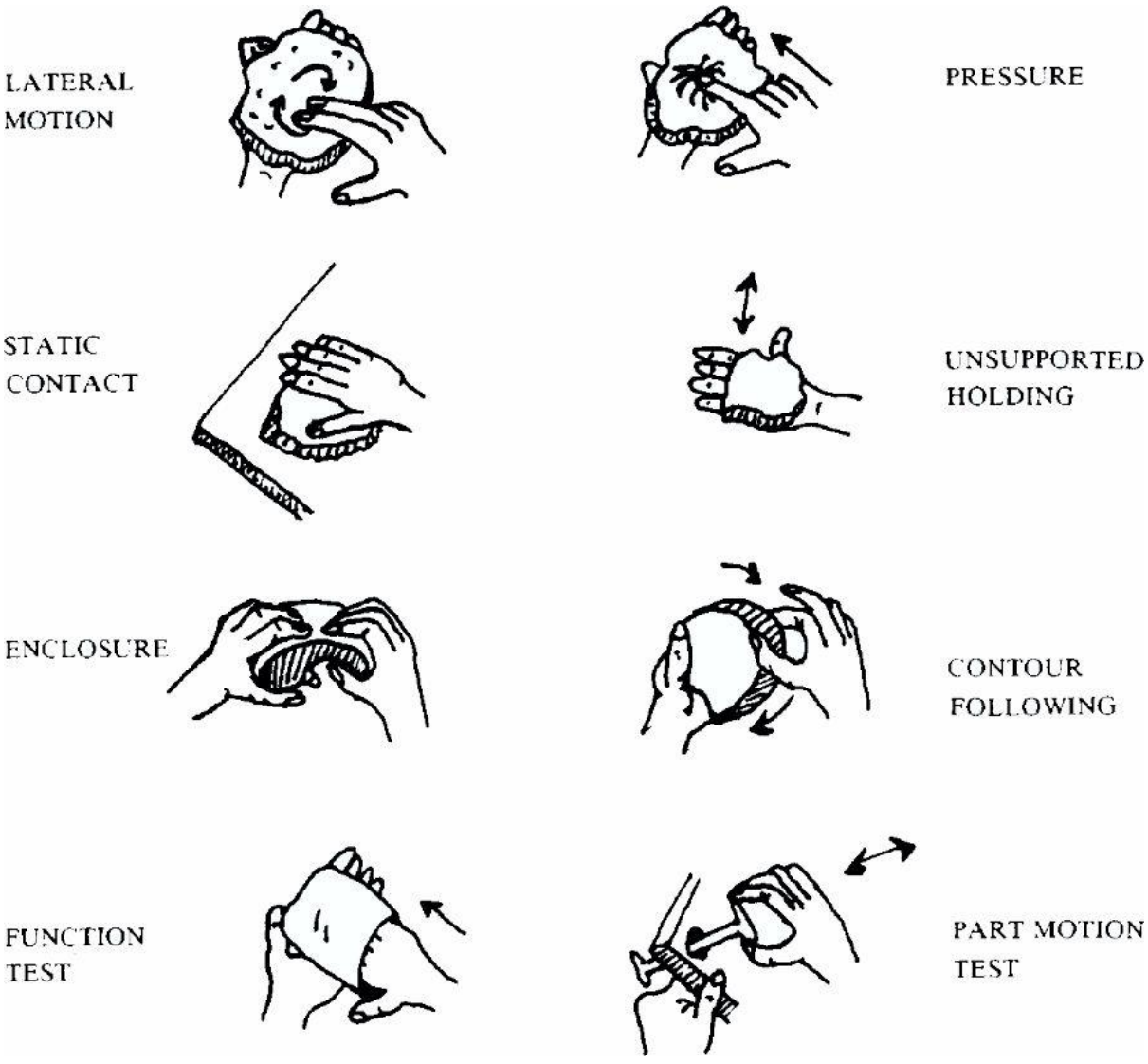

Figure 1.1 Exploratory procedures from Lederman & Klatzky (1987).

1.3 The neurobiology of touch and movement

Nerve fibres in the hand can be classified into two functional types; afferent fibres conduct impulses towards the spinal cord, whilst efferent fibres carry signals away from the spinal cord to the skeletal muscle, blood vessels and sweat glands (Gardner & Johnson, 2012b).

1.3.1 Afferent neurons

Afferent neurons, also known as sensory neurons, transmit signals from distinct types of cutaneous mechanoreceptors, proprioceptors, thermoreceptors, nociceptors, and at least one type of itch receptor from the periphery to the central nervous system. Cutaneous mechanoreceptors contribute to the tactile perception of texture, while proprioceptors contribute to the perception of limb position and movement in space, which is essential for active touch (Goodman & Bensmaia, 2020; Taylor, 2009).

Afferent fibres can be classified into four functional groups based on the fibres' diameter, myelination, conduction velocity, and whether they innervate muscles or skin (Lloyd, 1943; Sherrington, 1893). Groups I to III are myelinated and decrease in diameter and conduction velocity respectively, whereas group IV is unmyelinated and has the smallest diameter and slowest conduction velocity. In muscle nerves, group I fibres innervate muscle spindle receptors and Golgi tendon organs, and group II fibres innervate secondary spindle endings and receptors in joint capsules. Both group III and group IV fibres send signals relating to disorders in muscles and joints that may be sensed as painful. In cutaneous nerves, Aβ fibres (group II) innervate cutaneous mechanoreceptors, while Aδ (group III) and C (group IV) afferents play the same role as in muscle nerves, mediating thermal and noxious stimuli (Gardner & Johnson, 2012b).

Tactile perception relies on the activation of mechanosensitive sensory neurons, which are responsible for detecting both innocuous and noxious touch sensations. Mechanoreceptors can be divided into two categories: low-threshold mechanoreceptors (LTMR) that respond to innocuous mechanical stimulation and high-threshold mechanoreceptors (HTMR) that react to harmful mechanical stimulation (reviewed in Abraira & Ginty, 2013).

Four types of LTMR innervate the glabrous skin: Pacinian corpuscles, Meissner corpuscles, Merkel cells, and Ruffini endings (Hagbarth & Vallbo, 1967; Johansson & Vallbo, 1979; Vallbo & Johansson, 1984). These LTMR can be subdivided based on their receptor size, location, and whether they have slowly or rapidly adapting fibres. During sustained mechanical deformation of the skin, rapidly adapting (RA) afferents spike during the onset and/or offset of stimulation. These RA afferents are further split into two types of LTMR; type I (RAI-LTMR) and type II (RAII-LTMR), which innervate Meissner and Pacinian corpuscles respectively (Table 1.1). Slowly adapting (SA) afferents show sustained firing to continuous mechanical deformation. SA afferents are also subdivided further into two types of LTMR; type I (SAI-LTMR) and type II (SAII-LTMR), innervated by Merkel cell and Ruffini end organs respectively (Table 1.1).

Table 1.1. Cutaneous and subcutaneous mechanoreceptors adapted from Abraira & Ginty (2013).

Subtype	Fibre	Conduction velocity	Skin type	End organ	Stimuli
SAI-LTMR	Aβ	16–96m/s	Glabrous	Merkel cell	Indentation
SAII-LTMR	Aβ	20–100m/s	Glabrous Hairy	Ruffini unclear	Stretch
RAI-LTMR	Aβ	26–91m/s	Glabrous Hairy	Meissner corpuscle Longitudinal lanceolate ending	Skin movement Hair follicle deflection
RAII-LTMR	Aβ	30–90m/s	Glabrous	Pacinian corpuscle	Vibration
Ad-LTMR	Aδ	5–30m/s	Hairy	Longitudinal lanceolate ending	Hair follicle deflection
C-LTMR	C	0.2–2m/s	Hairy	Longitudinal lanceolate ending	Hair follicle deflection
HTMR	Aβ/Aδ/C	0.5–100m/s	Glabrous Hairy	Free nerve ending	Noxious mechanical

The location of end organs differs based on the type of afferent; end organs of type I afferents (Merkel cell and Meissner corpuscles) are located in the superficial layers of the skin at the dermo-epidermal junction, whereas end organs of type II afferents (Pacinian and Ruffini endings) are located deeper in the dermis (Figure 1.2). Further the receptive fields of type I and type II fibres differ, with type I afferents having a small receptive field and type 2 fibres have large receptive fields.

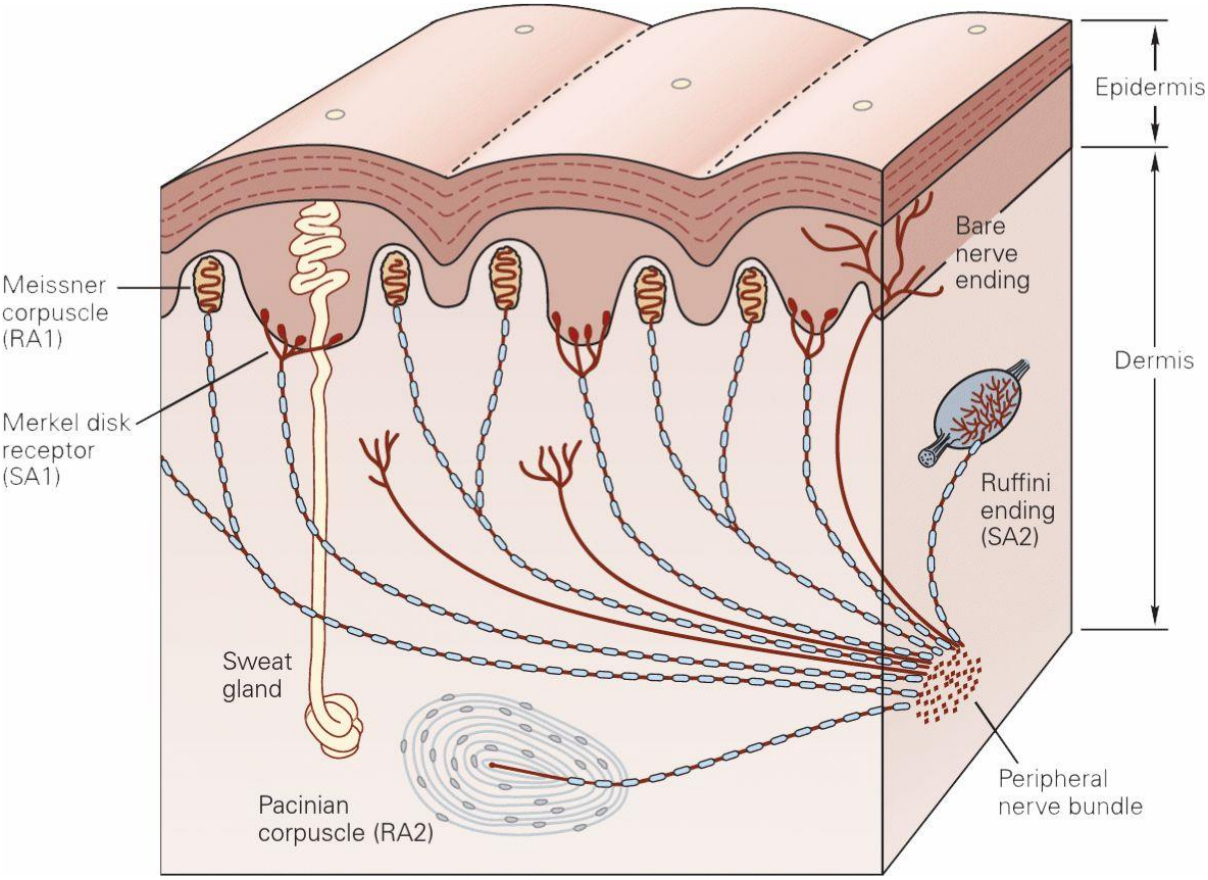

Figure 1.2 Organisation of cutaneous mechanoreceptors in the skin from Gardner et al. (2012).

Various aspects of tactile stimulation are encoded by LTMR afferents to facilitate discriminative touch. Merkel cells (SAI) are particularly sensitive to edges, corners, and points and indicate how much pressure has been applied to the skin. Ruffini endings (SAII) are more sensitive to skin stretching than skin indentation and are therefore particularly sensitive to the shape of large objects held in the hand. Meissner corpuscles (RA1) encode low-frequency vibration and therefore detect hand contact with objects, the slipping of handheld objects, as well as the motion of the hand over textured surfaces. Finally, Pacinian corpuscles (SAII) are extremely sensitive to high-frequency vibration and responds to motion in the nanometre range (Abraira & Ginty, 2013; Jänig et al., 1968; Lynn, 1971).

In humans, C-LTMR, referred to as CT afferents, have been found to innervate the hairy skin and respond to slowly moving (1-10 cm/s), low force mechanical stimulation (Johansson et al., 1988; Nordin, 1990; Vallbo et al., 1999). Further, CT afferents are associated with pleasantness encoding, subsequently, CT optimal touch has been termed "affective touch" since it is thought to convey positive affect (Morrison et al., 2010; Olausson et al., 2010; Pawling et al., 2017; Walker et al., 2022).

Sensory fibres that innervate the skin facilitate discriminative touch, while Aα and Aβ fibres that innervate the muscles enable proprioception. The sense of limb location, movement and joint positions is mediated by muscle and skeletal mechanoreceptors (Table 1.2), these include primary and secondary muscle spindles, which convey information about muscle stretch. Golgi tendon organs and joint capsule receptors which transduce muscle force and tension in the joint capsule, respectively (Loeb & Mileusnic, 2015). Humans need proprioception to update the desired behaviour and to estimate body positions resulting from motor commands (Taylor, 2009).

Table 1.2. Muscle and skeletal mechanoreceptors that facilitate proprioception from Gardner & Johnson (2012a).

Subtype	Fibre	Receptor type	Modality
Ia-LTMR	Aα	Muscle spindle primary	Muscle length and speed
II-LTMR	Aβ	Muscle spindle secondary	Muscle stretch
Ib-LTMR	Aα	Golgi tendon	Muscle contraction
II-LTMR	Aβ	Joint capsule	Joint angle

1.3.2 Efferent neurons

Motor neurons, also known as efferent neurons, can be categorised into upper and lower motor neurons. Lower motor neurons transduce signals from the central nervous system effector organs and tissue in order to facilitate muscle contraction and secretion of substances

from glands. Lower motor neurons can be split into three types, somatic, general visceral and special visceral motor neurons (Zayia & Tadi, 2021). Somatic motor neurons innervate skeletal muscles, controlling movement and muscle tone. They can be separated into three subtypes based on the muscle fibre type they innervate (Stifani, 2014): alpha motor neurons innervate extrafusal muscle fibres, beta motor neurons innervate both extrafusal and intrafusal fibres, and gamma motor neurons innervate muscle spindles.

1.3.3 Spinal pathways

The spinal cord is divided into thirty-one segments along its length corresponding to each vertebra, from the brain stem running inferiorly down the trunk of the body. Each spinal cord segment has a separate pair of dorsal and ventral nerve roots, which are numbered according to where they exit the vertebral column. Information from the body is conveyed to the central nervous system by afferent sensory nerve fibres contained within the dorsal root, whereas the ventral root carries efferent nerve fibres, which control muscles. The spinal cord is composed of both white matter containing nerve fibres, and grey matter containing the cell bodies and dentaries of the spinal neurons (Burke, 2008). The grey matter is organised into ten functionally distinct laminae, which are numbered from I to X from dorsal to ventral and distinguished according to cytoarchitecture (Gebhart & Schmidt, 2013; Rexed, 1952).

1.3.3.1 Dorsal column-medial lemniscal pathway

The dorsal column-medial lemniscal (DCML) system carries tactile and conscious proprioceptive information to the brain (Figure 1.3). Information is conveyed by first-order neurons, which have a cell body located in a ganglion on the dorsal root of a spinal or cranial nerve. These neurons have two branches, one projecting to the periphery and one projecting to the central nervous system. The central branches terminate in the spinal cord or brain stem and form the first synapses on the somatosensory pathway. The axon of each dorsal root

ganglion cell serves as a single transmission line between the receptor terminal and the central nervous system, called the primary afferent fibre (Gardner & Johnson, 2012b). In the spinal cord, lamina III to V neurons receive tactile input from Aβ fibres from LTMR (Abraira & Ginty, 2013; Brown, 1981; Li et al., 2011). Further, neurons in lamina V receive low-threshold input from Aβ as well as input from Aδ and C fibres, hence they are referred to as wide-dynamic-range neurons as they respond to more than one modality (Gardner & Johnson, 2012b; le Bars & Cadden, 2008).

Central branches of Aα and Aβ afferents are contained on each side of the dorsal column. Individual primary afferent fibres innervating a particular region of the body are grouped together into fascicles: the gracile fascicle conveys information from the legs and trunk, while the cuneate fascicle transmits information from the arms and trunk. The gracile and cuneate fascicle terminate in the anatomically distinct gracile and cuneate nuclei in the caudal brain stem, respectively (Gardner & Johnson, 2012b). Together they form the dorsal column nuclei and represent second-order neurons of the DCML pathway.

Axons of second-order neurons in the dorsal column nuclei cross over the midline, at the sensory decussation in the medulla, forming the medial lemniscus (Gardner & Johnson, 2012b). The medial lemniscus terminates and synapses in the ventral posterior nucleus (VPL) of the thalamus. VPL neurons are third-order neurons of the DCML pathway, axons project laterally out of the thalamus and ascend to the SI and secondary (SII) somatosensory cortex via the posterior limb of the internal capsule (Al-Chalabi et al., 2021). The DCML pathway maintains somatotopic organisation from fascicle to the SI and SII (Michael-Titus et al., 2010; Ruben et al., 2001).

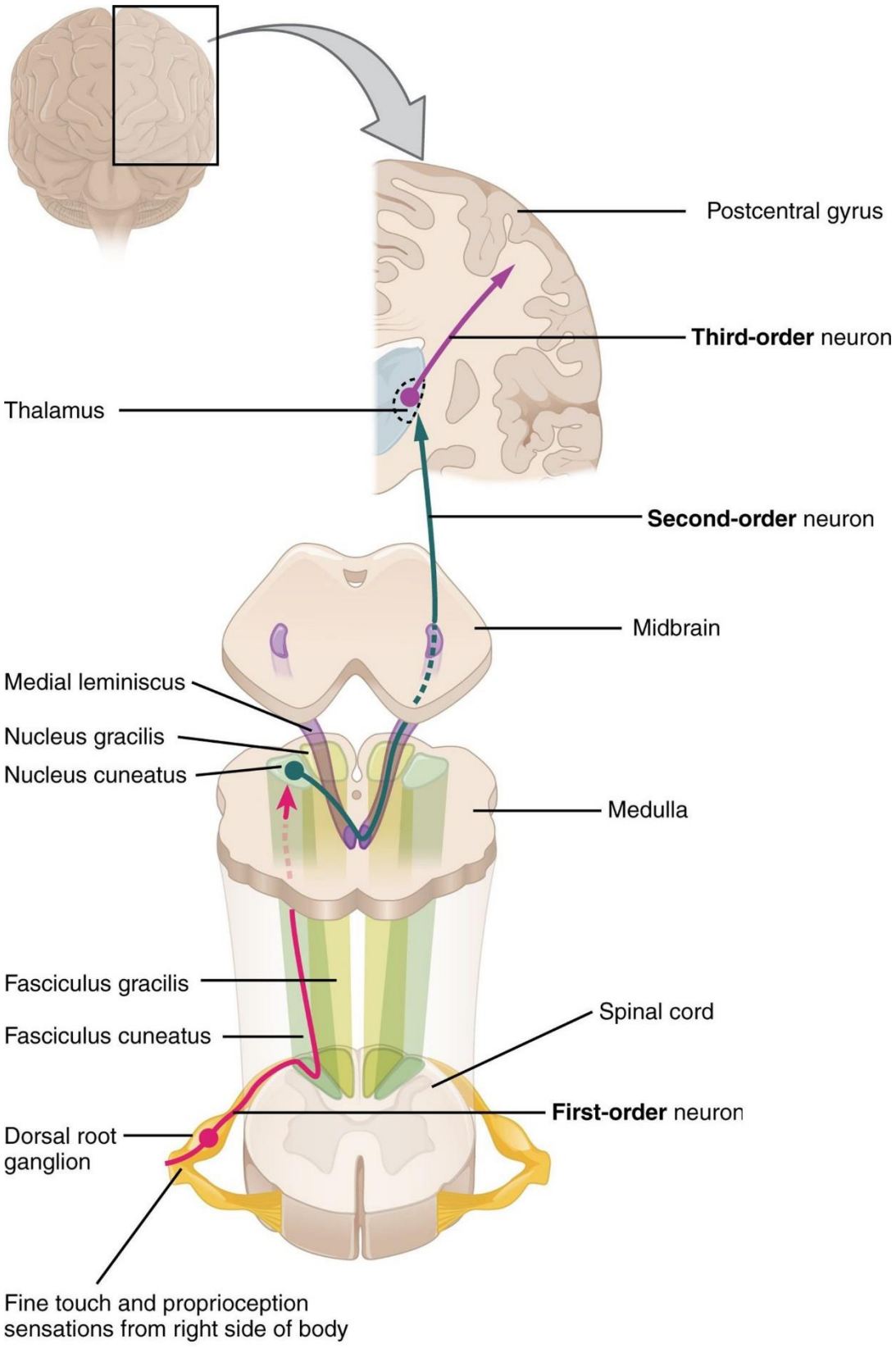

Figure 1.3 Neural connection sin the DCML pathway, adapted from Betts et al. (2013).

1.3.3.2 Corticospinal tract

Information from the brain is sent to the spinal cord via white matter tracts referred to as descending or motor tracts (Ganapathy et al., 2021). Tracts can be grouped by functionality into pyramidal or extrapyramidal tracts. Pyramidal tracts originate in layer V of the MI and are responsible for the control of voluntary movement, whereas extrapyramidal tracts originate in the brain stem and are responsible for involuntary and automatic control of muscle tone, balance, posture, and modulation of motor plans. Pyramidal tracts consist of the corticospinal tract controlling motor activity from the neck down, and corticobulbar tract responsible for control of facial, head, and neck muscles.

The corticospinal tract projects from axons of the MI to the ventral horn of the spinal cord. Axons from upper motor neurons of the MI descend through the internal capsule, the cerebral peduncle in the midbrain. In the medulla, most of the fibres in the tract cross to the opposite side of the spinal cord, forming the lateral corticospinal tract that sends fibres to extremity muscles (Javed et al., 2021). The fibres that do not cross in the medulla instead cross at the level of the spinal cord where they synapse, these fibres form the anterior corticospinal tract and are sent to the trunk or axial muscles (Amaral, 2012).

Both tracts descend through the spinal cord, the lateral corticospinal tract descends through the lateral funiculus and the anterior corticospinal tract descends via the anterior funiculus (Khan & Lui, 2021). Both tracts then synapse with lower motor neurons on the ventral horn and leave the spinal cord through the ventral root to innervate and contract muscles (Javed & Daly, 2021; Welniarz et al., 2017). Lamina IX of the ventral horn receives somatic motor neurons which innervate skeletal muscles responsible for movement (Rexed, 1952). Somatotopic organisation is preserved from the cortex along the corticospinal tract (Emos & Agarwal, 2021).

1.4 Tactile texture perception

Information about surface texture may be obtained through vision (Heller, 1989), audition (Lederman, 1979) and touch (Bensmaia, 2009), although touch provides humans with richer and more complex textural information (reviewed in Lieber & Bensmaia, 2022). When humans actively touch a surface, they are processing information about the surface texture and material properties. Often textural properties are quantified across perceptual scales; with roughness/smoothness, hardness/softness, stickiness/slipperiness, and warm/cool argued as the most salient dimensions (Hollins et al., 1993, 2000). However, a more recent review suggests that roughness/smoothness, hardness/softness, and coldness/warmness are the most prominent psychophysical dimensions of tactile texture (Okamoto et al., 2013).

1.4.1 Psychophysics of tactile texture perception

Psychophysics is the study of perception, with a particular focus on the relationship between stimuli and sensations (Baird & Elliot, 1978). The investigation of texture perception in previous psychophysical experiments tends to focus on roughness/smoothness (Bensmaia, 2009). As the distance between tactile elements increases the perceived roughness increases, this effect has been found using magnitude estimations during stimulation with varying grit sandpaper (Lederman & Abbott, 1981; Stevens & Harris, 1962), gratings (Cascio & Sathian, 2001; Lederman, 1974, 1976, 1981; Morley et al., 1983), and raised dots (Connor et al., 1990; Connor & Johnson, 1992; Li et al., 2022; Sutu et al., 2013).

Roughness estimation of dot patterns and gratings follow an inverted U-shaped function, whereby stimuli with a spatial period in the middle of the continuum are perceived as the roughest relative to either end of the spectrum where they are perceived as least rough (Connor & Johnson, 1992; Morley et al., 1983). Dot height has also been found to play a role in the perceived roughness, with greater height resulting in increased roughness estimates

(Sutu et al., 2013). The perceived roughness of gratings is also modulated by the groove and ridge width of the gratings, with wider groove and narrower ridge width resulting in greater perceived roughness (Lederman & Taylor, 1972; Sathian et al., 1989). Further, tangential force, which is the force acting along the direction of motion, is thought to play a role in the perception of roughness (Smith et al., 2002b). Overall, this suggests that the spatial patterns of skin deformation play an important role in the perceived roughness of a stimulus.

The perception of hardness/softness is related to the compliance of the surface (Harper & Stevens, 1964; Srinivasan & LaMotte, 1995). When the hand or digits are pressed against a hard surface or object the skin is intended, whereas the skin indents soft surfaces or objects. This means that hard and soft surfaces have differing spatial patterns of skin deformation. During passive stimulation of the skin, LTMR provide information about skin displacement. During active exploration, the perception of softness is also facilitated by proprioceptors which provide information about hand movement and force (Srinivasan & LaMotte, 1996; Xu et al., 2021a). This suggests that the perception of hardness/softness may be enhanced during active exploration.

Stickiness/slipperiness perception is linked to the friction between skin and surface. Tangential force is considered a contributing factor in the perception of stickiness (Smith & Scott, 1996). The perception of stickiness is often associated with roughness (Hollins & Risner, 2000), where smoother textures are distinguished by increases in tangential forces between the skin and material surface (Gueorguiev et al., 2016). The perception of stickiness is important for handling objects, as it allows for the applications of appropriate levels of grip force (Augurelle et al., 2003).

Further, the perception of surface temperature contributes to the recognition of materials (Katz, 1925, 1989), e.g., at room temperature metal generally feels cooler than

plastic (Ho & Jones, 2006). The perception of surface temperature depends on the thermal conductivity of the material, which determines the duration required for heat to be conducted in and out of the skin (Ho & Jones, 2008). The perception of warmth/cool is mediated by thermoreceptors afference in the skin instead of by LTMR which mediate other aspects of texture (i.e., roughness, softness, and stickiness; Darian-Smith et al., 1973, 1979; Johnson et al., 1973, 1979).

1.4.2 Texture perception and mechanoreceptors

There are three LTMR in the glabrous skin, all innervated by large myelinated Aβ fibres, that are thought to transduce incoming textural information (Bensmaia, 2009); SAI-, RAI-, and RAII-LTMR, which are associated with the anatomical end organs of Merkel cells, Meissner corpuscles, and Pacinian corpuscles, respectively (Gardner & Johnson, 2012b).

1.4.2.1 Slowly adapting fibres

Sustained indentation activates SAI-LTMR, fibres with small receptive fields, a conduction velocity of 16–96 m/s, which innervate the skin of the finger at a period of approximately 1 mm (Johansson & Vallbo, 1979, 1983; Vallbo et al., 1995). SAI-LTMR are sensitive to edges, corners, and curvatures of objects, with firing rates greater when touching an edge rather than touching a flat surface (Gardner et al., 2012). Further, SAI-LTMR have high spatial resolution of up to 0.5 mm for individual human SAI afferents, making them sensitive to stimulus position and velocity (Abraira & Ginty, 2013). Taken together, this means that the spatial configuration of coarse tactile elements is reflected in the spatial pattern of SAI-LTMR activation (Blake et al., 1997).

1.4.2.2 Rapidly adapting fibres

Movement produces vibrations that arise from the skin-surface interaction, which reflect the micro geometric properties of the surface and fingerprint, thus enabling one to perceive fine texture (Bensmaïa et al., 2005a; Bensmaia & Hollins, 2003; Hollins et al., 2001a, 2001b, 2002; Manfredi et al., 2014; Scheibert et al., 2009). Fine textures are incredibly complex and can be defined as textures with element sizes measuring less than 100 μm (Hollins et al., 1996; Hollins & Risner, 2000). Without movement, perception of fine textures is near impossible (Hollins & Risner, 2000).

RA receptors respond to motion between a surface and the skin rather than static indentation. RAI-LTMR encode low-frequency vibrations, with small receptive fields and a conduction velocity of 26–91 m/s, which can detect tactile elements as small as 10 μm (Piccinin et al., 2022). RAII-LTMR are extremely sensitive afferent fibres, with larger receptive fields, a conduction velocity of 30–90 m/s, which respond to high-frequency vibrations in the 250 nm range (Jänig et al., 1968; Lynn, 1971). Both RAI- and RAII-LTMR provide humans with a vibrotactile pattern related to the surface texture, which allows for the identification and discrimination of texture (Weber et al., 2013).

1.4.2.3 The Duplex theory

The Duplex theory of tactile texture perception, as proposed by Katz (1925, 1989), posited that perception of fine textures is facilitated by temporal cues in the form of high-frequency vibrations; investigations of vibratory coding support this hypothesis (Bensmaia & Hollins, 2003; Hollins et al., 2002). Vibrotactile cues were found to contribute to the perception of smoothness, with an increase in vibratory amplitude leading to a decrease in smoothness ratings (Hollins et al., 2001b). RAII afferents transduce high frequency vibrotactile information that arise from motion between the skin and a textured surface. Adaptation to

high frequency vibrotactile stimuli diminishes the discrimination of fine surfaces but has negligible effect on coarse surfaces (Hollins et al., 2001a, 2006), whilst adaptation to low-frequency stimuli does not affect the perception of fine textures (Bensmaïa et al., 2005b). Research suggests that RAII-LTMR are important for the textural processing of fine textures (Bensmaïa et al., 2005a; Bensmaïa & Hollins, 2005; Bensmaia & Hollins, 2003), thus supporting the Duplex theory that perception of fine surface textures is modulated by vibration.

Spatial cues, determined by the size, shape, and distribution of surface elements, are proposed to facilitate the perception of coarse textures (Hollins et al., 1998; Katz, 1989). Coarse surface elements can be perceived through static touch (Lederman, 1974; Taylor & Lederman, 1975), suggesting that coarse elements are encoded by SAI-LTMR since they have sustained firing without movement (Hollins & Risner, 2000). Although, Cascio & Sathian, (2001) suggest that roughness magnitude estimates depend on both spatial and temporal frequency. Investigation of vibratory adaption has shown that SAI- and RAI-LTMR can be desensitised with 10 Hz vibration, which did not affect the discrimination of fine textures (Bensmaïa et al., 2005b). Further Weber et al. (2013) suggests that textures that are exclusively coarse or fine will rely on spatial or temporal cues respectively, but textures that include a range of tactile elements will require both mechanisms. Therefore, RAI-LTMR may not contribute to the discrimination of fine texture but may play a role in the perception of roughness (Gamzu & Ahissar, 2001).

1.5 Brain correlates of tactile texture perception and active touch

Tactile and proprioceptive information from LTMR travel through the DCML pathway and terminate in the thalamus. Thalamocortical afferents convey signals to the SI and SII in the parietal lobe (Raju & Tadi, 2021). Projections to the SI and SII are thought to be processed

either in parallel (i.e., thalamus to SI and SII) or in serial (i.e., thalamus to SI and then to SII; Kaas & Garraghty, 1991; Song et al., 2021). A combined functional magnetic resonance imaging (fMRI) and magnetoencephalography (MEG) study hypothesised that parallel projections are made to the SI and SII during in the first 100 ms of somatosensory stimulation and serial projections are made from the SI to the SII subsequently (Klingner et al., 2016). From the SI, projections are made to the MI and the posterior parietal cortex (PPC; Gardner et al., 2012).

The MI, supplementary motor area (SMA), dorsal premotor cortex (PMd) and ventral premotor cortex (PMv) have reciprocal connections with each other, while the PPC and premotor areas also are reciprocally connected (Kalaska & Rizzolatti, 2012). Somatosensory and parietal inputs provide sensory information to the MI and premotor areas to inform motor planning and control. The corticospinal tract receives input from the MI, SI, and superior (SPL) and inferior parietal lobules (IPL) of the PPC. Premotor areas including the SMA, PMd and PMv send indirect projection to the corticospinal tract via other subcortical structures (AbuHasan & Munakomi, 2022). These connections and projections play a crucial role in coordinating and executing voluntary movements, making them essential for texture perception during active touch.

Positron emission tomography (PET) and fMRI measure haemodynamic changes in the brain (Doria, 1995). Both techniques have excellent spatial resolution and are used to image the brain to identify regions associated with external stimulation. Electroencephalography (EEG) and MEG measure the summation of postsynaptic potentials, these techniques have a relatively poorer spatial resolution but have a high temporal resolution in the magnitude of milliseconds (Hari & Puce, 2017). As described in Chapter 2, this range of neuroimaging techniques allows for the investigation of both the regions

associated with the processing of textured stimuli but also the period in which the brain processes the information.

1.5.1 Brain regions associated with tactile stimulation and voluntary movement

Motor function is key for active tactile explorations, sensory and motor information is integrated in the brain. This allows humans to use sensory information from their environment to inform motor actions, this integrated system is referred to as the sensorimotor system (Helms Tillery & Sainburg, 2012).

1.5.1.1 Somatosensory regions

The contralateral SI and bilateral SII have been found to be reliably activated in response to glabrous skin stimulation with textured stimuli (Burton et al., 1997, 1999; Ledberg et al., 1995; O'Sullivan et al., 1994; Roland et al., 1998), with effects reproducible over time (Carey et al., 2008). It is well established that the SI is responsible for processing tactile stimuli as well as discriminating between tactile stimuli (Morley et al., 2007; Tamè & Holmes, 2016). Lesions in the SI result in the diminished ability to discriminate objects and surfaces when exclusively using touch (Pause et al., 1989; Raju & Tadi, 2021).

Interestingly, SI response is greater during active touch paradigms rather than passive touch paradigms (Simões-Franklin et al., 2011). The MI is thought to send an efference copy (von Holst & Mittelstaedt, 1950), or corollary discharge (Sperry, 1950), to the SI for the prediction and processing of the sensory consequences of motor actions. Recently, a series of fMRI experiments have been conducted to examine the link between motor planning in the MI and somatosensory processing in the SI. These studies provide evidence that motor planning activates the human SI (Ariani et al., 2022; Gale et al., 2021). Suggesting that increased SI activation during active touch is possibly due to sensorimotor control which

manifests as projections of an efference copy from the MI to the SI to allow prediction of sensory feedback from motor commands.

Receptive fields of neurons in the SII are often bilateral and contain symmetrical maps of the contralateral and ipsilateral body halves (Lin & Forss, 2002; Picard et al., 1990; Woolsey & Fairman, 1946). The SII is located on the parietal operculum on the upper bank of the Sylvian fissure, extending medially to the insular cortex (Eickhoff et al., 2006). Humans with SII lesions suffer from tactile apraxia, where they have trouble performing purposeful and coordinated movements when manipulating objects, despite having normal sensation the stimuli and normal movements of the hand without the use of an object (Raju & Tadi, 2021). Suggesting deficits are more cognitive rather than sensorimotor (Binkofski et al., 2001). Research also suggests that the SII engages in the processing of other higher-order features such as attention (Chen et al., 2008; Hämäläinen et al., 2000), learning (Mishkin, 1979; Ridley & Ettlinger, 1976), and tactile memory and decision making (Romo et al., 2002).

The insular cortex is activated in response to tactile and proprioceptive stimulation (Craig, 2002). Kurth et al. (2010) conducted a coordinate-based activation-likelihood estimation (ALE) investigating the human insula, showing that somatosensory stimuli evoked activations of the left central region of the insula. More specifically, insula activation has been reported during stimulation of the hand/digits with textured stimuli (Gurtubay-Antolin et al., 2018; Kim et al., 2015; Kitada et al., 2006; Mueller et al., 2019; Sathian et al., 2011; Simões-Franklin et al., 2011; Stilla & Sathian, 2008; Yang et al., 2017). The insula is conceptualised as an integration hub and has been linked with cognitive and emotional evaluation (Craig et al., 2000; Jensen et al., 2016; Segerdahl et al., 2015). Therefore, it is possible that the insula integrates somatosensory information with higher-order cognitive and emotional processing.

Pleasant affective touch stimulation of the hairy skin is commonly associated with posterior insula (PI) activation (Morrison, 2016) through the CT pathway (Björnsdotter et al., 2009, 2010; Olausson et al., 2002, 2008). A recent ALE meta-analysis investigating the effect of CT optimal brushing demonstrated significant PI activation during pleasant affective touch of the glabrous and hairy skin (Morrison, 2016). Further, the glabrous skin has been consistently associated with subjective pleasantness despite the lack of CT fibres (Etzi et al., 2014; Klöcker et al., 2012, 2013; Löken et al., 2012; Perini et al., 2015), and no difference has been found between pleasantness ratings in the hairy and glabrous skin (Cruciani et al., 2021). Therefore, it is possible that the PI plays a role in perceived subjective pleasantness during discriminative touch as well as affective touch.

1.5.1.2 Motor regions

Voluntary movement requires continuous sensory feedback (Prochazka, 2015). Motor neurons carry information from the brain and spinal cord to the muscle fibres throughout the body, allowing one to take physical action in response to stimuli in the environment (Gautam, 2017). The MI, SMA and premotor cortex are the main motor regions associated with action execution, imitation, observation, motor learning, preparation, and imagery (Papitto et al., 2020).

The MI is in the frontal lobe and projections are mapped contralateral to stimulation in somatotopic organisation (Penfield & Boldrey, 1937; Penfield & Broldrey, 1950). The MI is responsible for generating neural impulses to control the execution of movement with brain activation seen contralaterally to the muscle movement (Brown & Staines, 2015). Lesions in the MI typically result in motor deficits such as muscle weakness, slowing of movements, and discoordination of joint motions (Friel & Nudo, 1998; Glees & Cole, 1950).

The human premotor cortex is split into ventral and dorsal regions. The PMv is predominantly linked with grasping and object manipulation hand movements (Davare et al., 2006, 2008, 2009; Fogassi et al., 2001; Reader & Holmes, 2018; Vingerhoets et al., 2013), and evaluating sensory information to inform motor action (Romo et al., 2004). The PMd plays a role in goal-directed reach actions and is concerned with motor preparation and execution (Beurze et al., 2007; Hoshi & Tanji, 2007). Lesions PMd result in deficits in visual guidance of goal-orientated movements, whilst damage to the PMv results in deficits in object manipulation (Chang et al., 2010; Rizzolatti et al., 1983). Together the premotor cortex plays a key role in formulation of motor actions and object manipulation.

The SMA is split into two functional regions, the pre-SMA and SMA (Vorobiev et al., 1998; Woolsey et al., 1952). The pre-SMA is thought to play a more cognitive role, whilst the SMA is concerned more with the planning of motor commands (Obeso et al., 2013; Picard & Strick, 2003). The SMA has been established as playing a role in movement preparation and bimanual coordination (Welniarz et al., 2019).

1.5.1.3 Sensorimotor integration

The PPC is thought to be a multimodal association area as it combines inputs from several brain areas (Buneo & Andersen, 2006; Whitlock, 2017). Importantly, the area receives information from both the SI and MI and plays a role in sensory guidance of movement rather than discriminative touch (Hyvärinen, 1982; Mountcastle, 1998; Mountcastle et al., 1975, 1995; Rushworth et al., 1997). In humans, the PPC is split into two regions: the SPL and IPL. The role of the SPL is to integrate proprioceptive information to guide movements (Johns, 2014), whilst the role of the IPL is to aid in preparation of motor acts such as hand grasping movements (Elk, 2014; Fogassi et al., 2005; Fogassi & Luppino, 2005; Jeannerod et al., 1995). Lesions in the PPC lead to tactile apraxia, which is characterised by kinematic deficits

when interacting with objects (Binkofski et al., 2001; Pause et al., 1989). Further, lesions of the SPL can impair sensorimotor integration of proprioceptive signals and cause optic ataxia, a deficit in control of arm movements under visual and proprioceptive guidance (Andersen et al., 2014). Neuroimaging studies demonstrate that the PPC is activated by grasping, reaching, and interacting with objects (Vingerhoets, 2014). Taken together, this suggests that the PPC plays a significant role in motor control by integrating sensory information, known as sensorimotor control.

1.5.2 Electrophysiological correlates of tactile stimulation and voluntary movement

EEG can be used to measure electrophysiological changes that arise from the cortex, these comprise of phase- and non-phase-locked activity. As discussed in Chapter 2, EEG activity which is phase-locked can be investigated by measuring event-related potentials (ERP), whereas non-phase-locked EEG activity can be examined during rest or following a time-locked stimulus (Kalcher & Pfurtscheller, 1995).

1.5.2.1 Cortical oscillations

EEG oscillations can be classified by their frequency, and changes in the amplitude, suppression, or enhancement of oscillations within specific frequency bands are associated with different functional characteristics.

Alpha-band oscillations occur within the 8-13 Hz range and can be observed over occipital, parietal, and sensorimotor cortices (Kropotov, 2009). The first report of oscillatory changes was made by Hans Berger (1929; as cited in Gloor, 1970) in the alpha-band, whereby alpha-band rhythms are enhanced during EEG recordings when the eyes are closed and are attenuated when the eyes are opened (Adrian & Matthews, 1934; Jung & Berger, 1979). The enhancement of occipital alpha-band rhythms is thought to be due to decreased

visual input to occipital areas. Therefore, occipital alpha-band oscillations have been proposed to reflect idling, whereas attenuation of alpha-band rhythms is thought to be a correlate of cortical activation (Adrian & Matthews, 1934). Enhancement of occipital alpha-band rhythms as a reflection of idling or cortical deactivation has also been evidenced through investigation of simultaneous EEG and fMRI; opening and closing the eyes produced suppression and enhancement of occipital alpha-band activity which corresponds to increased and decreased activation in blood-oxygen-level-dependent (BOLD) signals, respectively (Feige et al., 2005).

Alpha-band rhythms that occur over sensorimotor regions at ~10 Hz can be referred to as mu rhythms or sensorimotor rhythms. The mu rhythm gets its name from its distinctive sharp negative peaks which appear similar to the Greek letter μ (mu) and is sometimes referred to as rolandic mu due to its presence above the rolandic fissure (Kropotov, 2009). Alpha-band rhythms over sensorimotor regions are observed in the absence of movement and are attenuated during voluntary movement, motor imagery or tactile stimulation (Chatrian et al., 1958; Cheyne et al., 2003; Gaetz & Cheyne, 2006; Pfurtscheller & Neuper, 1997; Salmelin & Hari, 1994; Stancak & Pfurtscheller, 1996a). As with occipital alpha, attenuation of sensorimotor alpha-band rhythms reflects cortical activation, whilst enhancement is considered a correlate of active inhibition of task-irrelevant stimuli (Fry et al., 2016; Jensen & Mazaheri, 2010; Neuper & Pfurtscheller, 2001). Simultaneous EEG-fMRI investigations demonstrate a negative correlation between BOLD signals and sensorimotor alpha-band power (Ritter et al., 2009).

In further research, Berger found alpha-band waves were attenuated when subjects opened their eyes and if their attention was occupied, leading to the discovery of "beta waves" (Adrian & Matthews, 1934; Kropotov, 2009). Beta-band rhythms are classified as

occurring within the 14-30 Hz range and manifest over frontal and sensorimotor regions (Kropotov, 2009). Sensorimotor alpha- and beta-band oscillations originate from the SI and MI, respectively (Hari & Salmelin, 1997; Salmelin & Hari, 1994).

Attenuation of beta rhythms occur following voluntary movement, motor planning and tactile stimulation (Neuper & Pfurtscheller, 2001; Pfurtscheller, 1981; Pfurtscheller et al., 1998; Stancak et al., 2003; Stancak & Pfurtscheller, 1996b). Enhancement of beta-band oscillations are observed in the MI following movement-related beta suppression, referred to as beta rebound (Cheyne et al., 2003; Gaetz & Cheyne, 2006; Pfurtscheller et al., 2005). Beta-band oscillations are sensitive to Gamma-aminobutyric acid (GABA) agonists, whereby the power of beta rhythms is enhanced after administration of GABA agonists (Jensen et al., 2005). Movement induced beta-band event-related desynchronisation (ERD) has been linked to levels of GABA (Hall et al., 2010, 2011). Importantly, GABA has been found to decline with age (Gao et al., 2013), which may contribute to changes in motor control. Therefore, attenuation of beta-band rhythms during voluntary movement, motor planning and tactile stimulation may be impacted by age.

Theta-band oscillations occur within the 4–8 Hz frequency range over frontal midline regions in response to cognitive tasks and attention-related processes (Kropotov, 2009). A positive correlation between theta-band power and working memory load has been demonstrated, suggesting that theta-band oscillations are linked with top-down memory processes (Gevins, 1997; Klimesch, 1999; Klimesch et al., 2008). In addition, theta-band oscillations are thought to play a role in sensorimotor integration via connectivity between the hippocampus and sensorimotor areas (Karakaş, 2020). Thus, suggesting a role for theta-band oscillation during active touch.

1.6 Effects of texture processing on electrophysiological and haemodynamic response

Neuroimaging studies using fMRI have also reliably demonstrated SI activation after stimulation of the hand with sandpaper (Kim et al., 2015; Simões-Franklin et al., 2011), gratings (Kitada et al., 2005, 2006), ridged textures (Mueller et al., 2019; Tang et al., 2021a), dot patterns (Yang et al., 2017), and textiles (Wang et al., 2016). The haemodynamic response from SI has been shown to vary based on roughness (Kim et al., 2015), amplitude of vibratory stimuli (Nelson et al., 2004), attention (Hämäläinen et al., 2000), and to unexpected stimuli (Gurtubay-Antolin et al., 2018). Studies using fMRI have also confirmed the role of bilateral activation of the SII in response to textured stimuli (Kitada et al., 2005, 2006; Sathian et al., 2011; Stilla & Sathian, 2008; Yang et al., 2017). Evidence suggests that the SII may be responsible for encoding surface roughness (Kitada et al., 2005; Sathian et al., 2011; Servos et al., 2001; Stilla & Sathian, 2008). Together, neuroimaging studies have demonstrated the consistent activation of the SI and SII during processing of textured stimuli.

Using ERP analysis, textured stimuli have been found to evoke N100, P100, P200 and P300 ERPs (Ballesteros et al., 2009; Chen & Ge, 2017; Muñoz et al., 2014; Tang et al., 2020, 2021b). Further, surface properties modulate the ERP response, with increased P300 amplitude for rough compared to smooth textures (Chen & Ge, 2017; Muñoz et al., 2014; Tang et al., 2020). Although, Moungou et al. (2016) found that the amplitude of steady-state evoked-potentials (SS-EP) were greater in magnitude with increased surface smoothness, hypothesised to be due to increased high-frequency vibrations induced by movement across the texture. Further, the N100 and P200 peaks occur earlier for smoother textures compared to rough textures (Ballesteros et al., 2009).

Time-frequency analysis of ongoing oscillations has revealed bilateral alpha- and beta-band ERD, with greater alpha-band ERD with decreased stimulus roughness (Genna et al., 2018). A recent study by Taleei et al. (2022) demonstrated that functional conectivity in alpha- and beta-band were responsible for discrimination between surfaces. More recently, machine learning techniques have been employed to classify the EEG signal between different surface properties; EEG nonlinear characteristics were affected by alteration of surface roughness (Baghdadi et al., 2021) and EEG spectral features provided higher accuracy in discriminating surface roughness in alpha- and beta-band (Eldeeb et al., 2019).

1.7 Tactile suppression/movement-related gating

Active touch is associated with highly refined tactile abilities (Chapman, 1994), though, voluntary movement has been associated with a reduction in tactile perception, referred to as tactile suppression or movement-related gating (Chapman et al., 1987; Williams et al., 1998). Internal models of motor control can predict the sensory consequence of a motor command and calculate motor outputs from sensory inputs, referred to as the forward and inverse models respectively (Figure 1.4; Flanagan et al., 2003). In order to achieve a desired sensory consequence, the inverse model computes motor commands needed to produce movements. Motor areas in the brain send a copy of the descending motor command, known as the efference copy (Sperry, 1950; von Holst & Mittelstaedt, 1950), to somatosensory regions of the cortex. This process provides information to the forward model on intended actions and facilitates the prediction of neural response to tactile stimuli. This efference copy is thought to suppress redundant movement-related feedback; as a result, the perception of tactile stimulation that was not predicted is enhanced.

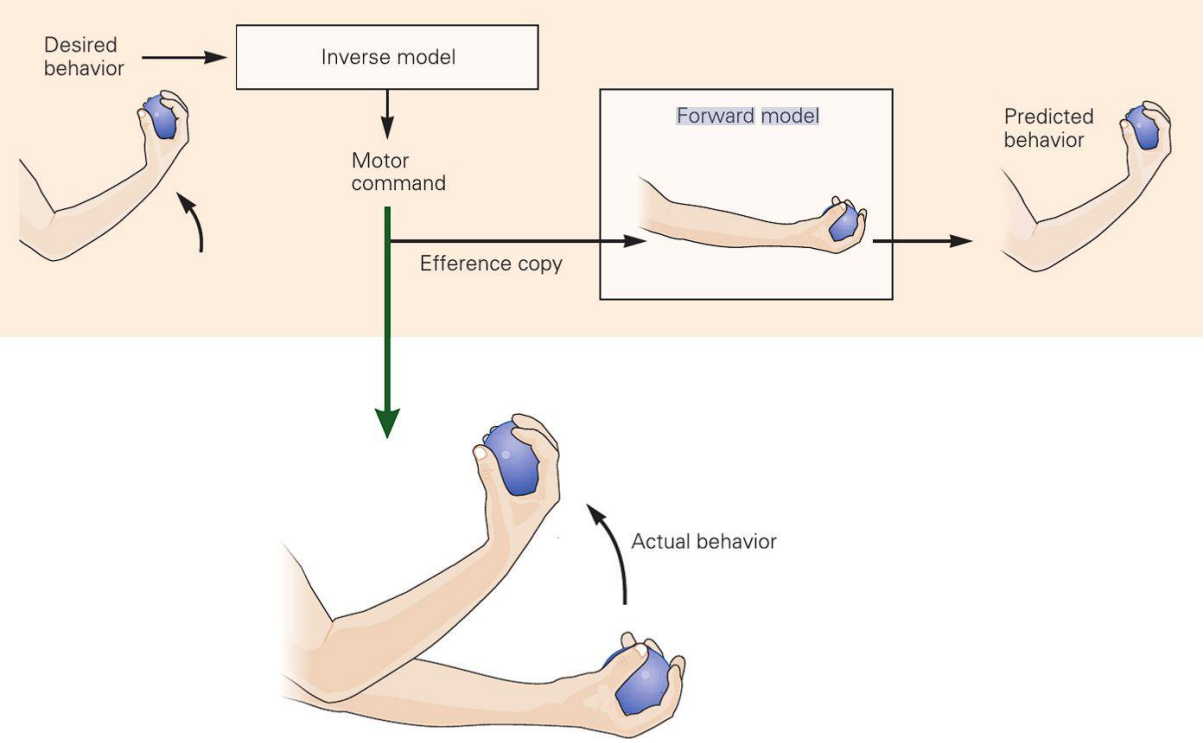

Figure 1.4 Inverse and forward model of motor control from Amaral (2012).

Tactile suppression begins before the onset of voluntary movement and passive movement of the limbs (Chapman & Beauchamp, 2006; Williams & Chapman, 2002). It is thought that movement itself does not induce tactile suppression, but motor planning initiates the efference copy (Voss et al., 2005, 2008). Tactile suppression is most prominent on the moving limb (Williams et al., 1998), and during tactile stimulation at near-threshold intensities, as the intensity of the stimuli increases tactile suppression decreases (Chapman et al., 1987; Post et al., 1994; Williams & Chapman, 2000). Further, the relative difference between two stimulus intensities is maintained during tactile suppression, meaning that humans can still discriminate between stimuli during onset of voluntary movement (Chapman et al., 1987; Post et al., 1994).

The speed of movement modulates tactile suppression, wherein, the faster the movement the greater the suppression (Angel et al., 1982; Cybulska-Klosowicz et al., 2011; Schmidt et al., 1990). Although, exploration of surfaces is associated with slow movement

speeds, which may facilitate tactile processing (Fraser & Fiehler, 2018; Juravle et al., 2013). Therefore, the accurate recording of touch behaviour is necessary when considering the neural correlates of texture processing.

Despite the evidence supporting tactile suppression during movement and tactile stimulation, we know that movements made to gain information about a surface (i.e., active touch) enhance perception and reflect how humans gather textural information in the real-world (Juravle et al., 2013, 2016a). In the human brain, tactile suppression results in a reduction of short-latency somatosensory evoked potentials (SEP) during EEG recordings (Giblin, 1964; Papakostopoulos et al., 1975; Rossini et al., 1996, 1999). Investigation of SEP responses in single neurons of the non-human primate SI demonstrated a decreased response during movement of the limb (Chapman et al., 1988; Jiang et al., 1990, 1991). Whilst evidence from humans suggests a decrease in short-latency SEP in both contralateral and ipsilateral SI (Cohen & Starr, 1987; Lei & Perez, 2017), thus evidencing that decreased cortical response is present in somatosensory processing areas during movement.

Investigation of SEP has included the study of both short- and long-latency evoked potentials, providing evidence that while voluntary movement diminishes short-latency SEP, the amplitude of long-latency SEP is increased (Lee & White, 1974; Nakata et al., 2003, 2011). Furthermore, goal-directed movements elicit an enhancement of SEP during movement and tactile stimulation compared to pre- and post-movement (Juravle et al., 2016b), which supports the theory that movements made to gain information about surface properties enhance tactile perception (Juravle et al., 2016a). Therefore, to fully understand the neural correlates of texture processing during active touch, investigation over a prolonged exploration period may be necessary to overcome the initial tactile suppression.

Chapter 2
General methods

2.1 Principles of electroencephalography

2.1.1 Physiological basis of the EEG signal

EEG can be used to investigate task-related changes in brain activation by measuring differences in electrical potentials at the scalp. The human brain consists of several billions of neurons which conduct electrical activity (Azevedo et al., 2009). Each neuron in the human brain consists of a cell body, dendrites, and an axon. When a neuron receives a signal, an electrical impulse, referred to as an action potential, is transmitted along the axon. This induces a temporary shift in the neuron's membrane potential, which is caused by the flow of sodium and potassium ions into and out of the neuron (Schneider & Strüder, 2012). Action potentials are brief, lasting between one to two milliseconds, and are not generally synchronised. Further, action potentials are biphasic, and the nature of the depolarising and repolarising currents may result in mean electrical field cancellation. Consequently, action potentials are not detectable at scalp electrodes (Buzsáki et al., 2012; Speckmann et al., 2011).

Postsynaptic potentials, however, are monophasic and sustained for hundreds of milliseconds (Buzsáki et al., 2012). An influx of positive sodium ions at dendrites causes depolarisation of the postsynaptic cell (excitatory), whereas an influx of negative chloride ions causes hyperpolarization of the postsynaptic cell (inhibitory; Purves et al., 2001). However, it is not possible to ascertain through EEG whether excitatory or inhibitory postsynaptic potentials are being recorded. Signals recorded by EEG reflect the summation of

synchronous postsynaptic potentials across a neuronal population, referred to as a field potential (Bastiaansen et al., 2011).

Pyramidal cells make up 70 to 85% of all neurons in the mammalian cortex and are the major excitatory neuron type in the cerebral cortex (DeFelipe & Fariñas, 1992; Markram et al., 2015). The neocortex is organised into six layers, numbered from the outer surface of the cortex to the white matter (Amaral & Strick, 2012). Pyramidal cells are found in layers II/III and V, and are organised so the primary axis is perpendicular to the cortical surface. Consequently, EEG signals are mostly generated by pyramidal neurons from both radial (from the gyri) and tangential (from the sulci) sources (Cohen & Halgren, 2015). Signals that are not nonaligned cancel each other out (cancellation effect). Therefore, EEG is dominated by radial sources, as they generate large electrical fields that are perpendicular to the scalp and therefore are easily recorded by the scalp electrodes. On the other hand, tangential sources produce weaker EEG signals, but still contribute to the measurable signal due to their proximity to the scalp. Overall, the open field layout of postsynaptic potentials from pyramidal cells is detectable with EEG.

2.1.2 EEG acquisition

EEG records fluctuating electrical fields of the brain across time via electrodes placed on the scalp (Malmivuo & Plonsey, 1995). Electrodes are typically placed according to a derivative of the 10-20 system, which is an internationally recognised method for the application of scalp electrodes to maintain standardised placement across research studies, thus aiding reproducibility, interpretation, and comparison of findings. Electrodes are placed at 10% and 20% points from the nasion to the inion, and from the left to the right preauricular points (Jasper, 1958; Klem et al., 1999). Dense electrode nets are often placed according to alternative systems, for example, the Geodesic layout specifies that electrodes are placed

equidistant to one another (Magstim EGI, UK), though many electrodes correspond to electrodes in the 10-10 system (Luu & Ferree, 2005), which is an extension of the original 10-20 system with a higher channel density (Chatrian et al., 1985).

Amplitudes recorded from raw EEG are typically under 100 μV, therefore, the signal for each electrode is usually amplified by a factor of 1000-100000, referred to as the gain of the amplifier (Luck, 2014). EEG uses three types of electrodes: active, reference, and ground. The EEG signal is recorded as the potential for a current to pass from the active electrode to the ground electrode. However, there is often noise in the ground circuit, which is solved by use of a differential amplifier, wherein activity at active electrode sites is computed as the difference between active-ground electrodes and reference-ground electrodes (Luck, 2014).

In this thesis, EEG studies employed the use of a 129-channel sponge-based Geodesic sensor net (Magstim EGI, UK), the electrodes location map is illustrated in Figure 2.1. Use of a Geodesic sensor net allows researchers to quickly place a dense array of electrodes, which covers the whole head including the forehead and suborbital regions of the face. A saline solution was used as the conducting medium and the position of the Geodesic sensor net was aligned to three anatomical landmarks, two preauricular points and the nasion. Electrode to skin impedances were kept below 50 kΩ, and a recording band-pass filter was set at 0.001–200 Hz with a sampling rate of 1000 Hz. Electrode Cz, located at the vertex, was used as a reference electrode for recording, and COM, located posterior to electrode Cz, was used as the isolated common/ground electrode, Figure 2.1.

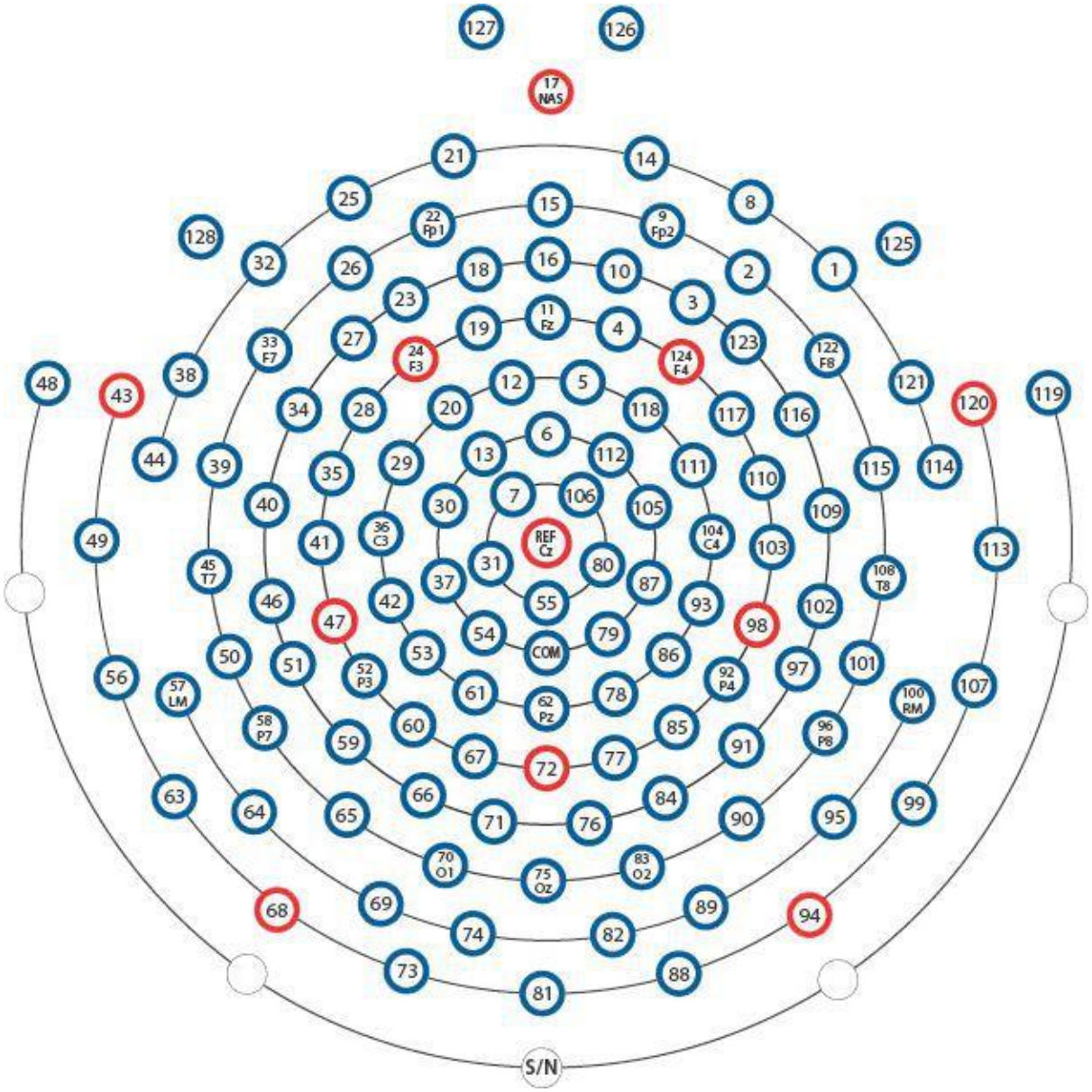

Figure 2.1 Distribution of 129 electrodes across the scalp for the sponge based EGI net.

2.1.3 Artefact correction

EEG is susceptible to artefacts from extracerebral sources which may impact the interpretation of the EEG signal. These artefacts can be classified into two types: physiological and non-physiological. Physiological artefacts encompass electrooculographic (EOG), electrocardiographic (ECG), electromyographic, electrodermal, and respiration-related activity. Non-physiological artefacts are primarily due to hardware problems, poor electrode-to-skin contact, and electrical interference caused by alternating mains power supply of either 50 Hz in Europe or 60 Hz in the USA (Luck, 2014). Researchers can visually inspect EEG data for the presence of artefacts, where contaminated trials are marked for rejection. Alternatively, reoccurring artefacts such as EOG and ECG can be removed from the EEG signal with adaptive artefact correction in the Brain Electrical Source Analysis software (BESA, GmbH; Berg & Scherg, 1994; Ille et al., 2002). This method uses a spatial filter to disentangle neural activity from artefacts without distorting the data. Segments of data are determined to represent brain activity if they demonstrate a low correlation with the artefact topography, and if the signal amplitudes are below a specified threshold. Data sections identified as an artefact are subjected to principal component analysis (PCA), where artefacts are removed from the raw data by decomposing the data into a linear combination of independent brain and artefact activities, enabling the estimation and subtraction of artefact signals from the raw data (Ille et al., 2002; Lagerlund et al., 1997).

2.1.4 Time-frequency analysis

2.1.4.1 Quantifying cortical oscillations

There are several characteristics of EEG oscillations that one can use for classification, including amplitude, frequency, and morphology (Nayak & Anilkumar, 2022). The most commonly used method to classify EEG oscillations is by frequency, where the classical

bands for EEG analysis are: delta- (1-4 Hz), theta- (4-7 Hz), alpha- (8-13 Hz), beta- (14-30 Hz), and gamma-band (>30 Hz). Each frequency band has different functional characteristics (Saby & Marshall, 2012), with somatosensory and motor processing typically inducing oscillatory activity in alpha- and beta-bands. Though, it should be noted that frequency bands can differ across populations (Hashemi et al., 2016; Newson & Thiagarajan, 2019; Polich, 1997)

Fourier analysis is the most widely used algorithm for decomposing the EEG signal from the time domain into specific frequency components, modelled by sine and cosine waves. The Fourier transformation contains two Fourier components, which are the weights of the cosine and sine basis functions. From these components, power and phase may be extracted (Nunez et al., 2016). A sliding time window is used when conducting a Fourier transform. A taper is a mathematical function which is multiplied with the data to reduce spectral leakage, where the power spectrum is smeared across the frequency spectrum due to the measured signal being non-periodic in the sample window (Cohen, 2014). The power spectrum is then calculated for each time window, which is a frequency domain representation of the magnitude of activity present in a series of data points for different frequencies (Keil et al., 2022). Time-frequency decomposition is limited by the Fourier uncertainty principle, which requires researchers to make a trade-off between temporal resolution and frequency resolution, where the higher the frequency resolution, the lower the temporal resolution and vice versa (Cohen, 2014).

Edge artefacts are spectral distortions that occur due to large variations at the beginning and end of the time series. A further issue of Fourier transformation, as previously mentioned, is spectral leakage. To minimise the effects of edge artefacts and spectral leakage, researchers can apply window or taper functions, where the data at either end of the segment

are weighted to zero. Common window functions include Hann(ing) and Hamming, Kayser, Bartlett, Tukey, Blackman, and cosine-square functions (Keil et al., 2022). Further, multitaper analysis can be used, where multiple window functions are applied prior to the moving-window Fourier Transformation (e.g., the Slepian sequence; Slepian, 1978). The multitaper method is beneficial for controlling smoothing and is typically used for frequencies above 30 Hz. In this thesis, Chapter 5 and Chapter 7 implemented a time-frequency analysis with a Fourier transform and a Hanning window to investigate the effect of texture processing.

An alternate method for time-frequency decomposition is wavelet analysis. Wavelets have the advantage of variable time and frequency smoothing, whereby lower frequencies are more precisely represented in the frequency domain and higher frequencies are more precisely represented in the time domain (Cohen, 2014; Tallon-Baudry & Bertrand, 1999). In neuroscience, the most used mother wavelet function is Morlet wavelets: they represent segments of sine and cosine functions at the frequencies of interest in a window of time, which is multiplied by a Gaussian. The width of the Gaussian is given by the researcher and is often between 5 and 10, this determines the temporal and frequency smoothing. A consequence of this is the Fourier uncertainty principle, where a wider Gaussian decreases temporal resolution whilst increasing frequency resolution, and vice-versa for a narrower Gaussian (Keil et al., 2022). In Chapter 6 of this thesis, time-frequency decomposition was performed using a wavelet analysis with a Morlet wavelet mother function and five wavelet cycles.

The power spectrum can be evaluated in terms of absolute or relative power. Absolute power can differ greatly between individuals due to neurophysiological, anatomical, and physical properties of the brain and surrounding tissue (Kropotov, 2009). Conversely, relative

power has lower variability when compared to absolute power. Researchers can investigate relative power of each frequency band by dividing the absolute power of each band by the total power, or by the sum of powers in the frequency band of interest.

2.1.4.2 Event-related de/synchronisation

The ERD method can be used to investigate time-locked oscillatory changes associated with an event such as somatosensory stimulation (Chatrian et al., 1958; Pfurtscheller, 1981; Stancak et al., 2003) or movement (Pfurtscheller et al., 1993; Pfurtscheller & Neuper, 1992; Stancak & Pfurtscheller, 1996a). Computation of the time course of ERD includes bandpass filtering all trials, followed by squaring the amplitude samples to obtain power samples. After this, power values are averaged across all trials and averaging of time samples is performed to smooth data and reduce variability (Pfurtscheller & Lopes da Silva, 1999).

Equation 1. The ERD transformation

$$\mathrm{ERD\%} = \left(\frac{A - R}{R} * 100\right)$$

In Equation 1, $\mathrm{ERD\%}$ is the percentage power change during event epochs (A) relative to the baseline period (R; Pfurtscheller, 2001; Pfurtscheller & Aranibar, 1979). Negative values of $\mathrm{ERD\%}$ refer to the amplitude decreases of band power which signify the presence of cortical activation (ERD; Pfurtscheller & Aranibar, 1977; Pfurtscheller & Neuper, 1992). In contrast, positive $\mathrm{ERD\%}$ values refer to the amplitude increases of band power, known as event-related synchronisation (ERS), which in certain circumstances can be interpreted as a correlate of deactivation (Pfurtscheller, 1992, 2001; Pfurtscheller et al., 1996a, 1996b).

Where no suitable baseline period is available, oscillatory changes can be quantified in terms of event-related band power by computing *z*-scores after the band power calculation across the frequency band of interest for each participant, electrode, and experimental condition (Klimesch et al., 1998; Pfurtscheller, 1999). In this thesis, Chapter 5–7 investigate the neural correlates of texture processing using EEG and relative power: Chapter 5 and Chapter 6 use the ERD/S method, while Chapter 7 uses a z-score transformation.

2.1.5 Statistical analysis of time-frequency data

EEG yields rich data with many time points, frequencies, and electrodes to consider. Therefore, statistical analysis of EEG data is confounded by the multiple comparison problem, due to the vast number of comparisons necessary to evaluate the difference between experimental conditions at different electrode-time-frequency pairs. Assumptions for data analysis may be based on previous research (Luck, 2014), particularly with the time-frequency approach where the researcher is aware of certain frequency bands of interest, e.g., movement-related beta-band ERD. However, while averaging over frequency reduces the number of data points, multiple comparisons is still an issue when evaluating the vast number of electrodes.

2.1.5.1 Permutation analysis

To help solve the problem of multiple comparisons, one can employ a permutation analysis (Maris & Oostenveld, 2007). During a permutation test, all the trials from the experimental conditions are collated into a single set. Then, the total number of trials from each experimental condition are randomly drawn and placed into subsets, referred to as a random partition. The test statistic is then calculated on the randomly partitioned data. A Monte Carlo estimate is obtained by repeating the previous steps many times and comparing these random test statistics with the observed test statistic, referred to as the permutation distribution

(Neumann & Ulam, 1945). The Monte Carlo estimate of the permutation p-value is the proportion of random partitions where the observed test statistic is larger than the value drawn from the permutation distribution. If the p-value is smaller than the critical alpha level one can conclude that the data in the experimental conditions are statistically significantly different (Maris & Oostenveld, 2007).

2.1.5.2 Statistical parametric mapping

Another approach for statistical analysis of exploratory research questions is the mass univariate approach, e.g., statistical parametric mapping (SPM; Friston, 1997). Classically, SPM is a method used to analyse functional images obtained by measuring the haemodynamic response (Friston, 2007a). Statistical parametric maps are images constructed with statistics that are calculated for each brain voxel. Data from each voxel is analysed independently using a general linear model (GLM) and standard univariate statistical tests. The resulting voxel-wise statistics are assembled into an image and interpreted as continuous statistical processes. Random field theory (RFT) is used to correct for multiple comparisons (Adler, 1981; Worsley et al., 1992, 1996), including adjusting degrees of freedom for non-sphericity (Brett et al., 2007). Classical inference is used to interpret regionally specific responses to experimental factors (Friston, 1994, 1997, 2004).

Over the past two decades SPM has been applied to EEG data to analyse evoked and induced responses (Friston, 2007a; Kilner et al., 2005). For EEG data, both 3D (X × Y × time) or 2D (time × frequency) images can be created, the former incorporating amplitude or power across peristimulus time and scalp location (X × Y) and the latter incorporating power and peristimulus time-frequency (Kiebel et al., 2007). A statistical value is calculated for each voxel (a volume created by SPM based on the desired image, e.g., scalp × time), representing the level of evidence against the null hypothesis (Friston, 1994, 2007b).

Statistical maps are produced based on the GLM which are corrected for multiple comparisons using RFT (Brett et al., 2007).

The statistical analysis of EEG data is performed in two stages; the first level is performed within individual subjects and the second level (also referred to as group-level) is conducted across subjects. During first level analysis each individual voxel is entered into a GLM; at this stage extra regressors (covariates) can be entered into the model (Kiebel & Holmes, 2007). Effects of interest are defined for each subject using a contrast vector; this generates an image containing the contrast of the parameter estimates at each voxel (Penny & Holmes, 2007). The second stage of analysis takes the contrast images from all subjects from the first stage and enters them into a GLM to test for the effect of interest using *t*- or *F*-statistics.

With SPM, researchers can analyse EEG data from large arrays of electrodes across all timepoints in a single model, allowing for the testing of several hypotheses without model refitting. Therefore, the SPM method for statistical analysis of EEG data is an appropriate approach to take when investigating more exploratory research questions (Friston & Stephan, 2007). In this thesis, SPM12 is used in Chapter 6 to compare EEG power in the form of ERD/S in alpha- and beta-band during tactile exploration of two textures under differing estimation conditions. Touch behaviours were used as GLM regressors.

2.1.6 Strengths and Limitations of EEG

As a neuroimaging technique, EEG is cost-effective when compared to other methods such as magnetic resonance imaging (MRI) or MEG, as EEG hardware is relatively inexpensive and has a long lifetime. Further, many pre-processing and analysis packages are available for free, for example, EEGLAB, FieldTrip, and SPM (Delorme & Makeig, 2004; Oostenveld et al., 2011; Penny et al., 2007), which enables researchers to develop customised data-analysis

pipelines without additional costs. The accessibility of EEG has led to a wealth of EEG research from labs across the world.

Further, other imaging methodologies, such as MRI, have many exclusion criteria, including participants who are fitted with a cardiac pacemaker, any shrapnel injuries over the lifetime, and claustrophobia. Meanwhile, EEG is a suitable method for participants with MRI contraindications as the method does not require a magnetic field. Furthermore, participants can sit comfortably during EEG recordings, or may even be navigating the environment if using mobile EEG (Tivadar & Murray, 2019). Therefore, EEG is appropriate for use across populations, from neonates to the elderly, including those with neurodevelopment and neuropsychiatric disorders, as well as those with neurological disease (Sanei, 2009).

The temporal resolution of EEG allows for ~1 ms sampling simultaneously from many channels (Schneider & Strüder, 2012). This allows researchers to assess the temporal dynamics of the brain and the underlying cognitive processes, which is more accurate than behavioural measures alone, for example, reaction times or hedonic ratings (Luck, 2014). Whilst the temporal resolution of EEG is excellent, the spatial resolution is poor when compared to other methods, such as MRI (Gage & Baars, 2018). This is because cortical current must travel through different resistive layers, such as the skull, before being recorded by scalp electrodes (Srinivasan et al., 1996), resulting in a distorted view of brain activity at the scalp level (Hämäläinen et al., 1993; Nunez et al., 1994). Therefore, the poor spatial resolution of EEG makes it difficult to infer the location of neuronal activity in cortex, referred to as the inverse problem. Source analysis is a technique used within in field of EEG to determine the origins of electrical activity recorded from scalp electrodes. However, the inverse problem is ill-posed, there are many possible solutions for the underlying sources of electrical activity in the brain that may produce the same observed EEG signals at the scalp

(Michel & He, 2011). As such, definitive source localisation is not possible from EEG alone (Iramina et al., 1996; Schneider & Strüder, 2012).

Deep or sub-cortical sources are small and enclosed by cortical activity and therefore have a low signal to noise ratio. The general rule of thumb is that at least 6 cm^2 of synchronous cortical activity is needed to generate a detectable signal (Nunez & Srinivasan, 2006). Further, deep and sub-cortical structures have a closed field; therefore, they do not reach far distances due to the cancellation effect. As such, recording from deep subcortical regions is challenging, though it is possible with the use of high-density EEG (Seeber et al., 2019).

2.2 Functional magnetic resonance imaging

fMRI is a widely used non-invasive neuroimaging technique that produces three dimensional images which can used for both clinical and research purposes (Mandeville & Rosen, 2002). In contrast to EEG, fMRI provides an indirect measure of neuronal activity by measuring changes in cerebral blood flow (Mandeville & Rosen, 2002).

2.2.1 Physics of fMRI

The principles underlying fMRI are based on nuclear magnetic resonance (Slichter, 1992), whereby certain nuclei absorb energy from an electromagnetic field at a specific frequency when placed within a magnetic field (Brown et al., 2007). In fMRI studies the measured signal arises from hydrogen nuclei as they have a large magnetic moment, and they are abundant in biological tissue (Narashiman & Jacobs, 2002). The strong magnetic field of fMRI during scanning aligns hydrogen protons in brain tissue in the direction of the magnetic field, referred to as longitudinal magnetisation (Hendee & Morgan, 1984). Short radio frequency (RF) pulses are delivered at a specific frequency, known as the Larmor frequency,

known to target hydrogen protons. The RF pulse disrupts the alignment of protons, causes protons to precess, and induces transverse magnetisation (Brown et al., 2007). After the RF pulse ends, the precessing protons quickly reorient to the static magnetic field through a process called longitudinal relaxation. Additionally, the excited hydrogen protons realign with the external magnetic field and lose their phase coherence, known as transverse relaxation. T1 and T2 are two parameters in MRI that describe the behaviour of hydrogen protons during relaxation processes; T1 represents longitudinal relaxation, reflecting the time it takes for protons to return to their original alignment after being disturbed by an RF pulse, whereas T2 represents transverse relaxation and indicated the time it takes for protons to lose phase coherence (Narashiman & Jacobs, 2002).

2.2.2 The BOLD signal

The brain cannot store oxygen or glucose; therefore, the normal functioning of brain tissue relies on a constant and adaptable blood supply to replenish energy levels. When an area of the brain is more active, more energy is needed to resupply cells with oxygen or glucose, and so blood flow through that area increases (Logothetis, 2008). However, the neural tissue cannot absorb all the excess oxygen in the blood, resulting in a localised increase in the ratio of oxygenated to deoxygenated haemoglobin (Logothetis, 2008). Deoxyhaemoglobin attenuates the MR signal, therefore, changes in regional haemodynamic response, known as the BOLD signal, are measurable with fMRI (Mandeville & Rosen, 2002). The BOLD contrast was proposed as a naturally occurring alternative to exogenous contrast agents, as it results from changes in the magnetic field associated with distortions caused by blood flow, and thus reflects regional activation (Glover, 2011; Kim & Ogawa, 2012; Ogawa et al., 1990b, 1990a). While this method is an indirect measurement of neural activity, simultaneous fMRI-EEG have established strong correlations between local field potentials and BOLD

signal, validating its use as a neuroimaging technique (Logothetis et al., 2001; Ogawa et al., 2000).

2.2.3 fMRI Meta-Analysis

As a research method, fMRI is expensive relative to EEG (Crosson et al., 2010). As a result, fMRI studies often recruit small samples of participants (Szucs & Ioannidis, 2020), making it difficult to draw conclusions from single studies due to low reliability and power (Bennett et al., 2010; Raemaekers et al., 2007; Zuo et al., 2019; Zuo & Xing, 2014). Further, the popularity of fMRI research has increased over the past 30 years (Wager et al., 2007), from around 44 journal articles published in 1992 to over 3000 published in 2022[1]. The increase in fMRI studies means that there is vast amount of neuroimaging data available. However, published findings from different labs often have a great deal of heterogeneity in task designs, such as differences in stimulus presentation and task instructions, and can vary in scanning procedures (Kober & Wager, 2010; Salimi-Khorshidi et al., 2009; Wager et al., 2007). These issues can contribute to the lack of reproducibility in fMRI studies (Bishop, 2019), and so it is vital that research findings are collated to give a more complete overview of the current literature.

Meta-analysis is a tool used by researchers to examine the convergence of findings by combining results from multiple independent studies (Herrera Ortiz et al., 2021). There are two standard approaches for conducting a meta-analysis on fMRI data: image-based meta-analyses (IBMA) or coordinate-based meta-analyses (CBMA; Salimi-Khorshidi et al., 2009). IBMA combines whole-brain statistic volumes by using the full *T* statistic images; this allows for the use of hierarchical mixed effects models that account for both intra-study and random

[1] A rough estimate based on an inclusive search in PsychInfo (which excludes many non-psychological medical studies) 'functional magnetic resonance imaging OR fMRI'.

inter-study variation (Salimi-Khorshidi et al., 2009; Samartsidis et al., 2017). Conversely, CBMA uses the *x y z* coordinates from each peak location reported, providing a sparser representation of findings in comparison to IBMA. While whole-brain statistical images can be shared on platforms such as NeuroVault (Gorgolewski et al., 2015), authors are typically not required by journals to share their data and as such rarely do so (Müller et al., 2018). Therefore, any researcher conducting IBMA must directly contact the authors of their cohort papers to obtain *T* statistic images that are not published to online repositories. This requirement can lead to bias of only collating data from authors who respond and bias of not being able to obtain images from older studies (Poldrack et al., 2008). As a result, IBMA is unable to answer most meta-analytic research problems (Müller et al., 2018).

2.2.3.1 Activation Likelihood Estimation

ALE is the most widely used CBMA (Eickhoff et al., 2009). ALE meta-analyses pool results across multiple studies in a systematic manner, allowing researchers to perform analysis with a standardised methodology that allows for identification of convergence of activation probabilities between research experiments (Eickhoff et al., 2012; Turkeltaub et al., 2002). To achieve this, ALE treats activation foci as spatial probability distributions which are centred at the coordinates specified and a 3D Gaussian spatial variance model is employed to replace coordinates (Eickhoff et al., 2009, 2016). Significance is determined by testing the null hypothesis of random spatial association between independent groups of coordinates (i.e., experiments; Eickhoff et al., 2012; Turkeltaub et al., 2002).

ALE analysis computes an ALE value for each voxel in the brain and performs tests to determine if there is any convergence among foci that cannot be explained by the null distribution of the ALE statistic (Eickhoff et al 2012). First, foci contributing to an ALE are grouped by experiment before being inputted into BrainMap GingerALE v3.0.2, where the

ALE algorithm is implemented (Eickhoff et al., 2009, 2012; Turkeltaub et al., 2012). Then, a modelled activation (MA) map is created for each experiment group using the mask, which defines the outer limits of Talairach or Montreal Neurologic Institute (MNI) space. The foci and a Gaussian kernel at full width at half maximum are determined from the subject size of the experimental group, with larger subject sizes yielding a tighter and taller Gaussian (Eickhoff et al., 2009). The ALE image is a combination of all the MA maps from the experiments entered into GingerALE (Eickhoff et al., 2009, 2012; Turkeltaub et al., 2012). A *p*-value image is created after calculation of the probability of finding voxels in MA maps, which is used to set a significance threshold on the ALE scores to create a thresholded ALE map. Conjunction and contrast analyses can then be employed to compare resulting ALE maps (Eickhoff et al., 2011).

2.2.3.2 Systematic review

The results from the ALE are affected by the foci given, which means that studies contributing foci should be carefully considered to ensure results are robust and replicable. To achieve this, a systematic review guided by the standards of the Preferred Reporting Items for Systematic Review and Meta-Analysis (PRISMA) statement (Page et al., 2021), is conducted to identify journal articles for inclusion in meta-analyses. Conducting a systematic review according to PRISMA guidelines involves following a procedural checklist and completing a flow diagram specifying the number of records identified and rejected at each stage of the review. The process of conducting a systematic review first involves creating a list of eligibility criteria where inclusion and exclusion criteria are specified. Then, a comprehensive literature search of specified databases with a set of predefined search terms is performed. Journal articles identified from the literature search are then screened for eligibility and the number of studies that met the criteria as well as those rejected are

reported. Data is then extracted from accepted journal articles, which is subsequently used in meta-analyses.

In this thesis, a systematic review was conducted to identify journal articles investigating texture perception with fMRI methods. Coordinates were extracted from accepted research articles and subjected to an ALE meta-analysis using GingerALE v3.0.2 (Eickhoff et al., 2009, 2012; Turkeltaub et al., 2012). The results of the systematic review and meta-analysis are discussed in Chapter 4.

2.3 Active touch

Active touch has often been neglected in previous EEG research as it is difficult to accurately quantify parameters necessary to epoch EEG data, e.g., precise stimulus onset times. Most of the previous research has utilised passive touch paradigms, where robotic stimulation devices are used to present stimuli to the skin. As a result, the neural correlates of active touch during texture perception are poorly understood. The use of touch sensor technology allows for the recording of both EEG and touch data simultaneously. During data-processing, touch and EEG triggers are integrated, allowing for the investigation of the neural correlates of active touch with appropriate temporal resolution. Further, behaviours quantified by touch sensor technology (i.e., load and friction) can be entered into the EEG analysis as covariates, allowing for the control of variance in exploration procedures.

2.3.1 Linear sensor

Initially, a linear sensor was purchased from Hopkinson Research, which allowed for measurement of finger load (g), which is the downward pressure, and finger position (mm) along a sample during unilateral finger movement. This was measured by two single-point load cells at two different positions on the X axis. Load is calculated from the sum of the two

load cells, whereas the calculation of position involves first calculating a torque moment around a horizontal Y axis which is orthogonal to the X axis and places at any arbitrary location along the X axis. This torque is then divided in Newtons-meters by the finger load in Newtons to derive a distance in meters, which is the distance between the centre of pressure from the finger and the Y axis where it was defined (Hopkinson, 2020). The linear sensor and its components are depicted in Figure 2.2. In this thesis, a Hopkinson Linear Sensor was used investigate the neural correlates of texture perception during active touch of different natural textures using EEG, discussed in Chapter 5.

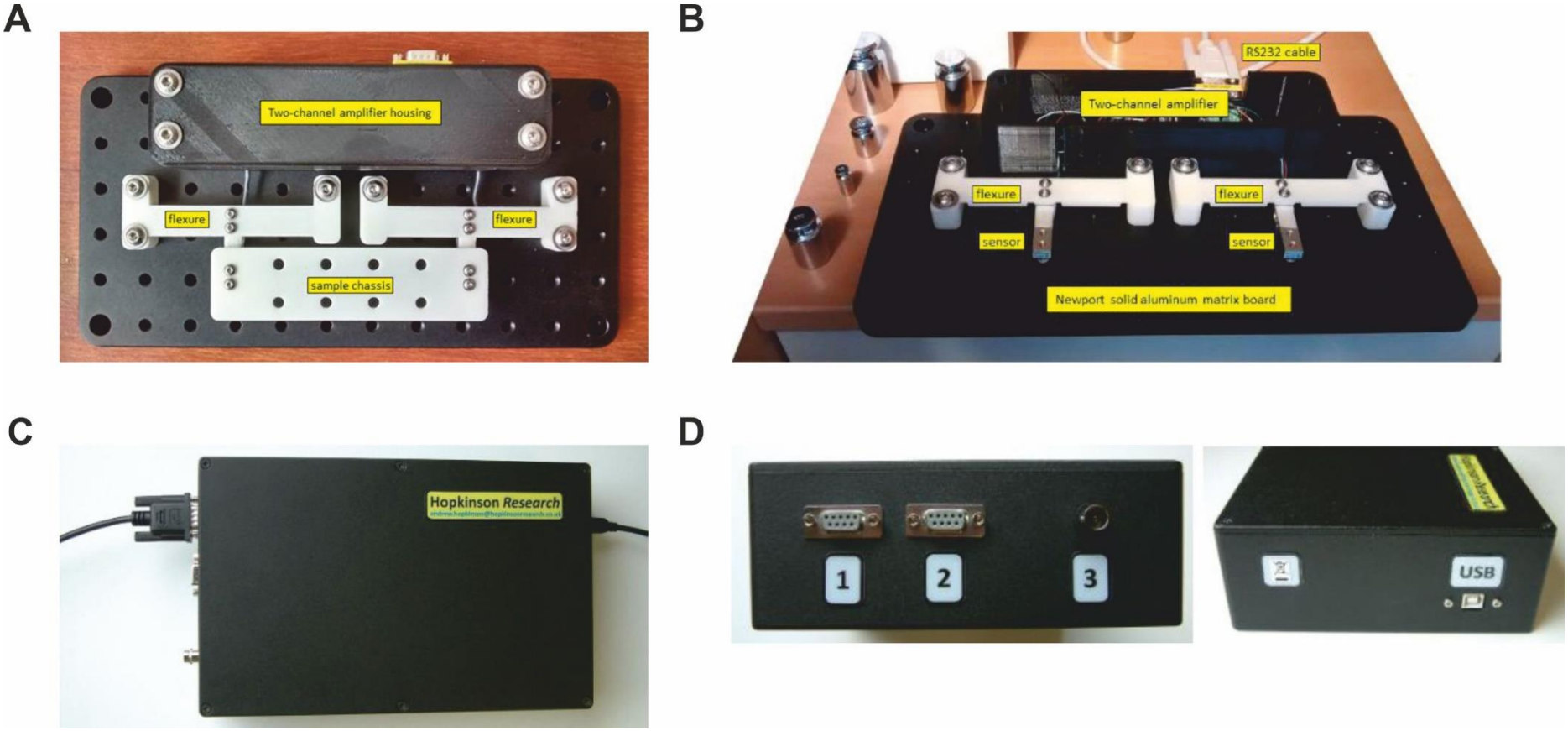

Figure 2.2 Hopkinson Research linear sensor. ***(A)*** *Top view of sensor system showing the amplifier housing, the flexures from which the strain-gauge sensors are mounted, and the sample chassis attached to the sensors.* ***(B)*** *Front view of the sensory system showing the amplifier housing with its cover removed, the RS232 connecting cable, the strain-gauge sensors (sample chassis removed).* ***(C)*** *The LabJackU6 housing, a diecast box containing the Lab Jack U6 multifunctional data acquisition system, a passive signal filter for the sensor signals, a passive voltage divider for user's timing voltage pulse, and sockets for cables to connect to the sensor system, the source of the user's timing voltage pulse, and a host PC or laptop via USB 2.0 or higher.* ***(D)*** *View of the diecast box. The left image shows the connections to the sensor system (labelled 1) and trigger pulse (labelled 3) are visible, the connection labelled 2 is currently unused and is for a planned future application involving more sensors. The right image shows the USB-A female socket for connection to the host laptop or PC. Adapted from Hopkinson (2020a).*

2.3.2 Six-axis sensors

Following the purchase of the linear sensor, a six-axis sensor was purchased from Hopkinson Research to allow for measurement of multidirectional finger movement, shown in Figure 2.3. The sensor was designed to measure finger load (g) in the Z axis, and finger position (mm) in both the X and Y axes. Three large load cells measure the downward force at three locations in a tripod arrangement. These load cells effectively measure the downward force and the torques around the X and Y axes. In addition, the six-axis sensor measures friction force along the X and Y axes as well as the torque around the Z axis with 3 smaller load cells (Hopkinson, 2020b). In this thesis, a Hopkinson Research six-axis sensor was used investigate electrophysiological changes during active texture change, discussed in Chapter 6, as well as the evaluation of textural properties during active touch, discussed in Chapter 7.

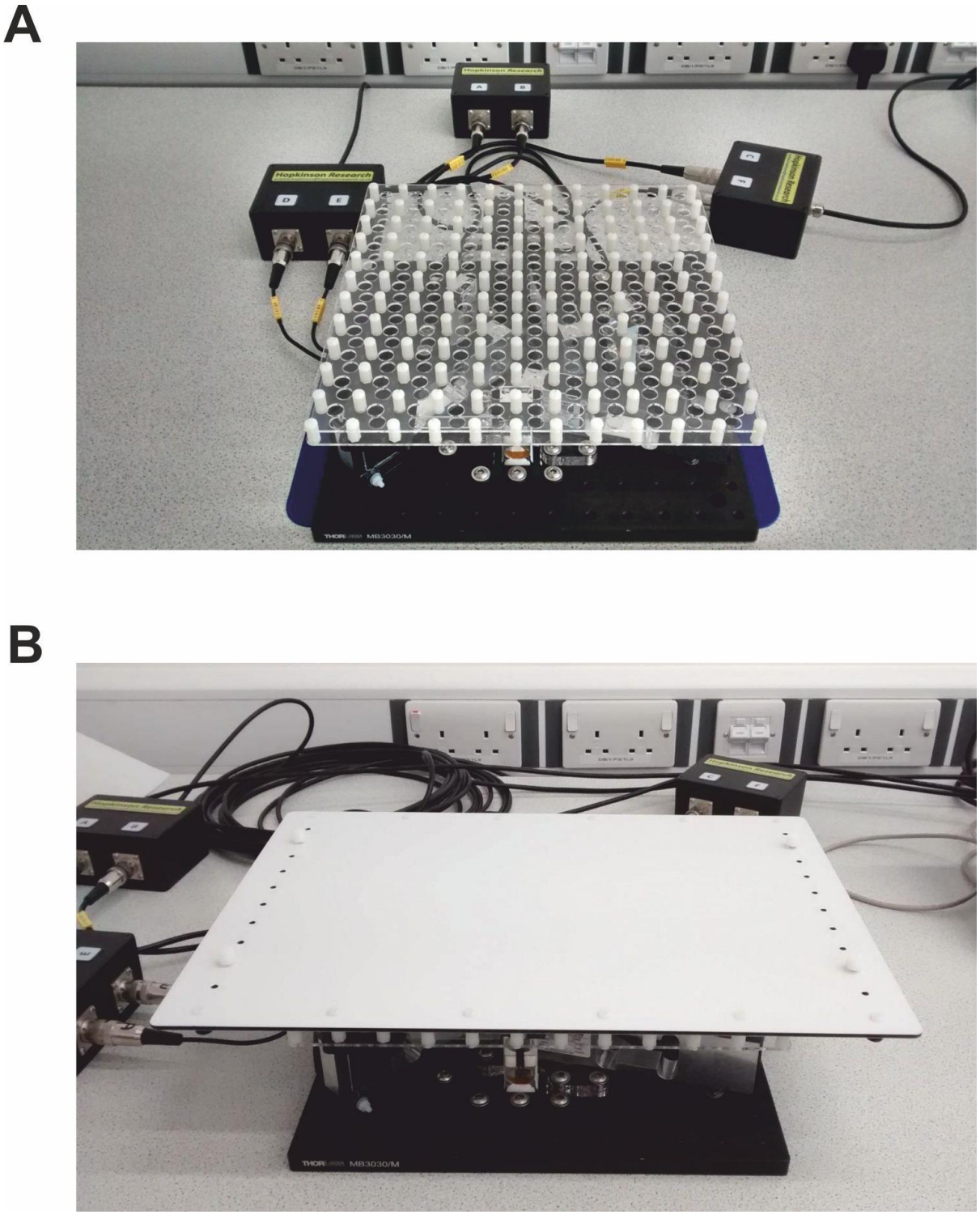

Figure 2.3 Hopkinson Research six-axis sensor. ***(A)*** *Set up of force plate with the load cells connected to the junction boxes.* ***(B)*** *Force plate with aluminium composite panel fitted. Adapted from Hopkinson (2020b).*

Chapter 3
Research problems and hypotheses

3.1 Research problems

The variability in perceptual scales used to quantify surface texture has led to researchers using a vast array of textured stimuli, from smooth natural textures such as silk to rough artificial gratings (Kitada et al., 2005; Wang et al., 2016). As a result, neuroimaging studies are difficult to compare. The SI is thought to be responsible for encoding tactile information related to surface texture (Lieber & Bensmaia, 2019), though previous research hypothesises that the SII plays a role in texture discrimination (Kitada et al., 2005; Roland et al., 1998; Sathian et al., 2011; Servos et al., 2001; Stilla & Sathian, 2008). Due to variations in paradigm and stimuli, fMRI studies demonstrate heterogeneous patterns of brain activity associated with texture processing. This thesis set out to investigate the relationship between neural activity and the processing of texture, taking into account physical characteristics of the texture as well as the influence of higher-level cognitive processes.

Humans navigate their tactile world through active touch, which allows for the modulation of movement speed and digit orientation to optimise skin-surface contact. EEG is used to record oscillatory brain activity, to examine the effect of external events on cortical rhythms data must be time locked to a common event, which is typically the onset of a stimulus. Consequently, current EEG literature investigating the neural correlates of texture processing mostly relies on passive stimulation devices (Ballesteros et al., 2009; Genna et al., 2018; Moungou et al., 2016). The results from passive touch paradigms may not be representative of how the brain processes texture under active touch conditions (Simões-

Franklin et al., 2011). Therefore, modulation of oscillatory brain rhythms during texture processing via active touch is not well understood and remains to be elucidated.

The investigation of texture perception often involves the researcher asking participants to provide a tactile estimation (Bensmaia, 2009; Hollins et al., 1993; Hollins & Risner, 2000). Perceptual judgements require both sensory and cognitive processing; incoming tactile information must be processed in order to inform perceptual judgements by comparing current information with past experiences. Estimation tasks have been shown to modulate the haemodynamic response during tactile discrimination tasks, demonstrating increased activation in higher-order brain regions such as the SII and the prefrontal cortex relative to no estimation conditions (Kitada et al., 2005). Therefore, perceptual judgements of surface texture likely alter brain activations. Despite this, investigations of perceptual judgements of texture using EEG are lacking, thus the electrophysiological underpinnings of perceptual judgement during active exploration of surface texture are yet to be delineated.

Investigation of active touch allows one to assess texture processing under more naturalistic conditions. During real-word explorations, humans perceive changes in surface texture. Typically, change detection in the brain is investigated using oddball tasks, wherein participants are exposed to one repetitive stimulus and then presented with a novel "oddball stimulus" (Naatanen et al., 1978). This method requires clean baselines where participants are at rest before the stimulation period for each trial, which does not reflect the continuous tactile exploration that is performed via active touch in the real word. Further, use of this type of paradigm assumes detection of change is an isolated feature, rather than an additive experience. Therefore, alternative methods that better simulate real-world conditions and consider the complexity of change detection in active touch should be explored.

3.2 Thesis chapters

Chapter 4 describes a systematic review and ALE meta-analysis of fMRI studies investigating texture processing (H_1, see section 3.3 below). The systematic review was conducted to identify studies that stimulated the glabrous skin on the hand, through either passive or active stimulation, with textured stimuli. Coordinates were collated from identified studies and subjected to an ALE meta-analysis which identified concordant activations across studies (H_1). Further, secondary analysis contrasted the processing of texture compared to a non-haptic baseline (e.g., rest or visual control) with texture processing compared to a haptic control (e.g., shape or orientation). This analysis aimed to reveal the structures associated with texture-specific processing, i.e., when other haptic processes are accounted for in the baseline or contrast (e.g., shape; H_2).

Chapter 5 examined the effect of natural textures, which varied in textural properties, on cortical oscillations during active touch (H_3). Three natural textures were chosen, smooth silk, soft brushed cotton, and rough hessian. EEG was used to record electrical field potentials from the scalp and the ERD method was used to investigate cortical activation changes during unilateral finger movement across each texture (H_3). Force plate technology was used to quantify active touch, allowing for computation of EEG trigger based on touch behaviour. Covariate analysis was used to assess whether hedonic and sensory estimations accounted for variance in the cortical oscillatory activity.

Chapter 6 investigated the neural underpinning of hedonic, sensory and no estimations during active exploration of natural textures (H_3, H_4). EEG and the ERD method were used to quantify neural oscillations during active exploration of two textures, smooth silk, and rough hessian. Prior to exploration, participants were instructed to either evaluate hedonic or sensory properties or told that they did not have to perform an evaluation (H_4). Sensory and

hedonic ratings were recorded after touch exploration was complete. Objective data from the force plate sensor recorded physical properties of touch, which were implemented as covariates in analysis on a single-trial level to account for individual variance in touch behaviour, thus allowing for the investigating of the invariant effect of texture and estimation on the neural response

Chapter 7 explored the electrophysiological correlates of texture change (H_5). A texture change tile was 3D printed, whereby the middle portion of the tile consisted of a transition between two distinct textures (one rough and one smooth). Force plate technology was used to calculate when the index finger crossed the texture change boundary. Absolute power (*z*-score normalised) was investigated to examine the neural markers of texture change detection in the brain (H_5). Subsequently, data were split into transitioning from rough to smooth and vice-versa to investigate differences in textural roughness whilst transitioning from one texture to the other (H_3).

Chapter 8 discusses the overall results from all experimental studies. In addition to discussing the implications of the findings, and future directions in the field of texture processing.

3.3 Overarching hypotheses

H_1 Texture processing will elicit brain activation in areas associated with tactile processing, including the SI, SII and the insula.

H_2 Texture-specific processing will recruit higher-order integrative structures such as the SII.

H_3 Decreasing textural roughness will be associated with increased alpha- and beta-band ERD in sensorimotor regions during active touch.

H_4 Encoding of hedonic and sensory evaluations of textural properties, relative to no estimation, during active exploration will increase ERD in prefrontal and temporoparietal regions.

H_5 Detection of textural change will manifest as an increase in theta-band power in frontocentral regions.

Chapter 4

The neural correlates of texture perception: A systematic review and activation likelihood estimation meta-analysis of functional magnetic resonance imaging studies

---

Jessica Henderson[1], Tyler Mari[1], Danielle Hewitt[1], Alice Newton-Fenner[1, 2], Timo Giesbrecht[3], Alan Marshall[4], Andrej Stancak[1, 2], Nicholas Fallon[1].

1 School of Psychology, University of Liverpool, Liverpool, UK.

2 Institute of Risk and Uncertainty, University of Liverpool, Liverpool, UK.

3 Unilever, Research and Development, Port Sunlight, UK.

4 Department of Electrical Engineering and Electronics, University of Liverpool, UK.

This experiment used ALE meta-analysis to investigate concordant activation during texture processing.

This paper has been submitted for publication in Brain and Behavior.
The format of the text has been modified to match the style of this thesis.

The roles of the co-authors are summarised below:

Jessica Henderson: Conceptualization, Methodology, Formal analysis, Investigation, Data curation, Writing – original draft, Writing – review & editing, Visualisation, Project administration. **Tyler Mari**: Investigation, Writing – review & editing. **Danielle Hewitt**: Writing – review & editing. **Alice Newton-Fenner**: Writing – review & editing. **Timo Giesbrecht**: Conceptualization, Funding acquisition, Supervision. **Alan Marshall**: Conceptualization, Supervision, Writing – review & editing. **Andrej Stancák**: Conceptualization, Supervision, Writing – review & editing. **Nicholas Fallon**: Conceptualization, Methodology, Writing – review & editing, Supervision, Funding acquisition.

Abstract

Humans use discriminative touch to perceive texture through dynamic interactions with surfaces, activating LTMR in the skin. It was largely assumed that texture was processed in primary somatosensory regions in the brain, however, imaging studies indicate heterogeneous patterns of brain activity associated with texture processing. To address this, we conducted a coordinate-based activation likelihood estimation meta-analysis of thirteen fMRI studies (comprising 15 experiments contributing 228 participants and 275 foci) selected by systematic review. Concordant activations for texture perception occurred in contralateral primary somatosensory and motor regions, with bilateral activations in the secondary somatosensory, insula, premotor and supplementary motor cortices. We also evaluated differences between studies that compared touch processing to non-haptic control (e.g., rest or visual control), or those which used haptic control (e.g., shape or orientation perception) to specifically investigate texture encoding. Studies employing a haptic control revealed concordance for texture processing only in contralateral secondary somatosensory cortex. Contrast analyses demonstrated greater concordance of activations in contralateral primary somatosensory regions and inferior parietal cortex for studies with a non-haptic control, compared to experiments accounting for other haptic aspects. These findings suggest that texture processing may recruit higher-order integrative structures, and the secondary somatosensory cortex may play a key role in encoding textural properties. The present study provides unique insight into the neural correlates of texture-related processing by assessing the influence of non-textural haptic elements and identifies opportunities for future research design to understand the neural processing of texture.

4.1 Introduction

Humans typically explore and gather haptic information using discriminative touch through the glabrous skin on their hands and digits (Gibson, 1962; Lederman & Klatzky, 1993; Wagner & Gibson, 2016). Previous research investigating texture perception and brain activation commonly focus on one textural feature, with roughness the most studied (Hollins et al., 2000). This meta-analysis aimed to collate research articles using fMRI methods to identify regions of the brain associated with texture perception of various stimuli during discriminative touch. For the purpose of this review, texture perception was defined as activation of LTMR and the DCML pathway. Importantly, this excludes thermal perception via thermoreceptors and the spinothalamic tract, which has previously been included as a dimension of texture (Okamoto et al., 2013).

The glabrous skin of the hands contains LTMR, which transduce incoming tactile information from surface texture (Gomez-Ramirez et al., 2016; Harvey et al., 2013; Johnson et al., 2000; McGlone & Reilly, 2010). Tactile information from LTMR travels through the DCML pathway to the brain, and thalamocortical afferents convey signals to the primary (SI) and secondary somatosensory cortex (SII; Klingner et al., 2016; Raju & Tadi, 2021). In humans, texture processing elicits bilateral activation in the SI and SII (Genna et al., 2018; Simões-Franklin et al., 2011). Lesions in the macaque SI and SII lead to impairment of texture perception (Garcha & Ettlinger, 1980; Randolph & Semmes, 1974). Moreover, the SII is hypothesised to be responsible for roughness discrimination (Kitada et al., 2005; Sathian et al., 2011; Servos et al., 2001; Stilla & Sathian, 2008).

Activation of LTMR requires voluntary movement or dynamic passive touch and contact pressure. The MI and non-primary motor regions, split into the SMA and premotor cortex, are responsible for planning and initiating limb movements (Rizzolatti & Kalaska,

2012; Rizzolatti & Luppino, 2001). Therefore, in contrasts employing voluntary movement (i.e., active touch), the MI and premotor areas would be activated due to motor preparation and execution.

Further, somatosensory information is processed in the insula, with the posterior region of the insular cortex found to be functionally connected to sensorimotor areas including the SI, SII, MI and SMA (Deen et al., 2011; Taylor et al., 2009). The insula is conceptualised as an integration hub as it is connected to many brain regions and is associated not only with sensory inputs (Craig et al., 2000; Jensen et al., 2016; Segerdahl et al., 2015) but also with affective processing (Björnsdotter et al., 2009, 2014; Morrison, 2016; Olausson et al., 2016) and higher-level cognition such as decision-making (Gogolla, 2017; Uddin et al., 2017). Therefore, texture perception in the brain likely involves the insula (Kitada et al., 2005; Stilla & Sathian, 2008).

Additionally, the PPC is associated with multisensory integration, combining inputs from several brain areas, including somatosensory, auditory, visual, motor, cingulate and prefrontal cortices (Whitlock, 2017). The PPC has been shown to play an important role in sensory guidance during active touch rather than texture perception specifically (Hyvärinen, 1982; Mountcastle et al., 1975), with increased activation during grasping (Konen et al., 2013; Vingerhoets, 2014), reaching (Blangero et al., 2009; Vesia & Crawford, 2012; Vingerhoets, 2014), and interaction with objects (Bodegård et al., 2001; O'Sullivan et al., 1994; Peltier et al., 2007; Zhang et al., 2004). Thus, texture discrimination through active touch is likely to include activation of PPC to aid in sensory guidance.

The present study performed a coordinate-based meta-analysis with an ALE of published fMRI findings relating to the neural correlates of texture perception (Eickhoff et al., 2009, 2012). Firstly, we aimed to identify key brain regions involved in texture

perception at hand and/or digit skin sites using concordance analysis to identify regions of the brain with the highest activation likelihood. Secondly, we attempted to identify key brain regions involved in texture-specific perception when controlling for other haptic elements involved in discriminative touch (e.g., location, orientation, and shape). For this purpose, we performed conjunction and contrast analyses to compare fMRI studies which contrasted texture perception with a resting or non-haptic control with those which used a haptic baseline to control for these non-texture aspects of discriminative touch.

We hypothesised that areas consistently reported in tactile perception studies would result in activation, which are bilateral SI, SII and insular cortices. Further, we expected areas associated with voluntary movement and motor planning would show activation, including bilateral MI, SMA, premotor cortex, and PPC. When controlling for the influence of haptic processing we anticipated an increased likelihood of activation in medial brain regions associated with higher-order processing or texture-specific processing such as the SII and insular cortex.

4.2 Method

This systematic review is reported following the PRISMA guidelines (Moher et al., 2009). The review protocol was registered on Open Science Framework on the 3rd November 2020.

4.2.1 Data search and extraction

Three electronic databases were examined during February 2023 (PubMed, PsycINFO, and Web of Science) using the Medical Subject Headings (MeSH) search terms (Magnetic resonance imaging OR fMRI) AND (functional OR brain activation OR neural activity OR BOLD) AND (texture OR rough* OR smooth* OR soft*) AND (touch OR tactile OR haptic OR somatosensory). No date limit was set for the searches. A citation search was conducted of the five most recent research papers accepted for analysis.

4.2.2 Article selection and extraction of data

Article selection consisted of two stages and was conducted by the same two authors (J.H. and T.M.). Firstly, the title and abstract for all unique search results were assessed separately by the two authors, studies identified as relevant were retrieved for full-text review. During the second stage, full-text articles, retrieved from stage one, were reviewed independently for inclusion, disagreements were resolved via discussion or presented to a third arbiter (N.F.). One author (J.H.) extracted the relevant coordinate data, which was cross-checked and confirmed by a second (T.M.). Studies that reported coordinates in Talairach space were converted into MNI using GingerALE software for analysis and reporting (Eickhoff et al., 2009, 2012; Turkeltaub et al., 2012). Studies that employed a region of interest (ROI) analysis to investigate the contrast of interest were included in the cohort when whole brain statistical data was available from online repositories, such as NeuroVault (Gorgolewski et al., 2015). In such instances, the unthresholded t-maps resulting from the fMRI analysis

were manually thresholded at $p < .001$ uncorrected voxelwise throughout the whole brain with a $p < .05$ cluster level correction to give whole brain results.

4.2.3 Eligibility criteria

The criteria for inclusion were: (i) fMRI studies; (ii) original English language articles; (iii) published in a peer-reviewed journal; (iv) healthy human participants aged 18+; (v) using a paradigm where the hand and/or fingers are either passively or actively stimulated by textured stimuli, i.e. three-dimensional (3D) printed texture, natural texture, or man-made textures; (vi) coordinates were reported in the paper or supplementary material in either MNI, (Evans et al., 1994) or Talairach space (Talairach & Tournoux, 1988); (vii) studies which analysed either of the two contrasts of interest: (1) texture perception through hand and/or finger stimulation compared to non-haptic control conditions, such as rest, visual control (e.g., visual instructions or rating scales with the absence of textured stimuli) or motor control (e.g., hand motion with the absence of textured stimuli), and (2) texture perception through hand and/or fingers stimulation compared to haptic control conditions, which included shape, location and orientation tasks. See Figure 4.1 for a flowchart showing the study selection steps.

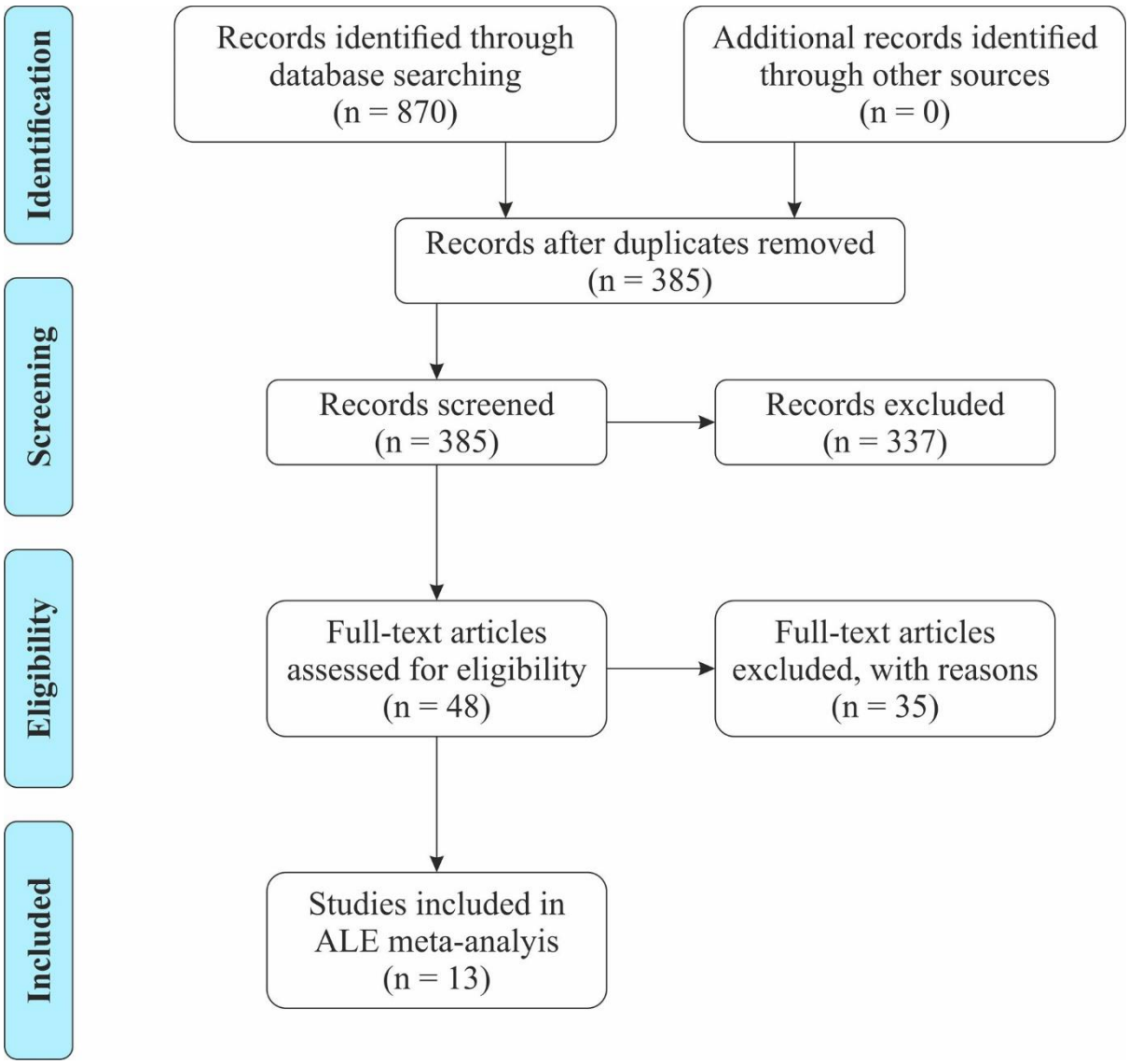

Figure 4.1 Flow chart depicting the screening process.

ALE meta-analyses were performed in BrainMap GingerALE v3.0.2 (Eickhoff et al., 2009, 2012; Turkeltaub et al., 2012). The ALE method computes an ALE value for each voxel in the brain and performs tests to determine the null distribution of the ALE statistic at each voxel, with increased ALE values suggestive of more studies reporting activated peaks in specific loci or at neighbouring voxels using a Gaussian distribution. Next, *p* values computed from the previous step, are used to calculate a thresholded ALE map, and thereafter, cluster analysis is performed on the thresholded map.

For the primary analyses, the comparison of texture perception > control, texture perception> non-haptic control and texture perception > haptic control were evaluated with permutation analyses performed with 5,000 permutations. Firstly, a cluster forming threshold of uncorrected $p < .001$ was applied (Eickhoff et al., 2012), followed by cluster-level Family-wise error (FWE) correction ($p < .05$) as recommended (Eickhoff et al., 2016). For the secondary analyses, the thresholded ALE images from the primary analysis were compared using conjunction and contrast analyses; this was executed by permutation analysis with 10,000 permutations and a cluster-level false discovery rate (FDR) threshold of $p < .05$, with a minimum cluster size of 200 mm^3 as recommended (Eickhoff et al., 2016), and in line with previous research (Morrison, 2016).

4.3 Results

A total of 870 articles were identified from searches (PubMed; 244, PsycInfo; 362, Web of Science; 264; Figure 4.1). Of these, 485 articles were removed due to duplication from repeated searches. An additional 337 articles were removed during the titles and abstracts review stage. Studies excluded at this stage included: those where it was clear and obvious that no suitable population was reported (106), not an experimental report published in a peer-reviewed journal (16), did not use fMRI methods (80), not using suitable textured stimuli (130), and not addressing one of the outcomes outlined (5). Following full-text review, a further 35 articles were removed including those which used an unsuitable contrast (121), did not utilise appropriate textured stimuli (13), did not conduct an fMRI contrast study (5), were not an experimental report journal article (3), only reported ROI analysis and whole brain data was not available (1; see section 4.2.2 above), or which did not report findings in English (1). This resulted in a final cohort of 13 studies for the analyses of texture perception (Table 4.1), with the age range of participants recruited being 18-47 years. The citation search did not lead to the inclusion of any additional studies. Studies contributing to this ALE stimulated the right hand, with Kitada et al. (2006) stimulating both hands and combining results. Therefore, concordant activation in the left and right hemispheres correspond to contralateral and ipsilateral activation, respectively.

Table 4.1. Studies included in ALE meta-analysis.

Author	Year	Title	N	Mean age (SD)	Description of tactile stimuli	Stimulation site	Type of stimulation	Task used in contrast	Included experiments
Gurtubay-Antolin et al.	2018	Neural Evidence of Hierarchical Cognitive Control during Haptic Processing: An fMRI Study	17	23.4 (1.5)	Six real 3D objects and six textures	Right palm/hand	Active	Congruency	Haptic texture > Haptic shape
Kim et al.	2015	Decoding Accuracy in Supplementary Motor Cortex Correlates with Perceptual Sensitivity to Tactile Roughness	13	25.3 (3.8)	Five grades of aluminium oxide sandpaper	Right index fingertip	Active	Perception	Haptic texture (3 µm) > rest Haptic texture (5 µm) > rest Haptic texture (9 µm) > rest Haptic texture (12 µm) > rest Haptic texture (40 µm) > rest
Kitada et al.	2006	Multisensory activation of the intraparietal area when classifying grating orientation: A functional magnetic resonance imaging study	16	22-47* (range)	Nine rectangular gratings with three degrees of roughness	Right and left middle finger	Passive	Estimation	Roughness task > button press Roughness task > tactile orientation[+]

Kitada et al.	2005	Tactile estimation of the roughness of gratings yields a graded response in the human brain: an fMRI study	14	23-26* (range)	Linear gratings with three ridge heights	Right middle fingertip	Passive	Perception	No estimation > Rest
Mueller et al.	2019	Neural correlates of top-down modulation of haptic shape versus roughness perception	21	25.33 (3.44)	3D printed cuboids with five levels of shape and roughness	Right thumb and index finger	Active	Comparison	Roughness > Rest
Podrebarac et al.	2014	Are visual texture-selective areas recruited during haptic texture discrimination?	13	27*	Two 3D shapes with two indented texture patterns	Right hand	Active	Comparison	Haptic texture > haptic shape
Sathian et al.	2011	Dual pathways for haptic and visual perception of spatial and texture information.	18	20.8*	Textiles attached to a piece of cardboard	Right hand	Active	Comparison	Haptic texture > haptic location
Simões-Franklin et al.	2011	Active and passive touch differentially activate somatosensory cortex in texture perception	16	23.6*	Three grades of aluminium oxide sandpaper	Right middle finger	Active & passive	Estimation	Active & passive > control

Stilla & Sathian.	2008	Selective visuo-haptic processing of shape and texture.	6	22*	3D meaningless objects. Textiles attached to a piece of cardboard	Right hand	Active	Comparison	Haptic texture > haptic shape
Tang et al.	2022	Brain activation related to the tactile perception of touching ridged texture using fingers.	10	22 (2.3)	Ridged textures with different edge shapes	Right index finger	Passive	Perception	Sharp shape > rest Rounded shape > rest Flat shape > rest
Wang et al.	2016	Brain discriminative cognition on the perception of touching different fabric using fingers actively	8	28.6*	Silk and linen swatches	Right thumb and index finger	Active	Estimation	Linen > rest Silk > rest
Yang et al.	2021	Different activation signatures in the primary sensorimotor and higher-level regions for haptic three-dimensional curved surface exploration	20	22 (0.63)	3D printed surfaces with four levels of raised dot patterns and four types of curvature, plus one flat surface.	Right index and middle finger	Active	Estimation	Roughness estimation > hand motion and visual control (Roughness estimation - hand motion and visual control) > (curve estimation - hand motion and visual control)$^{+}$
Yang et al.	2017	Brain networks involved in tactile speed classification of	20	21.9 (2.6)	Two surfaces with identical or pseudo-randomly	Right middle fingertip	Passive	Estimation	Speed classification periodic > visual

	moving dot patterns: the effects of speed and dot periodicity	distributed dot patterns		motor control periodic Speed classification non-periodic > visual motor control non-periodic

**Did not report standard deviation (SD); Estimation = Participants estimated textural properties, e.g., roughness; Comparison = Presented participants with two stimuli in succession, participants had to indicate if the stimuli were identical or different; Congruency = Judge whether a touched stimulus corresponded to an expected stimulus which had been presented before stimulus exploration; Perception = Exploration of the textured stimuli with a rest period between trials. [+]Not combined as a single experiment because they contribute to different analyses (i.e., texture perception > non-haptic control or texture perception > haptic control).*

4.3.1 Primary analyses

4.3.1.1 Texture perception > control

Texture perception > control contrast ALE meta-analysis pooled data from 13 studies which contributed 15 experiments, with a total of 228 participants and 275 reported foci. The results revealed seven significant clusters (Table 4.2). One cluster originated in the right hemisphere and spanned from the superior temporal gyrus to the postcentral gyrus, corresponding to both the right PI and SII. One cluster was identified in the left hemisphere from the supramarginal gyrus (SMG) in the IPL to the SI. Further clusters were identified in the bilateral SMA with one peak in the right SMA, two clusters encompassed the bilateral PI, and two clusters encompassed the bilateral PMv. Significant ALE cluster locations are illustrated in Figure 4.2.

Table 4.2. Locations of significant clusters from the ALE map of texture perception > control.

Cluster #	Label	Volume (mm^3)	*x*	*y*	*z*	#Experiments	ALE
1	Insula R	1752	58	-20	20	7	0.021
	Postcentral Gyrus R		64	-16	22		0.021
2	Postcentral Gyrus L	1600	-54	-20	48	8	0.023
3	Precentral Gyrus L	1424	-48	6	24	7	0.019
	Precentral Gyrus L		-58	8	28		0.014
	Precentral Gyrus L		-58	2	32		0.012
4	Insula L	1224	-36	-6	10	6	0.022
	Insula L		-42	-4	2		0.014
5	Inferior Frontal Gyrus R	984	50	8	24	4	0.025
6	Insula R	816	40	-8	8	4	0.020
7	Superior Frontal Gyrus R	816	4	16	48	4	0.018

L, left hemisphere; R, right hemisphere.

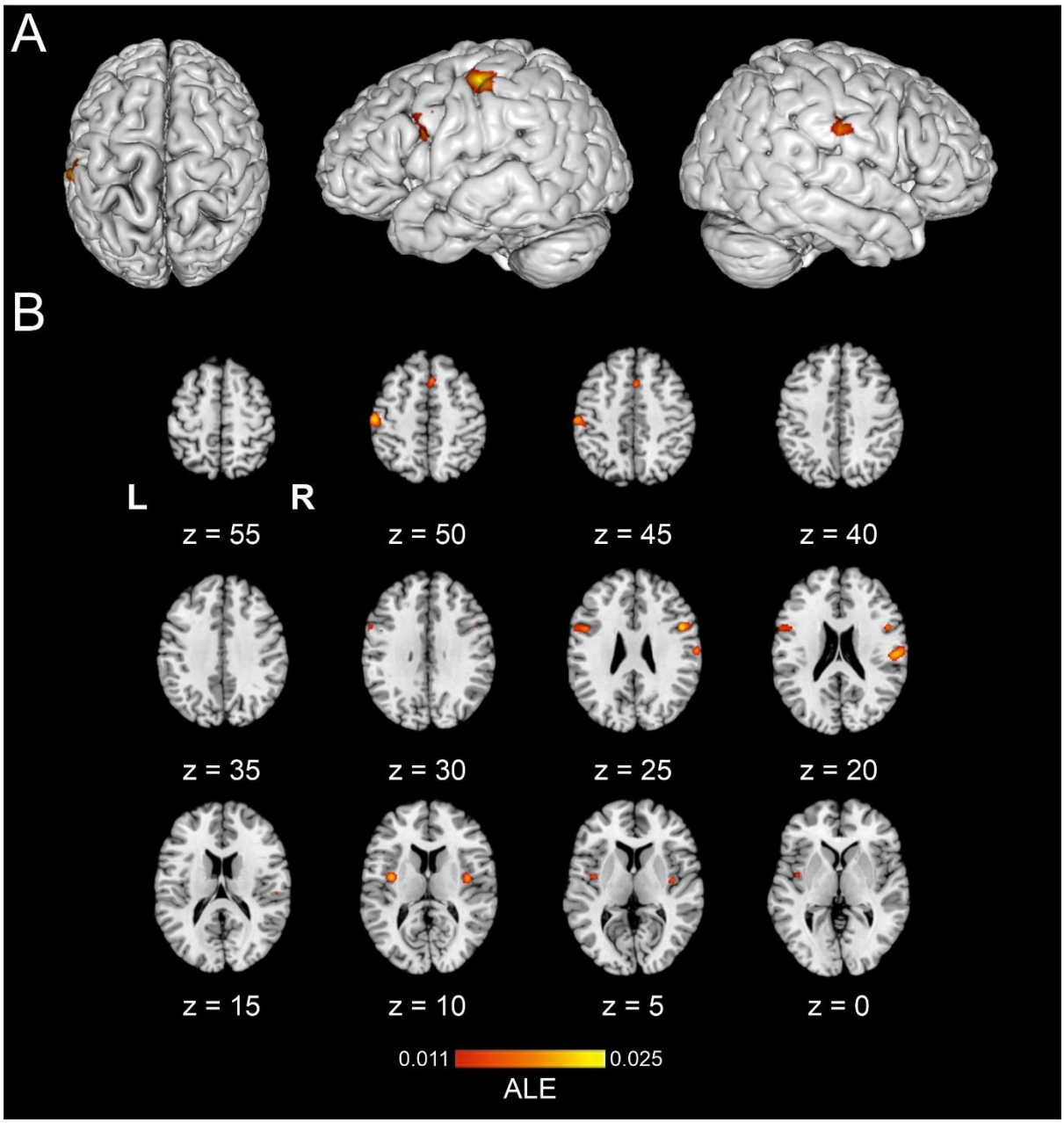

*Figure 4.2 The location of significant ALE clusters from the meta-analysis of concordant activations for texture perception > control. Results are displayed overlaid onto a standardized MNI template anatomical brain in **(A)**. 3D surface projection from superior, left, and right views, respectively. **(B)** As a montage of coronal slices throughout the whole brain, L and R denotes the left and right hemisphere, respectively. ALE scores are indicated by the colour bar.*

4.3.1.2 Texture perception > non-haptic control

The texture perception > non-haptic control (e.g., rest or visual control) contrast ALE meta-analysis pooled data from nine studies which contributed 9 experiments, with a total of 138 participants and 240 reported foci. The results revealed six significant clusters (Table 4.3); one cluster spanned from the right superior temporal gyrus to the postcentral gyrus, consistent with both PI and SII. Cluster two, in the left hemisphere, spanned from the SMG in the IPL to the SI. Cluster six corresponded to the left SI and MI. Further clusters encompassed the bilateral SMA and the bilateral PMv. Significant ALE cluster locations are illustrated in Figure 4.3.

Table 4.3. Locations of significant clusters from the ALE map of texture perception > non-haptic control.

Cluster #	Label	Volume (mm^3)	*x*	*y*	*z*	#Experiments	ALE
1	Insula R	1864	58	-20	20	7	0.021
	Postcentral Gyrus R		64	-16	22		0.021
2	Postcentral Gyrus L	1832	-54	-20	48	8	0.023
3	Inferior Frontal Gyrus L	1336	-58	6	22	5	0.016
	Precentral Gyrus L		-58	8	28		0.014
	Precentral Gyrus L		-58	6	14		0.013
	Precentral Gyrus L		-58	2	32		0.012
4	Inferior Frontal Gyrus R	1120	50	8	24	4	0.025
5	Superior Frontal Gyrus R	944	4	16	48	4	0.018
6	Postcentral Gyrus L	752	-44	-12	58		0.016
	Precentral Gyrus L		-38	-20	52	4	0.013

L, left hemisphere; R, right hemisphere.

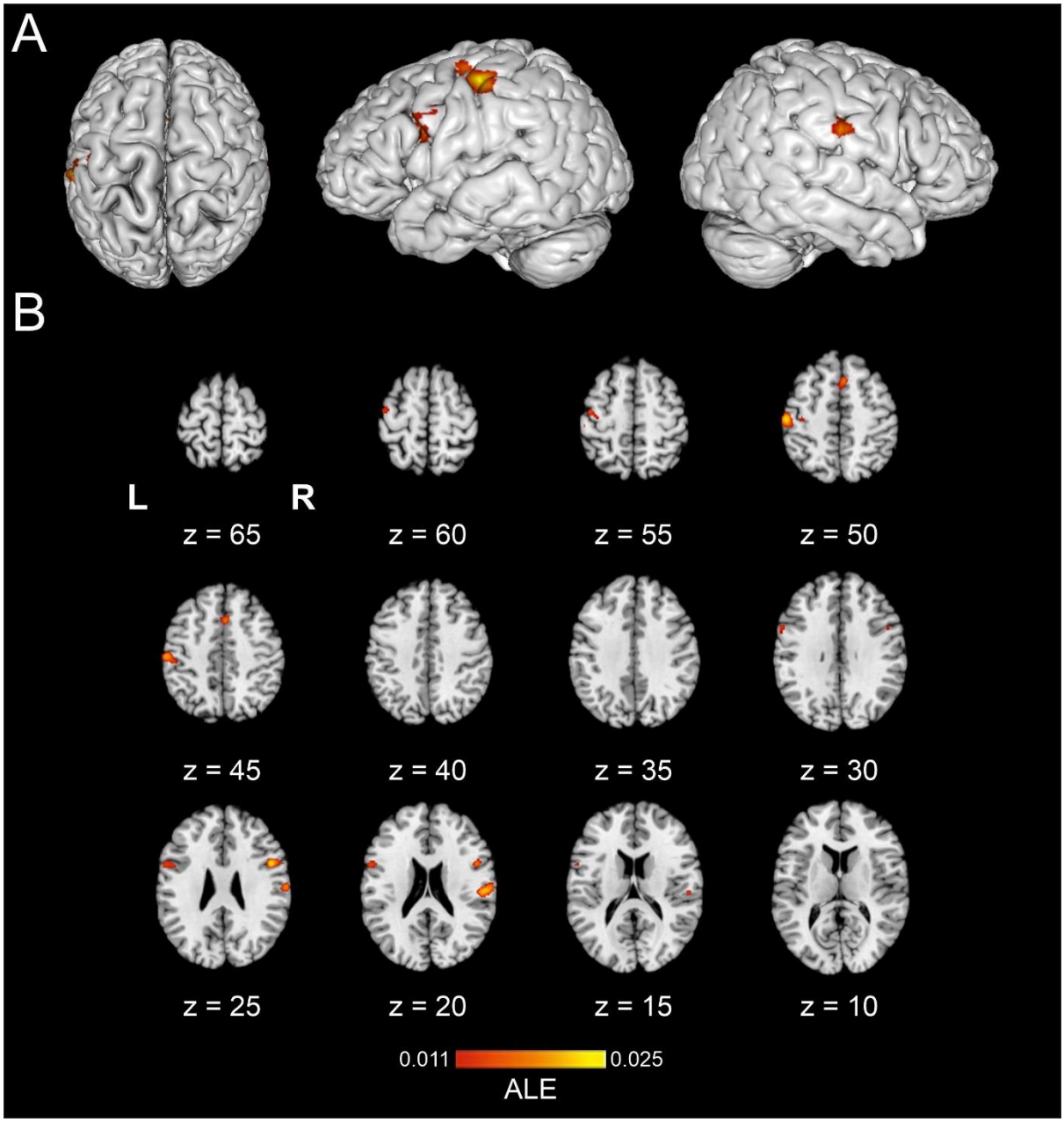

*Figure 4.3 The location of significant ALE clusters from the meta-analysis of concordant activations for texture perception > non-haptic control. Results are displayed overlaid onto a standardized MNI template anatomical brain in **(A)**. 3D surface projection from superior, left, and right view, respectively. **(B)** As a montage of coronal slices throughout the whole brain, L and R denotes the left and right hemisphere, respectively. ALE scores are indicated by the colour bar.*

4.3.1.3 Texture perception > haptic control

The texture > haptic control contrast ALE meta-analysis pooled data from a total of six studies which contributed six experiments, with 90 participants and 35 reported foci. Findings demonstrated one significant left hemisphere clusters located in the SII (Table 4.4). Figure 4.4 illustrates the location of significant ALE clusters from the meta-analysis of texture perception when controlling for other haptic processes.

Table 4.4. Locations of significant clusters from the ALE map of texture perception > haptic control.

Cluster#	Label	Volume (mm^3)	*x*	*y*	*z*	#Experiments (#Studies)	ALE
1	Postcentral Gyrus L	608	-54	-14	22	2 (2)	0.010
	Postcentral Gyrus L		-50	-10	16		0.009

L, left hemisphere.

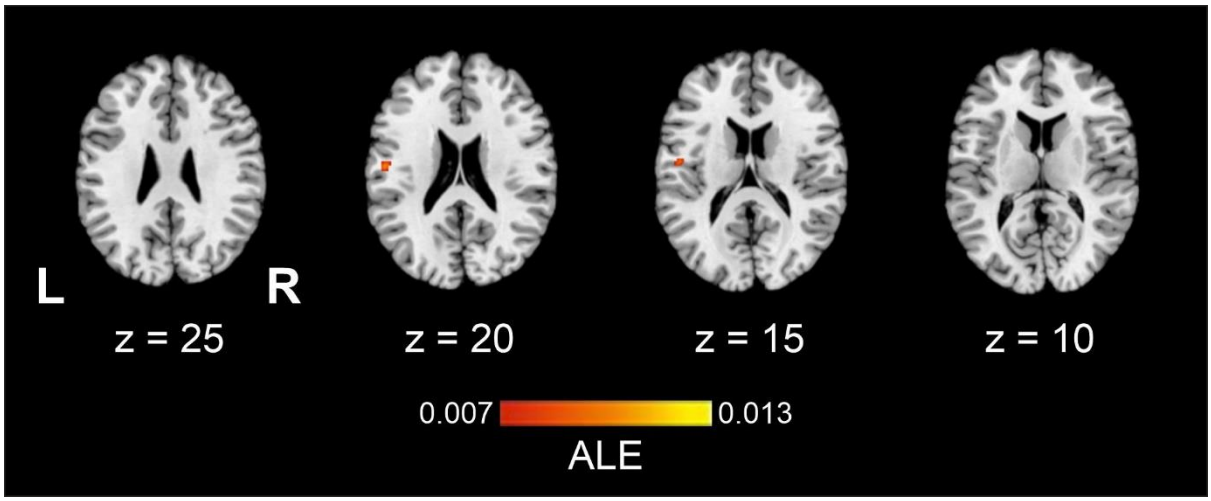

Figure 4.4 The location of significant ALE clusters from the meta-analysis of concordant activations for texture perception > haptic control. Results are displayed overlaid onto a standardized MNI template anatomical brain as a montage of coronal slices throughout the whole brain, L and R denotes the left and right hemisphere, respectively. ALE scores are indicated by the colour bar.

4.3.2 Secondary analyses

4.3.2.1 Conjunction analysis

The conjunction analysis of ALE maps representing texture perception relative to non-haptic control and texture-specific perception (relative to haptic control) pooled data from a total of 23 experiments, with a total of 245 participants and 273 reported foci. There were no findings of overlap of activation likelihood coordinates across both contrast types.

4.3.2.2 Contrast analyses

Contrast analysis comparing the ALE maps of concordant activations for each process pointed to a significantly greater likelihood of activation during general texture perception (texture perception > non-haptic control) relative to texture-specific perception (texture perception > haptic control) in three clusters (Figure 4.5, Table 4.5). Two contralateral clusters included the SI and the SMG in the IPL, as well as the SI, MI, and premotor areas. The third cluster was located in the ipsilateral IPL and corresponded to the SMG. The reverse contrast did not reveal any clusters indicative of increased activation likelihood estimates during texture-specific perception relative to general texture perception studies.

Table 4.5. Locations of significant clusters from contrast analysis of non-haptic - haptic control.

Cluster #	Label	Volume (mm^3)	*x*	*y*	*z*	#Experiments	Extrema (Z)
1	Inferior Parietal Lobule L	1832	-53.3	-22.3	48.2	8	3.156
	Postcentral Gyrus L		-41.2	-12.3	55.2	4	3.719
2	Postcentral Gyrus L	640	-40.9	-18.7	54.5		3.156
3	Inferior Parietal Lobule R	232	55.4	-24.6	19.8	1	3.036

L, left hemisphere; R, right hemisphere.

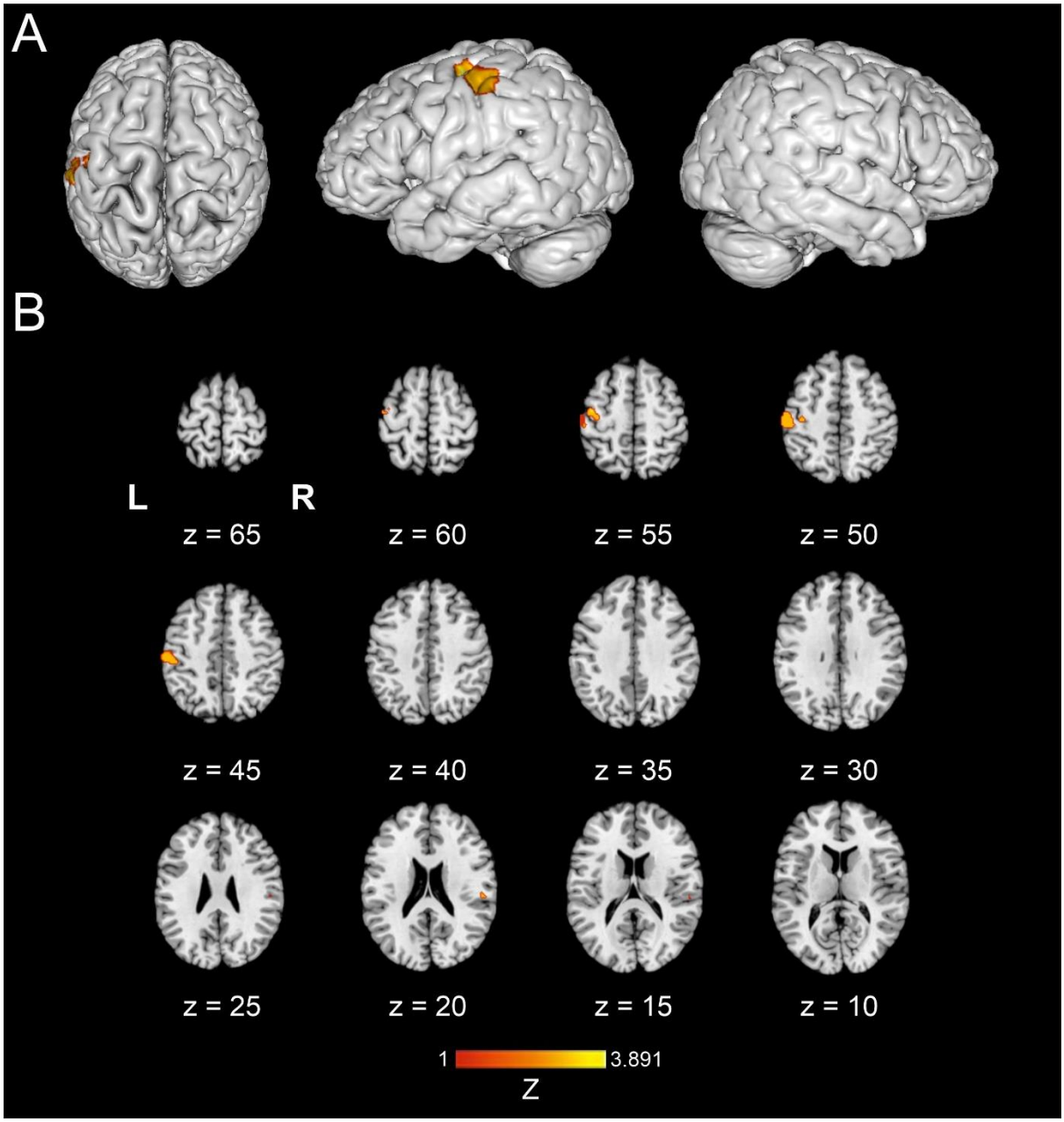

Figure 4.5 The location of significant clusters from contrast analysis of ALE maps for greater likelihood of texture perception > non-haptic control relative to texture perception > haptic control. All clusters are overlaid onto a standardized MNI template anatomical brain in ***(A)****. 3D surface projection from superior, left, and right views, respectively.* ***(B)*** *As a montage of coronal slices throughout the whole brain, L and R denotes the left and right hemisphere, respectively. Relative Z scores are indicated by the colour bar.*

4.3.3 Sensitivity analysis

To assess the stability of results, thirteen leave-one-out analyses (also known as jack-knife analyses) were conducted, whereby the primary analysis of texture perception > control was rerun, each time excluding a different single study (Supplementary material 1; Radua et al., 2012; Radua & Mataix-Cols, 2009). The sensitivity analysis confirmed the stability of the right SII cluster and left SI/IPL across all thirteen studies. Leaving out Yang et al. (2017) resulted in the left PMv and left PI clusters no longer reaching significance. The SMA cluster was not identified when leaving out Mueller et al. (2019), Yang et al. (2017), Simões-Franklin et al. (2011), and Kitada et al. (2006). In addition, leaving out Kitada et al. (2006) and Mueller et al. (2019) resulted in the loss of the right PMv cluster. The right PI cluster was not identified as significant when leaving out Kitada et al. (2006), Mueller et al. (2019), Sathian et al. (2011) and Stilla and Sathian (2008). Further, an additional cluster in the right PI/SII was identified when removing Simões-Franklin et al. (2011), Yang et al. (2021), Wang et al. (2016), Mueller et al. (2019), and Kim et al. (2015). Removing Kitada et al. (2005) and Yang et al. (2021) led to the identification of a further cluster in the left dorsolateral prefrontal cortex (DLPFC). Finally, a cluster from the left SI to the left MI was uncovered when removing Kitada et al. (2005), Sathian et al. (2011), Simões-Franklin et al. (2011), and Yang et al. (2017, 2021).

4.4 Discussion

Findings from the primary ALE meta-analysis of texture perception relative to control revealed nine significant clusters with activation in contralateral SI and SMG, bilateral PMv and SMA, and ipsilateral SII and PI, consistent with our hypotheses that texture perception would activate the sensorimotor regions that are well-associated with tactile perception and movement planning and execution. The presence of haptic control conditions during texture perception identified activation in contralateral SII, in line with our hypothesis that texture processing activates brain regions associated with higher-order processing. Further, contrast analyses revealed sensorimotor (SI, MI, and SMG) activations as more predominant in the non-haptic control contrast than when controlling for other haptic processing, suggesting that texture-specific processing may require the activation of higher-order cortical regions.

Contralateral SII was the only region selectively activated by contrasting texture processing with a haptic control, indicating its role in texture-specific processing. The SII has previously been implicated in higher-order processing such as: attention (Chen et al., 2008; Hämäläinen et al., 2000), learning (Mishkin, 1979; Ridley & Ettlinger, 1976), and roughness discrimination (Kitada et al., 2005; Sathian et al., 2011; Servos et al., 2001; Stilla & Sathian, 2008). Research with non-human primates show that lesions to the SII result in deficits in texture and shape discrimination (Garcha & Ettlinger, 1980; Murray & Mishkin, 1984), and humans with lesions in the area suffer from tactile apraxia (Binkofski et al., 2001). Further, single cell recordings from macaques demonstrated texture encoding in the SII (Jiang et al., 1997; Pruett et al., 2000; Sinclair & Burton, 1993). Taken together with the results from this meta-analysis, it is likely that the SII plays a significant role in the higher-order encoding of textural properties.

Conjunction and contrast analyses were computed to examine similarities and differences between the processing of generic discriminative touch, by comparing texture processing to non-haptic control conditions, relative to brain regions that are more selectively activated during texture processing/evaluations, which were determined by comparing texture processing to haptic control conditions. Concordant activation in the contralateral SI and bilateral SMG was more likely to be activated during texture perception compared to non-haptic control contrast, relative to touch minus haptic control contrast tasks which accounted for other aspects of discrimination (e.g., shape). Interestingly, the conjunction analysis did not identify any overlap of findings across studies with these differing approaches. Demonstrating that concordant activation of the SII cluster in the texture relative to haptic control ALE analysis may be specific to texture processing. These findings indicate that broad aspects of tactile information are processed in the sensorimotor areas, hence the dominance in contrasts which do not correct for this in the baseline. However, the absence of deeper SII or PI clusters indicates that important aspects of texture-specific processing may occur in higher-order medial regions such as the SII and insular cortex (Eck et al., 2016; Jiang et al., 1997; Roland et al., 1998), which may require careful consideration of experimental design, and particularly baseline, to investigate. This aligns with the presence of an SII cluster in the texture relative to haptic control ALE analysis.

Bilateral PI was found to be active when investigating texture processing compared to control (i.e., non-haptic and haptic control conditions combined). The insular cortex has been linked with somatosensation (Kurth et al., 2010), and has been associated with intensity processing of thermosensory (Craig et al., 2000) and noxious stimuli (Frot et al., 2007; Iannetti et al., 2005). Roughness-related activation has been reported in the parietal operculum and insula (Kitada et al., 2005). Therefore, the insula may play a role in processing or evaluation of texture intensity. Ten studies contributing to the present meta-

analysis asked participants to complete an estimation or comparison task where participants would evaluate textural features with a response (Gurtubay-Antolin et al., 2018; Kitada et al., 2006; Mueller et al., 2019; Podrebarac et al., 2014; Sathian et al., 2011; Simões-Franklin et al., 2011; Stilla & Sathian, 2008; Wang et al., 2016; Yang et al., 2017, 2021). As an integrative region associated with both sensory input (Craig et al., 2000; Jensen et al., 2016; Segerdahl et al., 2015) and decision-making (Gogolla, 2017; Uddin et al., 2017), insula activation may reflect the integration of sensory input which may be crucial for higher-order cognitive decisions based on sensory features.

SI and SMG were found to be active when comparing texture processing to both control and non-haptic control conditions, while the MI demonstrated concordant activation only when comparing to the non-haptic control condition. The SI is responsible for tactile processing (Case et al., 2016; Chapman, 1994; Lieber & Bensmaia, 2019, 2020; Lin et al., 1996). Active touch engages sensorimotor circuits in the PPC, including the SMG located in the IPL, activation in these regions has been associated with sensorimotor integration (Batista et al., 1999; Battaglia-Mayer et al., 2000; Buneo et al., 2002; Buneo & Andersen, 2006; Ferraina et al., 1997; Hyvärinen, 1982; Mountcastle et al., 1975; Snyder et al., 1997). MI activation is associated with execution of voluntary movement (Kalaska & Rizzolatti, 2012); an exploratory analysis of experiments employing active touch found concordant activation in premotor and motor areas, whilst passive touch did not (Supplementary material 2). Although, two studies contributing to the concordant activation identified in the SI/SMG/MI cluster employed dynamic passive touch (Kitada et al., 2005; Tang et al., 2021a); therefore, concordance of MI activation may also be due to force exerted by the finger during passive paradigms rather than solely due to active touch (Dettmers et al., 1995).

Concordant activation was identified in both the bilateral PMv and SMA across two ALE analyses, one that considered all studies irrespective of control condition, and the other that only considered baselines that did not account for other haptic elements (i.e., non-haptic control). The PMv is predominantly linked with grasping and object manipulation hand movements (Davare et al., 2006, 2008, 2009; Fogassi et al., 2001; Reader & Holmes, 2018; Vingerhoets et al., 2013), and evaluating sensory information to inform motor action (Romo et al., 2004). Five studies that contributed to the bilateral PMv clusters involved active touch (Mueller et al., 2019; Sathian et al., 2011; Simões-Franklin et al., 2011; Wang et al., 2016; Yang et al., 2021). Accordingly, SMA neurons discharge before and during coordinated voluntary movement (Tanji, 2001; Tanji and Shima, 1996), such as button pressing. Therefore, PMv and SMA activation may reflect evaluation of sensory information to inform response behaviour during experimental paradigms.

The current meta-analysis is impacted by the limited number of studies in the area. This can partly be attributed to the absence of a standardised paradigm, with 130 studies rejected due to stimuli/paradigm discrepancies. Therefore, the field would benefit from a standardised texture perception paradigm. Further, there is a vast range of tactile stimuli used when investigating texture perception, including gratings (Kitada et al., 2005, 2006), 3D printed textures (Mueller et al., 2019; Yang et al., 2021), dot patterns (Yang et al., 2021, 2017), and textiles (Gurtubay-Antolin et al., 2018; Wang et al., 2016). These types of stimuli differ greatly in their tactile properties, with textiles often finer-grained and therefore more likely to rely on vibrational cues generated through movement rather than coarse textures, such as gratings, which rely on distinct spatial patterns (Moungou et al., 2016; Weber et al., 2013). Consequently, findings are difficult to collate to investigate texture-specific processing. In the future, a standardised battery of textural stimuli would aid researchers to align and compare findings across studies, laboratories, and geographical regions.

Further, studies identified by systematic review are limited by modest participant numbers. The recommended sample size for investigating sensorimotor effects with 3T scanners is a minimum of 20, and preferably 27, participants (Thirion et al., 2007). The average number of participants recruited in the studies contributing to this meta-analysis was 15 ± 4.63 (M ± SD) with only three studies (Mueller et al., 2019; Yang et al., 2017, 2021) recruiting 20 participants or more. Therefore, contributing foci are potentially under powered. However, a leave-one-out analysis was conducted assess the sensitivity of results (Supplementary material 1; Acar et al., 2018), which demonstrated that clusters in the right SII and left SI/IPL were stable across all thirteen studies. During leave-one-out analyses, additional clusters were identified in the left SII, and left DLPFC and SI/MI, which may indicate that bilateral SII and higher-order prefrontal regions are important for texture processing. However, identification of concordant activation in these areas may be dependent upon task design and/or stimuli utilised, hence the sensitivity to leave-one-out procedures. Thus, highlighting the importance of a standardised procedure in the field of texture processing.

To conclude, findings revealed expected concordance in sensorimotor areas including higher-order structures associated with top-down mechanisms. Analysis of studies which included a haptic baseline to control for non-textual processing revealed concordance solely in contralateral SII. Furthermore, contrast analysis demonstrated that lateral SI and IPL are significantly more predominant when utilising a resting baseline, than in studies where textural aspects of discriminative touch are accounted for in the baseline. These findings point towards preferential processing of texture in higher-order structures, particularly the SII. Further research should carefully consider research design, and particularly the use of appropriate baseline contrasts to uncover the role of higher-order structures in texture processing. Overall, the present study has furthered our understanding of texture perception,

specifically when accounting for the influence of other haptic processes which offer unique insight into the neural correlates of texture-related processing.

Chapter 5

Neural correlates of texture perception during active touch

Jessica Henderson[1], Tyler Mari[1], Andrew Hopkinson[1, 2], Adam Byrne[1, 3], Danielle Hewitt[1], Alice Newton-Fenner[1, 3], Timo Giesbrecht[4], Alan Marshall[5], Andrej Stancák[1, 3], Nicholas Fallon[1].

1 School of Psychology, University of Liverpool, Liverpool, UK.

2 Hopkinson Research, Wirral, UK

3 Institute of Risk and Uncertainty, University of Liverpool, Liverpool, UK.

4 Unilever, Research and Development, Port Sunlight, UK.

5 Department of Electrical Engineering and Electronics, University of Liverpool, UK.

This experiment used touch sensor technology to investigate the neural correlates of active exploration of textured stimuli.

This paper was published in Behavioural Brain Research (2022)
doi: doi.org/10.1016/j.bbr.2022.113908
The format of the text has been modified to match the style of this thesis.

The roles of the co-authors are summarised below:
Jessica Henderson: Conceptualization, Methodology, Software, Formal analysis, Investigation, Data curation, Writing – original draft, Writing – review & editing, Visualisation, Project administration. **Tyler Mari**: Software, Formal analysis, Writing – review & editing. **Andrew Hopkinson**: Methodology, Software, Formal analysis, Writing – review & editing. **Adam Byrne**: Investigation, Writing – review & editing. **Danielle Hewitt**: Investigation, Writing – review & editing. **Alice Newton-Fenner**: Investigation, Writing – review & editing. **Timo Giesbrecht**: Conceptualization, Funding acquisition, Supervision. **Alan Marshall**: Conceptualization, Supervision, Writing – review & editing. **Andrej Stancák**: Conceptualization, Supervision, Writing – review & editing. **Nicholas Fallon**: Conceptualization, Methodology, Software, Formal analysis, Writing – review & editing, Supervision, Funding acquisition.

Abstract

Previous studies have shown attenuation of cortical oscillations over bilateral sensorimotor cortex areas during passive perception of smooth textures applied to the skin. However, humans typically explore surfaces using dynamic hand movements. As movements may both modulate texture-related cortical activity and induce movement-related cortical activation, data from passive texture perception cannot be extrapolated to active texture perception. In the present study, we used EEG to investigate cortical oscillatory changes during texture perception throughout active touch exploration. Three natural textured stimuli were selected: smooth silk, soft brushed cotton, and rough hessian. Texture samples were mounted on a purpose-built touch sensor which measured the load and position of the index finger, whilst EEG from 129 channels recorded oscillatory brain activity. The data were fused to investigate oscillatory changes relating to active touch. Changes in oscillatory band power (ERD/ERS) were investigated in alpha (8–12 Hz) and beta (16–24 Hz) frequency bands. Active texture exploration revealed bilateral activation patterns over sensorimotor cortical areas. Beta-band ERD increased over contralateral sensorimotor regions for soft and smooth textures, and over ipsilateral sensorimotor areas for the smoothest texture. Analysis of covariance revealed that individual differences in perception of softness and smoothness were related to variations in cortical oscillatory activity. Differences may be due to increased high frequency vibrations for smooth and soft textures compared to rough. For the first time, active touch was quantified and fused with EEG data streams, contributing to the understanding of the neural correlates of texture perception during active touch.

5.1 Introduction

Haptic perception enables humans to explore their environment (Lederman & Klatzky, 2009). There are two types of stimulation used in haptic perception research: passive and active touch (Chapman, 1994; Lederman, 1981). Passive touch involves the application of stimuli to the skin, typically using robotic presentation devices such as a tactile spinning wheel (Aviles et al., 2010; Essick et al., 2010; McGlone et al., 2012; Weber et al., 2013), which control the timing and properties of the stimulation. Conversely, active touch requires voluntary movement to optimise contact pressure, speed, and velocity during haptic exploration, thus being more representative of how humans interact with surfaces during real-world exploration (Gibson, 1962; Wagner & Gibson, 2016). Current literature investigating the neural correlates of texture perception predominantly relies on passive stimulation devices (Ballesteros et al., 2009; Eldeeb et al., 2019; Genna et al., 2018; Moungou et al., 2016; Tang et al., 2020), therefore, the neural correlates of active touch have yet to be elucidated.

LTMR of the glabrous skin contribute to texture perception (Lederman et al., 1982; McGlone & Reilly, 2010). Merkel cells respond to pressure, Meissner corpuscles process low-frequency vibrations, and Pacinian corpuscles respond to high-frequency vibrations (Gomez-Ramirez et al., 2016; Harvey et al., 2013; Johnson et al., 2000). The duplex theory of tactile texture perception (Katz, 1925) proposes that high-frequency vibrational cues encode tactile stimulation from fine textures, whereas spatial cues encode tactile stimulation from coarse textures via pressure (Blake et al., 1997; Hollins et al., 2001a; Hollins & Risner, 2000; Johnson & Hsiao, 1992; Yoshioka et al., 2001). The cerebral cortex appears to process low (5-50 Hz) and high-frequency stimuli (50-400 Hz) differently (Han et al., 2013). Low-frequency stimuli increase activation in the contralateral SI and bilateral SII, while high-frequency stimuli increase activation in the bilateral SII (Chung et al., 2013; Francis et al.,

2000; Harrington & Hunter Downs, 2001). Therefore, the perception of coarse and fine textures likely involve different neural mechanisms.

Roughness perception has been investigated in previous studies examining neural correlates of touch (Lederman & Klatzky, 2009). Coarse artificial stimuli such as gratings, (Ballesteros et al., 2009; Tang et al., 2020), three-dimensional (3D) printed textures (Eldeeb et al., 2019) and Braille dot patterns (Bauer et al., 2006) are often used to investigate the perception of roughness. Natural textures, such as silk and cotton, differ from coarse artificial textures as they are often finer grained and therefore more likely to rely on vibrational cues generated through movement (Moungou et al., 2016; Weber et al., 2013). Although natural textures typically lack large and pronounced spatial patterns, one can still perceive them as rough and unpleasant (Klöcker et al., 2012; Moungou et al., 2016).

Event-related amplitude decreases and increases of band power, known as ERD and ERS respectively, are known to vary with task-related changes (Pfurtscheller, 1977; Pfurtscheller & Aranibar, 1977). Voluntary movement and somatosensory stimulation are associated with ERD in alpha and beta frequency bands over primary motor and somatosensory cortices (Chatrian et al., 1958; Cheyne et al., 2003; Gaetz & Cheyne, 2006; Neuper & Pfurtscheller, 2001; Pfurtscheller, 1981, 2001; Stancak et al., 2003; Stancak & Pfurtscheller, 1996b, 1997), followed by beta-band ERS in the motor cortex after termination of stimulation (Cheyne et al., 2003; Gaetz & Cheyne, 2006; Houdayer et al., 2006). Alpha- and beta-band ERD are interpreted as increased cortical activation (Pfurtscheller & Aranibar, 1977; Pfurtscheller & Lopes da Silva, 1999); in contrast, ERS indicates cortical inhibition or idling (Berger, 1929; Legewie et al., 1969; Pfurtscheller et al., 1996b). Increased alpha-band ERS over occipito-parietal areas is found during self-paced voluntary hand movement and is thought to be the result of diverting attention from the visual system to the motor system,

increasing ERD in motor areas which supports hand/finger movement (Pfurtscheller et al., 2000). Investigation of texture perception has revealed bilateral alpha- and beta-band ERD during passive stimulation, with greater alpha-band ERD and increased magnitude of SS-EP with decreased stimulus roughness (Genna et al., 2018; Moungou et al., 2016). Further, ERD/S during voluntary movements are related to movement parameters such as force (Stancak et al., 1997) and speed (Stancak & Pfurtscheller, 1996a, 1996b). Therefore, the ERD/S method proposed by Pfurtscheller and Aranibar (1979) is likely to show differences during active touch exploration of different textures which may be due to textural and active movement differences.

Voluntary movement is associated with a reduction in tactile perception, known as tactile suppression or movement-related gating (Chapman et al., 1987; Post et al., 1994), as evidenced by reductions of short-latency SEP (Nakata et al., 2003, 2011; Rossini et al., 1996, 1999). However, movements made to gain information about surface properties enhance tactile perception (Juravle et al., 2017), with greater amplitudes of long-latency SEP (Juravle et al., 2016b; Lee & White, 1974; Nakata et al., 2003, 2011; Popovich & Staines, 2015). This suggests that tactile suppression is context dependent, with active tactile exploration playing a significant role in providing information about textural properties. Thus, while the evidence suggests that active touch is likely to enhance, rather than supress, tactile perception, this remains to be fully elucidated.

The current study investigated cortical oscillatory changes associated with texture perception during active exploration of natural textures. Active touch was quantified using novel touch sensor technology, enabling precise measurement of load and position of the index finger, thus allowing for computation of behavioural active touch timings. Fusion of computed active touch timings and EEG data streams allowed accurate investigation of

electrophysiological changes during active touch. Cortical oscillatory changes were investigated in alpha- and beta-bands during active touch exploration of three textures which varied in textural properties: smooth silk, soft brushed cotton, and rough hessian. We hypothesised that active touch exploration would elicit bilateral alpha- and beta-band ERD over the sensorimotor cortex. Based on evidence from passive touch studies (Genna et al., 2018), we predicted greater alpha-band ERD for smooth compared to rough textures. Furthermore, we hypothesised differences in cortical oscillatory activity for each texture would relate to individual differences in subjective perceptions of textural properties.

5.2 Method

5.2.1 Participants

Thirty-five participants were recruited (12 males) with no history of any neurological condition, or aversion or allergies to any textures. Nine participants were excluded due to excessive muscle artefacts or incomplete data recording from the touch sensor. The final sample for EEG analysis included 26 participants (7 males, 4 left-handed), aged 28.03 ± 11.06. Participants were reimbursed at a rate of £10 per hour for their time. The study was approved by the Research Ethics Committee of the University of Liverpool and all participants gave fully informed written consent at the start of the experiment in accordance with the Declaration of Helsinki.

5.2.2 Procedure

Participants were seated in a Faraday cage in front of a 19-inch LCD monitor. The study was carried out in a single 2-hour session. Participants were required to complete four tasks: initial subjective ratings of texture samples, pace training, an active touch task, and final subjective ratings. All tasks were presented using PsychoPy (Peirce et al., 2019). EEG and touch sensor data were recorded during the active touch task (see section 5.2.2.4 below). Elbow and wrist rests were used to stabilise and support the arm and wrist whilst maintaining position over the touch sensor. The height and position of the support were adjusted for each participant, minimising non-essential motor movements whilst allowing for active touch exploration using lateral finger movements. Texture exploration was performed using the glabrous skin of the distal phalanx of the index finger.

5.2.2.1 Stimuli

The stimuli included three textures selected from a preliminary pilot study: silk, brushed cotton, and hessian, Figure 5.1. The stimuli selected were natural textures that encompassed three tactile properties: pleasant/unpleasant, smooth/rough, and soft/hard. Texture samples were cut into 100 mm by 40 mm strips and mounted with double-sided tape to plastic stages lined with easily removable PVC electrical insulation tape. Plastic stages were slotted into the sample chassis of the touch sensor (Figure 5.2). The texture samples were replaced for each participant. The stages were removably attached to the touch sensor instrument for presentation to the participants.

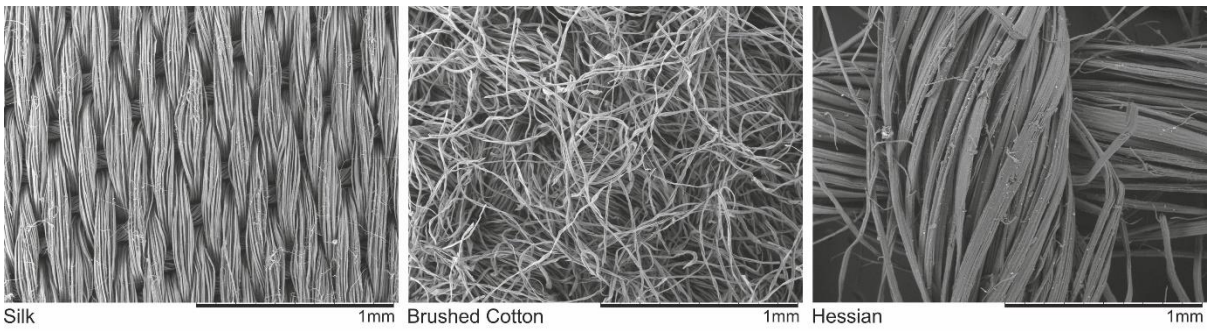

Figure 5.1 Hitachi TM-1000 scanning electron microscope images of the texture stimuli at 100x magnification.

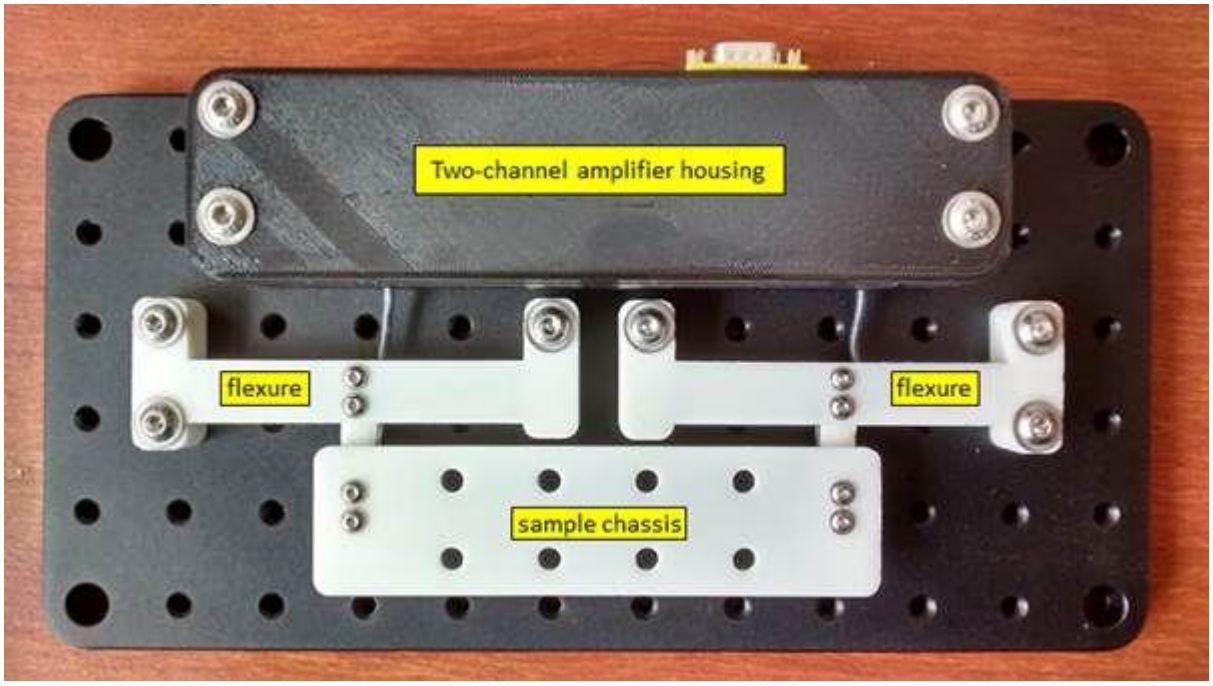

Figure 5.2 Top view of the touch sensor system showing the amplifier housing, the flexures from which the strain-gauge sensors are mounted, and the sample chassis attached to the sensors.

5.2.2.2 Subjective ratings

Initial and final subjective ratings were collected in response to the texture samples presented on stages attached to the touch sensor. Ratings were recorded using three 100-point visual analogue scales (VAS) to collect scores of pleasant/unpleasant, soft/hard, and smooth/rough for each texture, using a slide bar manipulated on-screen with a computer mouse. During subjective ratings, a partition to occlude vision of the sample stage was placed over the hand and touch sensor. Participants rated all three textures on all VAS in their own time. No touch sensor or EEG data were recorded at this time.

5.2.2.3 Pace training

The pacer task trained participants to explore the texture samples at approximately 5.5 cm/s to avoid large variations in finger movement speeds between participants. Participants were instructed to complete four sweeps of a plastic stage lined with a 100 mm by 40 mm strip of PVC electrical insulation tape, beginning and ending on the left side of the stage. A white dot was presented on a black screen, the dot moved horizontally across the screen in 1.5 s denoting one sweep. Participants followed the pacer dot with their index finger for as many repetitions as they wanted to train movement speed. The pacer dot was not shown during experimental trials of the active touch task. When participants felt confident with the pace, they completed five practice trials while the researcher visually assessed their pace and ability to perform the finger abduction movement. If their pace was inadequate (deemed to differ from 5.5 cm/s), they completed the pace training and practice trials again. During the active touch task, the researcher visually inspected participants' pace via the touch sensor recording app. The pacer dot was used to retrain participants between blocks if pace started to visually differ from 5.5 cm/s.

5.2.2.4 Active touch task

The active touch task consisted of three blocks which each encompassed three sub-blocks representing one texture. Participants experienced all three textures during each block. Blocks were repeated three times in a pseudo-randomised order which was counter-balanced between participants. Each sub-block contained 18 consecutive trials, totalling 54 trials for each texture over the course of the experiment.

Each trial consisted of a baseline period (4 s), touch experience (6 s) and recovery period (4 s). The baseline period was indicated by a white fixation cross on the screen, during which participants did not touch the texture. The touch experience began when the fixation cross turned from white to green, during which participants completed four sweeps of the texture: placing their index finger down on the left side of the texture sample, sweeping to the right then sweeping back to the left, and repeating before removing their index finger from the texture. The recovery period was indicated by the fixation cross turning from green to white, during which the participant did not touch the texture. At the end of each sub-block, participants were asked to rate how pleasant/unpleasant the texture was on a 100-point VAS; after which, the researcher checked that participants were comfortable and changed the stage to present the next texture sample.

5.2.3 Recordings

EEG data were recorded continuously using a 129-channel Geodesics EGI System (Electrical Geodesics, Inc., Eugene, Oregon, USA) and a sponge-based HydroCel Sensor Net. The net positioning was aligned to three anatomical landmarks, two preauricular points and the nasion. Electrode impedances were kept below 50 kΩ. A recording band-pass filter was set at 0.001–200 Hz with a sampling rate of 1000 Hz. Electrode Cz was used as a reference electrode for recording.

Finger load, representing downward pressure on the texture, finger position along a unidimensional axis across the texture sample, and time relative to the trial-onset marker (fixation cross) were recorded using a Hopkinson Research Touch sensor (Hopkinson Research, Wirral, UK), with a sampling rate of 1000 Hz.

5.2.4 Pre-processing

EEG pre-processing was conducted using BESA v 6.1 (MEGIS GmbH, Germany). Eye blinks and ECG artefacts were removed using PCA (Berg & Scherg, 1994). Data were filtered with a notch filter (50 Hz ± 2 Hz) and a visual inspection of data for the presence of any movement or muscle artefacts was performed. Trials affected by artefacts were excluded from subsequent analyses. EEG signals were downsampled to 256 Hz and were re-referenced using the common average method (Lehmann, 1984).

Touch sensor data were cleaned and visually inspected using in-house software developed in Python 3 (van Rossum & Drake, 2009). Position data were smoothed across time points using a Gaussian kernel ($\sigma = 20$), with 20 samples representing a window of 20 ms. Active touch timings (touch down; end of sweeps one, two and three; and lift off) were calculated relative to the trial-onset cue displayed on the LCD monitor. Trials were rejected when index finger touch down occurred one second or more after the trial-onset marker or less than 200 ms after the trial-onset marker. The latter step was implemented to remove trials where participants kept their finger on the touch sensor between trials. Furthermore, trials were rejected when index finger lift off occurred greater than one second after the trial-offset marker, or greater than two seconds before the trial-offset marker. Touch data were segmented into overlapping time windows to capture and extract active touch timings, with each time window individualised to the trial. The first time window captured touch down and the end of sweep one, the second captured end of sweep two, and the third captured the end

of sweep three and lift off. Trials were removed if participants missed a sweep. Subsequently, data were filtered by texture and *z*-scores were calculated for sweep duration and total load. Trials were removed when the *z*-score was ± 2 deviations from the normal distribution.

After EEG and touch sensor pre-processing was complete, the average number of trials and standard deviation (SD) per subject for ERD analysis in each condition was: silk, 27.57 ± 8.56; brushed cotton, 28.88 ± 8.86; hessian, 27.65 ± 7.90. The average number of rejected trials per condition was 25.96 ± 8.36. The number of accepted trials did not differ across conditions ($p > .05$).

5.2.5 Analysis

Time-locked ERD analysis was conducted using synchronised EEG and touch sensor data. Active touch timings, computed relative to the trial-onset visual cue on a trial-by-trial basis, were synchronised to EEG data. These individualised active touch timings included touch-onset, end of sweep one, two and three, and touch-offset. EEG data epochs were calculated using the touch sensor triggers and average sweep length to give four time-locked touch epochs per trial.

The power spectra were computed in MATLAB (The MathWorks, Inc., USA) using Welch's power spectral estimate method. The power spectra were calculated from EEG data −4–7.5 s relative to the trial onset visual cue and were then split into touch epochs. The power spectra were computed in 1 s windows shifted in overlapping 0.01 s steps. Data were smoothed using a Hanning window. The power spectral densities were estimated in the range of 1–80 Hz with a frequency resolution of 1 Hz. The baseline period utilised for analysis was 0.5–3.5 s of the four second rest period prior to each trial. Relative band power (RBP) changes in alpha- (8-12 Hz) and beta-band (16-24 Hz) were evaluated in each of the three

texture conditions using the ERD transformation (Pfurtscheller, 2001; Pfurtscheller & Aranibar, 1979).

$$\mathrm{ERD\%} = \left(\frac{A - R}{R} * 100\right)$$

In the above equation, $\mathrm{ERD\%}$ is a measure of RBP during active touch epochs (A) relative to rest during the baseline period (R). Negative values of $\mathrm{ERD\%}$ refer to the amplitude decreases of band power which signify the presence of cortical activation (ERD). In contrast, positive $\mathrm{ERD\%}$ values refer to the amplitude increases of band power (ERS).

Mean total load (g) and sweep duration (s) were computed for each sweep exploration and analysed using a 3×4 repeated measures analysis of variance (ANOVA), with three levels of texture (silk, brushed cotton, and hessian) and four levels representing sweeps one to four across the texture. The Greenhouse-Geisser epsilon correction was used for all ANOVA analyses to account for any violation of the sphericity assumption.

Mean pleasantness, smoothness, and softness ratings for each texture were calculated for all 35 participants (± 2 SD). Ratings were evaluated using 2×3 repeated measures ANOVA with two levels of time (initial and final) and three levels of texture (silk, brushed cotton, and hessian). Significant interaction effects were further examined using *post hoc t*-tests or Wilcoxon signed-rank tests for data that violated the Shapiro-Wilk test of normality, the Bonferroni correction was used to account for multiple comparisons.

Changes in ERD/S were investigated separately for alpha- and beta-band across 128 electrodes using 1×3 repeated measures ANOVA. Permutation analyses with 5000 repetitions, implemented using *statcond.m* in the EEGLAB library (Delorme & Makeig, 2004; Maris & Oostenveld, 2007), identified electrodes showing significant differences between textures ($p <$

.05). Secondly, we removed electrodes which demonstrated minimal changes in power from baseline, as these are unlikely to be involved in event-related sensory changes between texture conditions. Implementation of this second step was performed by calculating grand average ERD/S changes for all textures in each electrode identified from the permutation analyses. One sample *t*-tests with significance thresholds of $p < .01$ (uncorrected) were conducted on each grand average value to confirm that electrode ERD differed significantly from zero, i.e., that they demonstrated a significant change from baseline during sensory processing for all conditions. Electrodes that did not exhibit genuine changes during sensation were excluded from analysis of between-texture differences.

Repeated measures analysis of covariance (ANCOVA), performed with BMDP2V program (Statistical Solutions Ltd, 1995), were utilised to investigate whether subjective ratings for each texture were related to differences in ERD/S. ANCOVA were performed separately for electrodes identified as demonstrating significant differences between textures from the ANOVA analysis, with subjective ratings of pleasantness, smoothness and softness implemented as covariates.

5.3 Results

5.3.1 Subjective ratings

Mean subjective ratings for each texture are shown in Figure 5.3. 2×3 ANOVA indicated statistically significant interactions between the effects of texture (silk, brushed cotton, and hessian) and time (initial and final). Interactions were identified in ANOVA investigating pleasantness, $F(2, 2.62) = 4.57, p = .015, \eta_p^2 = 0.15$; softness, $F(2, 7.27) = 7.56, p = .001, \eta_p^2 = 0.24$; and smoothness, $F(2, 7.46) = 9.80, p < .001, \eta_p^2 = 0.26$. Significant main effects of texture were identified for pleasantness, $F(2, 371.89) = 153.63, p < .001, \eta_p^2 = 0.86$; softness, $F(2, 449.57) = 152.54, p < .001, \eta_p^2 = 0.86$; and smoothness, $F(2, 795.45) = 445.43, p < .001, \eta_p^2 = 0.95$. Pairwise comparisons revealed a reduction in pleasantness, softness and smoothness for hessian compared to brushed cotton and silk (all $p < .001$). Additionally, brushed cotton was revealed to be less smooth ($p < .001$) and less pleasant ($p = .009$) than silk. *Post-hoc* tests revealed that, over time, hessian was perceived as progressively rougher, $t(33) = 4.14, p < .001$ and harder $t(31) = 5.90, p < .001$.

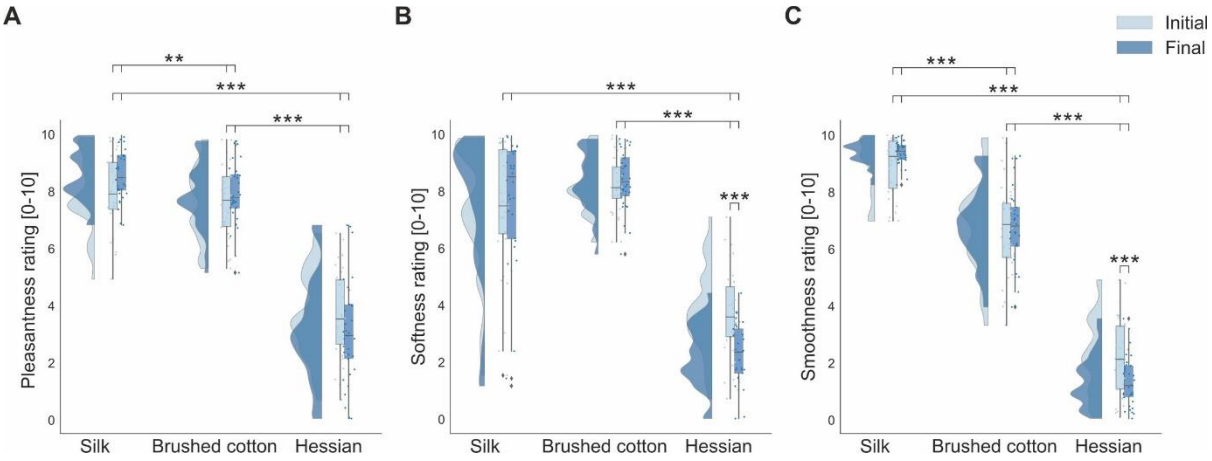

Figure 5.3 Raincloud plots (Allen et al., 2019) showing the distribution of mean subjective ratings, ***(A)*** *pleasantness rating,* ***(B)*** *softness rating, and* ***(C)*** *smoothness rating, for textured stimuli for both initial and final hedonic ratings. The half violin plots depict the probability distributions of the data. The individual dots show data points from each participant. The boxplots indicate the median, upper and lower quartiles, as well as the interquartile range (IQR) between the 25th and 75th percentile, whilst the whiskers represent scores outside of the IQR. Statistically significant differences are denoted as * for <.05, ** for <.01 and *** for <.001.*

5.3.2 Touch behaviour

Mean values of total load were 44.01 ± 4.13 g (mean ± standard error) in sweep one, 50.44 ± 5.05 g in sweep two, 49.5 ± 4.13 g in sweep three and 56.76 ± 5.96 g in sweep four. Figure 5.4 depicts a case example of load and duration over one trial. A 3×4 repeated measures ANOVA, with three levels of texture and four levels of sweep, revealed a significant main effect of sweeps, $F(1.32, 6349.97) = 21.18, p < .001, \eta_p^2 = 0.39$. Pairwise comparisons revealed a significant reduction in total load (g) for sweep one compared to sweeps two, three, and four (all $p < .001$). Additionally, sweep four demonstrated significant increased total load (g) relative to sweep two and three (all $p < .001$).

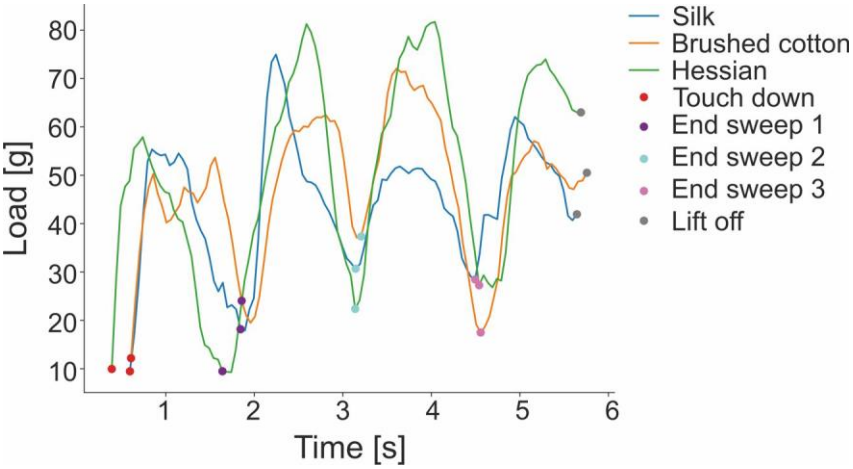

Figure 5.4 Line plot depicting load (g) for one complete trial for all three textures, with markers denoting the sweep time.

Mean duration (s) for each sweep were 1.17 ± 0.02 s (mean ± standard error) in sweep one, 1.30 ± 0.02 s in sweep two, 1.37 ± 0.02 s in sweep three and 1.50 ± 0.03 s in sweep four. A 3×4 ANOVA was performed on sweep duration (3 textures × 4 sweeps). Results indicated a significant main effect of sweep, $F\ (1.69, 2.65) = 48.04, p < .001, \eta_p^2 = 0.66$. Pairwise comparisons revealed a significant increase in sweep duration (s) over the duration of the trial for all sweeps (all $p < .001$), with sweep 1 and 4 showing the largest difference (0.332) and sweep 2 and 3 showing the least difference (0.068).

Differences in load and duration are possibly due to touch down and lift off, which have the potential to confound EEG interpretation. Therefore, sweep one and sweep four were excluded from the subsequent ERD analysis and EEG data were averaged over sweeps two and three.

5.3.3 ERD/S

During active touch exploration, alpha-band ERD was evident bilaterally over central electrodes representing sensorimotor regions (Figure 5.5A). Alpha-band ERS were prominent over the midline and ipsilateral occipito-parietal electrodes. Beta-band ERD was distributed bilaterally over central electrodes (Figure 5.5D). Electrodes manifesting statistically significant effects of texture, were identified for alpha- (Figure 5.5A) and beta-bands (Figure 5.5D). The analysis, comprising permutation analyses with 5000 repetitions ($p < .05$) and one sample *t*-tests (uncorrected $p < .01$), identified three electrodes which demonstrated a significant effect of texture on alpha- and beta-band oscillations.

A statistically significant effect for texture was found for alpha-band overlying left central parietal regions (electrode 42, CP3 according to the 10-10 system; Luu & Ferree, 2005) which corresponds to contralateral sensorimotor areas. The effect of texture,

$F(2, 390.05) = 4.40, p = .017, \eta_p^2 = 0.15$, was revealed to be due to hessian eliciting a stronger ERD than silk, as shown in Figure 5.5C.

In beta-band, statistically significant effects of texture were found overlying left parietal regions (electrode 52, P3 according to the 10-10 system; Luu & Ferree, 2005) and right central parietal regions (electrode 87, CP2 according to the 10-10 system; Luu & Ferree, 2005), both of which correspond to contralateral and ipsilateral sensorimotor areas, respectively. The effect of texture over contralateral sensorimotor region, $F(2, 299.85) = 5.09, p = .010, \eta_p^2 = 0.17$, was revealed to be due to silk eliciting a significantly greater degree of ERD relative to hessian ($p = .008$) and brushed cotton ($p = .005$). Over ipsilateral sensorimotor regions the effect of texture, $F(2, 265.52) = 4.05, p = .023, \eta_p^2 = 0.14$, was revealed to be due to hessian eliciting a significant reduced degree of ERD compared to silk ($p = .019$) and brushed cotton ($p = .041$). ERD values for electrodes 52 and 87 are displayed in Figure 5.5C, Figure 5.5F, and Figure 5.5H, respectively.

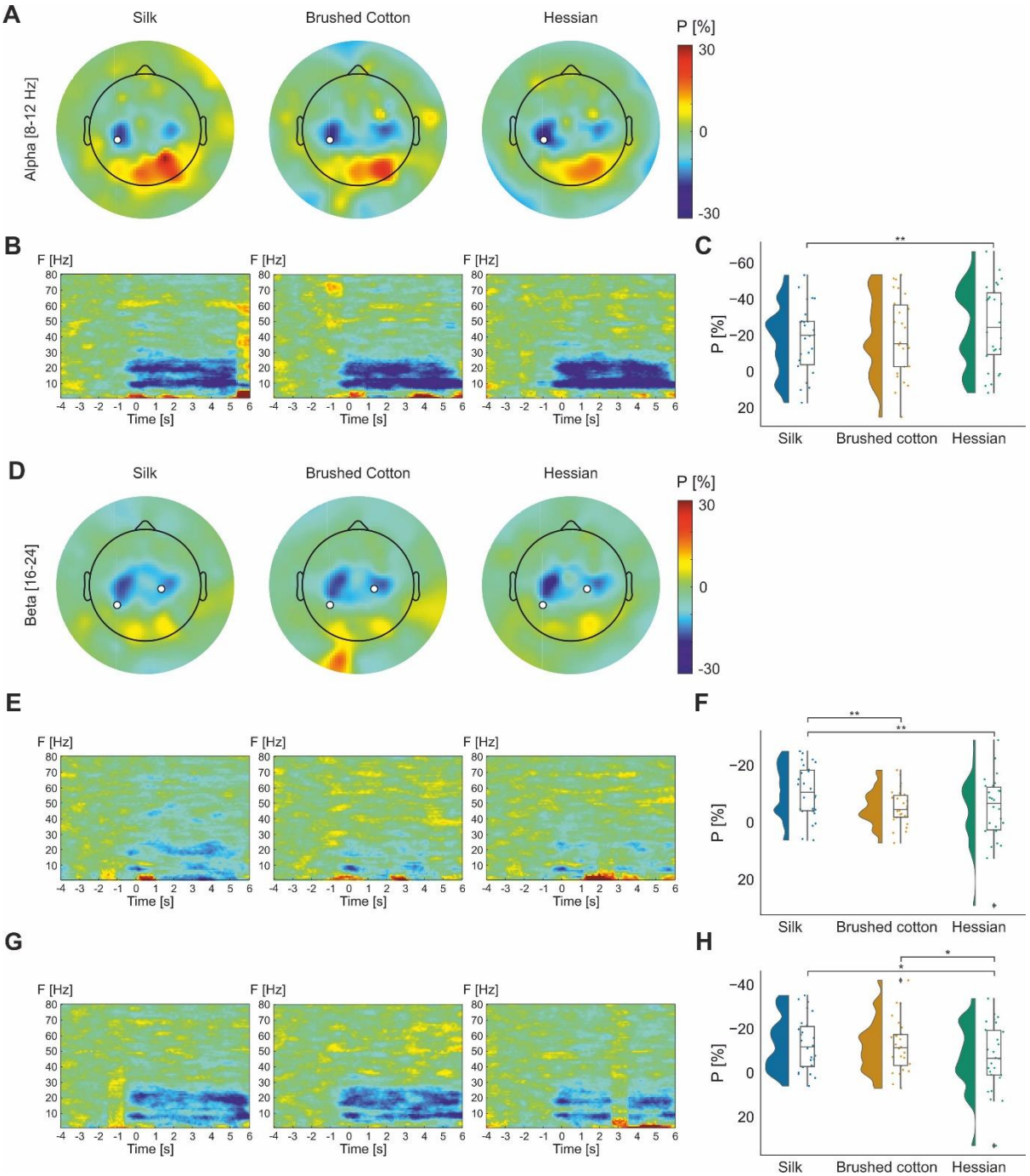

*Figure 5.5 Band power changes for each texture condition (silk, brushed cotton, and hessian). Grand average topographic maps of each frequency band of interest, alpha- **(A)** and beta-band **(D)**, are shown alongside an overhead view of electrodes showing statistically significant changes ($p < .05$). Time–frequency spectrograms for electrode 42 **(B)**, 52 **(E),** and 87 **(G)**, are pictured below the corresponding frequency band and condition. Raincloud plots (Allen et al., 2019) showing grand average alpha-band ERD/S values for textures conditions for electrode 42 **(C)**, 52 **(F)** and 87 **(H)**, are presented under the corresponding frequency band. The half violin plots depict the probability distributions of the data. The individual dots show data points from each participant. The boxplots indicate the median, upper and lower quartiles, as well as the IQR between the 25th and 75th percentile, whilst the whiskers represent scores outside of the IQR. Statistically significant differences are denoted as * for < .05, ** for < .01 and *** for < .001.*

5.3.3.1 Covariate analysis

Repeated measures ANCOVA were computed in electrodes demonstrating significant differences in ERD/S between textures, with subjective ratings of pleasantness, smoothness, and softness as covariates. Results indicated that smoothness ratings significantly covaried with differences in alpha-band ERD observed in electrode 42 overlying contralateral sensorimotor areas ($F(1, 862.43) = 11.47, p = .0016$). After controlling for the smoothness ratings, the main effect of texture on alpha-band ERD was not significant ($F(2, 237.53) = 3.16, p = .058$). Softness ratings were identified as a significant covariant for changes in beta-band ERD recorded in electrode 52 over contralateral sensorimotor areas, $F(1, 384.63) = 7.35, p = .01$). Controlling for softness ratings led to an increased in significance for the main effect of texture $F(2, 468.79) = 8.95, p < .001$). No significant covariates were found for electrode 87 in beta-band.

5.4 Discussion

Previous literature has provided insights into the cortical processing of texture during passive touch (Ballesteros et al., 2009; Bauer et al., 2006; Moungou et al., 2016), however cortical processing during active touch is poorly understood. The present study aimed to establish how texture perception is processed during active touch by assessing oscillatory changes in alpha- and beta-bands. Active touch stimulation of the index finger produced expected bilateral alpha- and beta- ERD over sensorimotor regions for all textures (Figure 5.5), with differences across stimuli observed. Furthermore, texture-related differences in alpha- and beta-band ERD covaried with subjective ratings of smoothness and softness. For the first time, we quantified parameters of active touch exploration using a novel fusion of touch sensor and EEG data streams which facilitated the investigation of ERD/S during each time-locked active touch experience.

Ipsi- and contralateral increases in beta-band ERD over sensorimotor regions were observed for silk and brushed cotton, relative to hessian. Differences in the modulation of beta-band activity may be attributed to variations in textural properties, with silk and brushed cotton rated as more smooth, soft, and pleasant when compared to hessian. Covariate analysis found ratings of perceived softness exerted a confounding effect for ERD differences in beta-band activity over the contralateral sensorimotor region. Controlling for the influence of individual differences in softness ratings between stimuli improved the sensitivity of analyses for changes in electrophysiological processing between textures. Suggesting beta-band ERD, in part, is likely modulated by differences in the micro-geometric properties of the texture such as softness. According to the duplex theory (Katz, 1925), vibrational cues mediate tactile perception of fine textures (Hollins & Risner, 2000). Therefore, the stronger beta-ERD in both contra- and ipsilateral central-parietal electrodes for the smoothest texture (silk)

compared to a coarse texture (hessian) may be related to increased high-frequency vibrations from tactile elements. Brushed cotton likely generated less high-frequency vibrations compared to silk which explains the finding of an increased beta-ERD for bushed cotton compared to hessian only in the contralateral central-parietal electrode. As described, covariate analysis suggests that modulation of beta-band ERD is likely related to the processing of vibrotactile cues rather than hedonic perception. Thus, our findings on texture modulation during active touch accord with previous studies reporting increased neural activation for physical properties of smooth compared to rough textures (Genna et al., 2018; Moungou et al., 2016).

Interestingly, alpha-band ERD was greater in electrode 52 located over contralateral sensorimotor region during exploration of hessian, the roughest texture, compared to silk. This contradicts our hypothesis of increased ERD for fine compared to rough textures, although at present there is little research investigating active touch using EEG methods. Covariate analysis identified that subjective smoothness ratings accounted for the variation in alpha-band ERD, indicating that individual differences in perceived smoothness account for the differences seen in alpha-band ERD during texture processing. Rough textures increase activation of Merkel cells through pressure and skin deformation, whereas Meissner corpuscles and Pacinian corpuscles modulate finer textures through high-frequency vibrations (Blake et al., 1997; Hollins et al., 2001a; Johnson & Hsiao, 1992; Yoshioka et al., 2001). Hessian is more likely to activate Merkel cells than brushed cotton and silk due to the increased spatial period of tactile elements (Chapman et al., 2002; Connor et al., 1990; Connor & Johnson, 1992; Johnson & Hsiao, 1992). Alpha-band activity may be modulated by roughness due to activation of Merkel cells and Meissner corpuscles, similar to the modulation of low- and high-frequency vibrotactile stimuli by SI and SII respectively (Chung et al., 2013; Francis et al., 2000; Harrington & Hunter Downs, 2001). Although greater alpha-

band ERD has recently been observed when decreasing the stimulus roughness during passive stimulation of the fingertip (Genna et al., 2018). Further research investigating texture perception during active touch is necessary to fully delineate how varying textural properties modulate oscillatory activity.

ERD analysis uncovered novel differences in oscillatory processing between conditions. This suggests that accurate data fusion is essential for time-locking ERD/S to the onset/offset of touch, as well as to remove noisy or incomplete trials and confounding elements of the touch experience. Investigation of active touch in relation to oscillatory changes likely requires rich touch data at the trial level to support the high temporal resolution of EEG methods (Koenig et al., 2005). In future, recording of touch data will facilitate the investigation of different physical properties of touch and their effect on neural processing, such as the effect of friction (Klöcker et al., 2013).

Although the current study has greater ecologically validity than previous paradigms (Gibson, 1962), it does not fully represent natural touch experiences due to EEG laboratory settings and the use of hand and wrist supports and pace training for tactile exploration. Further, participants were exposed to the texture stimuli repeatedly over the testing period, which may reduce task engagement (Lelis-Torres et al., 2017) or lead to sensory desensitisation (Graczyk et al., 2018; Klingner et al., 2011). However, repeated trials are necessitated by the ERD method (Cohen, 2016). Future use of continuous trials may be a more naturalistic and stimulating way to circumvent these problems. Furthermore, data were subjected to two stages of trial rejection (25.96 ± 8.36 trials rejected per texture). As a result, there were insufficient trials to compute grand average ERD/S per experimental block. Consequently, investigating the impact of time on ERD/S was beyond the scope of this study.

Additionally, this study is limited by the age of the population. Movement-related beta-band ERD increases with age in healthy populations (Bardouille & Bailey, 2019; Heinrichs-Graham & Wilson, 2016; Spooner et al., 2019; Walker et al., 2020; Xifra-Porxas et al., 2019), and has been linked with the inhibitory neurotransmitter GABA, which has been found to decline with age (Gao et al., 2013; Hall et al., 2010, 2011). The present study included participants aged 20-65, although the mean age was 28.03 ± 11.06, therefore findings may not be generalisable to the aging population. Further, the final sample included four left-handed participants. The researcher ensured participants could comfortably perform the finger abduction movement with their right hand. Therefore, handedness did not impact task performance.

Total load during the first and final sweep of the index finger differed significantly. Muscle contractions increase during flexions and extensions of the wrist (Hirt et al., 2016; Schieber & Thach, 1985); this additional wrist movement, present at touch onset and offset, may contribute to differences in total load observed during the first and last sweep. Further, voluntary movement is preceded by motor preparation which manifests as beta-band ERD, with the last sweep also likely to contain wrist movement preparation (Little et al., 2018; Stancak & Pfurtscheller, 1996b, 1997; Tzagarakis et al., 2015). Therefore, motor preparation and additional wrist movements have the potential to confound ERD/S interpretation (Pfurtscheller et al., 1998); consequently, the first and final sweeps were excluded from the ERD analysis, allowing one to assess the periods most likely to display texture processing.

The novel fusion of EEG and touch data, allowing for the computation of accurate active touch timings and time-locking, was found to be crucial when analysing EEG data during active touch. Touch sensor technology should be implemented where feasible in subsequent investigations of the neural correlates of active touch. The use of targeted active

touch exploration highlighted differences in brain oscillatory activity due to texture perception. Beta-band differences in sensorimotor areas expand on previously observed ERD changes during passive touch, whereas alpha-band ERD showed a divergence from previous passive touch research. Further research to consider physical parameters of active touch can aid our understanding of the brains processing of tactile perception and texture, which, may ultimately aid our understanding of debilitating conditions such as complex regional pain syndrome or other neuropathic pain syndromes which are accompanied by sensorimotor abnormalities (Brun et al., 2019; Harris, 1999). Although, one must first understand the neural underpinning of active touch in healthy individuals so we can make comparisons to clinical conditions.

Chapter 6

Tactile estimation of hedonic and sensory properties during active touch: an electroencephalography study

---

Jessica Henderson[1], Tyler Mari[1], Danielle Hewitt[1], Alice Newton-Fenner[1, 2], Andrew Hopkinson[1, 3], Timo Giesbrecht[4], Alan Marshall[5], Andrej Stancak[1, 2], Nicholas Fallon[1].

1 School of Psychology, University of Liverpool, Liverpool, UK.

2 Institute of Risk and Uncertainty, University of Liverpool, Liverpool, UK.

3 Hopkinson Research, Wirral, UK

4 Unilever, Research and Development, Port Sunlight, UK.

5 Department of Electrical Engineering and Electronics, University of Liverpool, UK.

This experiment used EEG to investigate oscillatory activity in relation to perceptual judgements of tactile texture properties.

This paper has been submitted for publication in the European Journal of Neuroscience. The format of the text has been modified to match the style of this thesis.

The roles of the co-authors are summarised below:

Jessica Henderson: Conceptualization, Methodology, Formal analysis, Investigation, Data curation, Writing – original draft, Writing – review & editing, Visualisation, Project administration, Software. **Tyler Mari**: Investigation, Writing – review & editing. **Danielle Hewitt**: Conceptualization, Investigation, Writing – review & editing. **Alice Newton-Fenner**: Investigation, Writing – review & editing. **Andrew Hopkinson**: Methodology, Software, Writing – review & editing. **Timo Giesbrecht**: Conceptualization, Funding acquisition, Supervision. **Alan Marshall**: Conceptualization, Supervision, Writing – review & editing. **Andrej Stancák**: Conceptualization, Supervision, Writing – review & editing. **Nicholas Fallon**: Conceptualization, Methodology, Software, Writing – review & editing, Supervision, Funding acquisition.

Abstract

Perceptual judgements about our physical environment are informed by somatosensory information. In real-world exploration, this often involves dynamic hand movements to contact surfaces, termed active touch. The current study investigated cortical oscillatory changes during active exploration to inform estimation of surface properties and hedonic preferences of two textured stimuli: smooth silk and rough hessian. A purpose-built touch sensor quantified active touch, while oscillatory brain activity was recorded from 129-channel EEG. By fusing these data streams at a single trial level, oscillatory changes within the brain were examined while controlling for objective touch parameters (i.e., friction). Time-frequency analysis was used to quantify changes in cortical oscillatory activity in alpha (8–12 Hz) and beta (16–24 Hz) frequency bands. Results reproduce findings from our lab, whereby active exploration of rough textures increased alpha-band ERD in contralateral sensorimotor areas. Hedonic processing of less preferred textures resulted in an increase in temporoparietal beta-band and frontal alpha-band ERD relative to most preferred textures, suggesting that higher-order brain regions are involved in the hedonic processing of texture. Overall, the current study provides novel insight into the neural mechanisms underlying texture perception during active touch and how this process is influenced by cognitive tasks.

6.1 Introduction

Humans encode somatosensory input to inform perceptual judgements. Texture is an important surface feature and is explored via the glabrous skin on the hands and digits via voluntary movement to create dynamic contact with surfaces, a behaviour termed active touch (Gibson, 1962; Prescott et al., 2011; Turvey & Carello, 2011; Wagner & Gibson, 2016). During tactile stimulation, subjective judgements of texture alter the BOLD signal, whereby greater prefrontal cortex activation was observed during tasks requiring estimation of surface properties, relative to conditions which included touch stimulation, but without estimation tasks (Kitada et al., 2005). In EEG literature, estimation tasks have been employed to quantify subjective judgements of surface texture (Ballesteros et al., 2009; Henderson et al., 2022), though ratings are typically collected separately from stimulation tasks. Therefore, it is unknown how subjective judgments modulate the electrophysiological correlates of texture processing.

Tactile information from surface texture is transduced by low-threshold mechanoreceptors in the glabrous skin of the hands (Hagbarth & Vallbo, 1967; Johansson & Vallbo, 1979; Vallbo & Johansson, 1984; McGlone & Reilly, 2010; Abraira & Ginty, 2013). This information is conveyed to the primary and secondary somatosensory cortex via the dorsal-column medial lemniscus pathway (Klingner *et al.*, 2016; Raju & Tadi, 2021). Subsequently, the information can be transmitted to higher-order regions involved in cognitive processing and multisensory integration (Romanski, 2012; Morrison, 2016; Gogolla, 2017; Uddin *et al.*, 2017; Whitlock, 2017), where estimation of surface properties is more likely to occur.

Event-related spectral perturbation (ERSP; Makeig, 1993; Makeig et al., 2004) is a spectral estimation method that provides insight into event-related changes in the EEG

spectra that are induced by the onset of stimuli (Grandchamp & Delorme, 2011). Decreases and increases in narrowband power are referred to as ERD and ERS, respectively (Pfurtscheller, 1977; Pfurtscheller & Aranibar, 1977, 1979). It is robustly shown that both motor and somatosensory activation are associated with ERD in alpha- (8–12 Hz) and beta-band (16–24 Hz) frequencies, originating from the primary motor and somatosensory cortices, respectively (Brovelli et al., 2004; Pfurtscheller, 2001; Salmelin & Hari, 1994). Beta-band ERS is then observed in the motor cortex after stimulation termination (Cheyne et al., 2003; Gaetz & Cheyne, 2006; Houdayer et al., 2006). Investigation of texture processing has revealed bilateral activation across sensorimotor areas, with an increase in cortical activation for smoother textures during passive touch (Genna et al., 2018; Moungou et al., 2016). On the other hand, active touch was found to elicit increased alpha-band ERD for rough textures and increased beta-band ERD for smooth textures (Henderson et al., 2022). Therefore, time-frequency analysis of induced cortical oscillations is an appropriate analysis method for active touch and is shown to elucidate bilateral sensorimotor cortex activation associated with texture processing.

The prefrontal cortex is thought to be involved in cognitive control and executive processing (Menon & D'Esposito, 2021; Nejati *et al.*, 2021), and has been identified as an important area during tactile discrimination tasks (Stoeckel *et al.*, 2003; Harada *et al.*, 2004; Kitada *et al.*, 2005; Marschallek *et al.*, 2023). The prefrontal cortex serves a well-established role in the processing of affective value of stimuli (Rolls & Grabenhorst, 2008), including tactile stimuli delivered to glabrous skin (Francis et al., 1999; Rolls et al., 2003a). Specifically, the DLPFC is active during somatosensory estimation and comparison tasks (Sathian et al., 2011; Simões-Franklin et al., 2011; Yang et al., 2017), and is thought to reflect the storage of tactile information in working memory to later inform goal-oriented motor behaviour (Barbey et al., 2013; Botvinick & An, 2009; Zhao et al., 2018a). The

orbitofrontal cortex (OFC) is associated with reward value and subjective pleasantness (Rolls, 2000, 2004), suggesting that prefrontal regions may also play an important role in hedonic preference for tactile stimuli, including surface texture (Gallace & Spence, 2011; Rolls et al., 2003a). Research using EEG has linked frontal alpha-band ERD to decision-making (Ramsøy et al., 2018; Ravaja et al., 2013) and emotional valence (Al-Nafjan et al., 2017; Poel et al., 2012; Schmidt & Trainor, 2010; Zhao et al., 2018b). Further, beta-band oscillations are thought to play a role in establishing a feed-forward loop which connects somatosensory regions to higher-order parietal and frontal brain regions (Adhikari et al., 2014). Taken together, research indicates that frontal alpha- and beta-band ERD may be increased during somatosensory processing with estimation tasks, relative to tasks where no subjective estimation is required.

Alpha-band oscillations are known to be modulated by attention (Klimesch, 2012; Pfurtscheller & Lopes da Silva, 1999). Cued attention during somatosensory tasks demonstrates decreased alpha-band power in the SI (Jones et al., 2010; van Ede et al., 2011). In addition, attention increases beta-band ERD prior to stimulus offset over sensorimotor areas (Bardouille et al., 2010; van Ede et al., 2011). Furthermore, the SII is associated with tactile attention (Hämäläinen et al., 2000; Hoechstetter et al., 2000; Wu et al., 2014) and tactile discrimination (Kitada et al., 2005; Sathian et al., 2011; Stilla & Sathian, 2008). Estimation tasks are more likely to increase attentional demands which may result in greater modulation of alpha- and beta-band ERD in sensorimotor regions in contrast to tasks with no estimation.

The present study aimed to investigate cortical oscillatory changes during active touch exploration of rough and smooth textures during estimation and no estimation conditions. We hypothesised that active texture exploration would elicit bilateral alpha- and beta-band ERD

over sensorimotor regions. Specifically, we predicted increased beta-band ERD for smooth when compared to rough textures, whilst alpha-band ERD was hypothesised to increase for rough compared to smooth textures, following our previous research (Henderson et al., 2022). Further, we hypothesised that estimation tasks would result in increased sensorimotor and frontal ERD in alpha- and beta-band, relative to no estimation conditions. Estimation tasks were split into two categories: sensory and hedonic estimations. We predicted that hedonic estimations would result in increased ERD in frontal regions when compared to sensory and no estimations conditions. Additionally, this study sought to investigate the potential differences between estimation type and texture by examining the interaction between the two variables.

6.2 Method

6.2.1 Participants

Thirty-five right-handed or ambidextrous participants were recruited (11 males, aged 18–49), left-handed participants were excluded due to difficulty exploring the texture with their right hand. All participants had no history of any neurological condition, or aversion or allergies to any textures. Four participants were excluded due to excessive muscle artefacts or technical problems resulting in incomplete data recording from the touch sensor. The final sample for analysis included 31 participants (8 males, 2 ambidextrous), aged 28.13 ± 6.54 years. Participants were reimbursed at a rate of £10 per hour for their time. The study was approved by the Research Ethics Committee of the University of Liverpool and all participants gave fully informed written consent at the start of the experiment in accordance with the Declaration of Helsinki.

6.2.2 Procedure

Participants were seated in a dimly lit Faraday cage with a 19-inch LCD monitor approximately 1 m in front of them. The tactile exploration task and practice trials were presented using PsychoPy (Peirce et al., 2019). EEG and six-axis sensor data were recorded during the tactile perception task. An arm support was used to stabilise and support the forearm whilst maintaining position over the six-axis sensor.

6.2.2.1 Stimuli

The stimuli included two textures selected from a previous study (Henderson et al., 2022): hessian and silk, Figure 6.1. The stimuli measured 150 × 255 mm and were mounted using double-sided tape (tesa® 64621) to a paper sample mount measuring 410 × 255 mm lined with masking tape (tesa® Precision Mask® 4333). Samples were mounted in a portrait

orientation; hessian was mounted on the left and silk on the right, with 40 mm spaces on each side and a 30 mm space between the samples. The paper sample mount was subsequently attached to an A3 size (420 × 300 × 3 mm) aluminium composite panel secured to the Hopkinson Research six-axis sensor (Hopkinson Research, 2020). The texture samples were replaced for each participant.

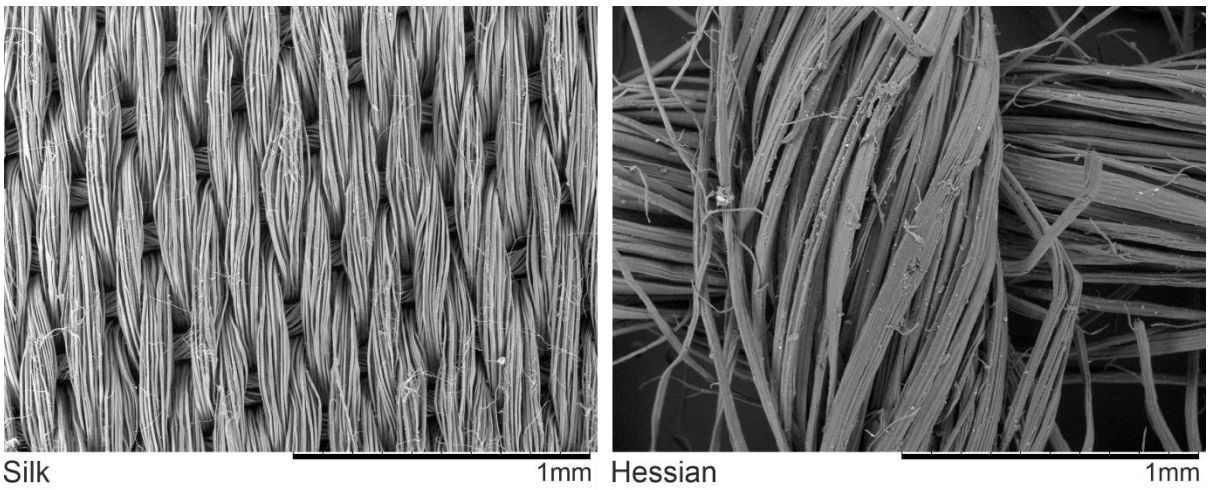

Figure 6.1 Hitachi TM-1000 scanning electron microscope images of the texture stimuli at 100x magnification.

6.2.2.2 Tactile exploration task

Participants completed four blocks, each lasting approximately 18 minutes. At the beginning of the block, participants were instructed to explore one of the two textures, and at the halfway point, participants were instructed to explore the other texture. A short break was given between blocks to increase task engagement and reduce desensitisation. There were 360 trials in total, 60 for each texture and each estimation condition (no estimation, sensory, and hedonic). Each block consisted of 90 trials, including all three trial types, this task design aimed to maximise participant engagement by ensuring continuous attention to the condition indicators throughout the session. Block order was counter-balanced, and the presentation order of trials conditions was pseudorandomised.

During the task, participants explored textures with the distal phalanx of their right index finger. Each trial consisted of a baseline period (4 s), condition indicator on screen (1 s) and tactile exploration (4 s), followed by an estimation response period for sensory and hedonic trials, Figure 2. The baseline period was indicated by a white fixation cross on the screen, during which participants kept their finger stationary on the texture. The condition indicators, which were a white square, circle, or triangle, were presented to specify whether the trial was sensory, hedonic, or no estimation. Condition indicators were randomised between participants, meaning that each shape corresponded to each condition equally, thereby ensuring that the shape of the condition indicator did not influence the trial (Benikos *et al.*, 2013).

Participants were trained to attend to sensory (i.e., ‘focus on how the texture feels. For example, is the texture smooth or rough, hard or soft?’) or hedonic features (i.e., ‘focus on how the texture makes you feel. For example, is the texture pleasant or unpleasant, comfortable or uncomfortable?’) during the respective trials. Subsequently, textures were

rated on a visual analogue scale (VAS) corresponding to their respective trial type; for hedonic ratings this included rating on pleasant/unpleasant and uncomfortable/comfortable scales, while sensory ratings included smooth/rough and soft/hard scales. During the no estimation trials participants were not given any instruction to attend to any textural aspect and were not asked to evaluate the texture after the trial. Full task instructions and the VAS used are detailed in Supplementary material 3.

During the touch exploration period, a green fixation cross appeared, indicating that the participant should start exploring the texture employing their preferred exploration behaviour, including multi-directional movements as well as optimising their speed and load according to their preference. Exploration stopped when the green cross was removed from the screen. Participants were instructed to keep their finger stationary on the texture when the green cross was not present (i.e., outside of the exploratory periods). Six practice trials following the same procedure were completed before beginning the tactile exploration task.

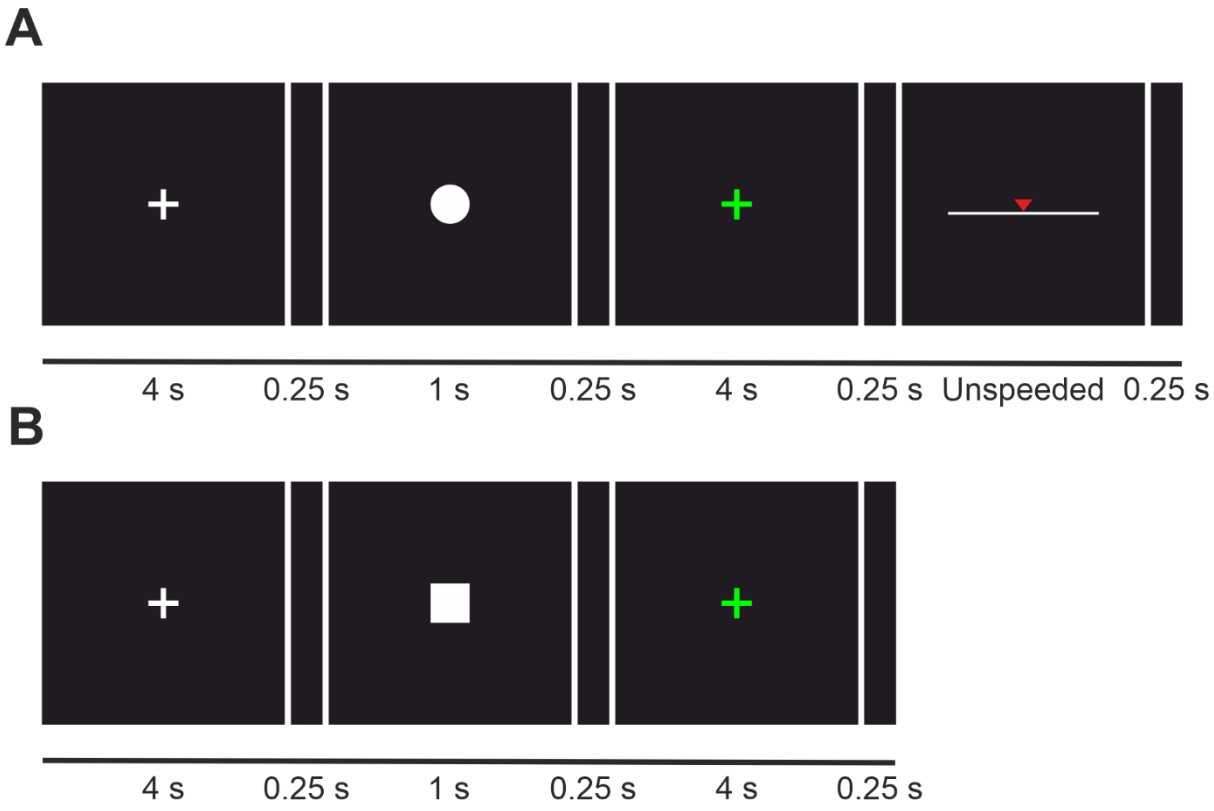

*Figure 6.2 An example of a hedonic or sensory estimation trial **(A)** and a no estimation trial **(B)**. For both conditions, each trial started with a baseline period indicated by a white fixation cross for 4 s, followed by the condition indicator for 1 s. Next, the tactile exploration period began, indicated by a green fixation cross presented for 4 s. For estimation trials, participants were instructed to rate the texture on the scale (i.e., smooth/rough, or soft/hard for sensory trials, and pleasant/unpleasant or comfortable/uncomfortable for hedonic trials). In the no estimation task, participants did not perform ratings.*

.

6.2.3 Recordings

A 129-channel saline-based Geodesic sensor net (Magstim EGI, UK) was used to record continuous EEG data. Positioning of the net was based on three anatomical landmarks, two preauricular points and the nasion. A recording band-pass filter was set at 0.001–200 Hz with a sampling rate of 1000 Hz, and electrode impedances were kept below 50 k. Electrode Cz was used as a reference electrode, and was not reinstated in the electrode array, leaving 128 recording channels. The six forces and torques acting on the texture samples due to the finger touch were recorded using the six-axis sensor, Figure 6.3, with a sampling rate of 1000 Hz. Finger position and friction force in the XY plane and finger load along the Z axis were calculated from the block averaged (20 Hz) forces and torques. The speed of finger movement was calculated by determining the distance between two positions at different time points.

A

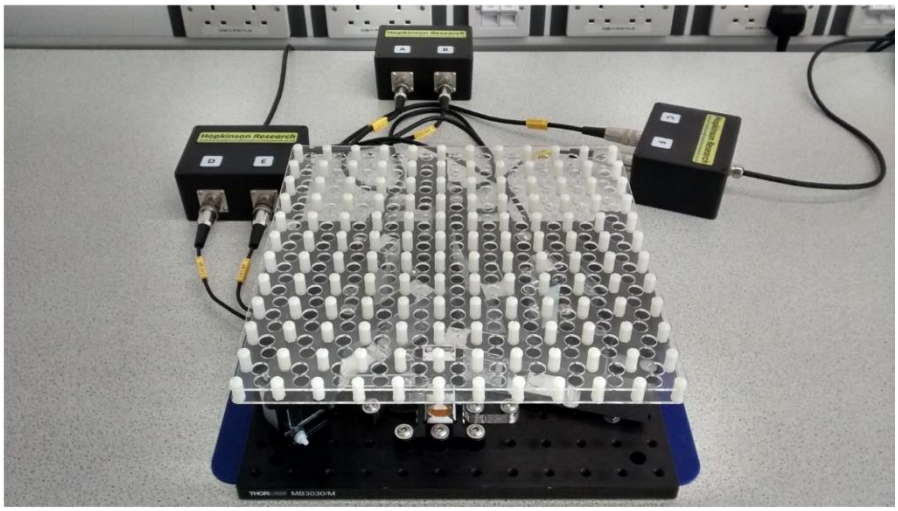

B

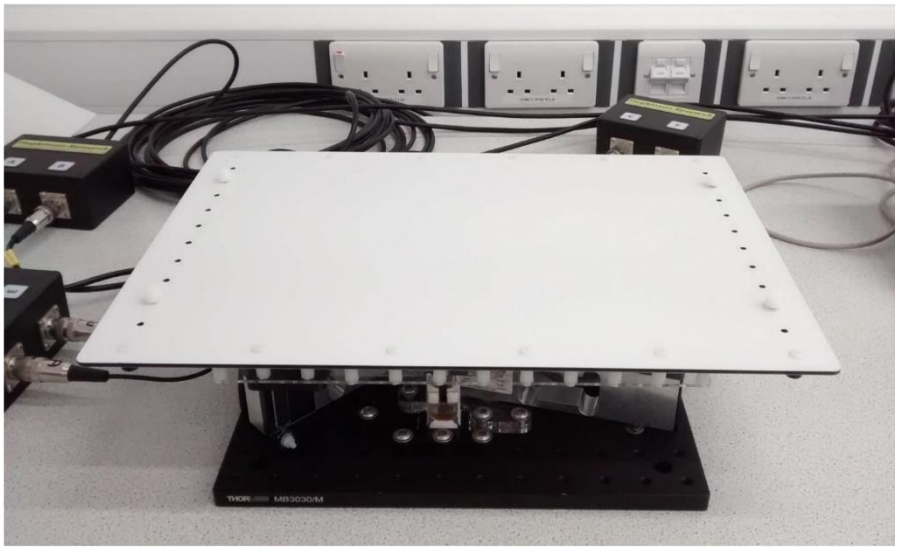

C

*Figure 6.3 Set up of the six axis sensor with the load cells connected to the junction boxes **(A)**, and with the ACP fitted **(B)**. Textures mounted the the paper sample mount and fixed to the ACP **(C)**.*

6.2.4 Pre-processing

EEG pre-processing was conducted using BESA v 6.1 (MEGIS GmbH, Germany). Eye blinks and ECG artefacts were removed using PCA (Berg and Scherg 1994). Data were filtered using 1 Hz high-pass and 100 Hz low-pass filters, with a 50 Hz ± 2 Hz notch filter. A visual inspection of data for the presence of any movement or muscle artefacts was performed, trials affected by artefacts were excluded from subsequent analyses.

Six-axis sensor data were cleaned and visually inspected using in-house software developed in Python 3 (Van Rossum & Drake, 2009). Trials were rejected where no suitable triggers were identified, as an error during data recording. The trial period was epoched −5–5 s from visual trigger onset. Trials were rejected where movement was detected in the baseline or visual cue period. Data were then epoched −200–4000 ms relative to the trial onset cue. Movement onset was identified for trials by calculating and identifying the first minima and maxima peaks of velocity, with the height set at half the minimum and maximum value, and prominence and distance set to 1. Trials were rejected when movement onset did not occur within 400 ms of visual cue onset. Median speed, friction and load were calculated from movement onset to the end of the trial period, Figure 6.4 depicts a case example of one trial. *Z*-scores were computed for each participant's measured touch behaviour during each block and texture. Trials were excluded if the z-score of any measure exceeded ± 2 SD.

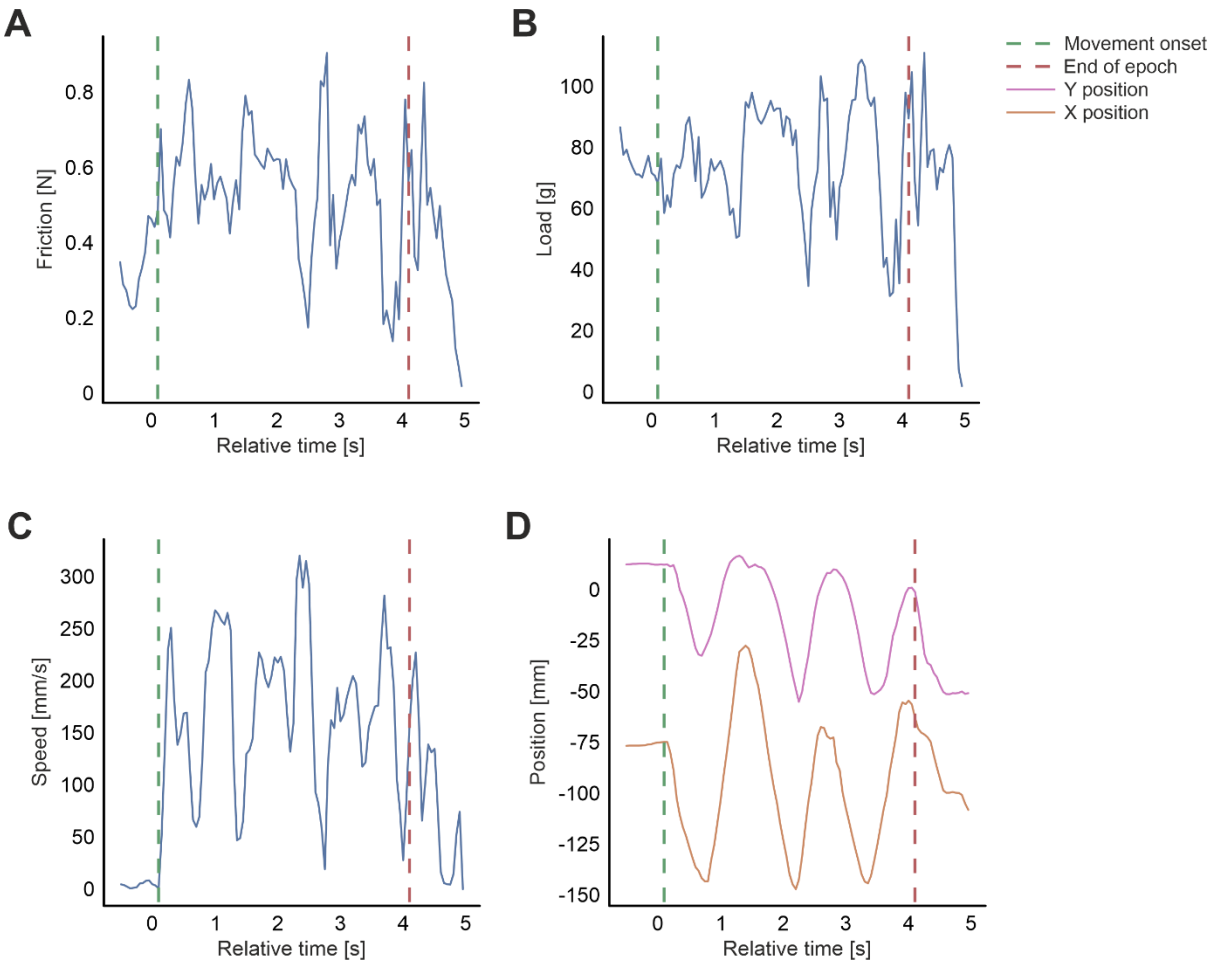

*Figure 6.4 Line plots for one complete trial depict friction **(A)**, load **(B)**, speed **(C)**, and X-axis position in orange and Y-axis position in pink **(D)**. Dashed lines denote movement onset and the end of the epoch, which was the period used for the calculation of median parameters.*

After completing EEG and six-axis sensor pre-processing, the average number of trials for analysis in each condition was as follows: sensory hessian, 39.52 ± 8.93 (M ± SD); hedonic hessian, 39.19 ± 9.35; no estimation hessian, 39.52 ± 8.88; sensory silk, 37.16 ± 8.84; hedonic silk, 39.39 ± 9.02; no estimation silk, 37.65 ± 8.70. The average number of accepted trials did not differ across conditions ($p > 0.05$). EEG pre-processing resulted in the rejection of 100.42 ± 47.97 trials over the entire experiment due to artefacts and noise. Furthermore, an additional 23.42 ± 20.48 trials were rejected as a result of the six-axis sensor pre-processing.

6.2.5 Analysis

Event-related time-frequency analysis was conducted using synchronised EEG and touch sensor data. Movement onset timings, computed on a trial-by-trial basis relative to the trial-onset visual cue, were synchronised to EEG data. EEG data were epoched −5.5–5 s relative to the movement onset marker.

Data were imported into the SPM12 software package (Statistical Parametric Mapping, University College London, England) in MATLAB (The MathWorks, Inc., USA). Epochs were baseline corrected (−4 – −2 s). EEG signals were downsampled to 256 Hz and were re-referenced using the common average method (Lehmann, 1984). Time-frequency analysis was performed by convolving the EEG signal with a set of complex Morlet wavelets, which are complex sine wave tapered by a Gaussian. The wavelets spanned a frequency range from 1 to 40 Hz with 1 Hz steps and each wavelet had 5 cycles (Cohen, 2019). The choice in cycle number ensured an acceptable trade-off between time and frequency smoothing, with a slight preference for temporal precision (Tallon-Baudry & Bertrand, 1999; Cohen, 2019). The power spectra obtained were rescaled with a log-ratio transformation (−4 – −2s), producing the baseline-normalised ERSP. Subsequently, the power spectra were cropped from 0 to 4s relative to movement onset and averaged over alpha (8–12 Hz) and beta frequency bands (16–24 Hz), giving narrow band ERD/S values.

For each trial, 3D scalp-time images were generated by projecting the location of the 128 electrodes onto a 2D plane, and then interpolating linearly between the point onto a standardised scalp grid sized 32 × 32 pixels (pixel size 4.25 × 5.38 mm^2); the resulting topographies of power spectra planes are continuously stacked over each timepoint to give the 3D representation (X × Y × time). To address spatial and temporal variability between subjects and improve the conformity of images to the assumptions of random field theory,

images were smoothed with a Gaussian kernel of 9 × 9 × 20 mm² ms (full width at half maximum; Kilner et al., 2005; Worsley, 2007), as commonly utilised in previous research (Cook *et al.*, 2015, 2017). SPM uses a technique called summary statistic approach (Kiebel *et al.*, 2007), where contrast images are generated in first level analyses to summarise the effects for each individual, subsequently, these images are utilised as data in second level models where the variability of the effects is assessed over the group of subjects.

First level analysis was conducted by applying the GLM to each subject's single-trial scalp-time data. The GLM design matrix, consisted of six dummy variables specifying the trials texture (silk or hessian) and estimation condition (sensory estimation, hedonic estimation, or no estimation), and 6 parametric regressors coding the summation of load and friction under the respective texture (silk and hessian) and estimation condition (sensory, hedonic, or no estimation; e.g., summation of load and friction under sensory estimations of hessian), this can be seen in Supplementary material 4. Regressors were mean centred to avoid multicollinearity issues. Three contrast images were produced to test for main effects: one imaged was produced to test the difference between hessian vs. silk for the main effect of texture, and two images were produced to test the difference between sensory vs. hedonic and hedonic vs. no estimation for the main effect of estimation. Two contrast images were produced to test the interaction effect: the difference between sensory hessian and hedonic silk vs. hedonic hessian and sensory silk, and the difference between hedonic hessian and no estimation of silk vs. no estimation of hessian and hedonic silk.

For the second level analysis, all 31 participants' individual contrast spectra from the first level were analysed using mass-univariate analysis at the group level. The main effect of texture was tested using a one-sampled t-test and an *F*-contrast of [1] with the 31 contrast images as input. A two-sample t-test design was employed to examine the main effect of

estimation and the interaction effect. The 62 contrast images (two per subject) were entered, and an *F*-contrast of [1 0; 0 1] was applied to test for these effects. An uncorrected cluster forming threshold of $p < .001$ and a cluster size of 35 contiguous space-time voxels, as commonly utilised in previous research (Cook et al., 2018), were used to determine significant effects. Power data from significant clusters were extracted and analysed in SPSS v. 28 (IBM Inc., USA) to determine the direction of observed effects; a paired samples t-test for the main effect of texture, one-way ANOVA for the main effect of texture, and two-way ANOVA for the interaction effect.

Mean subjective ratings of comfort and pleasantness (hedonic evaluations), and smoothness and softness (sensory evaluations) were calculated separately for each texture across all blocks. Subjective ratings were evaluated separately using 2 × 4 repeated measures ANOVA with two levels of texture (silk and hessian) and four levels of time (blocks one, two, three, and four). Median speed (mm/s), friction (N) and load (g) were computed for each tactile epoch that was used in the EEG analysis. These data were analysed using a 2 × 3 repeated measures ANOVA with two levels of texture (hessian and silk) and three levels categorising the experimental condition (sensory estimation, hedonic estimation, and no estimation) for each touch behaviour (speed, load, and friction). Statistical outliers (±2 SD) were removed for all behavioural data.

The Greenhouse-Geisser epsilon correction was applied to all ANOVA analyses in cases where the data violated the assumptions of sphericity. Additionally, to account for multiple comparisons during *post-hoc* analyses, the α level was adjusted using the Bonferroni correction.

Correlational analyses were performed on touch behaviour (speed, load, and friction) for each texture (silk and hessian) independently. Factors found to be correlated were linearly

combined by summation for subsequent SPM analysis to address issues of multicollinearity (Kalnins & Business, 2018). Further, touch behaviours showing no statistical differences between texture or estimation were not entered as regressors in the SPM analysis. Therefore, the linear combination of friction and load under each condition were used as regressors in the SPM model (see section 6.3.3 below). Additional correlational analyses were performed to examine the relationship between subjective ratings (comfort, pleasantness, softness, and smoothness) and touch behaviour (speed, load, and friction).

6.3 Results

6.3.1 Subjective ratings

Mean subjective ratings for each texture are shown in Figure 6.5. 2 × 4 ANOVA indicated statistically significant main effects of texture for ratings of comfort, $F(1, 2479.56) = 317.48, p < .001, \eta_p^2 = 0.93$; pleasantness, $F(1, 2469.43) = 263.49, p < .001, \eta_p^2 = 0.91$; smoothness, $F(1, 2908.67) = 610.11, p < .001, \eta_p^2 = 0.96$; and softness, $F(1, 2306.62) = 346.01, p < .001, \eta_p^2 = 0.93$. Pairwise comparisons revealed a reduction in comfort, pleasantness, smoothness, and softness when comparing hessian to silk (all $p < .001$). Further, significant interactions between the effects of texture and time were identified for comfort, $F(2.17, 3.44) = 9.12, p < .001, \eta_p^2 = 0.27, \varepsilon = .72$; pleasantness, $F(2.08, 5.22) = 15.11, p < 0.001, \eta_p^2 = 0.37, \varepsilon = .69$; smoothness, $F(1.90, 1.85) = 6.04, p = .005, \eta_p^2 = 0.19, \varepsilon = .63$; and softness, $F(1.73, 2.94) = 7.49, p = .002, \eta_p^2 = 0.22, \varepsilon = .58$.

The interaction between texture and time revealed that comfort, pleasantness, smoothness, and softness ratings differed between exploration of hessian and silk when comparing against each respective block (all $p < .001$). Further, comfort ratings of hessian significantly decreased when comparing block 1 to 3 ($p = .003$) and 4 ($p < .001$). Pleasantness ratings for hessian decreased over time, with a significant difference between block 1 when compared with block 3 ($p < .001$) and block 4 ($p < .001$), and when comparing block 3 with block 4 ($p = .007$). Softness ratings of hessian were significantly reduced when comparing block 1 with block 3 ($p = .005$). By contrast, ratings of silk did not significantly differ across time for all ratings.

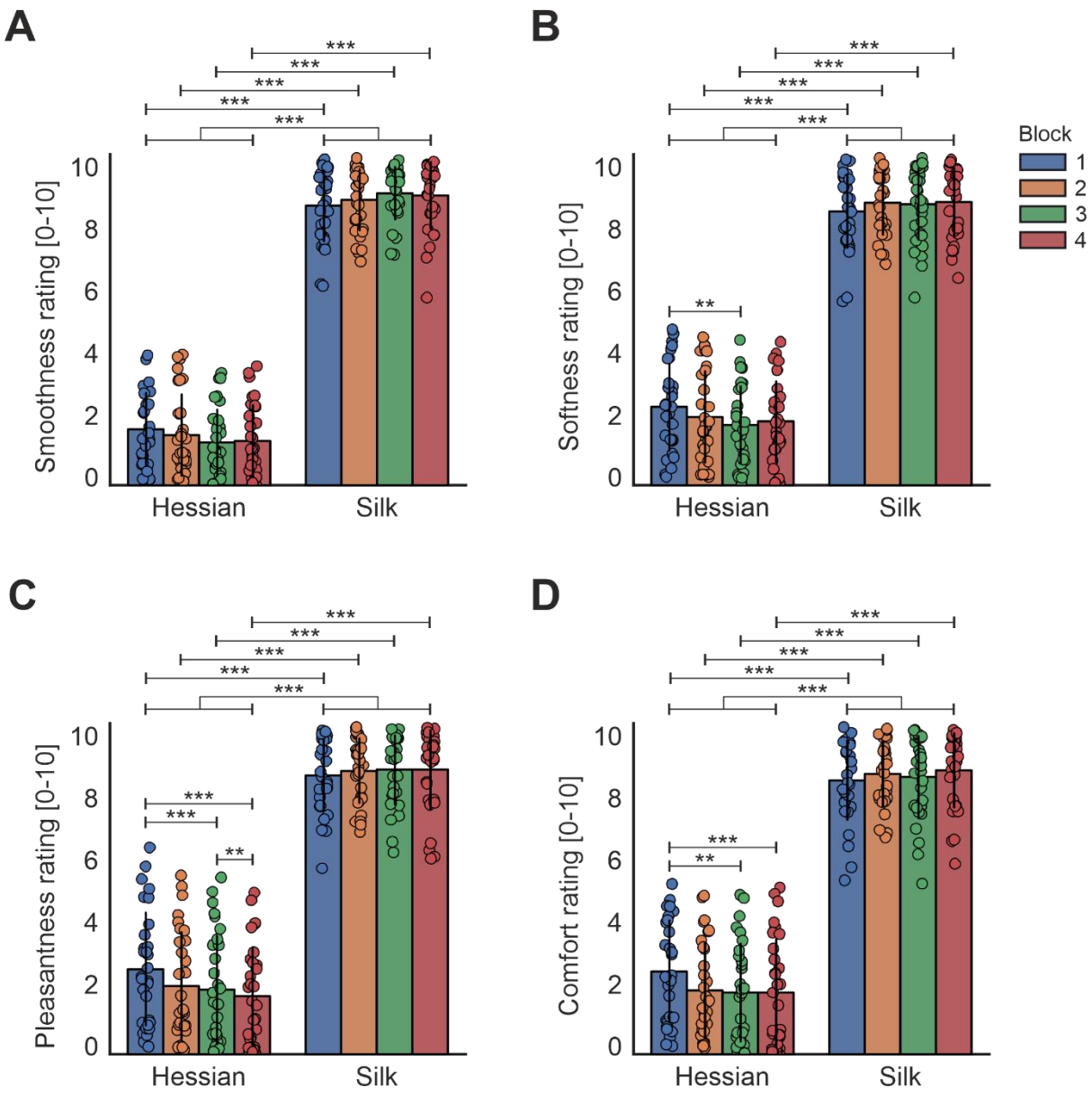

Figure 6.5 Bar charts showing mean subjective ratings, ***(A)*** *smoothness rating,* ***(B)*** *softness rating,* ***(C)*** *pleasantness rating, and* ***(D)*** *comfort rating, for textured stimuli across experimental blocks. The individual dots show data points from each participant. Statistically significant differences are denoted as * for < .05, ** for < .01 and *** for < .001.*

6.3.2 Touch behaviour

Mean touch behaviour values of friction, speed and load for each texture are displayed in Figure 6.6. 2 × 3 repeated measures ANOVA, with two levels of texture and three levels of estimation, were conducted for each touch parameter. A significant main effect of texture was identified for friction $F(1, 0.11) = 15.54, p < .001, \eta_{p^2} = 0.36$ and a significant main effect of estimation was demonstrated for load $F(2, 72.55) = 6.94, p = .002, \eta_{p^2} = 0.20$. No significant differences were observed for speed. Pairwise comparisons revealed a significant reduction in friction (N) for silk compared to hessian ($p < .001$), and a significant reduction in load (g) for no estimation trials compared hedonic estimation conditions ($p = .001$).

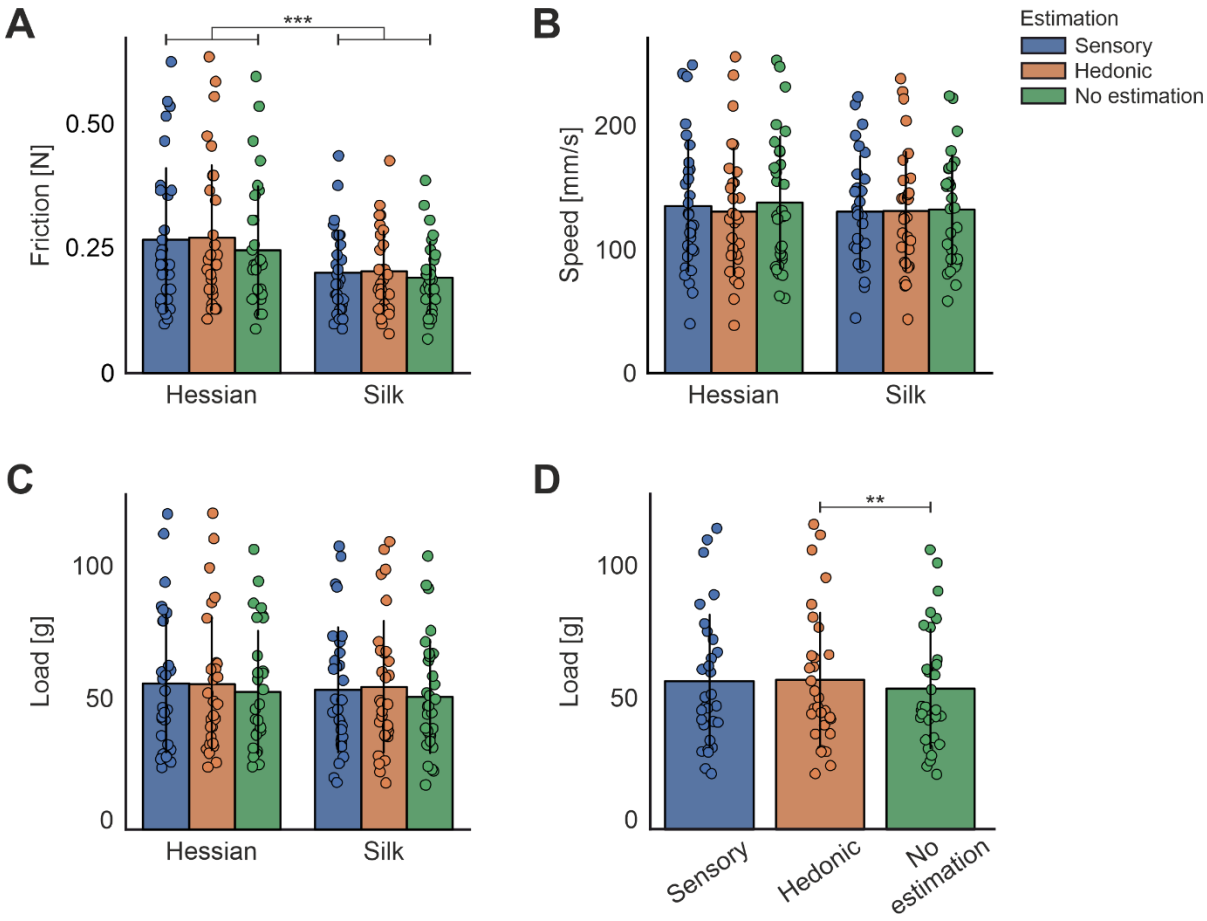

Figure 6.6 Bar charts showing mean touch behaviour, ***(A)*** *friction,* ***(B)*** *speed, and* ***(C)*** *load, for textured stimuli across estimation trial type.* ***(D)*** *Bar chart showing mean touch behaviour for load averaged across textures to display the main effect of estimation. The individual dots show data points from each participant. Statistically significant differences are denoted as * for p < .05, ** for < .01 and *** for < .001.*

6.3.3 Correlational analyses

Correlational analyses performed on touch behaviour revealed a positive correlation between friction and load for exploration of hessian $r(29) = .86, p < .001$; and silk $r(29 = .75, p < .001$. This was expected as friction force is directly proportional to load (Amontons, 1699; Bogy & Chen, 2013). Therefore, friction and load were linearly combined by summation for inclusion in subsequent SPM analysis. Likewise, speed was not included as a covariate due to not differentiating between textures or rating types. Correlational analyses performed between subjective ratings and touch behaviour revealed no significant correlation between any factors.

6.3.4 EEG

ERD/S was investigated relative to movement onset after accounting for the influence of load and friction on a single-trial level. Group-level analysis revealed significant scalp-time clusters in alpha-band, showing one cluster for the main effect of texture, one cluster for the main effect of estimation, and two clusters for the interaction effect. In beta-band, five clusters were identified for the main effect of estimation and two clusters for the interaction between texture and estimation type. No significant main effect of texture was revealed in beta-band. The direction of observed effects was determined by subjecting power data, from significant clusters extracted from SPM12, to further statistical analysis in SPSS v. 28 (IBM Inc., USA).

6.3.4.1 Alpha-band

6.3.4.1.1 Main effects

A significant main effect of texture was identified in contralateral parietal regions, corresponding to left sensorimotor areas, spanning approximately 234 ms duration and peaking at 357 ms and 436 ms after movement onset, illustrated in Figure 6.7A. A subsequent paired samples *t*-test demonstrated significantly greater ERD for hessian (-3.36 ± 1.64 dB; M $\pm$ SD) when compared to silk (-1.91 ± 1.58 dB), $t(30) = -4.92, p < .001$.

Over ipsilateral posterior parietal regions, as demonstrated in Figure 6.7E, a significant scalp-time cluster demonstrated a main effect of estimation on induced power peaking at 3268 ms after movement onset and lasting for approximately 191 ms in duration, $F(2, 23.13) = 10.431, p < .001, \eta_p^2 = 0.26$. Pairwise comparisons revealed a significant decrease in ERD for hedonic (-0.16 ± 1.58 dB) when compared with sensory (-1.87 ± 1.35 dB; $p < .001$) and no estimation (-1.23 ± 1.25 dB; $p = .014$).

Overall, findings demonstrate a significant effect of texture on contralateral parietal regions, with greater ERD for hessian than silk during active touch. In ipsilateral posterior parietal regions, a significant main effect of estimation was observed, with a decrease in ERD for hedonic compared to sensory and no estimation.

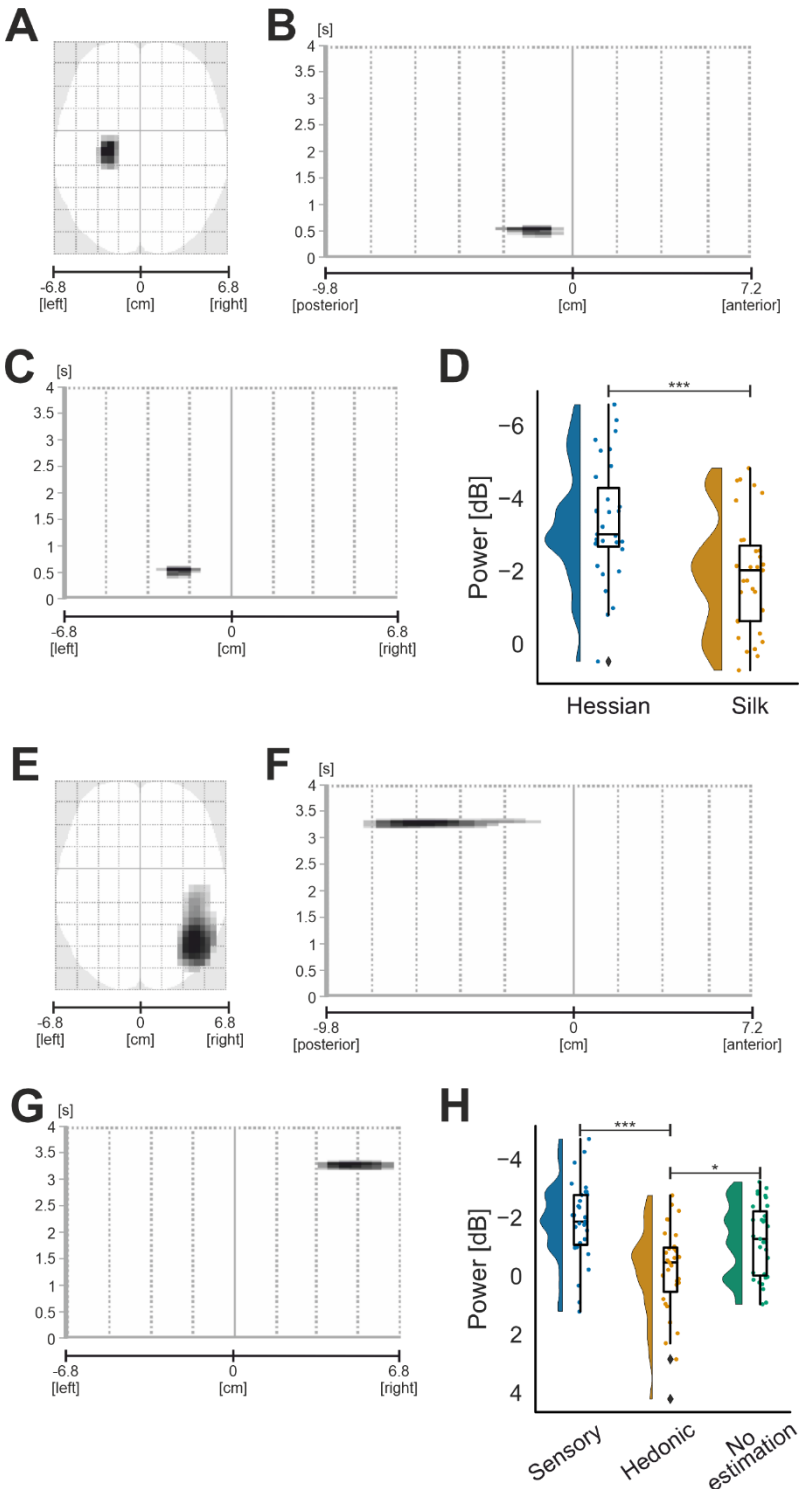

*Figure 6.7 Standard scalp map of the statistically significant clusters in alpha-band for the main effect of texture **(A)** and the main effect of estimation **(E)**. Statistically significant latency periods 0–4 s relative to the onset of movement are displayed over the horizontal axis of the scalp (from left −6.8 cm to right 6.8 cm) for the main effect of texture **(C)** and estimation **(G)**, and over the vertical axis of the scalp (from posterior −9.8 cm to anterior 7.2 cm) for the main effect of texture **(B)** and estimation **(F)**. Raincloud plots (Allen et al., 2019) show the distribution of grand average alpha-band power values for significant clusters for the main effect of texture **(D)**, and the main effect of estimation **(H)**. The half violin plots depict the probability distributions of the data. The individual dots show data points from each participant. The boxplots indicate the median, upper and lower quartiles, as well as the IQR between the 25th and 75th percentile, whilst the whiskers represent scores outside of the IQR. Statistically significant differences are denoted as * for < .05, ** for < .01 and *** for < .001.*

6.3.4.1.2 Interaction effects

An interaction between texture and estimation produced two significant clusters, Figure 6.8A. The largest cluster (k=399) was located over bilateral occipital areas and encompassed approximately 173 ms duration, peaking at 2213 ms, $F(2, 73.91) = 9.69, p < .001, \eta_p^2 = 0.24$. Exploration of hessian under hedonic estimation trials produced ERD, whilst exploration of silk produced slight ERS, resulting in a significant difference between the two conditions ($p = .002$; Table 6.1). In addition, sensory estimations of silk produced ERD, leading to a significant difference between sensory and hedonic estimation of silk ($p = .002$; Table 6.1). Sensory estimations demonstrated increased ERD for silk compared to hessian ($p = .021$; Table 6.1). Further, greater ERD was observed for hedonic contrasted with sensory estimations ($p = .016$; Table 6.1).

Table 6.1. Descriptive statistics for each significant cluster for the interaction effect in alpha-band

	Sensory				Hedonic				No Estimation			
	Hessian		Silk		Hessian		Silk		Hessian		Silk	
Cluster	M	SD	M	SD	M	SD	M	SD	M	SD	M	SD
One	−0.08	3.34	−1.86	2.25	−2.17	2.36	0.32	3.00	−0.76	3.09	−1.20	3.32
Two	−1.29	3.41	−1.16	2.01	−2.08	2.13	0.14	2.92	−0.62	2.94	−1.89	2.18

Cluster two (k=216) for the interaction effect peaked at 2232 ms and spanned approximately 173 ms duration. The cluster was located contralaterally in the left hemisphere and encompassed lateral and medial frontal areas, $F(2, 47.82) = 10.75, p < .001, \eta_p^2 = 0.26$. An interaction between texture and estimation was uncovered in the hedonic estimation condition, specifically ERD was observed for hessian and ERS for silk ($p < .001$; Table 6.1). Further ERD was increased for silk when contrasting no estimation with hedonic estimations ($p = .006$; Table 6.1). No estimation resulted in increased ERD for silk compared to hessian ($p = .025$; Table 6.1).

In summary, a significant interaction effect of texture and estimation was identified for contralateral frontal and bilateral occipital regions. Notably, greater ERD was observed for hedonic estimations of hessian relative to hedonic estimations of silk in both clusters.

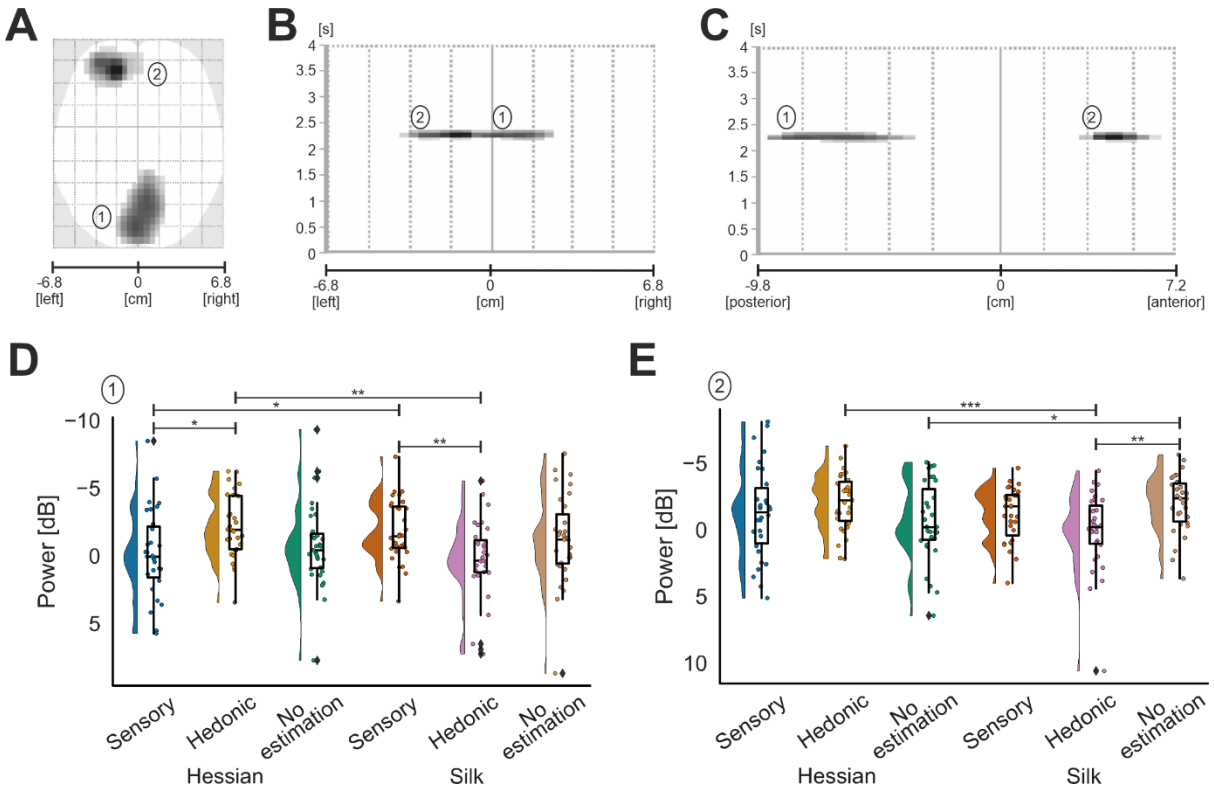

Figure 6.8 Standard scalp map of the statistically significant clusters in alpha-band for the interaction effect between texture and estimation ***(A)****. Statistically significant latency periods 0–4 s relative to the onset of movement are displayed over the horizontal axis of the scalp (from left −6.8 cm to right 6.8 cm)* ***(B)****, and over the vertical axis of the scalp (from posterior −9.8 cm to anterior 7.2 cm)* ***(C)****. Raincloud plots (Allen et al., 2019) showing the distribution grand average alpha-band power values for significant clusters for the interaction effect in cluster 1****(D)****, and cluster 2* ***(E)****. The half violin plots depict the probability distributions of the data. The individual dots show data points from each participant. The boxplots indicate the median, upper and lower quartiles, as well as the IQR between the 25th and 75th percentile, whilst the whiskers represent scores outside of the IQR. Statistically significant differences are denoted as * for p < .05, ** for < .01 and *** for < .001.*

6.3.4.2 Beta-band

6.3.4.2.1 Main effects

Five clusters were identified as statistically significant when investigating the main effect of estimation. The largest cluster (k=181) spanned from contralateral frontal towards frontocentral areas, Figure 6.9A, peaking at 3873 ms, 3893 ms and 3912 ms after movement onset and encompassing approximately 157 ms duration. Subsequent one-way ANOVA performed on EEG power data confirmed the significant main effect of estimation and tested the direction of observed effects, Table 6.2. Beta-band ERD/S differences were observed between hedonic estimations, which elicited a marginal ERS response in this late period, and sensory and no estimations, which produced ERD. This led to significant differences when contrasting hedonic with sensory ($p = .002$; Table 6.2) and no estimation conditions ($p < .001$; Table 6.2). Cluster two (k=69) and cluster four (k=43) were located in contralateral posterior parietal regions and peaked at 1275 ms and 3893 ms whilst lasting approximately 95 and 138 ms duration, respectively. Pairwise comparisons revealed a significant decrease in ERD for cluster two and four when comparing hedonic to sensory (cluster two: $p = .001$; cluster four: $p = .002$; Table 6.2) and no estimation (both $p < .001$; Table 6.2).

Table 6.2. ANOVA and descriptive statistics for each significant cluster for the main effect of estimation in beta-band.

					Sensory		Hedonic		No Estimation	
Cluster	*df*	*F*	*p*	η_p^2	M	SD	M	SD	M	SD
One	2, 10.98	12.67	<.001	0.30	−0.53	0.78	0.22	0.92	−0.95	0.92
Two	2, 16.30	9.10	<.001	0.23	−1.19	1.21	−0.04	1.21	−1.38	1.17
Three	2, 4.65	8.10	<.001	0.21	−0.59	0.78	−0.05	0.6	−0.8	0.75
Four	2, 16.62	9.32	<.001	0.24	−1.64	1.46	−0.38	1.21	−1.66	1.1
Five	2, 14.50	8.88	<.001	0.23	−1.7	0.93	−0.41	1.26	−1.44	1.2

Cluster three (k=44) was laterally adjacent to cluster two and lasted approximately 76 ms duration, peaking at 1393 ms after movement onset. Pairwise comparisons demonstrated differences were due to reduced ERD for hedonic estimations when compared with sensory ($p = .004$; Table 6.2) and no estimation ($p < .001$; Table 6.2) conditions. Finally, cluster five (k=35) was ipsilateral to cluster two and four and peaked at 3365 ms, spanning approximately 77 ms duration. Subsequent analysis revealed that the main effect of estimation was due to significantly decreased ERD for hedonic estimations relative to sensory ($p < .001$; Table 6.2) and no estimations ($p = .006$; Table 6.2).

The main effect of estimation for beta-band can be summarised as eliciting a network of contralateral frontal and bilateral posterior parietal clusters, which all demonstrated a decrease in ERD for hedonic estimations relative to sensory and no estimation conditions.

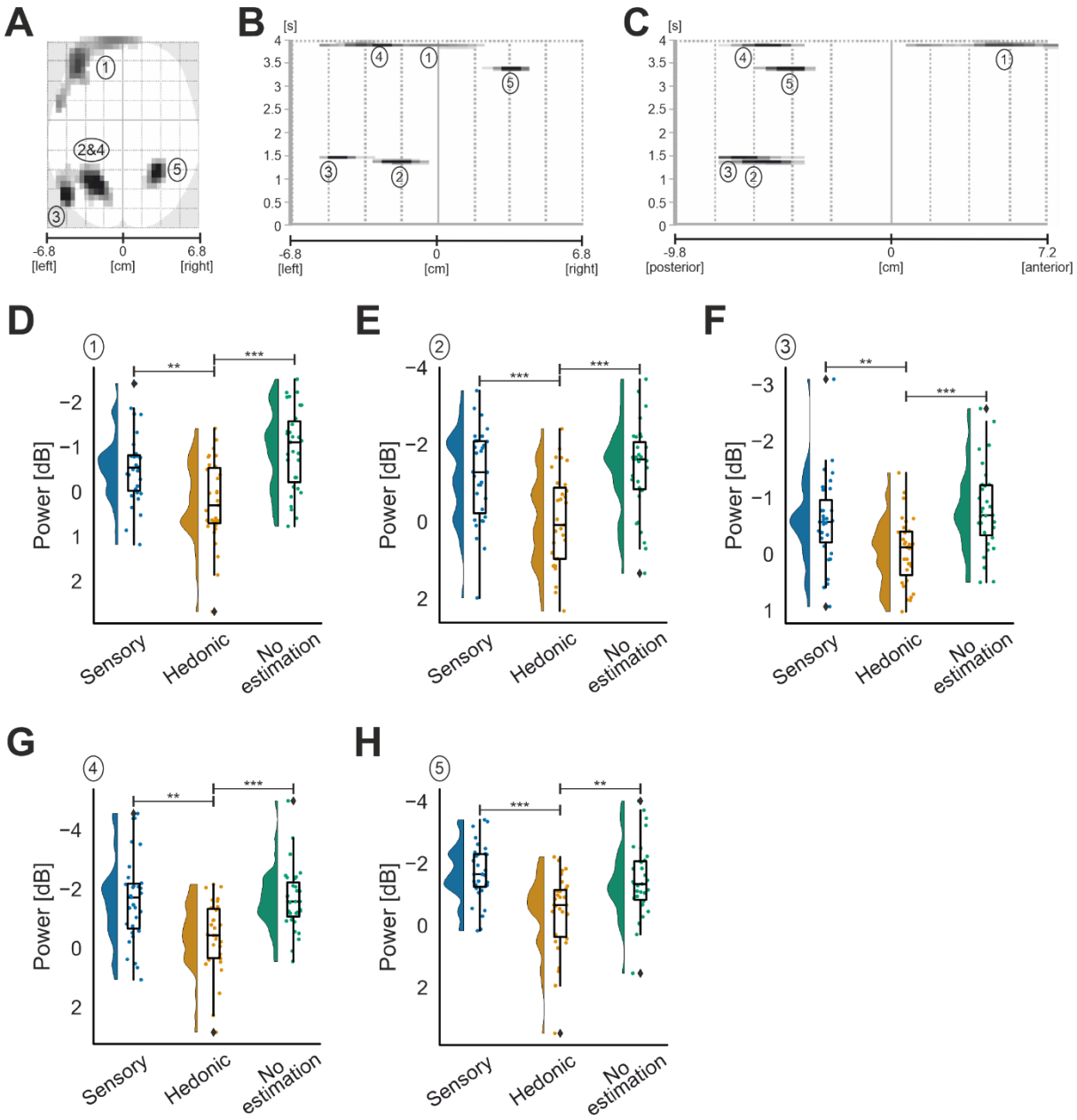

Figure 6.9 Standard scalp map of the statistically significant clusters in beta-band for the main effect of estimation ***(A)****. Statistically significant latency periods 0–4 s relative to the onset of movement are displayed over the horizontal axis of the scalp (from left −6.8 cm to right 6.8 cm)* ***(B)****, and over the vertical axis of the scalp (from posterior −9.8 cm to anterior 7.2 cm)* ***(C)****. Raincloud plots (Allen et al., 2019) showing the distribution grand average beta-band power values for significant clusters for the main effect of estimation in cluster 1* ***(D)****, cluster 2* ***(E)****, cluster 3* ***(F)****, cluster 4* ***(G)****, and cluster 5* ***(H)****. The half violin plots depict the probability distributions of the data. The individual dots show data points from each participant. The boxplots indicate the median, upper and lower quartiles, as well as the IQR between the 25th and 75th percentile, whilst the whiskers represent scores outside of the IQR. Statistically significant differences are denoted as * for p < .05, ** for < .01 and *** for < .001.*

6.3.4.2.2 Interaction effects

Two significant clusters were identified for the interaction effect between texture and estimation, Figure 6.10A. The largest cluster (k=94) was located over temporoparietal areas and spread to precentral regions, $F(2, 16.14) = 15.05, p < .001, \eta_p^2 = 0.33$. The cluster peaked at 963 ms and 982 ms and encompassed approximately 57 ms duration. Increased ERD was observed for hessian compared to silk when exploring under hedonic estimation ($p < .001$; Table 6.3), whilst no estimation ($p = .005$; Table 6.3) produced greater ERD for silk compared to hessian. In addition, ERD increased during hedonic estimation condition when compared to no estimations for hessian ($p < .001$; Table 6.3).

Table 6.3. Descriptive statistics for each significant cluster for the interaction effect in beta-band

	Sensory				Hedonic				No Estimation			
	Hessian		Silk		Hessian		Silk		Hessian		Silk	
Cluster	M	SD	M	SD	M	SD	M	SD	M	SD	M	SD
One	−0.69	1.18	−0.45	0.94	−1.67	1.56	−0.33	1.19	−0.05	1.27	−0.75	1.36
Two	−0.6	1.53	−0.36	1.13	−1.41	1.77	0.2	1.66	0.01	2.12	−0.87	1.61

Cluster two (k=76) for the interaction effect lasted for approximately 75 ms in duration and peaked at 1021 ms, the cluster was located over contralateral occipital areas, $F(2, 23.95) = 9.72, p < .001, \eta_p^2 = 0.24$. The interaction between texture and estimation revealed that ERD significantly increased for hedonic estimation of hessian compared to silk ($p < .001$; Table 6.3), whilst no estimation produced greater ERD for silk relative to hessian ($p = .043$; Table 6.3). Further, ERD increased for hedonic estimations compared to no estimations for hessian ($p = .013$; Table 6.3).

Overall, the interaction effect between texture and estimation revealed two clusters: one in contralateral temporoparietal regions and one in contralateral occipital regions. Notably, the results showed an increase in ERD for hedonic estimations of hessian relative to hedonic estimations of silk.

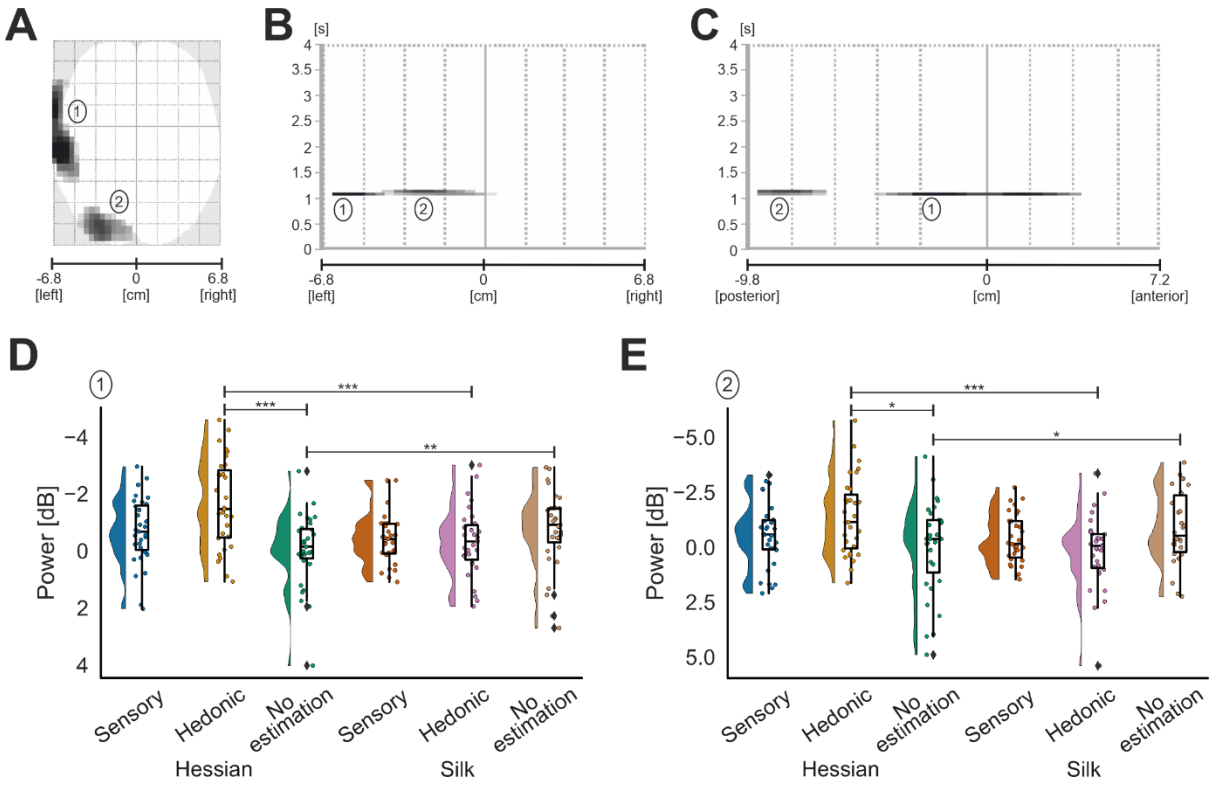

Figure 6.10 Standard scalp map of the statistically significant clusters in beta-band for the interaction effect between texture and estimation ***(A)****. Statistically significant latency periods 0–4 s relative to the onset of movement are displayed over the horizontal axis of the scalp (from left −6.8 cm to right 6.8 cm)* ***(B)****, and over the vertical axis of the scalp (from posterior −9.8 cm to anterior 7.2 cm)* ***(C)****. Raincloud plots (Allen et al., 2019) show the distribution of grand average beta-band power values for significant clusters for the interaction effect in cluster 1* ***(D)****, and cluster 2* ***(E)****. The half violin plots depict the probability distributions of the data. The individual dots show data points from each participant. The boxplots indicate the median, upper and lower quartiles, as well as the IQR between the 25th and 75th percentile, whilst the whiskers represent scores outside of the IQR. Statistically significant differences are denoted as * for p < .05, ** for < .01 and *** for < .001.*

6.4 Discussion

The purpose of this study was to examine oscillatory brain activity during active exploration of rough and smooth surface textures under conditions which necessitate estimation of sensory or hedonic characteristics compared to no estimation conditions. Active tactile exploration with the index finger resulted in contralateral alpha-band ERD over sensorimotor regions with greater ERD for rough (hessian) compared to smooth (silk) textures. Interestingly, hedonic estimations of hessian were associated with increased alpha-band ERD in frontal and occipital regions and increased beta-band ERD for temporoparietal and occipital regions, relative to hedonic estimations of silk. For the first time, touch behaviours were used as parametric regressors to investigate the effect of texture and estimation on neural responses while accounting for variation in touch behaviour at a single trial level.

Alpha-band ERD was stronger in contralateral sensorimotor regions during exploration of rough hessian compared to smooth silk, consistent with previous findings (Henderson et al., 2022). Rough textures likely increase the firing rate of Merkel cells and Meissner corpuscles, which may produce greater alpha-band ERD (Cascio & Sathian, 2001; Gamzu & Ahissar, 2001; Johansson & Vallbo, 1979; Vallbo et al., 1995). Further, the cluster peaked within a few hundred milliseconds of movement onset, suggesting the first neural response to the processing of physical attributes such as roughness (Ballesteros et al., 2009; McComas & Cupido, 1999). Previous passive touch research reported that smoother textures increase cortical activation (Ballesteros et al., 2009; Genna et al., 2018; Moungou et al., 2016), suggesting that activation in response to rough and smooth textures may differ depending on the mode of tactile stimulation. Future research should investigate active and passive modes of stimulation whilst manipulating surface roughness.

Sensory and no estimation conditions showed increased alpha- and beta-band ERD relative to hedonic estimations. Alpha-band ERD manifested as an ipsilateral posterior parietal cluster, an area associated with sensory integration (Hyvärinen, 1982; Mountcastle et al., 1975), while beta-band ERD demonstrated a network of contralateral frontal and bilateral posterior parietal regions. Alpha-band ERD in parietal regions enhances processing of task-relevant sensory information (Klimesch et al., 2007; Pfurtscheller & Klimesch, 1991), while beta-band connects somatosensory regions to higher-order parietal and frontal regions (Adhikari et al., 2014). Contrary to our hypothesis, hedonic estimations generally demonstrated a decrease in ERD relative to sensory and no estimation conditions. Positivity and negativity are proposed to serve as bipolar opposites, implying that an increase in one dimension corresponds to a decrease in the other (Becker et al., 2019; Wundt, 1897). A fMRI meta-analysis suggests regions of the prefrontal and anterior cingulate cortex demonstrate dissimilarity in concordant activation to positive and negative affect, supporting bipolarity in regions of the brain (Lindquist et al., 2016). Pleasant and unpleasant stimuli may result in differential changes in ERD/S, which cancel out activation when averaging trials across both types of hedonic estimations (negative/positive). The interaction effect between texture and estimation type supports this hypothesis, as differences were observed between hedonic estimations of hessian and silk in frontal, temporoparietal and occipital regions.

Hedonic estimations of hessian elicited significantly greater ERD than silk in contralateral temporoparietal beta-band. Decreases in beta-band power are associated with increased subjective preference for food, face, olfactory, auditory, and thermal stimuli (Bauer et al., 2015; Son & Chun, 2018; Tashiro et al., 2019; Yuan & Liu, 2022). In temporoparietal regions, beta-band power distinguishes pleasant from unpleasant tactile stimuli during passive stimulation of the hairy skin, where the least preferred texture elicited greater ERD than more preferred textures (Singh et al., 2014). Further, ERPs elicited in response to rough

tactile gratings were found to originate from the insular cortex (Ballesteros et al., 2009), a region tightly linked with the processing of hedonic preference (Morrison, 2016; Perini et al., 2015). Increased temporoparietal beta-band ERD during hedonic ratings of hessian may be due to activation of higher-order somatosensory association regions, with the insula potentially playing a role in distinguishing the hedonic value of perceived unpleasant tactile stimuli.

Activation of visual areas by tactile stimulation with textured surfaces suggests the role of the visual cortex in integrating visuo-haptic information to facilitate texture perception (Eck et al., 2013, 2016; Merabet et al., 2007; O'Callaghan et al., 2018; Sathian, 2016; Sathian et al., 2011; Simões-Franklin et al., 2011; Stilla & Sathian, 2008). The textured stimuli were visible to participants in this study, suggesting that alpha- and beta-band ERD in occipital areas reflects cross-modal visuo-haptic processing. Previous fMRI investigations of haptic texture processing demonstrate that estimation of surface roughness activates visual areas (Eck et al., 2013, 2016; Sathian et al., 2011; Stilla & Sathian, 2008), and visual texture modulates pleasantness ratings of haptically explored textures (Etzi et al., 2018). Therefore, increased occipital ERD during hedonic estimation of rough textures may reflect greater reliance on visual information than haptic information in sensory and no-estimation tasks. However, further investigation is necessary to confirm this hypothesis.

Increased alpha-band ERD was observed in contralateral frontal regions, both medially and laterally, during hedonic estimations of hessian relative to silk. The OFC has previously been implicated in the processing of a range of un/pleasant stimuli, including scents, words, temperature, and touch stimuli (Frey et al., 2009; Grabenhorst et al., 2007; Kringelbach, 2005; Lewis et al., 2007; Rolls et al., 2003a, 2003b, 2008; Rolls, 2010, 2020). The observed frontal activation may correspond to the DLPFC, which demonstrates increased

activation during estimation and comparison tasks with textured stimuli (Sathian et al., 2011; Simões-Franklin et al., 2011; Yang et al., 2017), and may reflect storage of tactile information in working memory to later inform estimation tasks (Barbey et al., 2013; Zhao et al., 2018a). Notably, a recent investigation of texture processing during active exploration of surface textures with functional near-infrared spectroscopy revealed prefrontal activation related to hedonic preference (Marschallek et al., 2023), further demonstrating the critical role of the prefrontal cortex in hedonic processing and estimation of surface texture during active touch.

The use of force plate technology to investigate texture perception during active touch increases ecological validity by allowing participants to optimise their exploratory procedure to gather somatosensory information. This approach also enables accurate data fusion, allowing for the time-locking of ERD/S to the onset of tactile exploration, and the removal of noisy trials with atypical touch behaviour, and the recording of touch behaviour such as load, friction and speed (Henderson et al., 2022). Interestingly, load increased for estimation tasks compared to no estimation tasks, suggesting exploratory behaviour varies by task type. Previous research shows that roughness estimates are modulated by exerted force, revealing a link between haptic exploration and perception of surface and object properties (Lederman & Taylor, 1972; Tanaka et al., 2014). Tactile data was also used by implementing covariates on a single-trial basis to account for variance in touch behaviour and understand the invariant effect of texture and estimation on the neural response, therefore, ERD differences seen between conditions cannot be ascribed to behavioural differences in active touch.

However, the present study is limited in replicating natural tactile experiences due to the use of forearm support and the EEG laboratory setting. Participants were also exposed to the two textured stimuli repeatedly over the testing period, which could lead to sensory

desensitisation (Klingner *et al.*, 2011; Graczyk *et al.*, 2018), though, repeated trials are necessitated by the time-frequency method (Cohen, 2017). Nevertheless, subjective ratings showed that participants were not desensitised to the textured stimuli per se, but rather sensitised to unpleasant rough stimuli. Furthermore, each block contained all three types of trial, which aimed to maximise participant engagement. However, this choice of task may be limited by the potential influence of prior knowledge from the estimation trials on participants' responses during the no-estimation trials. Additionally, active touch paradigms inherently increase the likelihood of motor-related artefacts in EEG data. However, despite this limitation, studying active touch is crucial for enhancing ecological validity and gaining insights into the potential unique neural mechanisms associated with active touch.

This study offers novel insights into texture perception during active touch and highlights the potential to improve ecological validity in future research by using force plate technology. In particular, the current paradigm may be used with neuroimaging methods with higher spatial resolution, such as magnetoencephalography, to explore the involvement of region-specific processing during hedonic estimation of texture. Additionally, future investigation should consider increasing the number of stimuli; this could be achieved using a gel-based EEG system which allows for longer recording times compared to saline-based EEG systems. Alternatively, employing neuroimaging techniques, such as functional near-infrared spectroscopy, that requires fewer trials for averaging could be explored (Marschallek *et al.*, 2023).

In conclusion, the study found that active exploration of textures had differential impacts on oscillatory brain activity, with rough textures increasing alpha-band ERD in contralateral sensorimotor regions. Hedonic processing of rough textures elicited increased temporoparietal beta-band and frontal alpha-band ERD, indicating selective activation of

higher-order brain regions for the processing of less preferred stimuli. Future research should continue to explore the neural mechanisms underlying the perception of textures during active touch, and their modulation by different modes of stimulation and cognitive tasks.

Chapter 7

Neural correlates of perceptual texture change during active touch

---

Jessica Henderson[1], Tyler Mari[1], Andrew Hopkinson[1, 2], Danielle Hewitt[1], Alice Newton-Fenner[1, 3], Timo Giesbrecht[4], Alan Marshall[5], Andrej Stancak[1, 3], Nicholas Fallon[1].

1 School of Psychology, University of Liverpool, Liverpool, UK.

2 Hopkinson Research, Wirral, UK

3 Institute of Risk and Uncertainty, University of Liverpool, Liverpool, UK.

4 Unilever, Research and Development, Port Sunlight, UK.

5 Department of Electrical Engineering and Electronics, University of Liverpool, UK.

This experiment used EEG to investigate texture change detection during ongoing active exploration.

This paper was published in Frontiers in Neuroscience (2023)
doi: doi.org/10.3389/fnins.2023.1197113
The format of the text has been modified to match the style of this thesis.

The roles of the co-authors are summarised below:

Jessica Henderson: Conceptualization, Methodology, Software; Formal analysis, Investigation, Data curation, Writing – original draft, Writing – review & editing, Visualisation, Project administration. **Tyler Mari**: Investigation, Writing – review & editing. **Andrew Hopkinson**: Methodology, Software, Writing – review & editing. **Danielle Hewitt**: Investigation, Writing – review & editing. **Alice Newton-Fenner**: Investigation, Writing – review & editing. **Timo Giesbrecht**: Conceptualization, Funding acquisition, Supervision. **Alan Marshall**: Conceptualization, Supervision, Writing – review & editing. **Andrej Stancák**: Conceptualization, Supervision, Writing – review & editing. **Nicholas Fallon**: Conceptualization, Methodology, Software, Formal analysis, Writing – review & editing, Supervision, Funding acquisition.

Abstract

Texture changes occur frequently during real-world haptic explorations, but the neural processes that encode perceptual texture change remain relatively unknown. The present study examines cortical oscillatory changes during transitions between different surface textures during active touch. Participants explored two differing textures whilst oscillatory brain activity and finger position data were recorded using 129-channel EEG and a purpose-built touch sensor. These data streams were fused to calculate epochs relative to the time when the moving finger crossed the textural boundary on a 3D-printed sample. Changes in oscillatory band power in alpha (8–12 Hz), beta (16–24 Hz) and theta (4–7 Hz) frequency bands were investigated. Alpha-band power reduced over bilateral sensorimotor areas during the transition period relative to ongoing texture processing, indicating that alpha-band activity is modulated by perceptual texture change during complex ongoing tactile exploration. Further, reduced beta-band power was observed in central sensorimotor areas when participants transitioned from rough to smooth relative to transitioning from smooth to rough textures, supporting previous research that beta-band activity is mediated by high-frequency vibrotactile cues. The present findings suggest that perceptual texture change is encoded in the brain in alpha-band oscillatory activity whilst completing continuous naturalistic movements across textures.

7.1 Introduction

The human brain processes ongoing sensory information by comparing incoming sensory information to previous stimulation, which enables humans to detect changes in their environment (Laufer et al., 2008). As humans, we explore our haptic environment through active touch and the glabrous skin on our hands and digits (Gibson, 1962; Wagner & Gibson, 2016). Active touch is integral in identifying and evaluating objects and surfaces by optimising contact pressure, speed, and velocity (Lederman & Klatzky, 2009). The present study aimed to investigate how the brain encodes continuous tactile information associated with changes in touch experience by assessing neural oscillations related to perceptual texture change.

Processing of stimulus change in the brain has previously been investigated using EEG and oddball tasks (Naatanen et al., 1978), wherein participants are exposed to one repetitive stimulus and then presented with a novel oddball stimulus. This type of paradigm results in an ERP response called mismatch negativity (MMN); a correlate of auditory change perception that peaks around 100–300 ms following novel stimuli (Näätänen et al., 2005, 2007). Though primarily studied in the auditory domain, MMN effects have been reported in other sensory modalities such as vision (Stefanics et al., 2014) and somatosensation (sMMN; Butler et al., 2011, 2012; Chen et al., 2014; Hu et al., 2013; Restuccia et al., 2007). Oddball paradigms present stimuli for fixed intervals with a period of rest prior to stimulation, thus revealing information about the brain processing of individual events and features. A drawback of this approach is that this type of stimulation is not representative of real-world experiences, where ongoing sensory processing occurs, and change detection is an additive experience rather than an isolated feature.

In contrast to ERP analysis, investigating neural oscillations using time-frequency analysis provides a more accurate representation of ongoing sensory processing in the brain, by offering insights into neuronal synchrony and ongoing inter-neuronal communication (Mathalon and Sohal, 2015; Morales and Bowers, 2022). This approach enables the investigation of the summation of neural oscillations and ongoing changes in the brain in response to external stimuli (Cohen, 2014). Alpha-band and beta-band oscillations are attenuated during tactile stimulation or voluntary movement (Chatrian et al., 1958; Pfurtscheller, 1981; Salmelin and Hari, 1994) over the primary somatosensory and motor cortices, respectively (Brovelli et al., 2004). Attenuation of alpha- and beta-band oscillations are thought to reflect increased cortical activation, whereas the presence of synchronous oscillations is indicative of cortical areas at rest (Pfurtscheller, 1992, 1999).

Texture processing in the brain manifests bilaterally as attenuation of alpha-and beta-band rhythms relative to a rest period (Genna et al., 2018; Henderson et al., 2022). Whilst active exploration of texture has been investigated with EEG (Henderson et al., 2022), the neural mechanisms that underpin the processing of texture change during naturalistic explorations are relatively unknown. Processing of rough and smooth textures demonstrate altered cortical responses, with smooth textures typically eliciting increased brain activation relative to rougher surfaces during passive tactile stimulation (Genna et al., 2018; Moungou et al., 2016). Comparatively, our recent study investigating the neural correlates of texture perception with active touch found increased attenuation of beta-band oscillations for smooth textures and increased attenuation of alpha-band oscillations for rough textures (Henderson et al., 2022). Taken together, the literature indicates that cortical changes which occur during texture processing are modulated by textural properties, such as surface roughness. Therefore, change detection in the brain during ongoing processing is also likely to demonstrate altered neural oscillatory response as an indication of encoding textural change.

Change detection in the brain has been previously investigated using time-frequency analysis of MMN ERPs, which revealed increased theta-band power across auditory (Fuentemilla et al., 2008; Hsiao et al., 2009; Ko et al., 2012), visual (Liang et al., 2017; Stothart & Kazanina, 2013), and somatosensory modalities during unattended pressure stimulation to the finger pad (Zhang et al., 2019). Theta-band oscillations have also been linked with top-down memory processes, which led to increased power in frontal midline regions (Klimesch, 1999; Klimesch et al., 2008). Further, ERPs in the time-domain are suggested to manifest as theta-band changes in the time-frequency domain (Bernat et al., 2007; Harper et al., 2014). Therefore, theta-band power may reflect event-related changes in neural processing of texture change. However, it should be noted that findings from oddball tasks are not representative of complex environmental change, and therefore oscillatory brain activity may differ under active ongoing exploration.

The present study utilised touch sensor technology to investigate cortical oscillatory changes in alpha-, beta- and theta-bands during active touch of two adjacent textures. A touch sensor was used to quantify touch behaviour in real-time and compute time markers from when the index finger crossed the point of texture transition. Time markers were subsequently integrated with EEG data to consider event-related changes in oscillatory activity. We hypothesised that brain oscillations would show differences related to texture change; specifically, there will be reductions in alpha- and beta-band power over sensorimotor areas related to perception of texture change. Further, we hypothesise that theta-band power would increase as an oscillatory reflection of perceptual change mechanisms in frontal regions. A secondary analysis compared texture change from rough-to-smooth, relative to smooth-to-rough transitions. We hypothesised beta-band power would decrease over sensorimotor areas when transitioning from rough to smooth, whereas alpha-band power would decrease when transitioning from smooth to rough, demonstrating texture preference

for smoothness in frequency bands in line with our previous research.(Henderson et al., 2022).

7.2 Method

7.2.1 Participants

Thirty-five participants were recruited with no history of any neurological condition, or aversion or allergies to any textures. Visual inspection of the data for the presence of any movement or muscle artefacts was conducted. Five participants were excluded due to over 45% of trials being marked for rejection or when over 10% of channels were interpolated. The final sample included 30 participants (12 males, 2 left-handed), aged 28.43 ± 5.05 years (mean ± SD). Participants were reimbursed at a rate of £10 per hour for their time. The study was approved by the Research Ethics Committee of the University of Liverpool and all participants gave fully informed written consent at the start of the experiment in accordance with the Declaration of Helsinki.

7.2.2 Procedure

Participants were seated in a dimly lit Faraday cage with a 19-inch LCD monitor approximately 1 m in front of them. The tactile contrast task and practice trials were presented using PsychoPy (Peirce et al., 2019). Six-axis touch sensor and EEG data were recorded during the tactile contrast task. An elbow rest was used to stabilise and support the arm whilst maintaining position over the measuring plate of a six-axis touch sensor. The height and position of the support were adjusted for each participant.

7.2.2.1 Stimuli

Texture stimuli were designed using algorithms adapted from Kanafi (2022) implemented in MATLAB (The MathWorks, Inc., USA), which produce isotropic textures representative of rough surfaces found in the real-world with well-defined power spectral distribution (PSD) given by Equation 2:

Equation 2. Isotropic texture calculation.

$$\phi(|q|) = \begin{cases} C, & if\ q_0 \le |q| \le q_r. \\ C\left(\frac{|q|}{q_r}\right)^{-2(1+H)}, & if\ q_r \le |q| \le q_1. \\ O, & otherwise. \end{cases}$$

where *C* is a constant which determines roughness amplitude, q_0 and q_1 define the lower and upper limits of the wavenumbers *q*, and q_r is the wavenumber above which the power spectral density is reduced with increasing wavenumber at a rate which is dictated by *H*, the Hurst roughness exponent. For the texture used in the study, $q_0 = 1200$ rad/m, $q_1 = 3600$ rad/m and $q_r = 2400$. The corresponding range of wavelengths in the texture is from 2.62–5.24 mm. The constant *C* was adjusted to achieve an RMS surface roughness of 0.15 mm.

Textured stimuli were manufactured as a 100 × 50 mm resin tile, produced with a Formlabs Form 3 Stereolithography (SLA) 3D printer, where 40 mm of the tile was smooth and 40 mm was rough, with a 10 mm transition period in the centre where the two textures merged (Figure 7.1). During naturalistic texture exploration, humans typically use lateral movement across interior surfaces rather than edges (Lederman & Klatzky, 1987). Therefore, it was important the stimuli did not include a sharp edge between the textures, as the perception of edge properties is more indicative of structure-related perception, such as shape, rather than a textural change. Thus, the transition period was implemented in the MATLAB algorithm to reduce the sharp edge between the two stimuli to investigate the neural processing of texture rather than other haptic features. The tile was mounted on the measuring plate of the touch sensor in a landscape position.

*Figure 7.1 3D printed stimuli 100 mm × 50 mm where left is the smooth portion of the tile and right is the rough portion of the tile. Superior **(A)** and horizontal view **(B)**.*

7.2.2.2 Tactile contrast task

The tactile contrast task comprised of four blocks, each lasting approximately two minutes. Participants were instructed to use a unilateral movement with the distal phalanx of their right index finger to complete sweeps across the texture. An 18 mm circle, the average width of a human index fingertip (Srinivasan, 2003), was displayed on the screen to denote a finger sweep across a 10 cm line, in concordance with the 3D printed sample size. The dot moved across the plane at 2.5 cm/s; therefore, the index finger completed one sweep of the 3D texture in four seconds. Participants were trained to perform this movement prior to the experimental task by following the same visual cues whilst exploring an entirely smooth tile. Trials lasted four seconds and were performed back-to-back in a continuous block, meaning each block contained both smooth-to-rough transitions and vice-versa. Each block contained

30 trials (finger sweeps), totalling 120 trials over the experiment (60 trials per condition). Blocks were counterbalanced by starting texture (i.e., starting on smooth or rough). Participants kept their finger on the texture throughout the block. The researcher offered participants a break at the end of each block while changing the stage's orientation.

7.2.3 Recordings

EEG data were recorded continuously using a 129-channel sponge-based Geodesic sensor net (Magstim EGI, UK). The net positioning was aligned to three anatomical landmarks, two preauricular points and the nasion. Electrode impedances were kept below 50 kΩ. A recording band-pass filter was set at 0.001–200 Hz with a sampling rate of 1000 Hz. Electrode Cz was used as a reference electrode. The six forces and torques acting on the tile due to the finger touch were recorded using a Hopkinson Research six-axis sensor (Hopkinson Research, 2020), with a sampling rate of 1000 Hz. Finger position in the XY plane was calculated from the block averaged (100 Hz) forces and torques.

7.2.4 Pre-processing

EEG pre-processing was conducted using BESA v 6.1 (MEGIS GmbH, Germany). Eye blinks and electrocardiographic artefacts were removed using principal component analysis (Berg and Scherg, 1994), which allowed the researcher to assess the feasibility of components for each participant and each experimental block. Data were filtered using 0.5 Hz high-pass and 100 Hz low-pass filters, with a notch filter (50 Hz ± 2 Hz). Data were visually inspected for the presence of any movement or muscle artefacts. Trials containing artefacts were excluded from subsequent analyses. EEG signals were downsampled to 256 Hz and re-referenced using the common average method (Lehmann, 1984).

Six-axis sensor data were cleaned and visually inspected using in-house software developed in Python 3 (van Rossum & Drake, 2009). Data were epoched relative to the visual trial onset marker. Trials were rejected when 25% of samples were missed due to recording issues. Texture transition was calculated from position data from when the finger position crossed ± 5 mm on the x-axis corresponding to the centre point of the sample which corresponds to a timepoint within the transition period from one texture to the other. Relative time from the visual trigger to the texture transition was calculated. After EEG and six-axis sensor pre-processing were complete, the average number of trials for each condition across all participants was: smooth to rough, 39.57 ± 9.77; rough to smooth, 41.70 ± 7.78. The average number of accepted trials did not differ across conditions ($p > 0.05$).

7.2.5 Analysis

Texture transition markers were computed relative to trial onset marker times, which were synchronised to EEG data. Data were epoched −2–2 s relative to the transition marker. The power spectra were computed in MATLAB (The MathWorks, Inc., USA) using Welch's power spectral estimate method. The power spectral densities were computed from 1 s windows shifted in overlapping 0.01 s increments to yield a power time series of 400 points. Data were smoothed using a Hanning window. The power spectral densities were estimated in the range of 1–80 Hz with a frequency resolution of 1 Hz. *Z*-values were computed after the power calculation at each time bin using the median and median absolute deviation (MAD) across trials and conditions (Arnal et al., 2015; Klimesch et al., 1998; Pfurtscheller, 1999). Comparing the period texture change to an active baseline of texture processing during active touch allows for the isolation of the neural correlates associated with the phenomena of texture change detection during active touch. Therefore, the obtained z-transformed power values were evaluated prior to texture change (−650 – −200 ms) and during texture change (0–450 ms). The pre-transition period was selected as an active baseline instead of a pre-

stimulus baseline with rest, as ongoing tactile perception provides a more naturalistic paradigm to investigate the complexities of sensory experience during perceptual change paradigms; this approach has been previously demonstrated in EEG research investigating auditory and visual change detection within complex scenes and environments (Boubenec et al., 2017; Kelly & O'Connell, 2013; O'Connell et al., 2012).

Permutation analyses with 5000 repetitions were implemented using *statcond.m* from the EEGLAB library (Delorme & Makeig, 2004; Maris & Oostenveld, 2007). The permutation analysis was conducted as an exploratory data analysis across all 128 electrodes with power averaged over the time period and frequency band of interest. This approach helps to reduce the likelihood of Type 1 errors while improving the statistical power of the analysis (Maris, 2004; Maris & Oostenveld, 2007). Identified electrodes showing significant differences between conditions ($p < 0.05$) were grouped into clusters based on spatial neighbours, and changes in absolute power *z*-scores subjected to paired samples t-test to investigate the direction of the effect. The results were corrected for multiple comparisons using the Bonferroni correction. Artefactual data were removed from identified electrodes where the *z*-score exceeded 5 MAD, in line with previous recommendations on identification of statistical outliers (Thatcher et al., 2019).

To assess the variability in the unilateral finger exploration, mean load (g) was computed for each pre-transition and transition period used in the EEG analysis. These data were then averaged over each participant and compared using paired samples *t*-test.

7.3 Results

7.3.1 Load

Mean values of total load were 30.45 ± 19.54 g (M ± SD) for the pre-transition period, and 50.44 ± 5.05 g during the transition period. A paired samples *t*-test demonstrated no significant difference between load in the two time periods.

7.3.2 EEG

Absolute power, normalised with a *z*-score transformation, was evaluated during pre-transition texture processing (−650 – −200 ms) and during texture transition (0–450 ms). Permutation analyses with 5000 repetitions ($p < 0.05$) identified one contralateral electrode and a cluster of two ipsilateral electrodes which demonstrated statistically significant effects of texture change, regardless of texture change direction, when compared to pre-transition texture processing in alpha-band (8–12 Hz). Both were located over bilateral sensorimotor areas. Permutation analysis found no statistically significant electrodes for beta- (16–24 Hz) or theta-band (4–7 Hz) when comparing pre-transition texture processing to texture transition. Further, texture transition was then split by condition for comparison of oscillatory changes associated with smooth-to-rough transitions and vice-versa. When comparing the two conditions using permutation analysis, one central electrode demonstrated a statistically significant effect of direction of texture change during the transition period for beta-band, whereas no statistically significant effect was identified for alpha- or theta-band.

Paired samples *t*-tests were computed for electrodes identified by permutation analysis. A significant decrease in alpha-band power during texture change when compared to ongoing texture processing was revealed for the contralateral electrode identified (electrode 35), $t(29) = 3.57, p = 0.001$, Figure 7.2A. A cluster of two electrodes over

ipsilateral sensorimotor regions (110 and 103, C6 according to the 10-10 system; Luu & Ferree, 2005) were found to be significant, Figure 7.2C. Paired samples *t*-test demonstrated a significant decrease in alpha-band power during texture transition relative to pre-transition texture processing, $t(29) = 3.03, p = 0.005$.

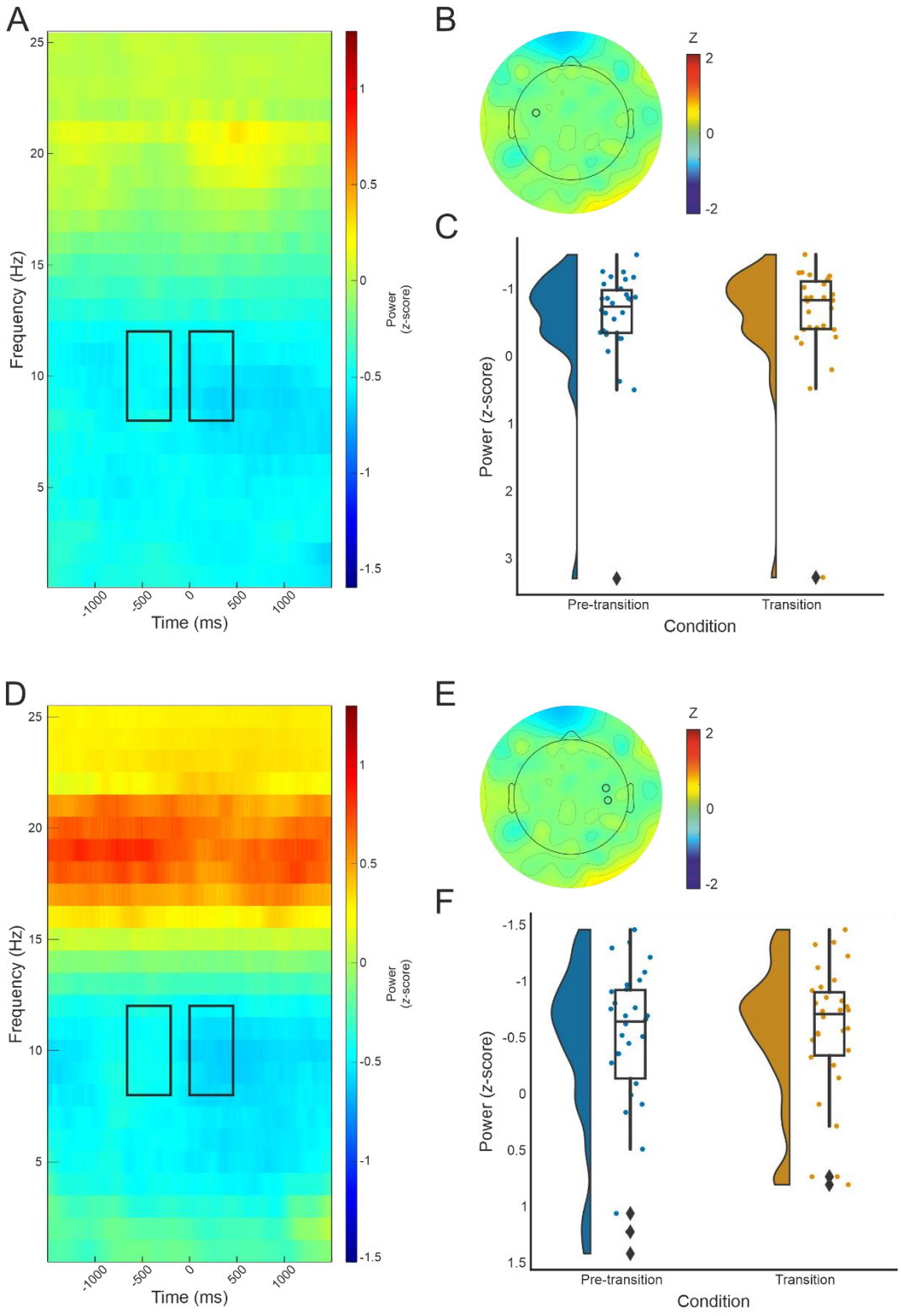

Figure 7.2 Time–frequency spectrograms for electrode 35 ***(A)*** *and cluster one (electrodes 103 and 110)* ***(D)****, black boxes indicate the time (pre-transition texture processing −600 – −200, and transition processing 0–450 ms) and frequency (8–12) Hz) where significant effects were identified. The half violin plots depict the probability distributions of the data in electrode 35* ***(C)*** *and cluster one (electrodes 103 and 110)* ***(F)****. The individual dots show data points from each participant. The boxplots indicate the median, upper and lower quartiles, as well as the interquartile range (IQR) between the 25th and 75th percentile, whilst the whiskers represent scores outside of the IQR. Grand average topographic maps for the alpha-band are shown, with electrode 35* ***(B)*** *and electrodes 110 and 103* ***(E)*** *locations overlayed.*

In the beta-band, a statistically significant effect was identified over central sensorimotor regions in electrode 55, Figure 7.3. Transitioning from rough to smooth textures demonstrated a significant decrease in power when compared with transitioning from smooth to rough, $t(29) = 3.03, p = 0.005$.

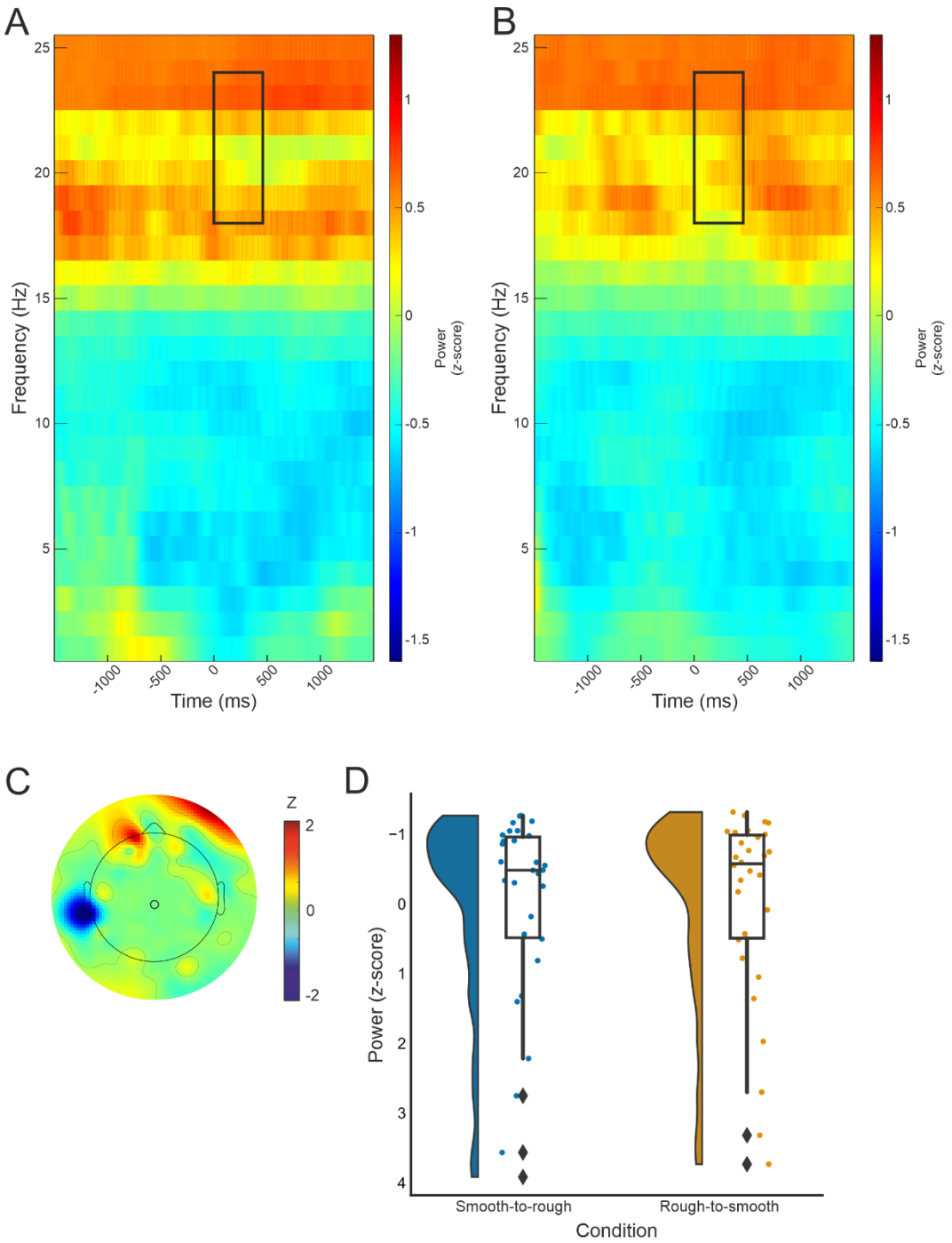

Figure 7.3 Time–frequency spectrograms for electrode 55 for smooth to rough transition ***(A)*** *and rough to smooth transition* ***(B)****, black boxes indicate the time (0–450 ms) and frequency (16–24) Hz) where statistically significant effects were identified. The half violin plots depict the probability distributions of the data in electrode 55* ***(D)****. The individual dots show data points from each participant. The boxplots indicate the median, upper and lower quartiles, as well as the IQR between the 25th and 75th percentile, whilst the whiskers represent scores outside of the IQR. Grand average topographic maps for beta-band are shown, with electrode 55 location overlayed* ***(C)****.*

7.4 Discussion

The present study aimed to establish how the brain encodes texture change by assessing oscillatory differences in alpha-, beta- and theta-bands as the finger transitions from one texture to another during active touch exploration. Texture transition produced significant differences in alpha and beta frequency bands, whereas no statistically significant effects were observed in theta-band. In line with our hypothesis, alpha-band power over sensorimotor cortical regions decreased during texture transition when compared to pre-transition texture processing. Further, beta-band power decreased during texture transition when transitioning from rough-to-smooth textures over central regions, relative to smooth-to-rough trials, supporting previous findings from our lab (Henderson et al., 2022). Results indicate that perceptual texture change is observable in oscillatory brain activation patterns recorded by EEG under a naturalistic paradigm.

Bilateral decreases in alpha-band power were observed for texture transition relative to pre-transition texture processing over sensorimotor regions. Alpha-band power is associated with bilateral activation following tactile stimulation (Tamè et al., 2016; Genna et al., 2018), wherein a decrease in power, or attenuation of oscillations, signifies an increase in cortical processing (Cheyne et al., 2003; Gaetz and Cheyne, 2006). The present results indicate that it is likely that alpha-band oscillations also reflect perceptual texture change mechanisms in the brain, which manifests as increased cortical activation (decrease in power) to encode novel or changing tactile input from mechanoreceptors. Previous research with active touch has suggested that alpha-band power is also associated with roughness, wherein rougher textures increase cortical activation (Henderson et al., 2022), whilst passive touch research reports increased cortical activation for smoother textures (Ballesteros et al., 2009; Moungou et al., 2016; Genna et al., 2018). In contrast to our hypothesis, the present study

demonstrated no significant effect in alpha-band when comparing rough to smooth transition and vice-versa. This suggests that the effects found in alpha-band for this study are representative of change detection, rather than roughness modulation. Therefore, it is possible that the role of alpha-and oscillations during change detection differs from that during roughness encoding in tactile stimulation, though further research is necessary to confirm this hypothesis.

Beta-band power was decreased over central sensorimotor regions when comparing transition from rough to smooth with the opposite condition. This supports our hypothesis that smooth textures increase cortical activation in the beta-band and accords with previous studies using passive (Genna et al., 2018; Moungou et al., 2016) as well as active touch paradigms (Henderson et al., 2022). The duplex theory states that the perception of fine textures is mediated by high-frequency vibrations from tactile elements (Hollins & Risner, 2000; Katz, 1925, 1989). Previous research suggests that beta-band activity is mediated by vibration intensity (Park et al., 2021), which contributes to observed difference in the EEG signal between rough and smooth textures (Henderson et al., 2022). Interestingly, the present study demonstrated that texture modulates beta-band power during transitioning between two textures, which, to the best of our knowledge, is the first instance demonstrating this effect.

Increased frontal theta-band oscillations have previously been shown to coincide with the enhancement of the sMMN component (Zhang et al., 2019). We hypothesised that such components may be visible in theta-band changes in time-frequency analysis. However, in this naturalistic active touch paradigm, perceptual texture change did not modulate theta-band power per se. Therefore, identification of change detection ERP components may not be detectable with the current temporal resolution (100 Hz) computation of time markers. Time-locking may need to be more precise to directly compare well known change perception

ERPs, such as the sMMN, in ongoing time-frequency changes. However, this is the first known study to investigate change perception in active touch in a naturalistic paradigm, offering a more ecologically valid approach than previous oddball paradigms with stationary participants. Therefore, it is also possible that ERP correlates of change detection seen in previous studies differ, or are not present, when performing ongoing explorations of texture.

The present study used continuous tactile stimulation to investigate perceptual texture change in the way that we typically encounter it in our environment, as change occurring on top of an ongoing sensory experience (Gallace et al., 2006, 2007). Contrasting with rest improves the signal-to-noise ratio of post-stimulus activity (Toro et al., 1994). There was no rest period included in this paradigm, which incidentally reduces the signal-to-noise ratio and results in small effect sizes due to the comparison of brain oscillations with active baseline conditions. However, to understand the features of change detection, it was essential to compare texture change to ongoing tactile perception. Previous EEG research has investigated perceptual change detection using complex ongoing auditory (Boubenec et al., 2017) and visual stimuli (Kelly & O'Connell, 2013; O'Connell et al., 2012). Therefore, ongoing stimulation is appropriate for perceptual change paradigms, as they allow researchers to understand the complexities of sensory experience during more naturalistic tasks. Though future paradigms may also benefit from a period of pre-stimulus rest to improve the signal-to-noise ratio for additional analyses in tandem with an active baseline approach.

There are limitations to the present design. As a lab-based study, and due to the trial requirements for time-frequency EEG analysis (Cohen, 2016), participants were exposed to the two textured stimuli repeatedly over the course of the experiment. Therefore, it is likely that changes in texture were predictable, which may have developed expectations and diminished stimulus novelty. Further, repeated stimulation may have led to sensory

desensitisation (Graczyk et al., 2018; Klingner et al., 2011) and reduced task engagement (Lelis-Torres et al., 2017). However, repeated trials are necessitated by the time-frequency method (Cohen, 2016). Future research could consider the use of one repetitive stimulus embedded within a more complex paradigm with various novel stimuli and various gradations of intensity to manipulate the degree to which the textural change was detectable whilst maintaining novelty, engagement and reducing desensitisation.

In conclusion, the present study demonstrates that alpha-band activity is related to perceptual texture change during continuous texture exploration, whilst beta-band may be linked to the processing of vibrotactile cues. Therefore, this study hypotheses that alpha- and beta-band both play a functional role in acting as a change detection mechanism as well as processing surface properties of the texture, respectively (Henderson et al., 2022). However, the neural underpinnings of texture processing require further elucidation. Future research should consider using active exploration of one repetitive stimulus alongside various novel stimuli, which will enable researchers to maintain novelty and test the hypothesis that alpha-band activity encodes perceptual texture change. To our knowledge, the results demonstrate for the first time that the encoding of textural change detection can be measured in the brain during ongoing active exploration of surfaces.

Chapter 8
General Discussion

Previously, regions of the brain associated with texture processing have been investigated using a wide range of paradigms and stimuli, making it challenging to draw conclusions from individual studies. One aim of this thesis was to identify brain areas that are consistently activated during texture processing by conducting an ALE meta-analysis. Additionally, texture-specific processing was investigated by contrasting texture processing with other haptic processes. Moreover, the investigation of the neural basis of texture processing in the brain using EEG methods has previously focused on passive stimulation paradigms, due to the necessity of time-locking the EEG signal to the onset of an event. As a result, the neural correlates of texture processing during active touch were not well understood. The EEG experimental chapters in this thesis aimed to uncover the temporal characteristics of texture processing during active touch by evaluating changes in oscillatory brain activity. Furthermore, texture estimation tasks are known to modulate the BOLD response, despite this, electrophysiological characteristics of texture processing and estimation of surface features had yet to be delineated. This thesis set out to investigated how tactile estimation of sensory and hedonic features of textures modulated oscillatory activity, aiming to uncover the potential involvement of higher-order brain regions. Finally, this thesis explored the brain's response to texture change detection. To achieve these aims, more naturalistic conditions were simulated by including ongoing active tactile exploration, rather than utilising classical methods that include structured trials with long periods of rest.

8.1 Summary of findings

- The general processing of textures evoked contralateral primary somatosensory and motor regions, with bilateral activations in the secondary somatosensory, insula, premotor and supplementary motor cortices (Chapter 4).
- Texture-specific processing was found to elicit activation in the contralateral SII, and the SI, MI and IPL were found to be selectively activated when contrasting general texture processing with texture-specific processing (Chapter 4).
- Rougher textures, when compared to smooth and soft textures, were associated with increased alpha-band ERD in contralateral sensorimotor regions (Chapter 5 & Chapter 6).
- Smooth and soft textures, when compared to rough textures, induced greater beta-band ERD in bilateral and central sensorimotor regions (Chapter 5 & Chapter 7, respectively).
- Sensory and no estimations were found to increase ERD relative to hedonic estimations in ipsilateral parietal alpha-band and in a network of contralateral frontal and bilateral posterior parietal regions for beta-band (Chapter 6).
- Hedonic estimations of rough compared to smooth textures elicited greater contralateral frontal alpha-band ERD, increased beta-band ERD in contralateral temporoparietal regions, and produced stronger occipital ERD in both alpha- and beta-band (Chapter 6).
- Change detection of texture manifested as a reduction of alpha-band power in bilateral sensorimotor regions (Chapter 7).
- Appropriate consideration of experimental design, particularly baseline or control comparisons, is crucial when investigating the neural correlates of texture perception and ongoing texture processing (Chapter 4 & Chapter 7).

8.2 Themes

The experimental chapters (Chapter 4–7) of this thesis discussed the individual results of four empirical studies, and multiple reoccurring themes were identified. The neural processes related to texture processing were investigated using fMRI meta-analysis (Chapter 4) and EEG measures (Chapter 5–7). The use of ALE meta-analysis allowed for the identification of convergence of activation probabilities between independent research experiments. Concordant activation for texture processing was demonstrated in sensorimotor and premotor areas as well as higher-order activation in the SII and insula, while the contralateral SII elicited texture-specific activation when controlling for other haptic processes. Time-frequency methods were used when employing EEG, which allowed for the investigation of the underlying cortical processes relating to different surface textures and tactile estimation. Oscillatory power was modulated by surface texture in bilateral sensorimotor areas. Estimation of surface texture demonstrated altered cortical excitability, which was further modulated when investigated across different textures. In addition, texture transition demonstrated that perceptual texture change is encoded in oscillatory activity.

Chapter 5–7 utilised touch sensor technology to quantify active touch, allowing for the fusion of EEG and touch data. This new data-analysis pipeline was found to be crucial in analysing electrophysiological changes during active touch. Furthermore, Chapter 6 utilised touch behaviours as covariates on a single-trial basis, allowing for the investigation of the invariant effect of texture and estimation on the resulting neural response. The finding of texture-selective activation in the SII from the ALE meta-analysis led to a suggestion that future research should carefully consider baseline or control comparison used. Subsequently, the neural processing of texture change detection employed an active baseline of texture

exploration, allowing for the investigation of nuanced brain activity changes associated with texture change detection using a more naturalistic paradigm than previous research.

8.2.1 Sensorimotor processing

Across all experimental chapters in this thesis, texture processing was found to induce cortical activation across sensorimotor regions. Investigation of the spatial characteristics of texture processing with fMRI and ALE showed concordant activations for texture processing in contralateral SI and MI as well as the PMv and SMA (Chapter 4). The investigation of ERD/S changes associated with texture processing found ERD during active exploration of textures in contralateral alpha-band for one centroparietal electrode and bilateral beta-band in central and parietal electrodes (Chapter 5). In addition, active ongoing exploration of a textured tile was found to elicit a decrease in bilateral alpha-band power in contra- and ipsilateral central electrodes corresponding to sensorimotor regions (Chapter 7). Moreover, the observed decrease in alpha-band power was modulated by a change in texture, suggesting texture change detection may be reflected in alpha-band oscillatory activity from sensorimotor regions. Furthermore, touch behaviour was quantified and used as covariates in EEG analysis in Chapter 6. The results demonstrated contralateral ERD in sensorimotor regions, demonstrating the effect of texture on neural activity, even when accounting for corresponding changes in touch behaviour parameters such as load and friction generated.

The effect of sensorimotor activation across all four experimental chapters suggests that texture processing during active touch recruits primary somatosensory and motor areas which are well-associated with tactile processing and motor control (Morley et al., 2007; Papitto et al., 2020; Raju & Tadi, 2021; Tamè & Holmes, 2016). In addition, voluntary movement, planning, and response behaviour are reflected through activation of the PMv and SMA (Davare et al., 2006, 2008, 2009; Fogassi et al., 2001; Reader & Holmes, 2018; Romo

et al., 2004; Tanji, 2001; Tanji & Shima, 1996; Vingerhoets et al., 2013), demonstrating activation of secondary motor areas during motor control in the context of texture processing.

8.2.2 Textural properties modulate oscillatory activity

In this thesis, Chapter 5 and Chapter 6 report the consistent pattern of increased alpha-band ERD for rough compared to smooth textures in contralateral sensorimotor regions. Previous attempts to investigate the neural correlates of texture processing via stimulation of the glabrous skin have depended upon passive stimulation paradigms to accurately time-lock the EEG signal to the onset of tactile stimuli. Passive touch research has contributed to the hypothesis that smoother textures elicit increased cortical activation in comparison to rough textures (Ballesteros et al., 2009; Genna et al., 2018; Moungou et al., 2016). Henderson et al. (2022) conducted the first study to quantify changes in ERD/S related to texture processing during active touch by utilising touch parameters recorded from touch sensor technology, these data were subsequently combined with the EEG signal to time-lock events (Chapter 4). This initial study found the contradictory finding of increased alpha-band ERD for rough compared to smooth textures, which was later corroborated by findings in Chapter 6. Findings suggest active exploration of texture elicits a differential pattern of activation in comparison to passive touch.

Texture processing in the brain is an understudied area, and as a result, previous investigations have been limited. One issue is the lack of statistical power due to small sample sizes, ranging from 3–12 participants (Ballesteros et al., 2009; Eldeeb et al., 2019; Genna et al., 2016, 2017, 2018). Previously, for EEG analysis, it was arbitrarily recommended that a minimum of 20 participants should be included in the sample (Cohen, 2016). The EEG chapters in this thesis (Chapter 5–7) have a sample size of 26–31 participants, suggesting that the results from these investigations are more reliable and robust

than preceding. Furthermore, only one previous study has investigated the differences in processing varying textured stimuli with time-frequency analysis (Genna et al., 2018). Therefore, it is possible that the replicated finding presented in this thesis, of increased alpha-band ERD during exploration of rough compared to smooth textures, may also be applicable across different stimulation paradigms, including passive touch. However, further research is necessary to confirm this.

Previous fMRI findings suggest that the magnitude of the SI response to textured stimuli is greater in active touch conditions relative to passive touch (Simões-Franklin et al., 2011), which is thought to reflect an efference copy of the motor command being sent to the SI (Ariani et al., 2022; Gale et al., 2021). The suppression of redundant movement-related feedback is believed to occur via the efference copy, which is sent to the forward model to predict sensory consequences. As a result, tactile stimulation that was not anticipated is enhanced. The large and irregular spatial patterns of rough textures may be more challenging to predict than smoother textures, which have a closer and more regular structure. Suggesting that smoother textures may be more supressed during active exploration and thus demonstrating increased alpha-band ERD for less anticipated rough textures.

Although oscillatory activity in beta-band demonstrates bilateral modulation in sensorimotor regions for both smooth (Chapter 5 and Chapter 7) and soft textures (Chapter 5), these results support the hypothesis that smooth textures increase cortical activation relative to rough textures. Therefore, differences in alpha- and beta-band activity may be the result of increased activation of different populations of LTMR in the glabrous skin. For instance, increases in beta-band ERD may be due to the higher frequency vibrations that arise when the fingertip scans smoother textures (Hollins & Risner, 2000; Katz, 1925, 1989), suggesting that beta-band may encode high-frequency vibrations (Park et al., 2021).

Conversely, alpha-band ERD may be modulated by pressure and skin deformation as well as low-frequency vibrations, which activate Merkel cells and Meissner corpuscles, respectively (Cascio & Sathian, 2001; Gamzu & Ahissar, 2001; Johansson & Vallbo, 1979; Vallbo et al., 1995). The function of afferent fibres during active touch is understudied due to the methodological limitations of microneurography which requires participants to remain still with their muscles relaxed. To overcome this, numerical models have been developed to simulate the response of LTMR in the glabrous skin during different conditions (Gerling et al., 2014; Lesniak & Gerling, 2009; Saal et al., 2017; Wei et al., 2022). Notably, Wei et al. (2022) developed a model for predicting afferent tactile signals during active exploration and concluded that perception during active touch may rely on multiple coding mechanisms elicited by different classes of LTMR. Therefore, differences in alpha- and beta-band may reflect the different coding mechanisms in the brain.

Importantly, the findings across experimental chapters demonstrate that texture properties can modulate neural response. This finding is particularly significant in Chapter 5–7, which use touch sensor technology to accurately time-lock the EEG signal to the onset of exploration. Accurate time-locking is essential when investigating the response to stimuli in time-frequency analysis (Chatrian et al., 1958; Pfurtscheller, 1981; Pfurtscheller et al., 1993; Pfurtscheller & Neuper, 1992; Stancak et al., 2003; Stancak & Pfurtscheller, 1996a). Therefore, the additional process of computing accurate touch triggers has been shown to be crucial in the investigation of texture processing during active touch.

8.2.3 Higher-order processing

The findings from Chapter 4 and Chapter 6 of this thesis suggest the involvement of higher-order brain structures in texture processing and hedonic preference. It has been hypothesised that the SII plays a role in higher-order texture processing, specifically as the region

responsible for discriminating roughness (Kitada et al., 2005; Sathian et al., 2011; Servos et al., 2001; Stilla & Sathian, 2008). The ALE meta-analysis (Chapter 4) found that the SII is selectively activated when contrasting texture perception with other forms of haptic processing (e.g., shape), thus highlighting its role in texture processing. Interestingly, this finding emerged from using an active haptic baseline and led to the suggestion that future research should carefully consider baseline or control comparisons when investigating the neural correlates of texture perception. This suggestion was carried forward to Chapter 7 which used an active baseline of texture exploration to investigate oscillatory texture change mechanisms.

Hedonic preference has long been associated with higher-order brain regions; however, it is thought that the processing of hedonic preference recruits anatomical regions of the prefrontal cortex, insula, and subcortical limbic structures, rather than higher-order texture processing regions such as the SII (Berridge & Kringelbach, 2015). Chapter 6 supports this hypothesis, as ERD was increased for the least preferred stimuli in prefrontal and temporoparietal regions. Further, concordant activation was observed in the DLPFC during leave-one-out analysis, with contributing studies employing either estimation or comparison tasks (Chapter 4 Sathian et al., 2011; Simões-Franklin et al., 2011; Yang et al., 2017). Interestingly, additional brain imaging research has identified prefrontal activation when discriminating speed (Bodegård et al., 2000), shape (Mueller et al., 2019; Stoeckel et al., 2003), haptic size (Perini et al., 2020), and dot patterns (Harada et al., 2004). Together this suggests that higher-order regions play a cognitive role in the evaluation and estimation of tactile properties, including surface texture and its hedonic value.

Concordant activation during texture processing from bilateral insula was confirmed with ALE analysis, and increased temporoparietal beta-band ERD was hypothesised to

originate from the insula, in line with previous research (Ballesteros et al., 2009). The integration of sensation, emotion, and cognition is linked with activation of the insula (Craig, 2002, 2009; Craig et al., 2000). Somatosensory and motor tasks engage the insula without the inclusion of cognitive or emotional evaluation (Kurth et al., 2010), although both increases in beta-band ERD and concordant activation were found when using estimation tasks. Therefore, this thesis suggests the role of the insula may be to integrate somatosensory information to inform higher-order cognitive decisions about textural properties or hedonic preference which warrants further research.

8.3 Limitations

Surface texture is often quantified by roughness/smoothness, hardness/softness, stickiness/slipperiness and warmth/cool (Lieber & Bensmaia, 2022). This thesis did not modulate surface temperature, thus focusing on texture processing through mechanoreceptors rather than thermoreceptors. The stimuli used in Chapter 5–7 are limited as they do not encompass the three remaining sensory continua. Instead, the stimuli focus on roughness/smoothness and softness/hardness, which were identified as they are argued to be the most salient dimensions of texture (Okamoto et al., 2013). However, in the real-world there is a wide range of diverse textures, most of which fall within the sensory continua outlined, though other distinctive surface attributes are not accounted for (e.g., fuzziness, bumpiness, velvetiness; Lieber & Bensmaia, 2022). EEG studies (Chapter 5–7) used two or three textures. This limited number of stimuli was necessary for the ERD/S method which requires repeated trials for each condition to obtain a good signal to noise ratio (Cohen, 2016). Therefore, the current investigations cannot draw conclusions about all textures but rather make generalisations based on the properties of the textures used.

Findings from Chapter 5–7 are limited by the spatial resolution of EEG (Gage & Baars, 2018). This issue arises from cortical current traveling though organic matter with varying levels of conductivity, before being measured across multiple neighbouring electrodes on the scalp (Srinivasan et al., 1996). Thus, making it difficult to infer the location of neuronal activity in the cortex from EEG signals. Therefore, the limited spatial resolution should be considered when interpreting the findings of experimental chapters using EEG methods.

The fMRI meta-analysis (Chapter 4) included 13 studies, which is less than the recommended 17 for a reliable ALE analysis (Eickhoff et al., 2016). Yet, recent guidance from Müller et al. (2018) advises that smaller sample sizes may be sufficient for conducting reliable meta-analyses when a strong effect is anticipated. Sensory paradigms with fMRI methods have shown higher reliability and stronger effects when compared with cognitive tasks (Bennett & Miller, 2010; de Haas, 2018; Han et al., 2022). Therefore, the somatosensory studies in the ALE analysis were expected to have a large effect size, suggesting that the results may be reliable. Although the sample size for the ALE analysis does not meet the recommended guideline, it does offer the most succinct coverage to reflect the currently available literature and provides promising recommendations for future research.

The sample population recruited for the EEG experimental chapters mostly consisted of undergraduate and postgraduate students from the United Kingdom. Therefore, the sample is biased towards participants from western, educated, industrialised, rich, and democratic societies (Henrich et al., 2010). Furthermore, the grand average age across all three EEG studies was 28.21 ± 7.69. The inhibitory neurotransmitter GABA has been found to decline with age in healthy populations (Gao et al., 2013; Hall et al., 2010, 2011), which has been

linked to age-related reduction in beta-band power during movement (Bardouille & Bailey, 2019; Heinrichs-Graham & Wilson, 2016; Spooner et al., 2019; Walker et al., 2020; Xifra-Porxas et al., 2019). Furthermore, tactile acuity decreases with natural ageing (Brodoehl et al., 2013; McGlone & Walker, 2016; Stevens & Choo, 1996; Tremblay et al., 2000, 2005; Verrillo, 1979, 1980; Verrillo et al., 2002). Taken together, this suggests that the extent to which the findings from Chapter 5–7 can be generalised to other populations should be considered.

8.4 Suggestions for future research

Texture processing during active touch manifests as an increase in alpha-band ERD when exploring rough compared to smooth textures (Chapter 5 and Chapter 6), contradicting paradigms using passive touch (Ballesteros et al., 2009; Genna et al., 2018; Moungou et al., 2016). Future research should aim to directly compare texture processing during passive and active touch to test the hypothesis that these different modes of stimulation result in distinct patterns of cortical activation. In addition, subsequent investigations should further manipulate surface roughness, by including a larger array of stimuli, to establish whether there is a linear relationship between cortical activation and textural properties.

Compared to EEG, fMRI techniques have greater spatial resolution (Glover, 2011). This thesis proposes that higher-order regions show increased activation during hedonic estimations of hessian compared to silk (Chapter 6). In particular, deep subcortical limbic structures have been linked with hedonic preference (Berridge & Kringelbach, 2015). While EEG signals may indicate the activation of deep brain structures, as suggested by previous joint EEG–fMRI studies (Daly et al., 2019; Dehghani et al., 2023; Keynan et al., 2016), localising the exact sources of these signals remains challenging (Grech et al., 2008), leaving the contribution of subcortical regions in this process unclear. To address this gap, it is

necessary to conduct further investigations using neuroimaging methods with higher spatial resolution. Although the spatial resolution of fMRI is preferred for examining anatomical regions, the touch sensor used to quantify active touch is incompatible with the strong magnetic field that accompanies this research method, and the supine positioning of participants would make it difficult to place the touch sensor. Therefore, MEG may be a more suitable method for investigating texture processing during active touch with increased spatial resolution. Recently, a MEG pilot study of tactile processing during active touch was conducted to validate the use of tactile virtual reality by delivering piezoelectric simulations to the finger whilst scanning (Bhattacharjee et al., 2020). Data from one participant was presented, despite this small sample, promising results demonstrated movement-induced somatosensory evoked responses, suggesting that MEG may be appropriate for investigating texture processing during active exploration.

Texture processing through active touch is important for discriminating textures and using tools for activities such as eating and writing. Individuals with sensory processing disorder may experience hypersensitivity, which can cause discomfort, pain, or avoidance of certain textures, or hyposensitivity to tactile stimuli, which manifests as a failure to register or respond to sensory inputs (Baranek et al., 2006; Foss-Feig et al., 2012; Lane et al., 2011). Furthermore, sensory processing disorder may co-occur with other conditions such as autism spectrum disorder, attention deficit hyperactivity disorder, and dyspraxia (Galiana-Simal et al., 2020). In addition, neuropathic pain syndromes, such as complex regional pain syndrome, can be accompanied by sensory and motor dysfunction (Harden et al., 2007, 2010). Specifically, complex regional pain syndrome is associated with a decrease in tactile acuity and changes in perception of hand shape and size due to functional reorganisation of the SI (di Pietro et al., 2015; Enax-Krumova et al., 2017; Lenz et al., 2011; Lewis & Schweinhardt, 2012; Peltz et al., 2011; Pleger et al., 2004, 2005; Schwenkreis et al., 2009), potentially

leading to altered texture perception during active touch. The findings of texture processing in the brain should be considered for further research within clinical populations to aid our understanding of neurodevelopmental disorders and pain syndromes that are accompanied by sensorimotor disturbances.

8.5 Concluding Remarks

To conclude, this thesis employed new methods and data analysis pipelines to investigate the neural basis of texture processing during active touch. This thesis discovered novel cortical activation patterns during active touch. Exploration of rough textures led to increased alpha-band ERD, whilst smooth textures elicited increased beta-band ERD, demonstrating altered cortical activation from previous passive touch paradigms which offers important new insight. Together, alpha- and beta-band ERD may demonstrate the brain's response to different peripheral tactile coding mechanisms during active touch. The findings of this thesis also suggest that estimation of hedonic preference elicits higher-order processing in frontal, temporoparietal, and occipital regions. In addition, texture-specific processing was evidenced by selective activation in the SII, supporting the hypothesis that the SII is a higher-order tactile processing region. Interestingly, this thesis sets the groundwork for investigation of texture change processing in the brain by demonstrating differences in oscillatory activity, particularly in alpha-band power, during complex ongoing tactile exploration. It is hoped that future research will further elucidate the spatial and temporal characteristics of brain processing of texture during active touch, and eventually lead to greater understanding, or clinical applications for people with sensorimotor disturbances.

References

Abraira, V. E., & Ginty, D. D. (2013). The Sensory Neurons of Touch. *Neuron*, *79*(4), 618–639. https://doi.org/10.1016/J.NEURON.2013.07.051

AbuHasan, Q., & Munakomi, S. (2022). Neuroanatomy, Pyramidal Tract. *StatPearls*. https://www.ncbi.nlm.nih.gov/books/NBK545314/

Acar, F., Seurinck, R., Eickhoff, S. B., & Moerkerke, B. (2018). Assessing robustness against potential publication bias in Activation Likelihood Estimation (ALE) meta-analyses for fMRI. *PLoS ONE*, *13*(11). https://doi.org/10.1371/JOURNAL.PONE.0208177

Adhikari, B. M., Sathian, K., Epstein, C. M., Lamichhane, B., & Dhamala, M. (2014). Oscillatory activity in neocortical networks during tactile discrimination near the limit of spatial acuity. *NeuroImage*, *91*, 300–310. https://doi.org/10.1016/J.NEUROIMAGE.2014.01.007

Adler, R. J. (1981). *The geometry of random fields* [Book]. Wiley.

Adrian, E. D., & Matthews, B. H. C. (1934). The Berger rhythm: potential changes from the occipital lobes in man. *Brain*, *57*(4), 355–385. https://doi.org/10.1093/brain/57.4.355

Al-Chalabi, M., Reddy, V., & Alsalman, I. (2021). Neuroanatomy, Posterior Column (Dorsal Column). *StatPearls*. https://www.ncbi.nlm.nih.gov/books/NBK507888/

Al-Nafjan, A., Hosny, M., Al-Wabil, A., & Al-Ohali, Y. (2017). Classification of Human Emotions from Electroencephalogram (EEG) Signal using Deep Neural Network. *IJACSA) International Journal of Advanced Computer Science and Applications*, *8*(9). www.ijacsa.thesai.org

Amaral, D. (2012). The Functional Organisation of Perception and Movement. In J. Schwartz, T. Jessell, S. Siegelbaum, & A. J. Hudspeth (Eds.), *Principles of Neural Science* (5th ed., p. 359). McGraw-Hill Publishing.

Amaral, D. G., & Strick, P. L. (2012). The Organization of the Central Nervous System [Book]. In E. R. Kandel (Ed.), *Principles of neural science* (Fifth edition., pp. 337–354). McGraw Hill.

Amontons, G. (1699). De la resistance cause'e dans les machines. In *Mémoires de l'Académie Royale A* (pp. 257–282). Chez Gerard Kuyper.

Andersen, R. A., Andersen, K. N., Hwang, E. J., & Hauschild, M. (2014). Optic ataxia: from Balint's syndrome to the parietal reach region. *Neuron*, *81*(5), 967. https://doi.org/10.1016/J.NEURON.2014.02.025

Angel, R., neurology, R. M.-E., & 1982, undefined. (1982). Velocity-dependent suppression of cutaneous sensitivity during movement. *Elsevier*, *77*, 266–274. https://www.sciencedirect.com/science/article/pii/0014488682902448

Ariani, G., Pruszynski, J. A., & Diedrichsen, J. (2022). Motor planning brings human primary somatosensory cortex into action-specific preparatory states. *ELife*, *11*. https://doi.org/10.7554/ELIFE.69517

Arnal, L. H., Doelling, K. B., & Poeppel, D. (2015). Delta-Beta Coupled Oscillations Underlie Temporal Prediction Accuracy. *Cerebral Cortex (New York, N.Y. : 1991)*, *25*(9), 3077–3085. https://doi.org/10.1093/CERCOR/BHU103

Augurelle, A. S., Smith, A. M., Lejeune, T., & Thonnard, J. L. (2003). Importance of cutaneous feedback in maintaining a secure grip during manipulation of hand-held

objects. *Journal of Neurophysiology*, *89*(2), 665–671. https://doi.org/10.1152/JN.00249.2002

Aviles, J. M. R., Muñoz, F. M., Kleinböhl, D., Sebastián, M., & Jiménez, S. B. (2010). A new device to present textured stimuli to touch with simultaneous EEG recording. *Behavior Research Methods*, *42*(2), 547–555. https://doi.org/10.3758/BRM.42.2.547

Azevedo, F. A. C., Carvalho, L. R. B., Grinberg, L. T., Farfel, J. M., Ferretti, R. E. L., Leite, R. E. P., Filho, W. J., Lent, R., & Herculano-Houzel, S. (2009). Equal numbers of neuronal and nonneuronal cells make the human brain an isometrically scaled-up primate brain. *The Journal of Comparative Neurology*, *513*(5), 532–541. https://doi.org/10.1002/CNE.21974

Baghdadi, G., Amiri, M., Falotico, E., & Laschi, C. (2021). Recurrence quantification analysis of EEG signals for tactile roughness discrimination. *International Journal of Machine Learning and Cybernetics*, *12*(4), 1115–1136. https://doi.org/10.1007/S13042-020-01224-1/FIGURES/20

Baird, J. C., & Elliot, N. (1978). *Fundamentals of Scaling and Psychophysics*. John Wiley & Sons.

Bajcsy, R. (1988). Active perception. *Proceedings of the IEEE*, *76*(8), 966–1005. https://doi.org/10.1109/5.5968

Ballesteros, S., Muñoz, F., Sebastián, M., García, B., & Reales, J. M. (2009). ERP evidence of tactile texture processing: Effects of roughness and movement. *Proceedings - 3rd Joint EuroHaptics Conference and Symposium on Haptic Interfaces for Virtual*

Environment and Teleoperator Systems, World Haptics 2009, 166–171. https://doi.org/10.1109/WHC.2009.4810901

Baranek, G. T., David, F. J., Poe, M. D., Stone, W. L., & Watson, L. R. (2006). Sensory Experiences Questionnaire: discriminating sensory features in young children with autism, developmental delays, and typical development. *Journal of Child Psychology and Psychiatry, and Allied Disciplines*, *47*(6), 591–601. https://doi.org/10.1111/J.1469-7610.2005.01546.X

Barbey, A. K., Koenigs, M., & Grafman, J. (2013). Dorsolateral Prefrontal Contributions to Human Working Memory. *Cortex; a Journal Devoted to the Study of the Nervous System and Behavior*, *49*(5), 1195. https://doi.org/10.1016/J.CORTEX.2012.05.022

Bardouille, T., & Bailey, L. (2019). Evidence for age-related changes in sensorimotor neuromagnetic responses during cued button pressing in a large open-access dataset. *NeuroImage*, *193*, 25–34. https://doi.org/10.1016/J.NEUROIMAGE.2019.02.065

Bardouille, T., Picton, T. W., & Ross, B. (2010). Attention modulates beta oscillations during prolonged tactile stimulation. *The European Journal of Neuroscience*, *31*(4), 761. https://doi.org/10.1111/J.1460-9568.2010.07094.X

Bastiaansen, M., Mazaheri, A., & Jensen, O. (2011). Beyond ERPs: Oscillatory Neuronal Dynamics [Book]. In S. J. Luck & E. S. Kappenman (Eds.), *The Oxford Handbook of Event-Related Potential Components* (1st ed., pp. 31–49). Oxford University Press. https://doi.org/10.1093/oxfordhb/9780195374148.001.0001

Batista, A. P., Buneo, C. A., Snyder, L. H., & Andersen, R. A. (1999). Reach plans in eye-centered coordinates. *Science (New York, N.Y.)*, *285*(5425), 257–260. https://doi.org/10.1126/SCIENCE.285.5425.257

Battaglia-Mayer, A., Ferraina, S., Mitsuda, T., Marconi, B., Genovesio, A., Onorati, P., Lacquaniti, F., & Caminiti, R. (2000). Early Coding of Reaching in the Parietooccipital Cortex. *Journal of Neurophysiology*, *83*(4), 2374–2391. https://doi.org/10.1152/jn.2000.83.4.2374

Bauer, A. K. R., Kreutz, G., & Herrmann, C. S. (2015). Individual musical tempo preference correlates with EEG beta rhythm. *Psychophysiology*, *52*(4), 600–604. https://doi.org/10.1111/PSYP.12375

Bauer, M., Oostenveld, R., Peeters, M., & Fries, P. (2006). Tactile spatial attention enhances gamma-band activity in somatosensory cortex and reduces low-frequency activity in parieto-occipital areas. *Journal of Neuroscience*, *26*(2), 490–501. https://doi.org/10.1523/JNEUROSCI.5228-04.2006

Bear, M., Connors, B., & Paradiso, M. A. (2020). *Neuroscience* (4th ed.) [Book]. Jones & Bartlett Learning, LLC.

Becker, S., Bräscher, A.-K., Bannister, S., Bensafi, M., Calma-Birling, D., Chan, R. C. K., Eerola, T., Ellingsen, D.-M., Ferdenzi, C., Hanson, J. L., Joffily, M., Lidhar, N. K., Lowe, L. J., Martin, L. J., Musser, E. D., Noll-Hussong, M., Olino, T. M., Pintos Lobo, R., & Wang, Y. (2019). *The role of hedonics in the Human Affectome*. https://doi.org/10.1016/j.neubiorev.2019.05.003

Benikos, N., Johnstone, S. J., & Roodenrys, S. J. (2013). Short-term training in the Go/Nogo task: Behavioural and neural changes depend on task demands. In *International Journal of Psychophysiology* (Vol. 87, Issue 3). https://doi.org/10.1016/j.ijpsycho.2012.12.001

Bennett, C. M., & Miller, M. B. (2010). How reliable are the results from functional magnetic resonance imaging? *Annals of the New York Academy of Sciences*, *1191*, 133–155. https://doi.org/10.1111/J.1749-6632.2010.05446.X

Bennett, C., of, M. M.-A. of the new Y. A., & 2010, undefined. (2010). How reliable are the results from functional magnetic resonance imaging? *Wiley Online Library*, *1191*, 133–155. https://doi.org/10.1111/j.1749-6632.2010.05446.x

Bensmaia, S. (2009). Texture from touch. In *Scholarpedia* (Vol. 4, Issue 8, p. 7956). Scholarpedia. https://doi.org/10.4249/scholarpedia.7956

Bensmaïa, S., & Hollins, M. (2005). Pacinian representations of fine surface texture. *Perception & Psychophysics*, *67*(5), 842–854. https://doi.org/10.3758/BF03193537

Bensmaïa, S., Hollins, M., & Yau, J. (2005a). Vibrotactile intensity and frequency information in the Pacinian system: A psychophysical model. *Perception & Psychophysics 2005 67:5*, *67*(5), 828–841. https://doi.org/10.3758/BF03193536

Bensmaia, S. J., & Hollins, M. (2003). The vibrations of texture. *Http://Dx.Doi.Org/10.1080/0899022031000083825*, *20*(1), 33–43. https://doi.org/10.1080/0899022031000083825

Bensmaïa, S. J., Leung, Y. Y., Hsiao, S. S., & Johnson, K. O. (2005b). Vibratory adaptation of cutaneous mechanoreceptive afferents. *Journal of Neurophysiology*, *94*(5), 3023–3036. https://doi.org/10.1152/JN.00002.2005

Berg, P., & Scherg, M. (1994). A multiple source approach to the correction of eye artifacts. *Electroencephalography and Clinical Neurophysiology*, *90*(3), 229–241. https://doi.org/10.1016/0013-4694(94)90094-9

Berger, H. (1929). Nach JBechterew: Die Energie des lebenden. *Organismus. S*, *102*, 25.

Bernat, E. M., Malone, S. M., Williams, W. J., Patrick, C. J., & Iacono, W. G. (2007). Decomposing delta, theta, and alpha time–frequency ERP activity from a visual oddball task using PCA. *International Journal of Psychophysiology*, *64*(1), 62–74. https://doi.org/10.1016/J.IJPSYCHO.2006.07.015

Berridge, K. C., & Kringelbach, M. L. (2015). Pleasure systems in the brain. *Neuron*, *86*(3), 646. https://doi.org/10.1016/J.NEURON.2015.02.018

Betts, J. G., College, T. J., Desaix, P., Johnson, J. E., Wise, J. A., Womble, M., & Young, K. A. (2013). *Anatomy & Physiology*.

Beurze, S. M., de Lange, F. P., Toni, I., & Medendorp, W. P. (2007). Integration of target and effector information in the human brain during reach planning. *Journal of Neurophysiology*, *97*(1), 188–199. https://doi.org/10.1152/JN.00456.2006/ASSET/IMAGES/LARGE/Z9K0120677910008.JPEG

Bhattacharjee, A., Kajal, D. S., Patrono, A., Li Hegner, Y., Zampini, M., Schwarz, C., & Braun, C. (2020). A Tactile Virtual Reality for the Study of Active Somatosensation. *Frontiers in Integrative Neuroscience*, *14*, 5. https://doi.org/10.3389/fnint.2020.00005

Binkofski, F., Kunesch, E., Classen, J., Seitz, R. J., & Freund, H. J. (2001). Tactile apraxiaUnimodal apractic disorder of tactile object exploration associated with parietal lobe lesions. *Brain*, *124*(1), 132–144. https://doi.org/10.1093/BRAIN/124.1.132

Bishop, D. (2019). Rein in the four horsemen of irreproducibility. *Nature*, *568*(7753), 435. https://doi.org/10.1038/D41586-019-01307-2

Björnsdotter, M., Gordon, I., Pelphrey, K. A., Olausson, H., & Kaiser, M. D. (2014). Development of brain mechanisms for processing affective touch. *Frontiers in Behavioral Neuroscience*, *8*, 24. https://doi.org/10.3389/fnbeh.2014.00024

Björnsdotter, M., Löken, L., Olausson, H., Vallbo, Å., & Wessberg, J. (2009). Somatotopic organization of gentle touch processing in the posterior insular cortex. *Journal of Neuroscience*, *29*(29), 9314–9320. https://doi.org/10.1523/JNEUROSCI.0400-09.2009

Björnsdotter, M., Morrison, I., & Olausson, H. (2010). Feeling good: on the role of C fiber mediated touch in interoception. *Experimental Brain Research*, *207*(3–4), 149–155. https://doi.org/10.1007/S00221-010-2408-Y

Blake, D. T., Hsiao, S. S., & Johnson, K. O. (1997). Neural Coding Mechanisms in Tactile Pattern Recognition: The Relative Contributions of Slowly and Rapidly Adapting Mechanoreceptors to Perceived Roughness. *Journal of Neuroscience*, *17*(19), 7480–7489. https://doi.org/10.1523/JNEUROSCI.17-19-07480.1997

Blangero, A., Menz, M. M., McNamara, A., & Binkofski, F. (2009). Parietal modules for reaching. *Neuropsychologia*, *47*(6), 1500–1507. https://doi.org/10.1016/J.NEUROPSYCHOLOGIA.2008.11.030

Bodegård, A., Geyer, S., Grefkes, C., Zilles, K., & Roland, P. E. (2001). Hierarchical processing of tactile shape in the human brain. *Neuron*, *31*(2), 317–328. https://doi.org/10.1016/S0896-6273(01)00362-2

Bodegård, A., Geyer, S., Naito, E., Zilles, K., & Roland, P. E. (2000). Somatosensory areas in man activated by moving stimuli: Cytoarchitectonic mapping and PET. *NeuroReport*, *11*(1), 187–191. https://doi.org/10.1097/00001756-200001170-00037

Bogy, D. B., & Chen, D. U. (2013). Amontons' Laws of Friction. *Encyclopedia of Tribology*, 71–71. https://doi.org/10.1007/978-0-387-92897-5_166

Botvinick, M., & An, J. (2009). Goal-directed decision making in prefrontal cortex: A computational framework. *Advances in Neural Information Processing Systems*, *21*, 169. /pmc/articles/PMC4171955/

Boubenec, Y., Lawlor, J., Górska, U., Shamma, S., & Englitz, B. (2017). Detecting changes in dynamic and complex acoustic environments. *ELife*, *6*. https://doi.org/10.7554/ELIFE.24910

Brett, M., Penny, W., & Kiebel, S. (2007). Parametric procedures [Book]. In K. J. (Karl J.) Friston (Ed.), *Statistical parametric mapping the analysis of functional brain images* (pp. 223–231). Academic.

Brodoehl, S., Klingner, C., Stieglitz, K., & Witte, O. W. (2013). Age-related changes in the somatosensory processing of tactile stimulation--an fMRI study. *Behavioural Brain Research*, *238*(1), 259–264. https://doi.org/10.1016/J.BBR.2012.10.038

Brovelli, A., Ding, M., Ledberg, A., Chen, Y., Nakamura, R., & Bressler, S. L. (2004). Beta oscillations in a large-scale sensorimotor cortical network: Directional influences

revealed by Granger causality. *Proceedings of the National Academy of Sciences of the United States of America*, *101*(26), 9849–9854. https://doi.org/10.1073/pnas.0308538101

Brown, A. G. (1981). *Organization in the Spinal Cord*. Springer London. https://doi.org/10.1007/978-1-4471-1305-8

Brown, G. G., Perthen, J. E., Liu, T. T., & Buxton, R. B. (2007). A primer on functional magnetic resonance imaging. *Neuropsychology Review*, *17*(2), 107–125. https://doi.org/10.1007/S11065-007-9028-8/FIGURES/7

Brown, M. J. N., & Staines, W. R. (2015). Somatosensory input to non-primary motor areas is enhanced during preparation of cued contraterlateral finger sequence movements. *Behavioural Brain Research*, *286*, 166–174. https://doi.org/10.1016/j.bbr.2015.02.052

Brun, C., Mercier, C., Grieve, S., Palmer, S., Bailey, J., & McCabe, C. S. (2019). Sensory disturbances induced by sensorimotor conflicts are higher in complex regional pain syndrome and fibromyalgia compared to arthritis and healthy people, and positively relate to pain intensity. *European Journal of Pain (London, England)*, *23*(3), 483–494. https://doi.org/10.1002/EJP.1322

Buneo, C. A., & Andersen, R. A. (2006). The posterior parietal cortex: Sensorimotor interface for the planning and online control of visually guided movements. *Neuropsychologia*, *44*(13), 2594–2606.

Buneo, C. A., Jarvis, M. R., Batista, A. P., & Andersen, R. A. (2002). Direct visuomotor transformations for reaching. *Nature*, *416*(6881), 632–636. https://doi.org/10.1038/416632A

Burke, R. E. (2008). Spinal cord. *Scholarpedia*, *3*(4), 1925. https://doi.org/10.4249/SCHOLARPEDIA.1925

Burton, H., Abend, N. S., MacLeod, A. M. K., Sinclair, R. J., Snyder, A. Z., & Raichle, M. E. (1999). Tactile attention tasks enhance activation in somatosensory regions of parietal cortex: a positron emission tomography study. *Cerebral Cortex (New York, N.Y. : 1991)*, *9*(7), 662–674. https://doi.org/10.1093/CERCOR/9.7.662

Burton, H., MacLeod, A. M. K., Videen, T. O., & Raichle, M. E. (1997). Multiple foci in parietal and frontal cortex activated by rubbing embossed grating patterns across fingerpads: A positron emission tomography study in humans. *Cerebral Cortex*, *7*(1), 3–17.

Butler, J. S., Foxe, J. J., Fiebelkorn, I. C., Mercier, M. R., & Molholm, S. (2012). Multisensory Representation of Frequency across Audition and Touch: High Density Electrical Mapping Reveals Early Sensory-Perceptual Coupling. *Journal of Neuroscience*, *32*(44), 15338–15344. https://doi.org/10.1523/JNEUROSCI.1796-12.2012

Butler, J. S., Molholm, S., Fiebelkorn, I. C., Mercier, M. R., Schwartz, T. H., & Foxe, J. J. (2011). *Common or Redundant Neural Circuits for Duration Processing across Audition and Touch*. https://doi.org/10.1523/JNEUROSCI.3296-10.2011

Buzsáki, G., Anastassiou, C. A., & Koch, C. (2012). The origin of extracellular fields and currents — EEG, ECoG, LFP and spikes. *Nature Reviews Neuroscience 2012 13:6*, *13*(6), 407–420. https://doi.org/10.1038/nrn3241

Carey, L. M., Abbott, D. F., Egan, G. F., & Donnan, G. A. (2008). Reproducible activation in BA2, 1 and 3b associated with texture discrimination in healthy volunteers over time. *NeuroImage*, *39*(1), 40–51. https://doi.org/10.1016/J.NEUROIMAGE.2007.08.026

Cascio, C. J., & Sathian, K. (2001). Temporal Cues Contribute to Tactile Perception of Roughness. *The Journal of Neuroscience*, *21*(14), 5289. https://doi.org/10.1523/JNEUROSCI.21-14-05289.2001

Case, L. K., Laubacher, C. M., Olausson, H., Wang, B., Spagnolo, P. A., & Bushnell, M. C. (2016). Encoding of touch intensity but not pleasantness in human primary somatosensory cortex. *Journal of Neuroscience*, *36*(21). https://doi.org/10.1523/JNEUROSCI.1130-15.2016

Chang, W.-H., Tang, P.-F., Wang, Y.-H., Lin, K.-H., Chiu, M.-J., & Chen, S.-H. A. (2010). Role of the premotor cortex in leg selection and anticipatory postural adjustments associated with a rapid stepping task in patients with stroke. *Gait & Posture*, *32*(4), 487–493. https://doi.org/10.1016/j.gaitpost.2010.07.007

Chapman, C. E. (1994). Active versus passive touch: factors influencing the transmission of somatosensory signals to primary somatosensory cortex. *Canadian Journal of Physiology and Pharmacology*, *72*(5), 558–570. https://doi.org/10.1139/y94-080

Chapman, C. E. (2008). Active Touch. *Encyclopedia of Neuroscience*, 35–41. https://doi.org/10.1007/978-3-540-29678-2_67

Chapman, C. E., & Beauchamp, E. (2006). Differential controls over tactile detection in humans by motor commands and peripheral reafference. *Journal of Neurophysiology*, *96*(3), 1664–1675. https://doi.org/10.1152/JN.00214.2006

Chapman, C. E., Jiang, W., & Lamarre, Y. (1988). Experimental Brain Research Modulation of lemniscal input during conditioned arm movements in the monkey. *Exp Brain Res*, *72*, 316–334.

Chapman, C. Elaine., Bushnell, M. C., Miron, D., Duncan, G. H., & Lund, J. P. (1987). Sensory perception during movement in man. *Experimental Brain Research*, *68*(3), 516–524. https://doi.org/10.1007/BF00249795

Chapman, C. Elaine., Tremblay, François., Jiang, Wan., Belingard, Loc., & Meftah, E. Mehdi. (2002). Central neural mechanisms contributing to the perception of tactile roughness. *Behavioural Brain Research*, *135*(1–2), 225–233. https://doi.org/10.1016/S0166-4328(02)00168-7

Chatrian, G. E. , Lettich, E., & Nelson, P. L. (1985). Ten Percent Electrode System for Topographic Studies of Spontaneous and Evoked EEG Activities. *American Journal of EEG Technology*, *25*(2), 83–92. https://doi.org/10.1080/00029238.1985.11080163

Chatrian, G., Petersen, M., & Lazarte, J. (1958). The blocking of the rolandic wicket rhythm and some central changes related to movement. *Neurophysiol*, *11*, 497–501.

Chen, J. C., Hämmerer, D., D'Ostilio, K., Casula, E. P., Marshall, L., Tsai, C. H., Rothwell, J. C., & Edwards, M. J. (2014). Bi-directional modulation of somatosensory mismatch negativity with transcranial direct current stimulation: An event related potential study. *Journal of Physiology*, *592*(4), 745–757. https://doi.org/10.1113/JPHYSIOL.2013.260331

Chen, S., & Ge, S. (2017). Experimental research on the tactile perception from fingertip skin friction. *Wear*, *376–377*, 305–314. https://doi.org/10.1016/J.WEAR.2016.11.014

Chen, T. L., Babiloni, C., Ferretti, A., Perrucci, M. G., Romani, G. L., Rossini, P. M., Tartaro, A., & del Gratta, C. (2008). Human secondary somatosensory cortex is involved in the processing of somatosensory rare stimuli: An fMRI study. *NeuroImage*, *40*(4), 1765–1771. https://doi.org/10.1016/J.NEUROIMAGE.2008.01.020

Cheyne, D., Gaetz, W., Garnero, L., Lachaux, J.-P. P., Ducorps, A., Schwartz, D., & Varela, F. J. (2003). Neuromagnetic imaging of cortical oscillations accompanying tactile stimulation. *Cognitive Brain Research*, *17*(3), 599–611. https://doi.org/10.1016/S0926-6410(03)00173-3

Chung, Y. G., Kim, J., Han, S. W., Kim, H. S., Choi, M. H., Chung, S. C., Park, J. Y., & Kim, S. P. (2013). Frequency-dependent patterns of somatosensory cortical responses to vibrotactile stimulation in humans: A fMRI study. *Brain Research*, *1504*, 47–57. https://doi.org/10.1016/j.brainres.2013.02.003

Cohen, D., & Halgren, E. (2015). *Magnetoencephalography (Neuromagnetism)*. *i*(January 2003).

Cohen, L. G., & Starr, A. (1987). Localization, timing and specificity of gating of somatosensory evoked potentials during active movement in man. *Brain : A Journal of Neurology*, *110 (Pt 2*(2), 451–467. https://doi.org/10.1093/brain/110.2.451

Cohen, M. X. (2014). *Analyzing neural time series data : theory and practice* [Book]. The MIT Press.

Cohen, M. X. (2016). *Rigor and replication in time-frequency analyses of cognitive electrophysiology data*. https://doi.org/10.1016/j.ijpsycho.2016.02.001

Connor, C. E., Hsiao, S. S., Phillips, J. R., & Johnson, K. O. (1990). Tactile roughness: Neural codes that account for psychophysical magnitude estimates. *Journal of Neuroscience*, *10*(12), 3823–3836. https://doi.org/10.1523/jneurosci.10-12-03823.1990

Connor, C. E., & Johnson, K. O. (1992). Neural coding of tactile texture: Comparison of spatial and temporal mechanisms for roughness perception. *Journal of Neuroscience*, *12*(9), 3414–3426. https://doi.org/10.1523/jneurosci.12-09-03414.1992

Cook, S., Fallon, N., Wright, H., Thomas, A., Giesbrecht, T., Field, M., & Stancak, A. (2015). Pleasant and Unpleasant Odors Influence Hedonic Evaluations of Human Faces: An Event-Related Potential Study. *Frontiers in Human Neuroscience*, *9*. https://doi.org/10.3389/fnhum.2015.00661

Cook, S., Kokmotou, K., Soto, V., Fallon, N., Tyson-Carr, J., Thomas, A., Giesbrecht, T., Field, M., & Stancak, A. (2017). Pleasant and unpleasant odour-face combinations influence face and odour perception: An event-related potential study. *Behavioural Brain Research*, *333*, 304–313. https://doi.org/10.1016/j.bbr.2017.07.010

Cook, S., Kokmotou, K., Soto, V., Wright, H., Fallon, N., Thomas, A., Giesbrecht, T., Field, M., & Stancak, A. (2018). Simultaneous odour-face presentation strengthens hedonic evaluations and event-related potential responses influenced by unpleasant odour. *Neuroscience Letters*, *672*, 22–27. https://doi.org/10.1016/j.neulet.2018.02.032

Craig, A. D. (2002). How do you feel? Interoception: the sense of the physiological condition of the body. *Nature Reviews. Neuroscience*, *3*(8), 655–666. https://doi.org/10.1038/NRN894

Craig, A. D. (2009). How do you feel - now? The anterior insula and human awareness. *Nature Reviews Neuroscience*, *10*(1), 59–70. https://doi.org/10.1038/NRN2555

Craig, A. D., Chen, K., Bandy, D., & Reiman, E. M. (2000). Thermosensory activation of insular cortex. *Nature Neuroscience*, *3*(2), 184–190. https://doi.org/10.1038/72131

Crosson, B., Ford, A., McGregor, K. M., Meinzer, M., Cheshkov, S., Xiufeng, L., Walker-Batson, D., & Briggs, R. W. (2010). Functional Imaging and Related Techniques: An Introduction for Rehabilitation Researchers. *Journal of Rehabilitation Research and Development*, *47*(2), vii. https://doi.org/10.1682/JRRD.2010.02.0017

Cruciani, G., Zanini, L., Russo, V., Boccardi, E., & Spitoni, G. F. (2021). Pleasantness ratings in response to affective touch across hairy and glabrous skin: A meta-analysis. *Neuroscience & Biobehavioral Reviews*, *131*, 88–95. https://doi.org/10.1016/J.NEUBIOREV.2021.09.026

Cybulska-Klosowicz, A., Meftah, E. M., Raby, M., Lemieux, M. L., & Chapman, C. E. (2011). A critical speed for gating of tactile detection during voluntary movement. *Experimental Brain Research*, *210*(2), 291–301. https://doi.org/10.1007/S00221-011-2632-0

Daly, I., Williams, D., Hwang, F., Kirke, A., Miranda, E. R., & Nasuto, S. J. (2019). Electroencephalography reflects the activity of sub-cortical brain regions during approach-withdrawal behaviour while listening to music. *Scientific Reports 2019 9:1*, *9*(1), 1–22. https://doi.org/10.1038/s41598-019-45105-2

Darian-Smith, I., Johnson, K. O., & Dykes, R. (1973). 'Cold' fiber population innervating palmar and digital skin of the monkey: responses to cooling pulses. *Https://Doi-*

Org.Liverpool.Idm.Oclc.Org/10.1152/Jn.1973.36.2.325, *36*(2), 325–346. https://doi.org/10.1152/JN.1973.36.2.325

Darian-Smith, I., Johnson, K. O., LaMotte, C., Shigenaga, Y., Kenins, P., & Champness, P. (1979). Warm fibers innervating palmar and digital skin of the monkey: responses to thermal stimuli. *Journal of Neurophysiology*, *42*(5), 1297–1315. https://doi.org/10.1152/JN.1979.42.5.1297

Davare, M., Andres, M., Cosnard, G., Thonnard, J. L., & Olivier, E. (2006). Dissociating the Role of Ventral and Dorsal Premotor Cortex in Precision Grasping. *Journal of Neuroscience*, *26*(8), 2260–2268. https://doi.org/10.1523/JNEUROSCI.3386-05.2006

Davare, M., Lemon, R., & Olivier, E. (2008). Selective modulation of interactions between ventral premotor cortex and primary motor cortex during precision grasping in humans. *The Journal of Physiology*, *586*(11), 2735–2742. https://doi.org/10.1113/JPHYSIOL.2008.152603

Davare, M., Montague, K., Olivier, E., Rothwell, J. C., & Lemon, R. N. (2009). Ventral premotor to primary motor cortical interactions during object-driven grasp in humans. *Cortex*, *45*(9), 1050–1057. https://doi.org/10.1016/J.CORTEX.2009.02.011

de Haas, B. (2018). How to Enhance the Power to Detect Brain–Behavior Correlations With Limited Resources. *Frontiers in Human Neuroscience*, *12*. https://doi.org/10.3389/FNHUM.2018.00421

Deen, B., Pitskel, N. B., & Pelphrey, K. A. (2011). Three systems of insular functional connectivity identified with cluster analysis. *Cerebral Cortex (New York, N.Y. : 1991)*, *21*(7), 1498–1506. https://doi.org/10.1093/CERCOR/BHQ186

DeFelipe, J., & Fariñas, I. (1992). The pyramidal neuron of the cerebral cortex: Morphological and chemical characteristics of the synaptic inputs. *Progress in Neurobiology*, *39*(6), 563–607. https://doi.org/10.1016/0301-0082(92)90015-7

Dehghani, A., Soltanian-Zadeh, H., & Hossein-Zadeh, G. A. (2023). Probing fMRI brain connectivity and activity changes during emotion regulation by EEG neurofeedback. *Frontiers in Human Neuroscience*, *16*, 881. https://doi.org/10.3389/FNHUM.2022.988890/BIBTEX

Delorme, A., & Makeig, S. (2004). EEGLAB: an open source toolbox for analysis of single-trial EEG dynamics including independent component analysis. *Journal of Neuroscience Methods*, *134*, 9–21. http://www.sccn.ucsd.edu/eeglab/

Dettmers, C., Fink, G. R., Lemon, R. N., Stephan, K. M., Passingham, R. E., Silbersweig, D., Holmes, A., Ridding, M. C., Brooks, D. J., & Frackowiak, R. S. (1995). Relation between cerebral activity and force in the motor areas of the human brain. *Journal of Neurophysiology*, *74*(2), 802–815. https://doi.org/10.1152/jn.1995.74.2.802

di Pietro, F., Stanton, T. R., Moseley, G. L., Lotze, M., & Mcauley, J. H. (2015). Interhemispheric somatosensory differences in chronic pain reflect abnormality of the healthy side. *Human Brain Mapping*, *36*(2), 508–518. https://doi.org/10.1002/HBM.22643

Doria, J. J. (1995). A Primer on Imaging. *Alcohol Health and Research World*, *19*(4), 261. /pmc/articles/PMC6875748/

Eck, J., Kaas, A. L., & Goebel, R. (2013). Crossmodal interactions of haptic and visual texture information in early sensory cortex. *NeuroImage*, *75*, 123–135. https://doi.org/10.1016/j.neuroimage.2013.02.075

Eck, J., Kaas, A. L., Mulders, J. L., Hausfeld, L., Kourtzi, Z., & Goebel, R. (2016). The Effect of Task Instruction on Haptic Texture Processing: The Neural Underpinning of Roughness and Spatial Density Perception. *Cerebral Cortex*, *26*(1), 384–401. https://doi.org/10.1093/CERCOR/BHU294

Eickhoff, S. B., Bzdok, D., Laird, A. R., Kurth, F., & Fox, P. T. (2012). Activation likelihood estimation meta-analysis revisited. *NeuroImage*, *59*(3), 2349–2361. https://doi.org/10.1016/J.NEUROIMAGE.2011.09.017

Eickhoff, S. B., Bzdok, D., Laird, A. R., Roski, C., Caspers, S., Zilles, K., & Fox, P. T. (2011). Co-activation patterns distinguish cortical modules, their connectivity and functional differentiation. *NeuroImage*, *57*(3), 938–949. https://doi.org/10.1016/J.NEUROIMAGE.2011.05.021

Eickhoff, S. B., Laird, A. R., Grefkes, C., Wang, L. E., Zilles, K., & Fox, P. T. (2009). Coordinate-based activation likelihood estimation meta-analysis of neuroimaging data: a random-effects approach based on empirical estimates of spatial uncertainty. *Human Brain Mapping*, *30*(9), 2907–2926. https://doi.org/10.1002/HBM.20718

Eickhoff, S. B., Nichols, T. E., Laird, A. R., Hoffstaedter, F., Amunts, K., Fox, P. T., Bzdok, D., & Eickhoff, C. R. (2016). Behavior, Sensitivity, and power of activation likelihood estimation characterized by massive empirical simulation. *NeuroImage*, *137*, 70. https://doi.org/10.1016/J.NEUROIMAGE.2016.04.072

Eickhoff, S. B., Schleicher, A., Zilles, K., & Amunts, K. (2006). The Human Parietal Operculum. I. Cytoarchitectonic Mapping of Subdivisions. *Cerebral Cortex*, *16*(2), 254–267. https://doi.org/10.1093/cercor/bhi105

Eldeeb, S., Ting, J., Erdogmus, D., Weber, D., & Akcakaya, M. (2019). EEG-Based Texture Classification during Active Touch. *IEEE International Workshop on Machine Learning for Signal Processing, MLSP*, *2019-Octob*. https://doi.org/10.1109/MLSP.2019.8918777

Elk, M. van. (2014). The left inferior parietal lobe represents stored hand-postures for object use and action prediction. *Frontiers in Psychology*, *5*(APR). https://doi.org/10.3389/FPSYG.2014.00333

Emos, M. C., & Agarwal, S. (2021). Neuroanatomy, Upper Motor Neuron Lesion. *StatPearls*. https://www.ncbi.nlm.nih.gov/books/NBK537305/

Enax-Krumova, E. K., Lenz, M., Frettlöh, J., Höffken, O., Reinersmann, A., Schwarzer, A., Westermann, A., Tegenthoff, M., & Maier, C. (2017). Changes of the Sensory Abnormalities and Cortical Excitability in Patients with Complex Regional Pain Syndrome of the Upper Extremity After 6 Months of Multimodal Treatment. *Pain Medicine (Malden, Mass.)*, *18*(1), 95–106. https://doi.org/10.1093/PM/PNW147

Essick, G. K., Mcglone, F., Dancer, C., Fabricant, D., Ragin, Y., Phillips, N., Jones, T., & Guest, S. (2010). Quantitative assessment of pleasant touch. *Neuroscience and Biobehavioral Reviews*, 192–203. https://doi.org/10.1016/j.neubiorev.2009.02.003

Essick, G. K., & Trulsson, M. (2009). Tactile Sensation in Oral Region. *Encyclopedia of Neuroscience*, 3999–4005. https://doi.org/10.1007/978-3-540-29678-2_5872

Etzi, R., Ferrise, F., Bordegoni, M., Zampini, M., & Gallace, A. (2018). The Effect of Visual and Auditory Information on the Perception of Pleasantness and Roughness of Virtual Surfaces. *Multisensory Research*, *31*(6), 501–522. https://doi.org/10.1163/22134808-00002603

Etzi, R., Spence, C., & Gallace, A. (2014). Textures that we like to touch: An experimental study of aesthetic preferences for tactile stimuli. *Consciousness and Cognition*, *29*, 178–188. https://doi.org/10.1016/j.concog.2014.08.011

Evans, A. C., Collins, D. L., Mills, S. R., Brown, E. D., Kelly, R. L., & Peters, T. M. (1994). 3D statistical neuroanatomical models from 305 MRI volumes. *IEEE Nuclear Science Symposium & Medical Imaging Conference*, *pt 3*, 1813–1817. https://doi.org/10.1109/nssmic.1993.373602

Feige, B., Scheffler, K., Esposito, F., di Salle, F., Hennig, J., & Seifritz, E. (2005). Cortical and subcortical correlates of electroencephalographic alpha rhythm modulation. *Journal of Neurophysiology*, *93*(5), 2864–2872. https://doi.org/10.1152/JN.00721.2004

Ferraina, S., Garasto, M. R., Battaglia-Mayer, A., Ferraresi, P., Johnson, P. B., Lacquaniti, F., & Carniniti, R. (1997). Visual Control of Hand-reaching Movement: Activity in Parietal Area 7m. *European Journal of Neuroscience*, *9*(5), 1090–1095. https://doi.org/10.1111/j.1460-9568.1997.tb01460.x

Flanagan, R. R., Vetter, P., Johansson, R. S., & Wolpert, D. M. (2003). Prediction precedes control in motor learning. *Current Biology : CB*, *13*(2), 146–150. https://doi.org/10.1016/S0960-9822(03)00007-1

Fogassi, L., Ferrari, P. F., Gesierich, B., Rozzi, S., Chersi, F., & Rizzolotti, G. (2005). Parietal lobe: from action organization to intention understanding. *Science (New York, N.Y.)*, *308*(5722), 662–667. https://doi.org/10.1126/SCIENCE.1106138

Fogassi, L., Gallese, V., Buccino, G., Craighero, L., Fadiga, L., & Rizzolatti, G. (2001). Cortical mechanism for the visual guidance of hand grasping movements in the monkey A reversible inactivation study. *Brain*, *124*, 571–586.

Fogassi, L., & Luppino, G. (2005). Motor functions of the parietal lobe. *Current Opinion in Neurobiology*, *15*(6), 626–631. https://doi.org/10.1016/J.CONB.2005.10.015

Foss-Feig, J. H., Heacock, J. L., & Cascio, C. J. (2012). Tactile responsiveness patterns and their association with core features in autism spectrum disorders. *Research in Autism Spectrum Disorders*, *6*(1), 337–344. https://doi.org/10.1016/j.rasd.2011.06.007

Francis, S., Rolls, E., Bowtell, R., McGlone, F., O'Doherty, J., Browning, A., Clare, S., & Smith, E. (1999). The representation of pleasant touch in the brain and its relationship with taste and olfactory areas. *NeuroReport*, *10*(3), 453–459. https://doi.org/10.1097/00001756-199902250-00003

Francis, S. T., Kelly, E. F., Bowtell, R., Dunseath, W. J. R., Folger, S. E., & McGlone, F. (2000). fMRI of the responses to vibratory stimulation of digit tips. *NeuroImage*, *11*(3), 188–202. https://doi.org/10.1006/nimg.2000.0541

Fraser, L. E., & Fiehler, K. (2018). Predicted reach consequences drive time course of tactile suppression. *Behavioural Brain Research*, *350*, 54–64. https://doi.org/10.1016/J.BBR.2018.05.010

Frey, S., Zlatkina, V., & Petrides, M. (2009). Encoding touch and the orbitofrontal cortex. *Human Brain Mapping*, *30*(2), 650–659. https://doi.org/10.1002/HBM.20532

Friedman, R. M., Hester, K. D., Green, B. G., & LaMotte, R. H. (2008). Magnitude estimation of softness. *Experimental Brain Research*, *191*(2), 133–142. https://doi.org/10.1007/S00221-008-1507-5

Friel, K. M., & Nudo, R. J. (1998). Recovery of motor function after focal cortical injury in primates: compensatory movement patterns used during rehabilitative training. *Somatosensory & Motor Research*, *15*(3), 173–189. https://doi.org/10.1080/08990229870745

Friston, K. (2007a). A short History of SPM. In W. D. Penny, K. J. Friston, J. T. Ashburner, S. J. Kiebel, & T. E. Nichols (Eds.), *Statistical Parametric Mapping: The Analysis of Functional Brain Images* (pp. 3–9). Elsevier Science & Technology.

Friston, K. J. (1994). Functional and effective connectivity in neuroimaging: A synthesis. *Human Brain Mapping*, *2*(1–2), 56–78. https://doi.org/10.1002/hbm.460020107

Friston, K. J. (1997). Analyzing brain images: Principles and overview [Book]. In R. Frackowiak, K. J. Friston, C. D. Frith, R. J. Dolaan, & J. C. Mazziotta (Eds.), *Human brain function* (pp. 25–41). Academic press.

Friston, K. J. (2004). Experimental Design and Statistical Parametric Mapping. In K. J. Friston, C. D. Frith, R. J. Dolan, C. J. Price, S. Zeki, J. T. Ashburner, & W. D. Penny (Eds.), *Human Brain Function* (pp. 599–632). Elsevier. https://doi.org/10.1016/B978-012264841-0/50033-0

Friston, K. J. (2007b). Statistical parametric mapping [Book]. In W. D. Penny, K. J. Friston, J. T. Ashburner, S. J. Kiebel, & T. E. Nichols (Eds.), *Statistical parametric mapping the analysis of functional brain images* (pp. 10–31). Academic.

Friston, K. J., & Stephan, K. (2007). Modelling brain responses [Book]. In K. J. (Karl J.) Friston (Ed.), *Statistical parametric mapping the analysis of functional brain images* (pp. 32–45). Academic.

Fry, A., Mullinger, K. J., O'Neill, G. C., Barratt, E. L., Morris, P. G., Bauer, M., Folland, J. P., & Brookes, M. J. (2016). Modulation of post-movement beta rebound by contraction force and rate of force development. *Human Brain Mapping, 37*(7). https://doi.org/10.1002/hbm.23189

Fuentemilla, L., Marco-Pallarés, J., Münte, T. F., & Grau, C. (2008). Theta EEG oscillatory activity and auditory change detection. *Brain Research, 1220,* 93–101. https://doi.org/10.1016/J.BRAINRES.2007.07.079

Gaetz, W., & Cheyne, D. (2006). Localization of sensorimotor cortical rhythms induced by tactile stimulation using spatially filtered MEG. *NeuroImage*, *30*(3), 899–908. https://doi.org/10.1016/j.neuroimage.2005.10.009

Gage, N. M., & Baars, B. J. (2018). Observing the Brain. *Fundamentals of Cognitive Neuroscience,* 53–97. https://doi.org/10.1016/B978-0-12-803813-0.00003-9

Gale, D. J., Flanagan, J. R., & Gallivan, J. P. (2021). Human Somatosensory Cortex Is Modulated during Motor Planning. *The Journal of Neuroscience, 41*(27), 5909. https://doi.org/10.1523/JNEUROSCI.0342-21.2021

Galiana-Simal, A., Vela-Romero, M., Manuel Romero-Vela, V., Oliver-Tercero, N., García-Olmo, V., Javier Benito-Castellanos, P., Muñoz-Martinez, V., Beato-Fernandez, L., & Beato, L. (2020). Sensory processing disorder: Key points of a frequent alteration in neurodevelopmental disorders. *Cogent Medicine*, *7*(1), 1736829. https://doi.org/10.1080/2331205X.2020.1736829

Gallace, A., & Spence, C. (2011). Tactile aesthetics: towards a definition of its characteristics and neural correlates. *Https://Doi.Org/10.1080/10350330.2011.591998*, *21*(4), 569–589. https://doi.org/10.1080/10350330.2011.591998

Gallace, A., Tan, H. Z., & Spence, C. (2006). The failure to detect tactile change: A tactile analogue of visual change blindness. *Psychonomic Bulletin & Review 2006 13:2*, *13*(2), 300–303. https://doi.org/10.3758/BF03193847

Gallace, A., Tan, H. Z., & Spence, C. (2007). Do "mudsplashes" induce tactile change blindness? *Perception & Psychophysics 2007 69:4*, *69*(4), 477–486. https://doi.org/10.3758/BF03193905

Gamzu, E., & Ahissar, E. (2001). Importance of Temporal Cues for Tactile Spatial-Frequency Discrimination. *Journal of Neuroscience*, *21*(18), 7416–7427. https://doi.org/10.1523/JNEUROSCI.21-18-07416.2001

Ganapathy, M. K., Reddy, V., & Tadi, P. (2021). Neuroanatomy, Spinal Cord Morphology. *StatPearls*. https://www.ncbi.nlm.nih.gov/books/NBK545206/

Gao, F., Edden, R. A. E., Li, M., Puts, N. A. J., Wang, G., Liu, C., Zhao, B., Wang, H., Bai, X., Zhao, C., Wang, X., & Barker, P. B. (2013). Edited magnetic resonance

spectroscopy detects an age-related decline in brain GABA levels. *NeuroImage*, *78*, 75–82. https://doi.org/10.1016/J.NEUROIMAGE.2013.04.012

Garcha, H. S., & Ettlinger, G. (1980). Tactile Discrimination Learning in the Monkey: The Effects of Unilateral or Bilateral Removals of the Second Somatosensory Cortex (Area SII). *Cortex*, *16*(3), 397–412. https://doi.org/10.1016/S0010-9452(80)80041-4

Gardner, E. P., & Johnson, K. O. (2012a). Sensory Coding. In E. R. Kandel, J. H. Schwartz, T. M. Jessell, S. A. Siegelbaum, & A. J. Hudspeth (Eds.), *Principles of Neural Science* (Fifth, pp. 449–472). McGraw-Hill Publishing.

Gardner, E. P., & Johnson, K. O. (2012b). The Somatosensory System: Receptors and Central Pathways. In J. Schwartz, T. Jessell, S. Siegelbaum, & A. J. Hudspeth (Eds.), *Principles of Neural Science* (5th ed., pp. 475–497). McGraw-Hill Publishing. https://ebookcentral.proquest.com/lib/liverpool/detail.action?docID=4959346

Gardner, E. P., Johnson, K. O., & M. (2012). Touch. In E. R. Kandel, J. H. Schwartz, T. M. Jessell, S. A. Siegelbaum, & A. J. Hudspeth (Eds.), *Principles of Neural Science* (Fifth, pp. 498–527). McGraw-Hill Publishing.

Gautam, A. (2017). Afferent and Efferent Impulses. In *Encyclopedia of Animal Cognition and Behavior* (pp. 1–2). Springer International Publishing. https://doi.org/10.1007/978-3-319-47829-6_1255-1

Gebhart, G. F., & Schmidt, R. F. (Eds.). (2013). *Rexed's Laminae BT - Encyclopedia of Pain* (pp. 3416–3417). Springer Berlin Heidelberg. https://doi.org/10.1007/978-3-642-28753-4_201936

Genna, C., Artoni, F., Fanciullacci, C., Chisari, C., Oddo, C. M., & Micera, S. (2016). Long-latency components of somatosensory evoked potentials during passive tactile perception of gratings. *Proceedings of the Annual International Conference of the IEEE Engineering in Medicine and Biology Society, EMBS*, *2016-Octob*, 1648–1651. https://doi.org/10.1109/EMBC.2016.7591030

Genna, C., Oddo, C., Fanciullacci, C., Micera, S., Artoni, F., Chisari, C., Micera, S., & Artoni, F. (2018). Bilateral cortical representation of tactile roughness. *Brain Research*, *1699*, 79–88. https://doi.org/10.1016/j.brainres.2018.06.014

Genna, C., Oddo, C. M., Fanciullacci, C., Chisari, C., Jörntell, H., Artoni, F., & Micera, S. (2017). Spatiotemporal Dynamics of the Cortical Responses Induced by a Prolonged Tactile Stimulation of the Human Fingertips. *Brain Topography*, *30*(4). https://doi.org/10.1007/s10548-017-0569-8

Gerling, G. J., Rivest, I. I., Lesniak, D. R., Scanlon, J. R., & Wan, L. (2014). Validating a population model of tactile mechanotransduction of slowly adapting type i afferents at levels of skin mechanics, single-unit response and psychophysics. *IEEE Transactions on Haptics*, *7*(2), 216–228. https://doi.org/10.1109/TOH.2013.36

Gevins, A. (1997). High-resolution EEG mapping of cortical activation related to working memory: effects of task difficulty, type of processing, and practice. *Cerebral Cortex*, *7*(4), 374–385. https://doi.org/10.1093/cercor/7.4.374

Giblin, D. R. (1964). Somatosensory evoked potentials in healthy subjects and in patients with lesions of the nervous system. *Annals of the New York Academy of Sciences*, *112*(1), 93–142. https://doi.org/10.1111/j.1749-6632.1964.tb26744.x

Gibson, J. J. (1962). Observations on active touch. *Psychological Review*, *69*(6), 477–491. https://doi.org/10.1037/h0046962

Glees, P., & Cole, J. (1950). Recovery of skilled motor functions after small repeated lesions of motor cortex in macaque. *Journal of Neurophysiology*, *13*(2), 137–148. https://doi.org/10.1152/jn.1950.13.2.137

Gloor, P. (1970). Hans Berger On The Electroencephalogram Of Man.(Book Review) [Article]. *Science*, 562–562.

Glover, G. H. (2011). Overview of Functional Magnetic Resonance Imaging. *Neurosurgery Clinics of North America*, *22*(2), 133. https://doi.org/10.1016/J.NEC.2010.11.001

Gogolla, N. (2017). The insular cortex. *Current Biology*, *27*(12), R580–R586. https://doi.org/10.1016/J.CUB.2017.05.010

Gomez-Ramirez, M., Hysaj, K., & Niebur, E. (2016). Neural mechanisms of selective attention in the somatosensory system. *Journal of Neurophysiology*, *116*(3), 1218–1231. https://doi.org/10.1152/jn.00637.2015

Goodman, J. M., & Bensmaia, S. J. (2020). The Neural Mechanisms of Touch and Proprioception at the Somatosensory Periphery. *The Senses: A Comprehensive Reference*, 2–27. https://doi.org/10.1016/B978-0-12-805408-6.00014-2

Gorgolewski, K. J., Varoquaux, G., Rivera, G., Schwarz, Y., Ghosh, S. S., Maumet, C., Sochat, V. v., Nichols, T. E., Poldrack, R. A., Poline, J. B., Yarkoni, T., & Margulies, D. S. (2015). NeuroVault.org: a web-based repository for collecting and sharing unthresholded statistical maps of the human brain. *Frontiers in Neuroinformatics*, *9*(APR). https://doi.org/10.3389/FNINF.2015.00008

Grabenhorst, F., Rolls, E. T., Margot, C., da Silva, M. A. A. P., & Velazco, M. I. (2007). How Pleasant and Unpleasant Stimuli Combine in Different Brain Regions: Odor Mixtures. *Journal of Neuroscience*, *27*(49), 13532–13540. https://doi.org/10.1523/JNEUROSCI.3337-07.2007

Graczyk, E. L., Delhaye, B. P., Schiefer, M. A., Bensmaia, S. J., & Tyler, D. J. (2018). Sensory adaptation to electrical stimulation of the somatosensory nerves. *Journal of Neural Engineering*, *15*(4), 046002. https://doi.org/10.1088/1741-2552/aab790

Grandchamp, R., & Delorme, A. (2011). Single-Trial Normalization for Event-Related Spectral Decomposition Reduces Sensitivity to Noisy Trials. *Frontiers in Psychology*, *2*(SEP). https://doi.org/10.3389/FPSYG.2011.00236

Grech, R., Cassar, T., Muscat, J., Camilleri, K. P., Fabri, S. G., Zervakis, M., Xanthopoulos, P., Sakkalis, V., & Vanrumste, B. (2008). Review on solving the inverse problem in EEG source analysis. *Journal of NeuroEngineering and Rehabilitation*, *5*, 25. https://doi.org/10.1186/1743-0003-5-25

Gueorguiev, D., Bochereau, S., Mouraux, A., Hayward, V., & Thonnard, J.-L. (2016). Touch uses frictional cues to discriminate flat materials. *Scientific Reports*, *6*(1), 25553. https://doi.org/10.1038/srep25553

Gurtubay-Antolin, A., León-Cabrera, P., & Rodríguez-Fornells, A. (2018). Neural Evidence of Hierarchical Cognitive Control during Haptic Processing: An fMRI Study. *ENeuro*, *5*(6). https://doi.org/10.1523/ENEURO.0295-18.2018

Hagbarth, K. -E, & Vallbo, B. (1967). Mechanoreceptor activity recorded percutaneously with semi-microelectrodes in human peripheral nerves. *Acta Physiologica Scandinavica*, *69*(1), 121–122. https://doi.org/10.1111/J.1748-1716.1967.TB03498.X

Hall, S. D., Barnes, G. R., Furlong, P. L., Seri, S., & Hillebrand, A. (2010). Neuronal network pharmacodynamics of GABAergic modulation in the human cortex determined using pharmaco-magnetoencephalography. *Human Brain Mapping*, *31*(4), 581–594. https://doi.org/10.1002/HBM.20889

Hall, S. D., Stanford, I. M., Yamawaki, N., McAllister, C. J., Rönnqvist, K. C., Woodhall, G. L., & Furlong, P. L. (2011). The role of GABAergic modulation in motor function related neuronal network activity. *NeuroImage*, *56*(3), 1506–1510. https://doi.org/10.1016/J.NEUROIMAGE.2011.02.025

Hämäläinen, H., Hiltunen, J., & Titievskaja, I. (2000). fMRI activations of SI and SII cortices during tactile stimulation depend on attention. *Neuroreport*, *11*(8), 1673–1676. https://doi.org/10.1097/00001756-200006050-00016

Hämäläinen, M., Hari, R., Ilmoniemi, R. J., Knuutila, J., & Lounasmaa, O. v. (1993). Magnetoencephalography—theory, instrumentation, and applications to noninvasive studies of the working human brain. *Reviews of Modern Physics*, *65*(2), 413. https://doi.org/10.1103/RevModPhys.65.413

Han, S. W., Chung, Y. G., Kim, H. S., Chung, S. C., Park, J. Y., & Kim, S. P. (2013). Evaluation of somatosensory cortical differences between flutter and vibration tactile stimuli. *Proceedings of the Annual International Conference of the IEEE Engineering in Medicine and Biology Society, EMBS*, 4402–4405. https://doi.org/10.1109/EMBC.2013.6610522

Han, X., Ashar, Y. K., Kragel, P., Petre, B., Schelkun, V., Atlas, L. Y., Chang, L. J., Jepma, M., Koban, L., Losin, E. A. R., Roy, M., Woo, C.-W., & Wager, T. D. (2022). Effect sizes and test-retest reliability of the fMRI-based neurologic pain signature. *NeuroImage*, *247*, 118844. https://doi.org/10.1016/j.neuroimage.2021.118844

Harada, T., Saito, D. N., Kashikura, K. I., Sato, T., Yonekura, Y., Honda, M., & Sadato, N. (2004). Asymmetrical neural substrates of tactile discrimination humans: A functional magnetic resonance imaging study. *Journal of Neuroscience*, *24*(34), 7524–7530. https://doi.org/10.1523/JNEUROSCI.1395-04.2004

Harden, R. N., Bruehl, S., Stanton-Hicks, M., & Wilson, P. R. (2007). Proposed new diagnostic criteria for complex regional pain syndrome. *Pain Medicine (Malden, Mass.)*, *8*(4), 326–331. https://doi.org/10.1111/J.1526-4637.2006.00169.X

Hari, M. P. R., & Puce, P. A. (2017). MEG-EEG Primer. *MEG-EEG Primer*. https://doi.org/10.1093/MED/9780190497774.001.0001

Hari, R., & Salmelin, R. (1997). Human cortical oscillations: a neuromagnetic view through the skull. *Trends in Neurosciences*, *20*(1), 44–49. https://doi.org/10.1016/S0166-2236(96)10065-5

Harper, J., Malone, S. M., & Bernat, E. M. (2014). Theta and delta band activity explain N2 and P3 ERP component activity in a go/no-go task. *Clinical Neurophysiology : Official Journal of the International Federation of Clinical Neurophysiology*, *125*(1), 124. https://doi.org/10.1016/J.CLINPH.2013.06.025

Harper, R., & Stevens, S. S. (1964). Subjective Hardness of Compliant Materials. *Quarterly Journal of Experimental Psychology*, *16*(3), 204–215. https://doi.org/10.1080/17470216408416370

Harrington, G. S., & Hunter Downs, J. (2001). FMRI mapping of the somatosensory cortex with vibratory stimuli: Is there a dependency on stimulus frequency? *Brain Research*, *897*(1–2), 188–192. https://doi.org/10.1016/S0006-8993(01)02139-4

Harris, A. J. (1999). Cortical origin of pathological pain. *The Lancet*, *354*(9188), 1464–1466. https://doi.org/10.1016/S0140-6736(99)05003-5

Harvey, M. A., Saal, H. P., Dammann, J. F., & Bensmaia, S. J. (2013). Multiplexing Stimulus Information through Rate and Temporal Codes in Primate Somatosensory Cortex. *PLoS Biology*, *11*(5), e1001558. https://doi.org/10.1371/journal.pbio.1001558

Hashemi, A., Pino, L. J., Moffat, G., Mathewson, K. J., Aimone, C., Bennett, P. J., Schmidt, L. A., & Sekuler, A. B. (2016). Characterizing Population EEG Dynamics throughout Adulthood. *ENeuro*, *3*(6). https://doi.org/10.1523/ENEURO.0275-16.2016

Heinrichs-Graham, E., & Wilson, T. W. (2016). Is an absolute level of cortical beta suppression required for proper movement? Magnetoencephalographic evidence from healthy aging. *NeuroImage*, *134*, 514–521. https://doi.org/10.1016/J.NEUROIMAGE.2016.04.032

Heller, M. A. (1984). Active and passive touch: The influence of exploration time on form recognition. *Journal of General Psychology*, *110*(2), 243–249. https://doi.org/10.1080/00221309.1984.9709968

Heller, M. A. (1986). Active and passive tactile braille recognition. *Bulletin of the Psychonomic Society*, *24*(3), 201–202. https://doi.org/10.3758/BF03330548

Heller, M. A. (1989). Texture perception in sighted and blind observers. *Perception & Psychophysics*, *45*(1), 49–54. https://doi.org/10.3758/BF03208032

Heller, M. A., Rogers, G. J., & Perry, C. L. (1990). Tactile pattern recognition with the optacon: Superior performance with active touch and the left hand. *Neuropsychologia*, *28*(9), 1003–1006. https://doi.org/10.1016/0028-3932(90)90114-4

Helms Tillery, S., & Sainburg, R. L. (2012). Multisensory integration for motor control and adaptation. *Journal of Motor Behavior*, *44*(6), 389–390. https://doi.org/10.1080/00222895.2012.747306

Hendee, W. R., & Morgan, C. J. (1984). Magnetic Resonance Imaging Part I—Physical Principles [Article]. *The Western Journal of Medicine*, *141*(4), 491–500.

Henderson, J., Mari, T., Hopkinson, A., Byrne, A., Hewitt, D., Newton-Fenner, A., Giesbrecht, T., Marshall, A., Stancák, A., & Fallon, N. (2022). Neural correlates of texture perception during active touch. *Behavioural Brain Research*, *429*(April), 113908. https://doi.org/10.1016/j.bbr.2022.113908

Henrich, J., Heine, S. J., & Norenzayan, A. (2010). The weirdest people in the world? *Behavioral and Brain Sciences*, *33*(2–3), 61–83. https://doi.org/10.1017/S0140525X0999152X

Herrera Ortiz, A. F., Cadavid Camacho, E., Cubillos Rojas, J., Cadavid Camacho, T., Zoe Guevara, S., Rincón Cuenca, N. T., Vásquez Perdomo, A., del Castillo Herazo, V., & Giraldo Malo, R. (2021). A Practical Guide to Perform a Systematic Literature Review

and Meta-analysis. *Principles and Practice of Clinical Research Journal*, *7*(4), 47–57. https://doi.org/10.21801/ppcrj.2021.74.6

Hertenstein, M. J., Keltner, D., App, B., Bulleit, B. A., & Jaskolka, A. R. (2006). Touch communicates distinct emotions. *Emotion*, *6*(3), 528–533. https://doi.org/10.1037/1528-3542.6.3.528

Hirt, B., Seyhan, H., & Wagner, M. (2016). *Hand and wrist anatomy and biomechanics : A comprehensive guide.* ProQuest Ebook Central.

Ho, H. N., & Jones, L. A. (2006). Contribution of thermal cues to material discrimination and localization. *Perception and Psychophysics*, *68*(1), 118–128. https://doi.org/10.3758/BF03193662

Ho, H. N., & Jones, L. A. (2008). Modeling the thermal responses of the skin surface during hand-object interactions. *Journal of Biomechanical Engineering*, *130*(2). https://doi.org/10.1115/1.2899574

Hoechstetter, K., Rupp, A., Meinck, H. M., Weckesser, D., Bornfleth, H., Stippich, C., Berg, P., & Scherg, M. (2000). Magnetic source imaging of tactile input shows task-independent attention effects in SII. *Neuroreport*, *11*(11), 2461–2465. https://doi.org/10.1097/00001756-200008030-00024

Hollins, M., Bensmaïa, S. J., & Washburn, S. (2001a). Vibrotactile adaptation impairs discrimination of fine, but not coarse, textures. *Somatosensory and Motor Research*, *18*(4), 253–262. https://doi.org/10.1080/01421590120089640

Hollins, M., Bensmaïa, S., Karlof, K., & Young, F. (2000). Individual differences in perceptual space for tactile textures: evidence from multidimensional scaling. *Perception & Psychophysics*, *62*(8), 1534–1544. https://doi.org/10.3758/BF03212154

Hollins, M., Bensmaïa, S., & Risner, R. (1998). The duplex theory of tactile texture perception. In S. Grondin & Y. Lacouture (Eds.), *Fechner Day 98. Proceedings of the Fourteenth Annual Meeting of the International Society for Psychophysics* (pp. 115–120). The International Society for Psychophysics.

Hollins, M., Bensmaïa, S. J., & Roy, E. A. (2002). Vibrotaction and texture perception. *Behavioural Brain Research*, *135*(1–2), 51–56. https://doi.org/10.1016/S0166-4328(02)00154-7

Hollins, M., Delemos, K. A., & Goble, A. K. (1996). Vebrotactile adaptation of a RA system: A psychophysical analysis. In *Somesthesis and the Neurobiology of the Somatosensory Cortex* (pp. 101–111). Birkhäuser Basel. https://doi.org/10.1007/978-3-0348-9016-8_9

Hollins, M., Faldowski, R., Rao, S., & Young, F. (1993). Perceptual dimensions of tactile surface texture: A multidimensional scaling analysis. *Perception & Psychophysics*, *54*(6), 697–705. https://doi.org/10.3758/BF03211795

Hollins, M., Fox, A., & Bishop, C. (2001b). Imposed Vibration Influences Perceived Tactile Smoothness. *Perception*, *29*(12), 1455–1465. https://doi.org/10.1068/p3044

Hollins, M., Lorenz, F., & Harper, D. (2006). Somatosensory Coding of Roughness: The Effect of Texture Adaptation in Direct and Indirect Touch. *The Journal of Neuroscience*, *26*(20), 5582. https://doi.org/10.1523/JNEUROSCI.0028-06.2006

Hollins, M., & Risner, S. R. (2000). Evidence for the duplex theory of tactile texture perception. *Perception & Psychophysics*, *62*(4), 695–705. https://doi.org/10.3758/BF03206916

Hopkinson, A. (2020a). *Linear Sensor for Touch Research EEG-Compatible Sensor for Finger Touch Position and Load on Linear 100 mm Samples*.

Hopkinson, A. (2020b). *Six-Axis Force Plate for Touch Research*.

Hoshi, E., & Tanji, J. (2007). Distinctions between dorsal and ventral premotor areas: anatomical connectivity and functional properties. *Current Opinion in Neurobiology*, *17*(2), 234–242. https://doi.org/10.1016/J.CONB.2007.02.003

Houdayer, E., Labyt, E., Cassim, F., Bourriez, J. L., & Derambure, P. (2006). Relationship between event-related beta synchronization and afferent inputs: Analysis of finger movement and peripheral nerve stimulations. *Clinical Neurophysiology*, *117*(3), 628–636. https://doi.org/10.1016/j.clinph.2005.12.001

Hsiao, F. J., Wu, Z. A., Ho, L. T., & Lin, Y. Y. (2009). Theta oscillation during auditory change detection: An MEG study. *Biological Psychology*, *81*(1), 58–66. https://doi.org/10.1016/J.BIOPSYCHO.2009.01.007

Hu, L., Zhao, C., Li, H., & Valentini, E. (2013). Mismatch responses evoked by nociceptive stimuli. *Psychophysiology*, *50*(2), 158–173. https://doi.org/10.1111/PSYP.12000

Hyvärinen, J. (1982). Posterior parietal lobe of the primate brain. *Https://Doi.Org/10.1152/Physrev.1982.62.3.1060*, *62*(3), 1060–1129. https://doi.org/10.1152/PHYSREV.1982.62.3.1060

Ille, N., Berg, P., & Scherg, M. (2002). Artifact correction of the ongoing EEG using spatial filters based on artifact and brain signal topographies. *Journal of Clinical Neurophysiology : Official Publication of the American Electroencephalographic Society*, *19*(2), 113–124. https://doi.org/10.1097/00004691-200203000-00002

Iramina, K., Ueno, S., & Matsuoka, S. (1996). MEG and EEG topography of frontal midline theta rhythm and source localization. *Brain Topography*, *8*(3), 329–331. https://doi.org/10.1007/BF01184793/METRICS

Iwamura, Y. (2009). Tactile Senses – Touch. *Encyclopedia of Neuroscience*, 4005–4009. https://doi.org/10.1007/978-3-540-29678-2_5873

Jänig, W., Schmidt, R. F., & Zimmermann, M. (1968). Single unit responses and the total afferent outflow from the cat's foot pad upon mechanical stimulation. *Experimental Brain Research*, *6*(2), 100–115. https://doi.org/10.1007/BF00239165

Jasper, H. (1958). The Ten-Twenty Electrode System of the International Federation. *Electroencephalography and Clinical Neurophysiology*, *10*, 371–375.

Javed, K., & Daly, D. T. (2021). Neuroanatomy, Lower Motor Neuron Lesion. *StatPearls*. https://www.ncbi.nlm.nih.gov/books/NBK539814/

Javed, K., Reddy, V., & Lui, F. (2021). Neuroanatomy, Lateral Corticospinal Tract. *StatPearls*. https://www.ncbi.nlm.nih.gov/books/NBK534818/

Jeannerod, M., Arbib, M. A., Rizzolatti, G., & Sakata, H. (1995). Grasping objects: the cortical mechanisms of visuomotor transformation. *Trends in Neurosciences*, *18*(7), 314–320. https://doi.org/10.1016/0166-2236(95)93921-J

Jensen, K. B., Regenbogen, C., Ohse, M. C., Frasnelli, J., Freiherr, J., & Lundström, J. N. (2016). Brain activations during pain: a neuroimaging meta-analysis of patients with pain and healthy controls. *Pain*, *157*(6), 1279–1286. https://doi.org/10.1097/J.PAIN.0000000000000517

Jensen, O., Goel, P., Kopell, N., Pohja, M., Hari, R., & Ermentrout, B. (2005). On the human sensorimotor-cortex beta rhythm: Sources and modeling. *NeuroImage*, *26*(2), 347–355. https://doi.org/10.1016/J.NEUROIMAGE.2005.02.008

Jensen, O., & Mazaheri, A. (2010). Shaping Functional Architecture by Oscillatory Alpha Activity: Gating by Inhibition. *Frontiers in Human Neuroscience*, *4*. https://doi.org/10.3389/FNHUM.2010.00186

Jiang, W., Chapman, C. E., & Lamarre, Y. (1991). Modulation of the cutaneous responsiveness of neurones in the primary somatosensory cortex during conditioned arm movements in the monkey. *Exp Brain Res*, *84*, 342–354.

Jiang, W., Lamarre, Y., & Chapman, C. E. (1990). Modulation of cutaneous cortical evoked potentials during isometric and isotonic contractions in the monkey. *Brain Research*, *536*(1–2), 69–78. https://doi.org/10.1016/0006-8993(90)90010-9

Jiang, W., Tremblay, F., & Chapman, C. E. (1997). Neuronal encoding of texture changes in the primary and the secondary somatosensory cortical areas of monkeys during passive texture discrimination. *Journal of Neurophysiology*, *77*(3), 1656–1662. https://doi.org/10.1152/JN.1997.77.3.1656

Johansson, R. S., Trulsson, M., Olsson, K. Å., & Abbs, J. H. (1988). Mechanoreceptive afferent activity in the infraorbital nerve in man during speech and chewing movements. *Experimental Brain Research*, *72*(1), 209–214. https://doi.org/10.1007/BF00248519

Johansson, R. S., & Vallbo, A. B. (1979). Tactile sensibility in the human hand: relative and absolute densities of four types of mechanoreceptive units in glabrous skin. *The Journal of Physiology*, *286*(1), 283–300. https://doi.org/10.1113/JPHYSIOL.1979.SP012619

Johansson, R. S., & Vallbo, Å. B. (1983). Tactile sensory coding in the glabrous skin of the human hand. *Trends in Neurosciences*, *6*(C), 27–32. https://doi.org/10.1016/0166-2236(83)90011-5

Johns, P. (2014). Functional neuroanatomy. *Clinical Neuroscience*, 27–47. https://doi.org/10.1016/B978-0-443-10321-6.00003-5

Johnson, K. O., Darian-Smith, I., & LaMotte, C. (1973). Peripheral neural determinants of temperature discrimination in man: a correlative study of responses to cooling skin. *Journal of Neurophysiology*, *36*(2), 347–370. https://doi.org/10.1152/JN.1973.36.2.347

Johnson, K. O., Darian-Smith, I., LaMotte et, a. C., & Oldfield, S. (1979). Coding of incremental changes in skin temperature by a population of warm fibers in the monkey: correlation with intensity discrimination in man. *Journal of Neurophysiology*, *42*(5), 1332–1353. https://doi.org/10.1152/JN.1979.42.5.1332

Johnson, K. O., & Hsiao, S. S. (1992). Neural mechanisms of tactual form and texture perception. In *Annual Review of Neuroscience* (Vol. 15, Issue 1). Annual Reviews 4139 El Camino Way, P.O. Box 10139, Palo Alto, CA 94303-0139, USA. https://doi.org/10.1146/annurev.ne.15.030192.001303

Johnson, K. O., Yoshioka, T., & Vega Bermudez, F. (2000). Tactile functions of mechanoreceptive afferents innervating the hand. *Journal of Clinical Neurophysiology*, *17*(6), 539–558. https://doi.org/10.1097/00004691-200011000-00002

Jones, L. A., & Lederman, S. J. (2006). Human Hand Function. *Human Hand Function*, 1–280. https://doi.org/10.1093/ACPROF:OSO/9780195173154.001.0001

Jung, R., & Berger, W. (1979). Hans Bergers Entdeckung des Elektrenkephalogramms und seine ersten Befunde 1924-1931. *Archiv Für Psychiatrie Und Nervenkrankheiten*, *227*(4), 279–300. https://doi.org/10.1007/BF00344814

Juravle, G., Binsted, G., & Spence, C. (2016a). Tactile suppression in goal-directed movement. *Psychonomic Bulletin & Review 2016 24:4*, *24*(4), 1060–1076. https://doi.org/10.3758/S13423-016-1203-6

Juravle, G., Binsted, G., & Spence, C. (2017). *Tactile suppression in goal-directed movement*. *24*, 1060–1076. https://doi.org/10.3758/s13423-016-1203-6

Juravle, G., Heed, T., Spence, C., & Röder, B. (2016b). Neural correlates of tactile perception during pre-, peri-, and post-movement. *Experimental Brain Research*, *234*, 1293–1305. https://doi.org/10.1007/s00221-016-4589-5

Juravle, G., McGlone, F., & Spence, C. (2013). Context-dependent changes in tactile perception during movement execution. *Frontiers in Psychology*, *4*(DEC). https://doi.org/10.3389/FPSYG.2013.00913

Kaas, J. H., & Garraghty, P. E. (1991). Hierarchical, parallel, and serial arrangements of sensory cortical areas: connection patterns and functional aspects. *Current Opinion in Neurobiology*, *1*(2), 248–251. https://doi.org/10.1016/0959-4388(91)90085-L

Kalaska, J. F., & Rizzolatti, G. (2012). Voluntary Movement: The Primary Motor Cortex. In E. R. Kandel, J. H. Schwartz, T. M. Jessell, S. A. Siegelbaum, & A. J. Hudspeth (Eds.), *Principles of neural science* (Fifth, pp. 835–863). McGraw-Hill Publishing.

Kalcher, J., & Pfurtscheller, G. (1995). Discrimination between phase-locked and non-phase-locked event-related EEG activity. *Electroencephalography and Clinical Neurophysiology*, *94*(5), 381–384. https://doi.org/10.1016/0013-4694(95)00040-6

Kalnins, A., & Business, P. (2018). Multicollinearity: How common factors cause Type 1 errors in multivariate regression. *Strategic Management Journal*, *39*(8), 2362–2385. https://doi.org/10.1002/SMJ.2783

Kanafi, M. (2022). *Surface generator: artificial randomly rough surfaces*. MATLAB Central File Exchange. https://www.mathworks.com/matlabcentral/fileexchange/60817-surface-generator-artificial-randomly-rough-surfaces

Karakaş, S. (2020). A review of theta oscillation and its functional correlates. *International Journal of Psychophysiology*, *157*, 82–99. https://doi.org/10.1016/J.IJPSYCHO.2020.04.008

Katz, D. (1925). Der Aufbau der Tastwelt. *Zeitschrift Für Psychologie, Leipzig: Barth*.

Katz, D. (1989). *The World of Touch* (L. E. Krueger, Ed.). Psychology Press. https://doi.org/10.4324/9780203771976

Keil, A., Bernat, E. M., Cohen, M. X., Ding, M., Fabiani, M., Gratton, G., Kappenman, E. S., Maris, E., Mathewson, K. E., Ward, R. T., & Weisz, N. (2022). Recommendations and publication guidelines for studies using frequency domain and time-frequency domain

analyses of neural time series. *Psychophysiology*, *59*(5), 1–37. https://doi.org/10.1111/psyp.14052

Kelly, S. P., & O'Connell, R. G. (2013). Internal and External Influences on the Rate of Sensory Evidence Accumulation in the Human Brain. *The Journal of Neuroscience*, *33*(50), 19434. https://doi.org/10.1523/JNEUROSCI.3355-13.2013

Keynan, J. N., Meir-Hasson, Y., Gilam, G., Cohen, A., Jackont, G., Kinreich, S., Ikar, L., Or-Borichev, A., Etkin, A., Gyurak, A., Klovatch, I., Intrator, N., & Hendler, T. (2016). Limbic Activity Modulation Guided by Functional Magnetic Resonance Imaging–Inspired Electroencephalography Improves Implicit Emotion Regulation. *Biological Psychiatry*, *80*(6), 490–496. https://doi.org/10.1016/J.BIOPSYCH.2015.12.024

Khan, Y. S., & Lui, F. (2021). Neuroanatomy, Spinal Cord. *StatPearls*. https://www.ncbi.nlm.nih.gov/books/NBK559056/

Kiebel, S. J., & Holmes, A. P. (2007). The General Linear Model [Book]. In K. J. (Karl J.) Friston (Ed.), *Statistical parametric mapping the analysis of functional brain images* (pp. 101–125). Academic.

Kiebel, S., Kilner, J., & Friston, K. (2007). Hierarchical models for EEG and MEG [Book]. In K. J. (Karl J.) Friston (Ed.), *Statistical parametric mapping the analysis of functional brain images* (pp. 211–220). Academic.

Kilner, J. M., Kiebel, S. J., & Friston, K. J. (2005). Applications of random field theory to electrophysiology. *Neuroscience Letters*, *374*(3), 174–178. https://doi.org/10.1016/J.NEULET.2004.10.052

Kim, J., Chung, Y. G., Park, J.-Y., Chung, S.-C., Wallraven, C., Bülthoff, H. H., & Kim, S.-P. (2015). Decoding Accuracy in Supplementary Motor Cortex Correlates with Perceptual Sensitivity to Tactile Roughness. *PloS One*, *10*(6), e0129777. https://doi.org/10.1371/journal.pone.0129777

Kim, S. G., & Ogawa, S. (2012). Biophysical and physiological origins of blood oxygenation level-dependent fMRI signals. *Journal of Cerebral Blood Flow and Metabolism : Official Journal of the International Society of Cerebral Blood Flow and Metabolism*, *32*(7), 1188–1206. https://doi.org/10.1038/JCBFM.2012.23

Kitada, R., Hashimoto, T., Kochiyama, T., Kito, T., Okada, T., Matsumura, M., Lederman, S. J., & Sadato, N. (2005). Tactile estimation of the roughness of gratings yields a graded response in the human brain: An fMRI study. *NeuroImage*, *25*(1), 90–100. https://doi.org/10.1016/j.neuroimage.2004.11.026

Kitada, R., Kito, T., Saito, D. N., Kochiyama, T., Matsumura, M., Sadato, N., & Lederman, S. J. (2006). Multisensory Activation of the Intraparietal Area When Classifying Grating Orientation: A Functional Magnetic Resonance Imaging Study. *Journal of Neuroscience*, *26*(28), 7491–7501. https://doi.org/10.1523/JNEUROSCI.0822-06.2006

Klem, G. H., Lüders, H. O., Jasper, H. H., & Elger, C. (1999). The ten-twenty electrode system of the International Federation. The International Federation of Clinical Neurophysiology. *Electroencephalography and Clinical Neurophysiology. Supplement*, *52*, 3–6. http://www.ncbi.nlm.nih.gov/pubmed/10590970

Klimesch, W. (1999). EEG alpha and theta oscillations reflect cognitive and memory performance: a review and analysis. *Brain Research. Brain Research Reviews*, *29*(2–3), 169–195. https://doi.org/10.1016/S0165-0173(98)00056-3

Klimesch, W. (2012). α-band oscillations, attention, and controlled access to stored information. *Trends in Cognitive Sciences*, *16*(12), 606–617. https://doi.org/10.1016/J.TICS.2012.10.007

Klimesch, W., Freunberger, R., Sauseng, P., & Gruber, W. (2008). A short review of slow phase synchronization and memory: Evidence for control processes in different memory systems? *Brain Research*, *1235*, 31–44. https://doi.org/10.1016/J.BRAINRES.2008.06.049

Klimesch, W., Russegger, H., Doppelmayr, M., & Pachinger, T. (1998). A method for the calculation of induced band power: implications for the significance of brain oscillations. *Electroencephalography and Clinical Neurophysiology*, *108*(2), 123–130. https://doi.org/10.1016/S0168-5597(97)00078-6

Klimesch, W., Sauseng, P., & Hanslmayr, S. (2007). EEG alpha oscillations: The inhibition–timing hypothesis. *Brain Research Reviews*, *53*(1), 63–88. https://doi.org/10.1016/J.BRAINRESREV.2006.06.003

Klingner, C. M., Brodoehl, S., Huonker, R., & Witte, O. W. (2016). The processing of somatosensory information shifts from an early parallel into a serial processing mode: A combined fMRI/MEG study. *Frontiers in Systems Neuroscience*, *10*(DEC), 103. https://doi.org/10.3389/FNSYS.2016.00103/BIBTEX

Klingner, C. M., Nenadic, I., Hasler, C., Brodoehl, S., & Witte, O. W. (2011). Habituation within the somatosensory processing hierarchy. *Behavioural Brain Research*, *225*(2), 432–436. https://doi.org/10.1016/j.bbr.2011.07.053

Klöcker, A., Arnould, C., Penta, M., & Thonnard, J.-L. (2012). Rasch-Built Measure of Pleasant Touch through Active Fingertip Exploration. *Frontiers in Neurorobotics*, *6*, 5. https://doi.org/10.3389/fnbot.2012.00005

Klöcker, A., Wiertlewski, M., Théate, V., Hayward, V., & Thonnard, J.-L. (2013). Physical Factors Influencing Pleasant Touch during Tactile Exploration. *PLoS ONE*, *8*(11), e79085. https://doi.org/10.1371/journal.pone.0079085

Ko, D., Kwon, S., Lee, G. T., Im, C. H., Kim, K. H., & Jung, K. Y. (2012). Theta Oscillation Related to the Auditory Discrimination Process in Mismatch Negativity: Oddball versus Control Paradigm. *Journal of Clinical Neurology*, *8*(1), 35–42. https://doi.org/10.3988/JCN.2012.8.1.35

Kober, H., & Wager, T. D. (2010). Meta-analysis of neuroimaging data. *WIREs Cognitive Science*, *1*(2), 293–300. https://doi.org/10.1002/wcs.41

Koenig, T., Studer, D., Hubl, D., Melie, L., & Strik, W. K. (2005). Brain connectivity at different time-scales measured with EEG. In *Philosophical Transactions of the Royal Society B: Biological Sciences* (Vol. 360, Issue 1457, pp. 1015–1023). Royal Society. https://doi.org/10.1098/rstb.2005.1649

Konen, C. S., Mruczek, R. E. B., Montoya, J. L., & Kastner, S. (2013). Functional organization of human posterior parietal cortex: Grasping- and reaching-related activations relative to topographically organized cortex. *Journal of Neurophysiology*, *109*(12), 2897–2908. https://doi.org/10.1152/JN.00657.2012/ASSET/IMAGES/LARGE/Z9K0121319550006.JPEG

Kringelbach, M. L. (2005). The human orbitofrontal cortex: Linking reward to hedonic experience. In *Nature Reviews Neuroscience* (Vol. 6, Issue 9, pp. 691–702). Nature Publishing Group. https://doi.org/10.1038/nrn1747

Kropotov, J. D. (2009). Quantitative EEG, Event-Related Potentials and Neurotherapy [Book]. In *Quantitative EEG, Event-Related Potentials and Neurotherapy* (1st ed.). Elsevier/Academic. https://doi.org/10.1016/B978-0-12-374512-5.X0001-1

Kurth, F., Zilles, K., Fox, P. T., Laird, A. R., & Eickhoff, S. B. (2010). A link between the systems: functional differentiation and integration within the human insula revealed by meta-analysis. *Brain Structure & Function*, *214*(5–6), 519. https://doi.org/10.1007/S00429-010-0255-Z

Lagerlund, T. D., Sharbrough, F. W., & Busacker, N. E. (1997). Spatial filtering of multichannel electroencephalographic recordings through principal component analysis by singular value decomposition. *Journal of Clinical Neurophysiology : Official Publication of the American Electroencephalographic Society*, *14*(1), 73–82. https://doi.org/10.1097/00004691-199701000-00007

Lamb, G. D. (1983). Tactile discrimination of textured surfaces: psychophysical performance measurements in humans. *The Journal of Physiology*, *338*(1), 551–565. https://doi.org/10.1113/JPHYSIOL.1983.SP014689

Lane, A. E., Dennis, S. J., & Geraghty, M. E. (2011). Brief report: Further evidence of sensory subtypes in autism. *Journal of Autism and Developmental Disorders*, *41*(6), 826–831. https://doi.org/10.1007/S10803-010-1103-Y

Laufer, I., Negishi, M., Rajeevan, N., Lacadie, C. M., & Constable, R. T. (2008). Sensory and cognitive mechanisms of change detection in the context of speech. *Brain Structure & Function*, *212*(5), 427. https://doi.org/10.1007/S00429-007-0167-8

le Bars, D., & Cadden, S. W. (2008). What is a Wide-Dynamic-Range Cell? *The Senses: A Comprehensive Reference*, *5*, 331–338. https://doi.org/10.1016/B978-012370880-9.00167-5

Ledberg, A., O'Sullivan, B. T., Kinomura, S., & Roland, P. E. (1995). Somatosensory activations of the parietal operculum of man. A PET study. *The European Journal of Neuroscience*, *7*(9), 1934–1941. https://doi.org/10.1111/J.1460-9568.1995.TB00716.X

Lederman, S. J. (1974). Tactile roughness of grooved surfaces: The touching process and effects of macro- and microsurface structure. *Perception & Psychophysics*, *16*(2), 385–395. https://doi.org/10.3758/BF03203958

Lederman, S. J. (1976). The 'callus-thenics' of touching. *Canadian Journal of Psychology/Revue Canadienne de Psychologie*, *30*(2), 89. https://doi.org/10.1037/H0082051

Lederman, S. J. (1979). Auditory texture perception. *Perception*, *8*(1), 93–103. https://doi.org/10.1068/P080093

Lederman, S. J. (1981). The perception of surface roughness by active and passive touch. *Bulletin of the Psychonomic Society*, *18*(5), 253–255. https://doi.org/10.3758/BF03333619

Lederman, S. J., & Abbott, S. G. (1981). Texture perception: Studies of intersensory organization using a discrepancy paradigm, and visual versus tactual psychophysics.

Journal of Experimental Psychology: Human Perception and Performance, *7*(4), 902–915. https://doi.org/10.1037/0096-1523.7.4.902

Lederman, S. J., & Klatzky, R. L. (1987). Hand movements: A window into haptic object recognition. *Cognitive Psychology*, *19*(3), 342–368. https://doi.org/10.1016/0010-0285(87)90008-9

Lederman, S. J., & Klatzky, R. L. (1993). Extracting object properties through haptic exploration. In *Acta Psychologica* (Vol. 84). https://ac.els-cdn.com/0001691893900708/1-s2.0-0001691893900708-main.pdf?_tid=33f36eeb-1572-4ac6-b75e-e16454ffb0f8&acdnat=1540299794_a2656bcb5ad7daf97f67afb5d9b3e6a6

Lederman, S. J., & Klatzky, R. L. (2009). Haptic perception: A tutorial. *Attention, Perception, and Psychophysics*, *71*(7), 1439–1459. https://doi.org/10.3758/APP.71.7.1439

Lederman, S. J., Loomis, J. M., & Williams, D. A. (1982). The role of vibration in the tactual perception of roughness. *Perception & Psychophysics*, *32*(2), 109–116. https://doi.org/10.3758/BF03204270

Lederman, S. J., & Taylor, M. M. (1972). Fingertip force, surface geometry, and the perception of roughness by active touch. *Perception & Psychophysics 1972 12:5*, *12*(5), 401–408. https://doi.org/10.3758/BF03205850

Lee, R. G., & White, D. G. (1974). Modification of the human somatosensory evoked response during voluntary movement. *Electroencephalography and Clinical Neurophysiology*, *36*(C), 53–62. https://doi.org/10.1016/0013-4694(74)90136-9

Legewie, H., Simonova, O., & Creutzfeldt, O. D. (1969). EEG changes during performance of various tasks under open- and closed-eye conditions. *Electroencephalography and Clinical Neurophysiology*, *27*(5), 470–479. https://doi.org/10.1016/0013-4694(69)90187-4

Lehmann, D. (1984). EEG assessment of brain activity: Spatial aspects, segmentation and imaging. *International Journal of Psychophysiology*, *1*(3), 267–276. https://doi.org/10.1016/0167-8760(84)90046-1

Lei, Y., & Perez, M. A. (2017). Cortical contributions to sensory gating in the ipsilateral somatosensory cortex during voluntary activity. *The Journal of Physiology*, *595*(18), 6203. https://doi.org/10.1113/JP274504

Lelis-Torres, N., Ugrinowitsch, H., Apolinário-Souza, T., Benda, R. N., & Lage, G. M. (2017). Task engagement and mental workload involved in variation and repetition of a motor skill. *Scientific Reports*, *7*(1), 1–10. https://doi.org/10.1038/s41598-017-15343-3

Lenz, M., Höffken, O., Stude, P., Lissek, S., Schwenkreis, P., Reinersmann, A., Frettlöh, J., Richter, H., Tegenthoff, M., & Maier, C. (2011). Bilateral somatosensory cortex disinhibition in complex regional pain syndrome type I. *Neurology*, *77*(11), 1096–1101. https://doi.org/10.1212/WNL.0B013E31822E1436

Lesniak, D. R., & Gerling, G. J. (2009). Predicting SA-I mechanoreceptor spike times with a skin-neuron model. *Mathematical Biosciences*, *220*(1), 15–23. https://doi.org/10.1016/J.MBS.2009.03.007

Lewis, J. S., & Schweinhardt, P. (2012). Perceptions of the painful body: the relationship between body perception disturbance, pain and tactile discrimination in complex

regional pain syndrome. *European Journal of Pain (London, England)*, *16*(9), 1320–1330. https://doi.org/10.1002/J.1532-2149.2012.00120.X

Lewis, P. A., Critchley, H. D., Rotshtein, P., & Dolan, R. J. (2007). Neural Correlates of Processing Valence and Arousal in Affective Words. *Cerebral Cortex*, *17*(3), 742–748. https://doi.org/10.1093/CERCOR/BHK024

Li, H., Yang, J., Yu, Y., Wang, W., Liu, Y., Zhou, M., Li, Q., Yang, J., Shao, S., Takahashi, S., Ejima, Y., & Wu, J. (2022). Global surface features contribute to human haptic roughness estimations. *Experimental Brain Research*, *240*(3), 773–789. https://doi.org/10.1007/S00221-021-06289-0/FIGURES/7

Li, L., Rutlin, M., Abraira, V. E., Cassidy, C., Kus, L., Gong, S., Jankowski, M. P., Luo, W., Heintz, N., Koerber, H. R., Woodbury, C. J., & Ginty, D. D. (2011). The functional organization of cutaneous low-threshold mechanosensory neurons. *Cell*, *147*(7), 1615. https://doi.org/10.1016/J.CELL.2011.11.027

Liang, T., Hu, Z., & Liu, Q. (2017). Frontal theta activity supports detecting mismatched information in visual working memory. *Frontiers in Psychology*, *8*(OCT), 1821. https://doi.org/10.3389/FPSYG.2017.01821/BIBTEX

Lieber, J. D., & Bensmaia, S. J. (2019). High-dimensional representation of texture in somatosensory cortex of primates. *Proceedings of the National Academy of Sciences of the United States of America*, *116*(8), 3268–3277. https://doi.org/10.1073/PNAS.1818501116/SUPPL_FILE/PNAS.1818501116.SAPP.PDF

Lieber, J. D., & Bensmaia, S. J. (2020). Emergence of an Invariant Representation of Texture in Primate Somatosensory Cortex. *Cerebral Cortex*, *30*(5), 3228–3239. https://doi.org/10.1093/cercor/bhz305

Lieber, J. D., & Bensmaia, S. J. (2022). The neural basis of tactile texture perception. *Current Opinion in Neurobiology*, *76*, 102621. https://doi.org/10.1016/J.CONB.2022.102621

Lin, W., Kuppusamy, K., Haacke, E. M., & Burton, H. (1996). Functional MRI in human somatosensory cortex activated by touching textured surfaces. *Journal of Magnetic Resonance Imaging : JMRI*, *6*(4), 565–572. https://doi.org/10.1002/jmri.1880060402

Lin, Y. Y., & Forss, N. (2002). Functional characterization of human second somatosensory cortex by magnetoencephalography. *Behavioural Brain Research*, *135*(1–2), 141–145. https://doi.org/10.1016/S0166-4328(02)00143-2

Lindquist, K. A., Satpute, A. B., Wager, T. D., Weber, J., & Barrett, L. F. (2016). The Brain Basis of Positive and Negative Affect: Evidence from a Meta-Analysis of the Human Neuroimaging Literature. *Cerebral Cortex (New York, NY)*, *26*(5), 1910. https://doi.org/10.1093/CERCOR/BHV001

Little, S., Bonaiuto, J., Barnes, G., & Bestmann, S. (2018). Motor cortical beta transients delay movement initiation and track errors. In *bioRxiv* (p. 384370). bioRxiv. https://doi.org/10.1101/384370

Lloyd, D. P. C. (1943). NEURON PATTERNS CONTROLLING TRANSMISSION OF IPSILATERAL HIND LIMB REFLEXES IN CAT. *Journal of Neurophysiology*, *6*(4), 293–315. https://doi.org/10.1152/jn.1943.6.4.293

Loeb, G. E., & Mileusnic, M. (2015). Proprioceptors and Models of Transduction. *Scholarpedia*, *10*(5), 12390. https://doi.org/10.4249/SCHOLARPEDIA.12390

Logothetis, N. K. (2008). What we can do and what we cannot do with fMRI. *Nature 2008 453:7197*, *453*(7197), 869–878. https://doi.org/10.1038/nature06976

Logothetis, N. K., Pauls, J., Augath, M., Trinath, T., & Oeltermann, A. (2001). Neurophysiological investigation of the basis of the fMRI signal. *Nature 2001 412:6843*, *412*(6843), 150–157. https://doi.org/10.1038/35084005

Löken, L. S., Evert, M., & Wessberg, J. (2012). *Pleasantness of touch in human glabrous and hairy skin: Order effects on affective ratings*. https://doi.org/10.1016/j.brainres.2011.08.011

Luck, S. J. (2014). *An introduction to the event-related potential technique* (2nd ed.) [Book]. The MIT Press.

Luu, P., & Ferree, T. (2005). *Determination of the HydroCel Geodesic Sensor Nets' Average Electrode Positions and Their 10-10 International Equivalents*.

Lynn, B. (1971). The form and distribution of the receptive fields of Pacinian corpuscles found in and around the cat's large foot pad. *The Journal of Physiology*, *217*(3), 755–771. https://doi.org/10.1113/JPHYSIOL.1971.SP009598

Makeig, S. (1993). Auditory event-related dynamics of the EEG spectrum and effects of exposure to tones. *Electroencephalography and Clinical Neurophysiology*, *86*(4), 283–293. https://doi.org/10.1016/0013-4694(93)90110-H

Makeig, S., Debener, S., Onton, J., & Delorme, A. (2004). Mining event-related brain dynamics. *Trends in Cognitive Sciences*, *8*(5), 204–210. https://doi.org/10.1016/j.tics.2004.03.008

Malmivuo, J., & Plonsey, R. (1995). Electroencephalography [Book]. In R. Plonsey (Ed.), *Bioelectromagnetism : principles and applications of bioelectric and biomagnetic fields*. Oxford University Press.

Mandeville, J. B., & Rosen, B. R. (2002). Functional MRI. *Brain Mapping: The Methods*, 315–349. https://doi.org/10.1016/B978-012693019-1/50015-0

Manfredi, L. R., Saal, H. P., Brown, K. J., Zielinski, M. C., Dammann, J. F., Polashock, V. S., & Bensmaia, S. J. (2014). Natural scenes in tactile texture. *Journal of Neurophysiology*, *111*(9), 1792–1802. https://doi.org/10.1152/JN.00680.2013/ASSET/IMAGES/LARGE/Z9K0091424010006.JPEG

Maris, E. (2004). Randomization tests for ERP topographies and whole spatiotemporal data matrices. *Psychophysiology*, *41*(1), 142–151. https://doi.org/10.1111/j.1469-8986.2003.00139.x

Maris, E., & Oostenveld, R. (2007). Nonparametric statistical testing of EEG- and MEG-data. *Journal of Neuroscience Methods*, *164*(1), 177–190. https://doi.org/10.1016/j.jneumeth.2007.03.024

Markram, H., Muller, E., Ramaswamy, S., Reimann, M. W., Abdellah, M., Sanchez, C. A., Ailamaki, A., Alonso-Nanclares, L., Antille, N., Arsever, S., Kahou, G. A. A., Berger, T. K., Bilgili, A., Buncic, N., Chalimourda, A., Chindemi, G., Courcol, J. D.,

Delalondre, F., Delattre, V., … Schürmann, F. (2015). Reconstruction and Simulation of Neocortical Microcircuitry. *Cell*, *163*(2), 456–492. https://doi.org/10.1016/J.CELL.2015.09.029

Marschallek, B. E., Löw, A., & Jacobsen, T. (2023). You can touch this! Brain correlates of aesthetic processing of active fingertip exploration of material surfaces. *Neuropsychologia*, 108520. https://doi.org/10.1016/J.NEUROPSYCHOLOGIA.2023.108520

Mathalon, D. H., & Sohal, V. S. (2015). Neural Oscillations and Synchrony in Brain Dysfunction and Neuropsychiatric Disorders: It's About Time. *JAMA Psychiatry*, *72*(8), 840–844. https://doi.org/10.1001/JAMAPSYCHIATRY.2015.0483

McComas, A. J., & Cupido, C. M. (1999). The RULER model. Is this how the somatosensory cortex works? *Clinical Neurophysiology*, *110*(11), 1987–1994. https://doi.org/10.1016/S1388-2457(99)00067-X

McGlone, F., Olausson, H., Boyle, J. A., Jones-Gotman, M., Dancer, C., Guest, S., & Essick, G. (2012). Touching and feeling: Differences in pleasant touch processing between glabrous and hairy skin in humans. *European Journal of Neuroscience*, *35*(11), 1782–1788. https://doi.org/10.1111/j.1460-9568.2012.08092.x

McGlone, F. P., & Walker, S. C. (2020). The Neurobiological Basis of Affective Touch. In *The Senses: A Comprehensive Reference* (pp. 67–78). Elsevier. https://doi.org/10.1016/B978-0-12-809324-5.24227-2

McGlone, F., & Reilly, D. (2010). The cutaneous sensory system. *Neuroscience and Biobehavioral Reviews*, *34*(2), 148–159. https://doi.org/10.1016/j.neubiorev.2009.08.004

McGlone, F., & Walker, S. (2016). Losing Touch: An unrecognised consequence of aging [Book]. In *Age-from the anatomy of life to the architecture of living* (pp. 98–109). Vubpress.

McGlone, F., Wessberg, J., & Olausson, H. (2014). Discriminative and Affective Touch: Sensing and Feeling. *Neuron*, *82*(4), 737–755. https://doi.org/10.1016/J.NEURON.2014.05.001

Menon, V., & D'Esposito, M. (2021). The role of PFC networks in cognitive control and executive function. *Neuropsychopharmacology 2021 47:1*, *47*(1), 90–103. https://doi.org/10.1038/s41386-021-01152-w

Merabet, L. B., Swisher, J. D., McMains, S. A., Halko, M. A., Amedi, A., Pascual-Leone, A., & Somers, D. C. (2007). Combined activation and deactivation of visual cortex during tactile sensory processing. *Journal of Neurophysiology*, *97*(2), 1633–1641. https://doi.org/10.1152/JN.00806.2006/ASSET/IMAGES/LARGE/Z9K0020780010004.JPEG

Michael-Titus, Adina., Revest, Patricia., & Shortland, Peter. (2010). The Spinal Cord. In Adina. Michael-Titus, Patricia. Revest, & Peter. Shortland (Eds.), *The nervous system basic science and clinical conditions* (2nd ed., pp. 67–87). https://archive.org/details/nervoussystembas0002mich

Michel, C. M., & He, B. (2011). EEG mapping and Source Imaging [Book]. In E. Niedermeyer, D. L. Schomer, & F. H. Lopes da Silva (Eds.), *Niedermeyer's electroencephalography : basic principles, clinical applications, and related fields* (6th ed., pp. 1179–1202). Lippincott Williams & Wilkins.

Mishkin, M. (1979). Analogous neural models for tactual and visual learning. *Neuropsychologia*, *17*(2), 139–151. https://doi.org/10.1016/0028-3932(79)90005-8

Moher, D., Liberati, A., Tetzlaff, J., & Altman, D. G. (2009). Preferred reporting items for systematic reviews and meta-analyses: The PRISMA statement. In *BMJ (Online)* (Vol. 339, Issue 7716, pp. 332–336). British Medical Journal Publishing Group. https://doi.org/10.1136/bmj.b2535

Morales, S., & Bowers, M. E. (2022). Time-frequency analysis methods and their application in developmental EEG data. *Developmental Cognitive Neuroscience*, *54*, 101067. https://doi.org/10.1016/J.DCN.2022.101067

Morley, J. W., Goodwin, A. W., & Darian-Smith, I. (1983). Tactile discrimination of gratings. *Experimental Brain Research*, *49*(2), 477–491. https://doi.org/10.1007/BF00238588

Morley, J. W., Vickery, R. M., Stuart, M., & Turman, A. B. (2007). Suppression of vibrotactile discrimination by transcranial magnetic stimulation of primary somatosensory cortex. *European Journal of Neuroscience*, *26*(4), 1007–1010. https://doi.org/10.1111/J.1460-9568.2007.05729.X

Morrison, I. (2016). ALE meta-analysis reveals dissociable networks for affective and discriminative aspects of touch. *Human Brain Mapping*, *37*(4), 1308–1320. https://doi.org/10.1002/hbm.23103

Morrison, I., Löken, L. S., & Olausson, H. (2010). The skin as a social organ. *Experimental Brain Research*, *204*(3), 305–314. https://doi.org/10.1007/S00221-009-2007-Y/FIGURES/2

Moungou, A., Thonnard, J. L., & Mouraux, A. (2016). EEG frequency tagging to explore the cortical activity related to the tactile exploration of natural textures. *Scientific Reports*, *6*(January), 1–10. https://doi.org/10.1038/srep20738

Mountcastle, V. B. (1998). *Perceptual neuroscience : the cerebral cortex* [Book]. Harvard University Press.

Mountcastle, V. B., Lynch, J. C., Georgopoulos, A., Sakata, H., & Acuna, C. (1975). Posterior parietal association cortex of the monkey: command functions for operations within extrapersonal space. *Journal of Neurophysiology*, *38*(4), 871–908. https://doi.org/10.1152/jn.1975.38.4.871

Mountcastle, V. B., Mind, K., & Brain, /. (1995). The Parietal System and Some Higher Brain Functions. *Cerebral Cortex*, *5*(5), 377–390. https://doi.org/10.1093/CERCOR/5.5.377

Mueller, S., de Haas, B., Metzger, A., Drewing, K., Fiehler, K., Haas, B., Metzger, A., Drewing, K., & Fiehler, K. (2019). Neural correlates of top-down modulation of haptic shape versus roughness perception. *Human Brain Mapping*, *40*(18), 5172–5184. https://doi.org/10.1002/hbm.24764

Müller, V. I., Cieslik, E. C., Laird, A. R., Fox, P. T., Radua, J., Mataix-Cols, D., Tench, C. R., Yarkoni, T., Nichols, T. E., Turkeltaub, P. E., Wager, T. D., & Eickhoff, S. B. (2018). Ten simple rules for neuroimaging meta-analysis. *Neuroscience & Biobehavioral Reviews*, *84*, 151–161. https://doi.org/10.1016/J.NEUBIOREV.2017.11.012

Muñoz, F., Reales, J. M., Sebastián, M. Á., & Ballesteros, S. (2014). An electrophysiological study of haptic roughness: Effects of levels of texture and stimulus uncertainty in the P300. *Brain Research*, *1562*, 59–68. https://doi.org/10.1016/J.BRAINRES.2014.03.013

Murray, E. A., & Mishkin, M. (1984). Relative contributions of SII and area 5 to tactile discrimination in monkeys. *Behavioural Brain Research*, *11*(1), 67–83. https://doi.org/10.1016/0166-4328(84)90009-3

Naatanen, R., Gaillard, A. W. K., Mantysalo, S., & Gaillard, W. K. (1978). EARLY SELECTIVE-AmENTION EFFECT ON EVOKED POTENTIAL REINTERPRETED*. *Acta Psychologica*, *42*, 313–329.

Näätänen, R., Jacobsen, T., & Winkler, I. (2005). Memory-based or afferent processes in mismatch negativity (MMN): A review of the evidence. *Psychophysiology*, *42*(1), 25–32. https://doi.org/10.1111/J.1469-8986.2005.00256.X

Näätänen, R., Paavilainen, P., Rinne, T., & Alho, K. (2007). The mismatch negativity (MMN) in basic research of central auditory processing: A review. *Clinical Neurophysiology*, *118*(12), 2544–2590. https://doi.org/10.1016/J.CLINPH.2007.04.026

Nakata, H., Inui, K., Wasaka, T., Nishihira, Y., & Kakigi, R. (2003). Mechanisms of differences in gating effects on short- and long-latency somatosensory evoked potentials

relating to movement. *Brain Topography*, *15*(4), 211–222. https://doi.org/10.1023/A:1023908707851

Nakata, H., Sakamoto, K., Yumoto, M., & Kakigi, R. (2011). The relationship in gating effects between short-latency and long-latency somatosensory-evoked potentials. *NeuroReport*, *22*(18), 1000–1004. https://doi.org/10.1097/WNR.0b013e32834dc296

Narashiman, P. T., & Jacobs, R. E. (2002). Neuroanatomical micromagnetic resonance imaging [Book]. In A. W. Toga & J. C. Mazziotta (Eds.), *Brain mapping : the methods* (2nd ed., pp. 399–426). Academic Press.

Nayak, C. S., & Anilkumar, A. C. (2022). EEG Normal Waveforms. *StatPearls*, 1–6. https://www.ncbi.nlm.nih.gov/books/NBK539805/

Nejati, V., Majdi, R., Salehinejad, M. A., & Nitsche, M. A. (2021). The role of dorsolateral and ventromedial prefrontal cortex in the processing of emotional dimensions. *Scientific Reports*, *11*(1), 1–12. https://doi.org/10.1038/s41598-021-81454-7

Nelson, A. J., Staines, W. R., Graham, S. J., & McIlroy, W. E. (2004). Activation in SI and SII; the influence of vibrotactile amplitude during passive and task-relevant stimulation. *Cognitive Brain Research*, *19*(2), 174–184. https://doi.org/10.1016/J.COGBRAINRES.2003.11.013

Neumann, J. von, & Ulam, S. (1945). The Monte Carlo Method. *Bulletin of the American Mathematical Society*, *51*(0), 165.

Neuper, C., & Pfurtscheller, G. (2001). Evidence for distinct beta resonance frequencies in human EEG related to specific sensorimotor cortical areas. In *Clinical Neurophysiology* (Vol. 112, Issue 11). Elsevier. https://doi.org/10.1016/S1388-2457(01)00661-7

Newson, J. J., & Thiagarajan, T. C. (2019). EEG Frequency Bands in Psychiatric Disorders: A Review of Resting State Studies. *Frontiers in Human Neuroscience*, *12*, 521. https://doi.org/10.3389/FNHUM.2018.00521/BIBTEX

Nordin, M. (1990). Low-threshold mechanoreceptive and nociceptive units with unmyelinated (C) fibres in the human supraorbital nerve. *The Journal of Physiology*, *426*(1), 229–240. https://doi.org/10.1113/JPHYSIOL.1990.SP018135

Nunez, M. D., Nunez, P. L., & Srinivasan, R. (2016). Electroencephalography (EEG): neurophysics, experimental methods, and signal processing. In H. Ombao, M. Linquist, W. Thompson, & J. Aston (Eds.), *Handbook of Neuroimaging Data Analysis* (pp. 175–197). Chapman & Hall/CRC. https://doi.org/10.13140/rg.2.2.12706.63687

Nunez, P. L., Silberstein, R. B., Cadusch, P. J., Wijesinghe, R. S., Westdorp, A. F., & Srinivasan, R. (1994). A theoretical and experimental study of high resolution EEG based on surface Laplacians and cortical imaging. *Electroencephalography and Clinical Neurophysiology*, *90*(1), 40–57. https://doi.org/10.1016/0013-4694(94)90112-0

Nunez, P. L., & Srinivasan, R. (2006). *Electric Fields of the Brain* [Book]. Oxford University Press. https://doi.org/10.1093/acprof:oso/9780195050387.001.0001

Obeso, I., Robles, N., Muñoz-Marrón, E., & Redolar-Ripoll, D. (2013). Dissociating the role of the pre-SMA in response inhibition and switching: A combined online and offline TMS approach. *Frontiers in Human Neuroscience*, *0*(APR 2013), 150. https://doi.org/10.3389/FNHUM.2013.00150/BIBTEX

O'Callaghan, G., O'Dowd, A., Simões-Franklin, C., Stapleton, J., & Newell, F. N. (2018). Tactile-to-Visual Cross-Modal Transfer of Texture Categorisation Following Training:

An fMRI Study. *Frontiers in Integrative Neuroscience*, *12*, 24. https://doi.org/10.3389/fnint.2018.00024

O'Connell, R. G., Dockree, P. M., & Kelly, S. P. (2012). A supramodal accumulation-to-bound signal that determines perceptual decisions in humans. *Nature Neuroscience 2012 15:12*, *15*(12), 1729–1735. https://doi.org/10.1038/nn.3248

Ogawa, S., Lee, T. M., Kay, A. R., & Tank, D. W. (1990a). Brain magnetic resonance imaging with contrast dependent on blood oxygenation. *Proceedings of the National Academy of Sciences*, *87*(24), 9868–9872. https://doi.org/10.1073/PNAS.87.24.9868

Ogawa, S., Lee, T. -M, Nayak, A. S., & Glynn, P. (1990b). Oxygenation-sensitive contrast in magnetic resonance image of rodent brain at high magnetic fields. *Magnetic Resonance in Medicine*, *14*(1), 68–78. https://doi.org/10.1002/MRM.1910140108

Ogawa, S., Lee, T. M., Stepnoski, R., Chen, W., Zhu, X. H., & Ugurbil, K. (2000). An approach to probe some neural systems interaction by functional MRI at neural time scale down to milliseconds. *Proceedings of the National Academy of Sciences of the United States of America*, *97*(20), 11026–11031. https://doi.org/10.1073/PNAS.97.20.11026/ASSET/473214E1-D720-4600-B444-DD7C3FFBE9C7/ASSETS/GRAPHIC/PQ1900057007.JPEG

Okamoto, S., Nagano, H., & Yamada, Y. (2013). Psychophysical dimensions of tactile perception of textures. *IEEE Transactions on Haptics*, *6*(1), 81–93. https://doi.org/10.1109/TOH.2012.32

Olausson, H., Lamarre, Y., Backlund, H., Morin, C., Wallin, B. G., Starck, G., Ekholm, S., Strigo, I., Worsley, K., Vallbo, B., & Bushnell, M. C. (2002). Unmyelinated tactile

afferents signal touch and project to insular cortex. *Nature Neuroscience*, *5*(9), 900–904. https://doi.org/10.1038/NN896

Olausson, H. W., Cole, J., Vallbo, Å., McGlone, F., Elam, M., Krämer, H. H., Rylander, K., Wessberg, J., & Bushnell, M. C. (2008). Unmyelinated tactile afferents have opposite effects on insular and somatosensory cortical processing. *Neuroscience Letters*, *436*(2), 128–132. https://doi.org/10.1016/J.NEULET.2008.03.015

Olausson, H., Wessberg, J., Morrison, I., & McGlone, F. (2016). Affective touch and the neurophysiology of CT afferents. In *Affective Touch and the Neurophysiology of CT Afferents*. https://doi.org/10.1007/978-1-4939-6418-5

Olausson, H., Wessberg, J., Morrison, I., McGlone, F., & Vallbo, Å. (2010). The neurophysiology of unmyelinated tactile afferents. *Neuroscience and Biobehavioral Reviews*, *34*(2), 185–191. https://doi.org/10.1016/J.NEUBIOREV.2008.09.011

Oostenveld, R., Fries, P., Maris, E., & Schoffelen, J. M. (2011). FieldTrip: Open source software for advanced analysis of MEG, EEG, and invasive electrophysiological data. *Computational Intelligence and Neuroscience*, *2011*. https://doi.org/10.1155/2011/156869

O'Sullivan, B. T., Roland, P. E., & Kawashima, R. (1994). A PET study of somatosensory discrimination in man Microgeometry versus macrogeometry. *European Journal of Neuroscience*, *6*(1), 137–148. https://liverpool.idm.oclc.org/login?url=https://search.ebscohost.com/login.aspx?direct=true&db=psyh&AN=2008-13509-014&site=eds-live&scope=site

Page, M. J., McKenzie, J. E., Bossuyt, P. M., Boutron, I., Hoffmann, T. C., Mulrow, C. D., Shamseer, L., Tetzlaff, J. M., Akl, E. A., Brennan, S. E., Chou, R., Glanville, J., Grimshaw, J. M., Hróbjartsson, A., Lalu, M. M., Li, T., Loder, E. W., Mayo-Wilson, E., McDonald, S., … Moher, D. (2021). The PRISMA 2020 statement: an updated guideline for reporting systematic reviews. *Systematic Reviews*, *10*(1), 1–11. https://doi.org/10.1186/S13643-021-01626-4/FIGURES/1

Papakostopoulos, D., Cooper, R., & Crow, H. J. (1975). Inhibition of cortical evoked potentials and sensation by self-initiated movement in man. *Nature 1975 258:5533*, *258*(5533), 321–324. https://doi.org/10.1038/258321a0

Papitto, G., Friederici, A. D., & Zaccarella, E. (2020). The topographical organization of motor processing: An ALE meta-analysis on six action domains and the relevance of Broca's region. *NeuroImage*, *206*, 116321. https://doi.org/10.1016/J.NEUROIMAGE.2019.116321

Park, W., Kim, S.-P., & Eid, M. (2021). Neural Coding of Vibration Intensity. *Frontiers in Neuroscience*, *15*. https://doi.org/10.3389/fnins.2021.682113

Pause, M., Kunesch, E., Binkofski, F., & Freund, H. J. (1989). Sensorimotor disturbances in patients with lesions of the parietal cortex. *Brain : A Journal of Neurology*, *112 (Pt 6*(6), 1599–1625. https://doi.org/10.1093/brain/112.6.1599

Pawling, R., Trotter, P. D., McGlone, F. P., & Walker, S. C. (2017). A positive touch: C-tactile afferent targeted skin stimulation carries an appetitive motivational value. *Biological Psychology*, *129*, 186–194. https://doi.org/10.1016/J.BIOPSYCHO.2017.08.057

Peirce, J., Gray, J. R., Simpson, S., MacAskill, M., Höchenberger, R., Sogo, H., Kastman, E., & Lindeløv, J. K. (2019). PsychoPy2: Experiments in behavior made easy. *Behavior Research Methods*, *51*(1), 195–203. https://doi.org/10.3758/s13428-018-01193-y

Peltier, S., Stilla, R., Mariola, E., LaConte, S., Hu, X., & Sathian, K. (2007). Activity and effective connectivity of parietal and occipital cortical regions during haptic shape perception. *Neuropsychologia*, *45*(3), 476–483. https://doi.org/10.1016/j.neuropsychologia.2006.03.003

Peltz, E., Seifert, F., Lanz, S., Müller, R., & Maihöfner, C. (2011). Impaired hand size estimation in CRPS. *The Journal of Pain*, *12*(10), 1095–1101. https://doi.org/10.1016/J.JPAIN.2011.05.001

Penfield, W., & Boldrey, E. (1937). Somatic motor and sensory representation in the cerebral cortex of man as studied by electrical stimulation. *Brain*, *60*(4), 389–443. https://doi.org/10.1093/brain/60.4.389

Penfield, W., Brain, E. B.-, & 1937, undefined. (1937). Somatic motor and sensory representation in the cerebral cortex of man as studied by electrical stimulation. *Citeseer*. https://citeseerx.ist.psu.edu/viewdoc/download?doi=10.1.1.873.4232&rep=rep1&type=pdf

Penfield, W., & Broldrey, E. (1950). The Cerebral Cortex of Man: A Clinical Study of Localization of Function. *Journal of the American Medical Association*, *144*(16), 1412. https://doi.org/10.1001/jama.1950.02920160086033

Penny, W. D., & Holmes, A. J. (2007). Random Effect Analysis [Book]. In K. J. (Karl J.) Friston (Ed.), *Statistical parametric mapping the analysis of functional brain images* (pp. 156–165). Academic.

Penny, W., Friston, K., Ashburner, J., Kiebel, S., & Nichols, T. (2007). Statistical Parametric Mapping: The Analysis of Functional Brain Images. In *Statistical Parametric Mapping: The Analysis of Functional Brain Images*. Elsevier Ltd. https://doi.org/10.1016/B978-0-12-372560-8.X5000-1

Perini, F., Powell, T., Watt, S. J., & Downing, P. E. (2020). Neural representations of haptic object size in the human brain revealed by multivoxel fMRI patterns. *Journal of Neurophysiology*, *124*(1), 218–231. https://doi.org/10.1152/JN.00160.2020/ASSET/IMAGES/LARGE/Z9K0072055180008.JPEG

Perini, I., Olausson, H., & Morrison, I. (2015). Seeking pleasant touch: Neural correlates of behavioral preferences for skin stroking. *Frontiers in Behavioral Neuroscience*, *9*(FEB). https://doi.org/10.3389/fnbeh.2015.00008

Pfurtscheller, G. (1977). Graphical display and statistical evaluation of event-related desynchronization. *Electroencephalogr Clin Neurophysiol*, *43*, 757–760. https://www.clinph-journal.com/article/0013-4694(77)90092-X/pdf

Pfurtscheller, G. (1981). Central beta rhythm during sensorimotor activities in man. In *Electroencephalography and Clinical Neurophysiology* (Vol. 51, Issue 3). Elsevier. https://doi.org/10.1016/0013-4694(81)90139-5

Pfurtscheller, G. (1992). Event-related synchronization (ERS): an electrophysiological correlate of cortical areas at rest. *Electroencephalography and Clinical Neurophysiology*, *83*(1), 62–69. https://doi.org/10.1016/0013-4694(92)90133-3

Pfurtscheller, G. (1999). Quantification of ERD and ERS in the time domain. In G. Pfurtscheller & F. H. Lopes da Silva (Eds.), *Handbook of Electroencephalography & Clinical Neurophysiology* (Vol. 6, Issue 1, pp. 89–105). Elsevier B.V. https://doi.org/10.2/JQUERY.MIN.JS

Pfurtscheller, G. (2001). Functional brain imaging based on ERD/ERS. *Vision Research*, *41*(10–11), 1257–1260. https://doi.org/10.1016/s0042-6989(00)00235-2

Pfurtscheller, G., & Aranibar, A. (1977). Event-related cortical desynchronization detected by power measurements of scalp EEG. *Electroencephalography and Clinical Neurophysiology*, *42*(6), 817–826. https://doi.org/10.1016/0013-4694(77)90235-8

Pfurtscheller, G., & Aranibar, A. (1979). Evaluation of event-related desynchronization (ERD) preceding and following voluntary self-paced movement. *Electroencephalography and Clinical Neurophysiology*, *46*(2), 138–146. https://doi.org/10.1016/0013-4694(79)90063-4

Pfurtscheller, G., & Klimesch, W. (1991). Event-related desynchronization during motor behavior and visual information processing. *Electroencephalography and Clinical Neurophysiology. Supplement*, *42*, 58–65. http://www.ncbi.nlm.nih.gov/pubmed/1915032

Pfurtscheller, G., & Lopes da Silva, F. H. H. (1999). Event-related EEG/MEG synchronization and desynchronization: basic principles. *Clinical Neurophysiology*, *110*(11), 1842–1857. https://doi.org/10.1016/S1388-2457(99)00141-8

Pfurtscheller, G., & Neuper, C. (1992). Simultaneous EEG 10 Hz desynchronization and 40 Hz synchronization during finger movements. *NeuroReport*, *3*(12), 1057–1060. https://doi.org/10.1097/00001756-199212000-00006

Pfurtscheller, G., & Neuper, C. (1997). Motor imagery activates primary sensorimotor area in humans. *Neuroscience Letters*, *239*(2–3), 65–68. https://doi.org/10.1016/S0304-3940(97)00889-6

Pfurtscheller, G., Neuper, C., Brunner, C., & Lopes Da Silva, F. (2005). Beta rebound after different types of motor imagery in man. *Neuroscience Letters*, *378*, 156–159. https://doi.org/10.1016/j.neulet.2004.12.034

Pfurtscheller, G., Neuper, C., & Kalcher, J. (1993). 40-Hz oscillations during motor behavior in man. *Neuroscience Letters*, *164*(1–2), 179–182. https://doi.org/10.1016/0304-3940(93)90886-P

Pfurtscheller, G., Neuper, C., & Krausz, G. (2000). Functional dissociation of lower and upper frequency mu rhythms in relation to voluntary limb movement. *Clinical Neurophysiology*, *111*(10), 1873–1879. https://doi.org/10.1016/S1388-2457(00)00428-4

Pfurtscheller, G., Stancak, A., & Neuper, C. (1996a). Post-movement beta synchronization. A correlate of an idling motor area? *Electroencephalography and Clinical Neurophysiology*, *98*(4), 281–293. https://doi.org/10.1016/0013-4694(95)00258-8

Pfurtscheller, G., Stancak, A., & Neuper, C. (1996b). Event-related synchronization (ERS) in the alpha band - An electrophysiological correlate of cortical idling: A review. *International Journal of Psychophysiology*, *24*(1–2), 39–46. https://doi.org/10.1016/S0167-8760(96)00066-9

Pfurtscheller, G., Zalaudek, K., & Neuper, C. (1998). Event-related beta synchronization after wrist, finger and thumb movement. *Electroencephalography and Clinical Neurophysiology - Electromyography and Motor Control*, *109*(2), 154–160. https://doi.org/10.1016/S0924-980X(97)00070-2

Picard, N., Lepore, F., Ptito, M., & Guillemot, J. P. (1990). Bilateral interaction in the second somatosensory area (SII) of the cat and contribution of the corpus callosum. *Brain Research*, *536*(1–2), 97–104. https://doi.org/10.1016/0006-8993(90)90013-2

Picard, N., & Strick, P. L. (2003). Activation of the Supplementary Motor Area (SMA) during Performance of Visually Guided Movements. *Cerebral Cortex*, *13*(9), 977–986. https://doi.org/10.1093/CERCOR/13.9.977

Piccinin, M. A., Miao, J. H., & Schwartz, J. (2022). Histology, Meissner Corpuscle. *StatPearls*. https://www.ncbi.nlm.nih.gov/books/NBK518980/

Pleger, B., Tegenthoff, M., Ragert, P., Förster, A. F., Dinse, H. R., Schwenkreis, P., Nicolas, V., & Maier, C. (2005). Sensorimotor retuning [corrected] in complex regional pain syndrome parallels pain reduction. *Annals of Neurology*, *57*(3), 425–429. https://doi.org/10.1002/ANA.20394

Pleger, B., Tegenthoff, M., Schwenkreis, P., Janssen, F., Ragert, P., Dinse, H. R., Völker, B., Zenz, M., & Maier, C. (2004). Mean sustained pain levels are linked to hemispherical

side-to-side differences of primary somatosensory cortex in the complex regional pain syndrome I. *Experimental Brain Research*, *155*(1), 115–119. https://doi.org/10.1007/S00221-003-1738-4

Podrebarac, S. K., Goodale, M. A., & Snow, J. C. (2014). Are visual texture-selective areas recruited during haptic texture discrimination? *NeuroImage*, *94*, 129–137. https://doi.org/10.1016/j.neuroimage.2014.03.013

Poel, M., Reuderink, B., & Mühl, C. (2012). Valence, arousal and dominance in the EEG during game play. *Int. J. Autonomous and Adaptive Communications Systems*, *6*(1), 45–62. https://doi.org/10.1504/IJAACS.2013.050691

Poldrack, R. A., Fletcher, P. C., Henson, R. N., Worsley, K. J., Brett, M., & Nichols, T. E. (2008). Guidelines for reporting an fMRI study. *NeuroImage*, *40*(2), 409–414. https://doi.org/10.1016/j.neuroimage.2007.11.048

Polich, J. (1997). EEG and ERP assessment of normal aging. *Electroencephalography and Clinical Neurophysiology*, *104*(3), 244–256. https://doi.org/10.1016/S0168-5597(97)96139-6

Popovich, C., & Staines, W. R. (2015). Acute aerobic exercise enhances attentional modulation of somatosensory event-related potentials during a tactile discrimination task. *Behavioural Brain Research*, *281*, 267–275. https://doi.org/10.1016/j.bbr.2014.12.045

Post, L. J., Zompa, I. C., & Chapman, C. E. (1994). Perception of vibrotactile stimuli during motor activity in human subjects. *Experimental Brain Research*, *100*(1), 107–120. https://doi.org/10.1007/BF00227283

Prescott, T. J., Diamond, M. E., & Wing, A. M. (2011). Active touch sensing. *Philosophical Transactions of the Royal Society B: Biological Sciences*, *366*(1581), 2989. https://doi.org/10.1098/RSTB.2011.0167

Prochazka, A. (2015). Sensory control of normal movement and of movement aided by neural prostheses. *Journal of Anatomy*, *227*(2), 167–177. https://doi.org/10.1111/joa.12311

Pruett, J. R., Sinclair, R. J., & Burton, H. (2000). Response patterns in second somatosensory cortex (SII) of awake monkeys to passively applied tactile gratings. *Journal of Neurophysiology*, *84*(2), 780–797. https://doi.org/10.1152/JN.2000.84.2.780/ASSET/IMAGES/LARGE/9K0801162014.JPEG

Purves, D., Augustine, G. J., Fitzpatrick, D., Katz, L. C., LaMantia, A.-S., McNamara, J. O., & Williams, S. M. (2001). *Excitatory and Inhibitory Postsynaptic Potentials*. https://www.ncbi.nlm.nih.gov/books/NBK11117/

Radua, J., & Mataix-Cols, D. (2009). Voxel-wise meta-analysis of grey matter changes in obsessive–compulsive disorder. *British Journal of Psychiatry*, *195*(5), 393–402. https://doi.org/10.1192/bjp.bp.108.055046

Radua, J., Mataix-Cols, D., Phillips, M. L., El-Hage, W., Kronhaus, D. M., Cardoner, N., & Surguladze, S. (2012). A new meta-analytic method for neuroimaging studies that combines reported peak coordinates and statistical parametric maps. *European Psychiatry*, *27*(8), 605–611. https://doi.org/10.1016/j.eurpsy.2011.04.001

Raemaekers, M., Vink, M., Zandbelt, B., van Wezel, R. J. A., Kahn, R. S., & Ramsey, N. F. (2007). Test-retest reliability of fMRI activation during prosaccades and antisaccades. *NeuroImage*, *36*(3), 532–542. https://doi.org/10.1016/J.NEUROIMAGE.2007.03.061

Raju, H., & Tadi, P. (2021). Neuroanatomy, Somatosensory Cortex. *StatPearls*. https://www.ncbi.nlm.nih.gov/books/NBK555915/

Ramsøy, T. Z., Skov, M., Christensen, M. K., & Stahlhut, C. (2018). Frontal Brain Asymmetry and Willingness to Pay. *Frontiers in Neuroscience*, *12*(MAR), 138. https://doi.org/10.3389/FNINS.2018.00138

Randolph, M., & Semmes, J. (1974). Behavioral consequences of selective subtotal ablations in the postcentral gyrus of Macaca mulatta. *Brain Research*, *70*(1), 55–70. https://doi.org/10.1016/0006-8993(74)90211-x

Ravaja, N., Somervuori, O., & Salminen, M. (2013). Predicting purchase decision: The role of hemispheric asymmetry over the frontal cortex. *Journal of Neuroscience, Psychology, and Economics*, *6*(1), 1–13. https://doi.org/10.1037/A0029949

Reader, A. T., & Holmes, N. P. (2018). The left ventral premotor cortex is involved in hand shaping for intransitive gestures: evidence from a two-person imitation experiment. *Royal Society Open Science*, *5*(10). https://doi.org/10.1098/RSOS.181356

Restuccia, D., Marca, G. della, Valeriani, M., Leggio, M. G., & Molinari, M. (2007). Cerebellar damage impairs detection of somatosensory input changes. A somatosensory mismatch-negativity study. *Brain*, *130*, 276–287. https://doi.org/10.1093/brain/awl236

Rexed, B. (1952). The cytoarchitectonic organization of the spinal cord in the cat. *Journal of Comparative Neurology*, *96*(3), 415–495. https://doi.org/10.1002/CNE.900960303

Ridley, R. M., & Ettlinger, G. (1976). Impaired tactile learning and retention after removals of the second somatic sensory projection cortex (SII) in the monkey. *Brain Research*, *109*(3), 656–660. https://doi.org/10.1016/0006-8993(76)90048-2

Ritter, P., Moosmann, M., & Villringer, A. (2009). Rolandic alpha and beta EEG rhythms' strengths are inversely related to fMRI-BOLD signal in primary somatosensory and motor cortex. *Human Brain Mapping*, *30*(4), 1168–1187. https://doi.org/10.1002/HBM.20585

Rizzolatti, G., & Kalaska, J. F. (2012). Voluntary Movement: The Parietal and Premotor Cortex. In J. Schwartz, T. Jessell, S. Siegelbaum, & A. J. Hudspeth (Eds.), *Principles of Neural Science* (Fifth, pp. 865–892). McGraw-Hill Publishing.

Rizzolatti, G., & Luppino, G. (2001). The Cortical Motor System. *Neuron*, *31*(6), 889–901. https://doi.org/10.1016/S0896-6273(01)00423-8

Rizzolatti, G., Matelli, M., & Pavesi, G. (1983). Deficits in attention and movement following the removal of postarcuate (area 6) and prearcuate (area 8) cortex in macaque monkeys. *Brain*, *106*(3), 655–673. https://doi.org/10.1093/brain/106.3.655

Rochat, P., & Senders, S. J. (1991). Active touch in infancy: Action systems in development. In *Newborn attention: Biological constraints and the influence of experience* (pp. 412–442).

Roland, P. E., O'Sullivan, B., & Kawashima, R. (1998). Shape and roughness activate different somatosensory areas in the human brain. *Proceedings of the National Academy of Sciences of the United States of America*, *95*(6), 3295–3300.

https://doi.org/10.1073/PNAS.95.6.3295/ASSET/887A97C5-67C3-42E1-B544-CDB3A4E81D0E/ASSETS/GRAPHIC/PQ0383981001.JPEG

Rolls, E., O'Doherty, J., Kringelbach, M., Francis, S., Bowtell, R., & McGlone, F. (2003a). Representations of pleasant and painful touch in the human orbitofrontal and cingulate cortices. *Cerebral Cortex*, *13*(3), 308–317. https://doi.org/10.1093/cercor/13.3.308

Rolls, E. T. (2000). The Orbitofrontal Cortex and Reward. *Cerebral Cortex*, *10*(3), 284–294. https://doi.org/10.1093/cercor/10.3.284

Rolls, E. T. (2004). The functions of the orbitofrontal cortex. *Brain and Cognition*, *55*(1), 11–29. https://doi.org/10.1016/S0278-2626(03)00277-X

Rolls, E. T. (2010). The affective and cognitive processing of touch, oral texture, and temperature in the brain. *Neuroscience & Biobehavioral Reviews*, *34*(2), 237–245. https://doi.org/10.1016/J.NEUBIOREV.2008.03.010

Rolls, E. T. (2020). The texture and taste of food in the brain. *Journal of Texture Studies*, *51*(1), 23–44. https://doi.org/10.1111/JTXS.12488

Rolls, E. T., & Grabenhorst, F. (2008). The orbitofrontal cortex and beyond: From affect to decision-making. In *Progress in Neurobiology* (Vol. 86, Issue 3, pp. 216–244). Pergamon. https://doi.org/10.1016/j.pneurobio.2008.09.001

Rolls, E. T., Grabenhorst, F., & Parris, B. A. (2008). Warm pleasant feelings in the brain. *NeuroImage*, *41*(4), 1504–1513. https://doi.org/10.1016/J.NEUROIMAGE.2008.03.005

Rolls, E. T., Kringelbach, M. L., & de Araujo, I. E. T. (2003b). Different representations of pleasant and unpleasant odours in the human brain. *European Journal of Neuroscience*, *18*(3), 695–703. https://doi.org/10.1046/J.1460-9568.2003.02779.X

Romo, R., Hernández, A., & Zainos, A. (2004). Neuronal Correlates of a Perceptual Decision in Ventral Premotor Cortex. *Neuron*, *41*(1), 165–173. https://doi.org/10.1016/S0896-6273(03)00817-1

Romo, R., Hernández, A., Zainos, A., Lemus, L., & Brody, C. D. (2002). Neuronal correlates of decision-making in secondary somatosensory cortex. *Nature Neuroscience*, *5*(11), 1217–1225. https://doi.org/10.1038/NN950

Rossini, P. M., Babiloni, C., Babiloni, F., Ambrosini, A., Onorati, P., Carducci, F., & Urbano, A. (1999). 'Gating' of human short-latency somatosensory evoked cortical responses during execution of movement. A high resolution electroencephalography study. *Brain Research*, *843*(1–2), 161–170. https://doi.org/10.1016/S0006-8993(99)01716-3

Rossini, P. M., Caramia, D., Bassetti, M. A., Pasqualetti, P., Tecchio, F., & Bernardi, G. (1996). Somatosensory evoked potentials during the ideation and execution of individual finger movements. *Muscle and Nerve*, *19*(2), 191–202. https://doi.org/10.1002/(SICI)1097-4598(199602)19:2<191::AID-MUS11>3.0.CO;2-Y

Ruben, J., Schwiemann, J., Deuchert, M., Meyer, R., Krause, T., Curio, G., Villringer, K., Kurth, R., & Villringer, A. (2001). Somatotopic organization of human secondary somatosensory cortex. *Cerebral Cortex (New York, N.Y. : 1991)*, *11*(5), 463–473. https://doi.org/10.1093/CERCOR/11.5.463

Rushworth, M. F. S., Nixon, P. D., & Passingham, R. E. (1997). Parietal cortex and movement I. Movement selection and reaching. *Experimental Brain Research 1997 117:2*, *117*(2), 292–310. https://doi.org/10.1007/S002210050224

Ryan, C. P., Bettelani, G. C., Ciotti, S., Parise, C., Moscatelli, A., & Bianchi, M. (2021). The interaction between motion and texture in the sense of touch. *Journal of Neurophysiology*, *126*(4), 1375–1390. https://doi.org/10.1152/JN.00583.2020/ASSET/IMAGES/LARGE/JN.00583.2020_F006.JPEG

Saal, H. P., Delhaye, B. P., Rayhaun, B. C., & Bensmaia, S. J. (2017). Simulating tactile signals from the whole hand with millisecond precision. *Proceedings of the National Academy of Sciences of the United States of America*, *114*(28), E5693–E5702. https://doi.org/10.1073/PNAS.1704856114/SUPPL_FILE/PNAS.1704856114.SM02.AVI

Saby, J. N., & Marshall, P. J. (2012). The Utility of EEG Band Power Analysis in the Study of Infancy and Early Childhood. *Developmental Neuropsychology*, *37*(3), 253. https://doi.org/10.1080/87565641.2011.614663

Salimi-Khorshidi, G., Smith, S. M., Keltner, J. R., Wager, T. D., & Nichols, T. E. (2009). Meta-analysis of neuroimaging data: A comparison of image-based and coordinate-based pooling of studies. *NeuroImage*, *45*(3), 810–823. https://doi.org/10.1016/J.NEUROIMAGE.2008.12.039

Salmelin, R., & Hari, R. (1994). Spatiotemporal Characteristics of Sensorimotor Neuromagnetic Rhythms Related to Thumb Movement. *Neuroscience*, *60*(2), 537–550.

Samartsidis, P., Montagna, S., Johnson, T. D., & Nichols, T. E. (2017). The Coordinate-Based Meta-Analysis of Neuroimaging Data. *Statistical Science*, *32*(4). https://doi.org/10.1214/17-STS624

Sanei, Saeid. (2009). *EEG signal processing* (Jonathon. Chambers, Ed.) [Book]. John Wiley & Sons.

Sathian, K. (2016). Analysis of haptic information in the cerebral cortex. *Journal of Neurophysiology*, *116*(4), 1795–1806. https://doi.org/10.1152/JN.00546.2015/ASSET/IMAGES/LARGE/Z9K0101638410003.JPEG

Sathian, K., Goodwin, A. W., John, K. T., & Darian-Smith, I. (1989). Perceived roughness of a grating: correlation with responses of mechanoreceptive afferents innervating the monkey's fingerpad. *The Journal of Neuroscience : The Official Journal of the Society for Neuroscience*, *9*(4), 1273–1279. https://doi.org/10.1523/JNEUROSCI.09-04-01273.1989

Sathian, K., Lacey, S., Stilla, R., Gibson, G. O., Deshpande, G., Hu, X., LaConte, S., & Glielmi, C. (2011). Dual pathways for haptic and visual perception of spatial and texture information. *NeuroImage*, *57*(2), 462–475. https://doi.org/10.1016/J.NEUROIMAGE.2011.05.001

Scheibert, J., Leurent, S., Prevost, A., & Debrégeas, G. (2009). The role of fingerprints in the coding of tactile information probed with a biomimetic sensor. *Science*, *323*(5920), 1503–1506. https://doi.org/10.1126/SCIENCE.1166467/SUPPL_FILE/SCHEIBERT_SOM.PDF

Schieber, M. H., & Thach, W. T. (1985). Trained slow tracking. I. Muscular production of wrist movement. *Journal of Neurophysiology*, *54*(5), 1213–1227. https://doi.org/10.1152/jn.1985.54.5.1213

Schmidt, L. A., & Trainor, L. J. (2010). Frontal brain electrical activity (EEG) distinguishes valence and intensity of musical emotions. *Http://Dx.Doi.Org/10.1080/02699930126048*, *15*(4), 487–500. https://doi.org/10.1080/02699930126048

Schmidt, R. F., Schady, W. J. L., & Torebjörk, H. E. (1990). Gating of tactile input from the hand - I. Effects of finger movement. *Experimental Brain Research*, *79*(1), 97–102. https://doi.org/10.1007/BF00228877

Schneider, S., & Strüder, H. K. (2012). Eeg: Theoretical background and practical aspects. *Functional Neuroimaging in Exercise and Sport Sciences*, 197–212. https://doi.org/10.1007/978-1-4614-3293-7_9/FIGURES/4

Schwenkreis, P., Maier, C., & Tegenthoff, M. (2009). Functional imaging of central nervous system involvement in complex regional pain syndrome. *AJNR. American Journal of Neuroradiology*, *30*(7), 1279–1284. https://doi.org/10.3174/AJNR.A1630

Seeber, M., Cantonas, L. M., Hoevels, M., Sesia, T., Visser-Vandewalle, V., & Michel, C. M. (2019). Subcortical electrophysiological activity is detectable with high-density EEG source imaging. *Nature Communications*, *10*(1). https://doi.org/10.1038/S41467-019-08725-W

Segerdahl, A. R., Mezue, M., Okell, T. W., Farrar, J. T., & Tracey, I. (2015). The dorsal posterior insula subserves a fundamental role in human pain. *Nature Neuroscience*, *18*(4), 499–500. https://doi.org/10.1038/NN.3969

Servos, P., Lederman, S., Wilson, D., & Gati, J. (2001). fMRI-derived cortical maps for haptic shape, texture, and hardness. *Brain Research. Cognitive Brain Research*, *12*(2), 307–313. https://doi.org/10.1016/s0926-6410(01)00041-6

Sherrington, C. S. (1893). IX. Experiments in examination of the peripheral distribution of the fibres of the posterior roots of some spinal nerves. *Philosophical Transactions of the Royal Society of London. (B.), 184*, 641–763. https://doi.org/10.1098/rstb.1893.0009

Simões-Franklin, C., Whitaker, T. A., & Newell, F. N. (2011). Active and passive touch differentially activate somatosensory cortex in texture perception. *Human Brain Mapping*, *32*(7), 1067–1080. https://doi.org/10.1002/hbm.21091

Sinclair, R. J., & Burton, H. (1993). Neuronal activity in the second somatosensory cortex of monkeys (Macaca mulatta) during active touch of gratings. *Journal of Neurophysiology*, *70*(1), 331–350. https://doi.org/10.1152/jn.1993.70.1.331

Singh, H., Bauer, M., Chowanski, W., Sui, Y., Atkinson, D., Baurley, S., Fry, M., Evans, J., & Bianchi-Berthouze, N. (2014). The brain's response to pleasant touch: an EEG investigation of tactile caressing. *Frontiers in Human Neuroscience*, *8*(November). https://doi.org/10.3389/FNHUM.2014.00893

Slepian, D. (1978). Prolate Spheroidal Wave Functions, Fourier Analysis, and Uncertainty—V: The Discrete Case. *Bell System Technical Journal*, *57*(5), 1371–1430. https://doi.org/10.1002/J.1538-7305.1978.TB02104.X

Slichter, C. P. (1992). *Principles of magnetic resonance* (3rd ed.) [Book]. Springer.

Smith, A., Gosselin, G., & Houde, B. (2002a). Deployment of fingertip forces in tactile exploration. *Experimental Brain Research*, *147*(2), 209–218. https://doi.org/10.1007/s00221-002-1240-4

Smith, A. M., Chapman, C. E., Deslandes, M., Langlais, J.-S., & Thibodeau, M.-P. (2002b). Role of friction and tangential force variation in the subjective scaling of tactile roughness. *Experimental Brain Research*, *144*(2), 211–223. https://doi.org/10.1007/s00221-002-1015-y

Smith, A. M., Chapman, C. E., Donati, F., Fortier-Poisson, P., & Hayward, V. (2009). Perception of simulated local shapes using active and passive touch. *Journal of Neurophysiology*, *102*(6), 3519–3529. https://doi.org/10.1152/JN.00043.2009/ASSET/IMAGES/LARGE/Z9K0120998320007.JPEG

Smith, A. M., & Scott, S. H. (1996). Subjective scaling of smooth surface friction. *Journal of Neurophysiology*, *75*(5), 1957–1962. https://doi.org/10.1152/jn.1996.75.5.1957

Snyder, L. H., Batista, A. P., & Andersen, R. A. (1997). Coding of intention in the posterior parietal cortex. *Nature*, *386*(6621), 167–170. https://doi.org/10.1038/386167A0

Son, Y. J., & Chun, C. (2018). Research on electroencephalogram to measure thermal pleasure in thermal alliesthesia in temperature step-change environment. *Indoor Air*, *28*(6), 916–923. https://doi.org/10.1111/INA.12491

Song, Y., Su, Q., Yang, Q., Zhao, R., Yin, G., Qin, W., Iannetti, G. D., Yu, C., & Liang, M. (2021). Feedforward and feedback pathways of nociceptive and tactile processing in

human somatosensory system: A study of dynamic causal modeling of fMRI data. *NeuroImage , 234 , Article 117957. (2021) , 234*. https://doi.org/10.1016/J.NEUROIMAGE.2021.117957

Speckmann, E.-Josef., Elger, C. E., & Gorji, A. (2011). Neurophysiologic Basis of EEG and DC Potentials [Book]. In E. Niedermeyer, D. L. Schomer, & F. H. Lopes da Silva (Eds.), *Niedermeyer's electroencephalography basic principles, clinical applications, and related fields* (Sixth edit). Wolters Kluwer/Lippincott Williams & Wilkins Health.

Sperry, R. W. (1950). Neural basis of the spontaneous optokinetic response produced by visual inversion. *Journal of Comparative and Physiological Psychology*, *43*(6), 482–489. https://doi.org/10.1037/H0055479

Spooner, R. K., Wiesman, A. I., Proskovec, A. L., Heinrichs-Graham, E., & Wilson, T. W. (2019). Rhythmic Spontaneous Activity Mediates the Age-Related Decline in Somatosensory Function. *Cerebral Cortex*, *29*(2), 680–688. https://doi.org/10.1093/CERCOR/BHX349

Srinivasan, M. A. (2003). *Kiran Dandekar Balasundar I. Raju 3-D Finite-Element Models of Human and Monkey Fingertips to Investigate the Mechanics of Tactile Sense*. https://doi.org/10.1115/1.1613673

Srinivasan, M. A., & LaMotte, R. H. (1995). Tactual discrimination of softness. *Journal of Neurophysiology*, *73*(1), 88–101. https://doi.org/10.1152/JN.1995.73.1.88

Srinivasan, M. A., & LaMotte, R. H. (1996). Tactual discrimination of softness: abilities and mechanisms. *Somesthesis and the Neurobiology of the Somatosensory Cortex*, 123–135. https://doi.org/10.1007/978-3-0348-9016-8_11

Srinivasan, R., Nunez, P. L., Tucker, D. M., Silberstein, R. B., & Cadusch, P. J. (1996). Spatial sampling and filtering of EEG with spline laplacians to estimate cortical potentials. *Brain Topography*, *8*(4), 355–366. https://doi.org/10.1007/BF01186911

Stancak, A., & Pfurtscheller, G. (1996a). Mu-rhythm changes in brisk and slow self-paced finger movements. *NeuroReport*, *7*(6), 1161–1164. https://doi.org/10.1097/00001756-199604260-00013

Stancak, A., & Pfurtscheller, G. (1996b). Event-related desynchronisation of central beta-rhythms during brisk and slow self-paced finger movements of dominant and nondominant hand. *Cognitive Brain Research*, *4*(3), 171–183. https://doi.org/10.1016/S0926-6410(96)00031-6

Stancak, A., & Pfurtscheller, G. (1997). Effects of handedness on movement-related changes of central beta rhythms. *Journal of Clinical Neurophysiology*, *14*, 419–428.

Stancák, A., Riml, A., & Pfurtscheller, G. (1997). The effects of external load on movement-related changes of the senorimotor EEG rhythms. *Electroencephalography and Clinical Neurophysiology*, *102*(6), 495–504. https://doi.org/10.1016/S0013-4694(96)96623-0

Stancak, A., Svoboda, Jirí., Rachmanová, Rosa., Vrána, Jirí., Králík, Jirí., & Tintera, Jaroslav. (2003). Desynchronization of cortical rhythms following cutaneous stimulation: Effects of stimulus repetition and intensity, and of the size of corpus callosum. *Clinical Neurophysiology*, *114*(10), 1936–1947. https://doi.org/10.1016/S1388-2457(03)00201-3

Statistical Solutions Ltd. (1995). *BMDP*.

Stefanics, G., Stefanics, G., Kremláček, J., & Czigler, I. (2014). Visual mismatch negativity: A predictive coding view. *Frontiers in Human Neuroscience*, *8*, 1–19. https://doi.org/10.3389/FNHUM.2014.00666/BIBTEX

Stevens, J. C., & Choo, K. K. (1996). Spatial acuity of the body surface over the life span. *Somatosensory & Motor Research*, *13*(2), 153–166. https://doi.org/10.3109/08990229609051403

Stevens, S. S., & Harris, J. R. (1962). The scaling of subjective roughness and smoothness. *Journal of Experimental Psychology*, *64*(5), 489–494. https://doi.org/10.1037/h0042621

Stifani, N. (2014). Motor neurons and the generation of spinal motor neuron diversity. *Frontiers in Cellular Neuroscience*, *8*(OCT), 293. https://doi.org/10.3389/FNCEL.2014.00293/BIBTEX

Stilla, R., & Sathian, K. (2008). Selective visuo-haptic processing of shape and texture. *Human Brain Mapping*, *29*(10), 1123–1138. https://doi.org/10.1002/hbm.20456

Stoeckel, M. C., Weder, B., Binkofski, F., Buccino, G., Shah, N. J., & Seitz, R. J. (2003). A fronto-parietal circuit for tactile object discrimination: an event-related fMRI study. *NeuroImage*, *19*(3), 1103–1114. https://doi.org/10.1016/S1053-8119(03)00182-4

Stothart, G., & Kazanina, N. (2013). Oscillatory characteristics of the visual mismatch negativity: what evoked potentials aren't telling us. *Frontiers in Human Neuroscience*, *7*. https://doi.org/10.3389/fnhum.2013.00426

Sutu, A., Meftah, E. M., & Elaine Chapman, C. (2013). Physical determinants of the shape of the psychophysical curve relating tactile roughness to raised-dot spacing: Implications

for neuronal coding of roughness. *Journal of Neurophysiology*, *109*(5), 1403–1415. https://doi.org/10.1152/JN.00717.2012

Szucs, D., & Ioannidis, J. P. (2020). Sample size evolution in neuroimaging research: An evaluation of highly-cited studies (1990-2012) and of latest practices (2017-2018) in high-impact journals. *NeuroImage*, *221*. https://doi.org/10.1016/J.NEUROIMAGE.2020.117164

Talairach, J., & Tournoux, T. (1988). Co-planar stereotaxic atlas of the human brain. In *Thieme Medical Publishers*. Thieme Medical Publishers.

Taleei, T., Nazem-Zadeh, M.-R., Amiri, M., & Keliris, G. A. (2022). EEG-based functional connectivity for tactile roughness discrimination. *Cognitive Neurodynamics*, 1–20. https://doi.org/10.1007/S11571-022-09876-1/TABLES/4

Tallon-Baudry, C., & Bertrand, O. (1999). Oscillatory gamma activity in humans and its role in object representation. *Trends in Cognitive Sciences*, *3*(4), 151–162. https://doi.org/10.1016/S1364-6613(99)01299-1

Tamè, L., Braun, C., Holmes, N. P., Farnè, A., & Pavani, F. (2016). Bilateral representations of touch in the primary somatosensory cortex. *Https://Doi.Org/10.1080/02643294.2016.1159547*, *33*(1–2), 48–66. https://doi.org/10.1080/02643294.2016.1159547

Tamè, L., & Holmes, N. P. (2016). Involvement of human primary somatosensory cortex in vibrotactile detection depends on task demand. *NeuroImage*, *138*, 184–196. https://doi.org/10.1016/J.NEUROIMAGE.2016.05.056

Tanaka, Y., Bergmann Tiest, W. M., Kappers, A. M. L., & Sano, A. (2014). Contact Force and Scanning Velocity during Active Roughness Perception. *PLOS ONE*, *9*(3), e93363. https://doi.org/10.1371/JOURNAL.PONE.0093363

Tang, W., Liu, R., Shi, Y., Hu, C., Bai, S., & Zhu, H. (2020). From finger friction to brain activation: Tactile perception of the roughness of gratings. *Journal of Advanced Research*, *21*, 129–139. https://doi.org/10.1016/j.jare.2019.11.001

Tang, W., Shu, Y., Bai, S., Peng, Y., Yang, L., & Liu, R. (2021a). Brain activation related to the tactile perception of touching ridged texture using fingers. *Skin Research and Technology : Official Journal of International Society for Bioengineering and the Skin (ISBS) [and] International Society for Digital Imaging of Skin (ISDIS) [and] International Society for Skin Imaging (ISSI)*. https://doi.org/10.1111/srt.13122

Tang, W., Zhang, M., Chen, G., Liu, R., Peng, Y., Chen, S., Shi, Y., Hu, C., & Bai, S. (2021b). Investigation of Tactile Perception Evoked by Ridged Texture Using ERP and Non-linear Methods. *Frontiers in Neuroscience*, *15*, 756. https://doi.org/10.3389/FNINS.2021.676837/BIBTEX

Tanji, J. (2001). Sequential Organization of Multiple Movements: Involvement of Cortical Motor Areas. *Annual Review of Neuroscience*, *24*(1), 631–651. https://doi.org/10.1146/annurev.neuro.24.1.631

Tanji, J., & Shima, K. (1996). Supplementary Motor Cortex in Organization of Movement. *European Neurology*, *36*(Suppl. 1), 13–19. https://doi.org/10.1159/000118878

Tashiro, N., Sugata, H., Ikeda, T., Matsushita, K., Hara, M., Kawakami, K., Kawakami, K., & Fujiki, M. (2019). Effect of individual food preferences on oscillatory brain activity. *Brain and Behavior*, *9*(5). https://doi.org/10.1002/BRB3.1262

Taylor, J. L. (2009). Proprioception. *Encyclopedia of Neuroscience*, 1143–1149. https://doi.org/10.1016/B978-008045046-9.01907-0

Taylor, K. S., Seminowicz, D. A., & Davis, K. D. (2009). Two systems of resting state connectivity between the insula and cingulate cortex. *Human Brain Mapping*, *30*(9), 2731. https://doi.org/10.1002/HBM.20705

Taylor, M. M., & Lederman, S. J. (1975). Tactile roughness of grooved surfaces: A model and the effect of friction. *Perception & Psychophysics 1975 17:1*, *17*(1), 23–36. https://doi.org/10.3758/BF03203993

Thatcher, R. W., Lubar, J. F., & Koberda, J. L. (2019). Z-Score EEG Biofeedback: Past, Present, and Future. *Biofeedback*, *47*(4), 89–103. https://doi.org/10.5298/1081-5937-47.4.04

Thirion, B., Pinel, P., Mériaux, S., Roche, A., Dehaene, S., & Poline, J. B. (2007). Analysis of a large fMRI cohort: Statistical and methodological issues for group analyses. *NeuroImage*, *35*(1), 105–120. https://doi.org/10.1016/J.NEUROIMAGE.2006.11.054

Tivadar, R. I., & Murray, M. M. (2019). A Primer on Electroencephalography and Event-Related Potentials for Organizational Neuroscience. *Organizational Research Methods*, *22*(1), 69–94. https://doi.org/10.1177/1094428118804657/ASSET/IMAGES/LARGE/10.1177_1094428118804657-FIG2.JPEG

Tremblay, F., Backman, A., Cuenco, A., Vant, K., & Wassef, M. A. (2000). Assessment of spatial acuity at the fingertip with grating (JVP) domes: validity for use in an elderly population. *Somatosensory & Motor Research*, *17*(1), 61–66. https://doi.org/10.1080/08990220070300

Tremblay, F., Mireault, A.-C., Dessureault, L., Manning, H., & Sveistrup, H. (2005). Postural stabilization from fingertip contact. *Experimental Brain Research*, *164*(2), 155–164. https://doi.org/10.1007/s00221-005-2238-5

Turkeltaub, P. E., Eden, G. F., Jones, K. M., & Zeffiro, T. A. (2002). Meta-analysis of the functional neuroanatomy of single-word reading: Method and validation. *NeuroImage*, *16*(3 I), 765–780. https://doi.org/10.1006/nimg.2002.1131

Turkeltaub, P. E., Eickhoff, S. B., Laird, A. R., Fox, M., Wiener, M., & Fox, P. (2012). Minimizing within-experiment and within-group effects in Activation Likelihood Estimation meta-analyses. *Human Brain Mapping*, *33*(1), 1–13. https://doi.org/10.1002/HBM.21186

Turvey, M. T., & Carello, C. (2011). Obtaining information by dynamic (effortful) touching. *Philosophical Transactions of the Royal Society B: Biological Sciences*, *366*(1581), 3123. https://doi.org/10.1098/RSTB.2011.0159

Tzagarakis, C., West, S., & Pellizzer, G. (2015). Brain oscillatory activity during motor preparation: effect of directional uncertainty on beta, but not alpha, frequency band. *Frontiers in Neuroscience*, *9*(JUN), 246. https://doi.org/10.3389/fnins.2015.00246

Uddin, L. Q., Nomi, J. S., Hébert-Seropian, B., Ghaziri, J., & Boucher, O. (2017). Structure and function of the human insula. *Journal of Clinical Neurophysiology : Official*

Publication of the American Electroencephalographic Society, *34*(4), 300. https://doi.org/10.1097/WNP.0000000000000377

Vallbo, A. B., & Johansson, R. S. (1984). Properties of cutaneous mechanoreceptors in the human hand related to touch sensation. *Human Neurobiology*, *3*(1), 3–14. http://www.ncbi.nlm.nih.gov/pubmed/6330008

Vallbo, Å. B., Olausson, H., & Wessberg, J. (1999). Unmyelinated afferents constitute a second system coding tactile stimuli of the human hairy skin. *Journal of Neurophysiology*, *81*(6), 2753–2763. https://doi.org/10.1152/JN.1999.81.6.2753

Vallbo, A. B., Olausson, H., Wessberg, J., & Kakuda, N. (1995). Receptive field characteristics of tactile units with myelinated afferents in hairy skin of human subjects. *Journal of Physiology*, 783–795.

van Ede, F., de Lange, F., Jensen, O., & Maris, E. (2011). Orienting Attention to an Upcoming Tactile Event Involves a Spatially and Temporally Specific Modulation of Sensorimotor Alpha- and Beta-Band Oscillations. *Journal of Neuroscience*, *31*(6), 2016–2024. https://doi.org/10.1523/JNEUROSCI.5630-10.2011

Van Rossum, G., & Drake, F. L. (2009). *Python 3 Reference Manual*. CreateSpace.

Verrillo, R. T. (1979). Change in vibrotactile thresholds as a function of age. *Sensory Processes*, *3*(1), 49–59.

Verrillo, R. T. (1980). Age related changes in the sensitivity to vibration. *Journal of Gerontology*, *35*(2), 185–193. https://doi.org/10.1093/GERONJ/35.2.185

Verrillo, R. T., Bolanowski, S. J., & Gescheider, G. A. (2002). Effect of aging on the subjective magnitude of vibration. *Somatosensory & Motor Research*, *19*(3), 238–244. https://doi.org/10.1080/0899022021000009161

Vesia, M., & Crawford, J. D. (2012). Specialization of reach function in human posterior parietal cortex. *Experimental Brain Research 2012 221:1*, *221*(1), 1–18. https://doi.org/10.1007/S00221-012-3158-9

Vingerhoets, G. (2014). Contribution of the posterior parietal cortex in reaching, grasping, and using objects and tools. *Frontiers in Psychology*, *5*(MAR), 151. https://doi.org/10.3389/FPSYG.2014.00151/BIBTEX

Vingerhoets, G., Nys, J., Honoré, P., Vandekerckhove, E., & Vandemaele, P. (2013). Human Left Ventral Premotor Cortex Mediates Matching of Hand Posture to Object Use. *PLOS ONE*, *8*(7), e70480. https://doi.org/10.1371/JOURNAL.PONE.0070480

Voisin, J., Lamarre, Y., & Chapman, E. C. (2002). Haptic discrimination of object shape in humans: contribution of cutaneous and proprioceptive inputs. *Experimental Brain Research 2002 145:2*, *145*(2), 251–260. https://doi.org/10.1007/S00221-002-1118-5

von Holst, E., & Mittelstaedt, H. (1950). Das Reafferenzprinzip - Wechselwirkungen zwischen Zentralnervensystem und Peripherie. *Die Naturwissenschaften*, *37*(20), 464–476. https://doi.org/10.1007/BF00622503

Vorobiev, V., Govoni, P., Rizzolatti, G., Matelli, M., & Luppino, G. (1998). Parcellation of human mesial area 6: cytoarchitectonic evidence for three separate areas. *European Journal of Neuroscience*, *10*(6), 2199–2203. https://doi.org/10.1046/J.1460-9568.1998.00236.X

Voss, M., Ingram, J. N., Haggard, P., & Wolpert, D. M. (2005). Sensorimotor attenuation by central motor command signals in the absence of movement. *Nature Neuroscience 2005 9:1*, *9*(1), 26–27. https://doi.org/10.1038/nn1592

Voss, M., Ingram, J. N., Wolpert, D. M., & Haggard, P. (2008). Mere expectation to move causes attenuation of sensory signals. *PloS One*, *3*(8). https://doi.org/10.1371/JOURNAL.PONE.0002866

Wager, T. D., Lindquist, M., & Kaplan, L. (2007). Meta-analysis of functional neuroimaging data: current and future directions. *Social Cognitive and Affective Neuroscience*, *2*(2), 150–158. https://doi.org/10.1093/scan/nsm015

Wagner, A., & Gibson, J. J. (2016). Pre-Gibsonian Observations on Active Touch. *History of Psychology*, *19*(2), 93–104. https://doi.org/10.1037/hop0000028

Walker, S. C., Marshall, A., & Pawling, R. (2022). Psychophysiology and motivated emotion: testing the affective touch hypothesis of C-tactile afferent function. *Current Opinion in Behavioral Sciences*, *43*, 131–137. https://doi.org/10.1016/J.COBEHA.2021.10.004

Walker, S., Monto, S., Piirainen, J. M., Avela, J., Tarkka, I. M., Parviainen, T. M., & Piitulainen, H. (2020). Older Age Increases the Amplitude of Muscle Stretch-Induced Cortical Beta-Band Suppression But Does not Affect Rebound Strength. *Frontiers in Aging Neuroscience*, *12*. https://doi.org/10.3389/FNAGI.2020.00117

Wang, Q., Yu, W., Chen, K., & Zhang, Z. (2016). Brain discriminative cognition on the perception of touching different fabric using fingers actively. *Skin Research and Technology*, *22*(1), 63–68. https://doi.org/10.1111/srt.12229

Weber, A. I., Saal, H. P., Lieber, J. D., Cheng, J. W. J.-W., Manfredi, L. R., Dammann, J. F., & Bensmaia, S. J. (2013). Spatial and temporal codes mediate the tactile perception of natural textures. *Proceedings of the National Academy of Sciences*, *110*(42), 17107–17112. https://doi.org/10.1073/pnas.1305509110

Wei, Y., McGlone, F. P., Marshall, A. G., Makdani, A., Zou, Z., Ren, L., & Wei, G. (2022). From Skin Mechanics to Tactile Neural Coding: Predicting Afferent Neural Dynamics During Active Touch and Perception. *IEEE Transactions on Biomedical Engineering*, *69*(12), 3748–3759. https://doi.org/10.1109/TBME.2022.3177006

Welniarz, Q., Dusart, I., & Roze, E. (2017). The corticospinal tract: Evolution, development, and human disorders. *Developmental Neurobiology*, *77*(7), 810–829. https://doi.org/10.1002/DNEU.22455

Welniarz, Q., Gallea, C., Lamy, J. C., Méneret, A., Popa, T., Valabregue, R., Béranger, B., Brochard, V., Flamand-Roze, C., Trouillard, O., Bonnet, C., Brüggemann, N., Bitoun, P., Degos, B., Hubsch, C., Hainque, E., Golmard, J. L., Vidailhet, M., Lehéricy, S., … Roze, E. (2019). The supplementary motor area modulates interhemispheric interactions during movement preparation. *Human Brain Mapping*, *40*(7), 2125. https://doi.org/10.1002/HBM.24512

Whitlock, J. R. (2017). Posterior parietal cortex. *Current Biology*, *27*(14), R691–R695. https://doi.org/10.1016/J.CUB.2017.06.007

Williams, S. R., & Chapman, C. E. (2000). Time Course and Magnitude of Movement-Related Gating of Tactile Detection in Humans. II. Effects of Stimulus Intensity. *Journal of Neurophysiology*, *84*(2), 863–875. https://doi.org/10.1152/jn.2000.84.2.863

Williams, S. R., & Chapman, C. E. (2002). Time Course and Magnitude of Movement-Related Gating of Tactile Detection in Humans. III. Effect of Motor Tasks. *Journal of Neurophysiology*, *88*(4), 1968–1979. https://doi.org/10.1152/jn.2002.88.4.1968

Williams, S. R., Shenasa, J., & Chapman, C. E. (1998). Time course and magnitude of movement-related gating of tactile detection in humans. I. Importance of stimulus location. *Journal of Neurophysiology*, *79*(2), 947–963. https://doi.org/10.1152/JN.1998.79.2.947

Woolsey, C. N., & Fairman, D. (1946). Contralateral, ipsilateral, and bilateral representation of cutaneous receptors in somatic areas I and II of the cerebral cortex of pig, sheep, and other mammals. *Surgery*, *19*(5), 684–702. http://www.surgjournal.com/article/003960604690061X/fulltext

Woolsey, C. N., Settlage, P. H., Meyer, D. R., Sencer W, Pinto Hamuy, T., & Travis, A. M. (1952). Patterns of localization in precentral and 'supplementary' motor areas and their relation to the concept of a premotor area. *Research Publications - Association for Research in Nervous and Mental Disease*, *30*, 238–264. http://www.ncbi.nlm.nih.gov/pubmed/12983675

Worsley, K. J., Evans, A. C., Marrett, S., & Neelin, P. (1992). A three-dimensional statistical analysis for CBF activation studies in human brain. *Journal of Cerebral Blood Flow and Metabolism : Official Journal of the International Society of Cerebral Blood Flow and Metabolism*, *12*(6), 900–918. https://doi.org/10.1038/JCBFM.1992.127

Worsley, K. J., Marrett, S., Neelin, P., Vandal, A. C., Friston, K. J., & Evans, A. C. (1996). A unified statistical approach for determining significant signals in images of cerebral

activation. *Human Brain Mapping*, *4*(1), 58–73. https://doi.org/10.1002/(sici)1097-0193(1996)4:1<58::aid-hbm4>3.0.co;2-o

Wu, Q., Li, C., Li, Y., Sun, H., Guo, Q., & Wu, J. (2014). SII and the fronto-parietal areas are involved in visually cued tactile top-down spatial attention: a functional MRI study. *Neuroreport*, *25*(6), 415–421. https://doi.org/10.1097/WNR.0000000000000128

Wundt, W. (1897). *Wundt: Outlines of psychology - Google Scholar* (W. Engelmann, Ed.). Williams and Norgate. https://doi.org/10.1037/12908-000

Xifra-Porxas, A., Niso, G., Larivière, S., Kassinopoulos, M., Baillet, S., Mitsis, G. D., & Boudrias, M. H. (2019). Older adults exhibit a more pronounced modulation of beta oscillations when performing sustained and dynamic handgrips. *NeuroImage*, *201*. https://doi.org/10.1016/J.NEUROIMAGE.2019.116037

Xu, C., Wang, Y., & Gerling, G. J. (2021a). An elasticity-curvature illusion decouples cutaneous and proprioceptive cues in active exploration of soft objects. *PLoS Computational Biology*, *17*(3). https://doi.org/10.1371/JOURNAL.PCBI.1008848

Xu, C., Wang, Y., & Gerling, G. J. (2021b). Individual Performance in Compliance Discrimination is Constrained by Skin Mechanics but Improved under Active Control. *2021 IEEE World Haptics Conference (WHC)*, 445–450. https://doi.org/10.1109/WHC49131.2021.9517269

Yang, J., Kitada, R., Kochiyama, T., Yu, Y., Makita, K., Araki, Y., Wu, J., & Sadato, N. (2017). Brain networks involved in tactile speed classification of moving dot patterns: the effects of speed and dot periodicity. *Scientific Reports*, *7*(1), 40931. https://doi.org/10.1038/srep40931

Yang, J., Molfese, P. J., Yu, Y., Handwerker, D. A., Chen, G., Taylor, P. A., Ejima, Y., Wu, J., & Bandettini, P. A. (2021). Different activation signatures in the primary sensorimotor and higher-level regions for haptic three-dimensional curved surface exploration. *NeuroImage*, *231*, 117754. https://doi.org/10.1016/j.neuroimage.2021.117754

Yoshioka, T., Craig, J. C., Beck, G. C., & Hsiao, S. S. (2011). Perceptual Constancy of Texture Roughness in the Tactile System. *Journal of Neuroscience*, *31*(48), 17603–17611. https://doi.org/10.1523/JNEUROSCI.3907-11.2011

Yoshioka, T., Gibb, B., Dorsch, A. K., Hsiao, S. S., & Johnson, K. O. (2001). Neural coding mechanisms underlying perceived roughness of finely textured surfaces. *Journal of Neuroscience*, *21*(17), 6905–6916. https://doi.org/10.1523/jneurosci.21-17-06905.2001

Yuan, G., & Liu, G. (2022). Mate preference and brain oscillations: Initial romantic attraction is associated with decreases in alpha- and lower beta-band power. *Human Brain Mapping*, *43*(2), 721. https://doi.org/10.1002/HBM.25681

Zayia, L. C., & Tadi, P. (2021). Neuroanatomy, Motor Neuron. *StatPearls*. https://www.ncbi.nlm.nih.gov/books/NBK554616/

Zhang, M., Weisser, V. D., Stilla, R., Prather, S. C., & Sathian, K. (2004). Multisensory cortical processing of object shape and its relation to mental imagery. *Cognitive, Affective & Behavioral Neuroscience*, *4*(2), 251–259. https://doi.org/10.3758/cabn.4.2.251

Zhang, Z., Guo, G., Zhang, J., Li, C., Huang, Q., Go, R., Fukuyama, H., Funahashi, S., Yan, T., & Wu, J. (2019). Do theta oscillations explain the somatosensory change detection

mechanism? *Biological Psychology*, *143*, 103–112. https://doi.org/10.1016/J.BIOPSYCHO.2019.02.001

Zhao, D., Zhou, Y. di, Bodner, M., & Ku, Y. (2018a). The Causal Role of the Prefrontal Cortex and Somatosensory Cortex in Tactile Working Memory. *Cerebral Cortex*, *28*(10), 3468–3477. https://doi.org/10.1093/CERCOR/BHX213

Zhao, G., Zhang, Y., & Ge, Y. (2018b). Frontal EEG asymmetry and middle line power difference in discrete emotions. *Frontiers in Behavioral Neuroscience*, *12*, 225. https://doi.org/10.3389/FNBEH.2018.00225/BIBTEX

Zuo, X. N., Biswal, B. B., & Poldrack, R. A. (2019). Editorial: Reliability and reproducibility in functional connectomics. *Frontiers in Neuroscience*, *13*(FEB), 117. https://doi.org/10.3389/FNINS.2019.00117/BIBTEX

Zuo, X. N., & Xing, X. X. (2014). Test-retest reliabilities of resting-state FMRI measurements in human brain functional connectomics: A systems neuroscience perspective. In *Neuroscience and Biobehavioral Reviews* (Vol. 45, pp. 100–118). https://doi.org/10.1016/j.neubiorev.2014.05.009

Appendices

Supplementary material 1

Thirteen leave-one-out analyses were conducted to assess the stability of the results. Below are the results from the primary analysis of texture perception > control each time excluding a different single study.

Gurtubay-Antolin et al. (2018)

Supplementary table 1. Locations of significant clusters when leaving out Gurtubay-Antolin et al. (2018).

Cluster #	Label	Volume (mm^3)	*x*	*y*	*z*	# Experiments	ALE
1	Insula R	1760	58	-20	20	7	0.021
	Postcentral Gyrus R		64	-16	22		0.021
2	Postcentral Gyrus L	1648	-54	-20	48	8	0.023
3	Precentral Gyrus L	1432	-48	6	24	7	0.019
	Precentral Gyrus L		-58	8	28		0.014
	Precentral Gyrus L		-58	2	32		0.012
4	Insula L	1248	-36	-6	10	6	0.022
	Insula L		-42	-4	2		0.014
5	Inferior Frontal Gyrus R	984	50	8	24	4	0.025
6	Insula R	832	40	-8	8	5	0.020
7	Superior Frontal Gyrus R	832	4	16	48	4	0.018

L, left hemisphere; R, right hemisphere.

Kim et al. (2015)

Supplementary table 2. Locations of significant clusters when leaving out Kim et al. (2015).

Cluster #	Label	Volume (mm^3)	*x*	*y*	*z*	# Experiments	ALE
1	Insula R	1840	58	-20	20	7	0.021
	Postcentral Gyrus R		64	-16	22		0.021
2	Precentral Gyrus L	1688	-48	6	24	7	0.019
	Precentral Gyrus L		-58	8	28		0.014
	Precentral Gyrus L		-58	6	14		0.013
	Precentral Gyrus L		-58	2	32		0.012
3	Inferior Parietal Lobule L	1480	-54	-22	48	7	0.022
4	Insula L	1096	-36	-6	10	6	0.022
	Insula L		-42	-4	0		0.013
5	Inferior Frontal Gyrus R	1048	50	8	24	4	0.025
6	Insula R	856	40	-8	8	5	0.020
7	Superior Frontal Gyrus R	784	4	18	48	4	0.018
8	Postcentral Gyrus L	728	-56	-20	20	4	0.017

L, left hemisphere; R, right hemisphere.

Kitada et al. (2005)

Supplementary table 3. Locations of significant clusters when leaving out Kitada et al. (2005).

Cluster #	Label	Volume (mm^3)	*x*	*y*	*z*	# Experiments	ALE
1	Precentral Gyrus L	1672	-48	6	24	7	0.019
	Precentral Gyrus L		-58	8	28		0.014
	Precentral Gyrus L		-58	6	14		0.013
	Precentral Gyrus L		-58	2	32		0.012
2	Postcentral Gyrus L	1488	-54	-20	50	7	0.022
3	Postcentral Gyrus R	1376	64	-16	22	6	0.020
	Insula R		54	-20	20		0.016
4	Insula L	1328	-36	-6	10	6	0.022
	Insula L		-42	-4	2		0.014
5	Inferior Frontal Gyrus R	1032	50	8	24	4	0.025
6	Insula R	856	40	-8	8	5	0.020
7	Superior Frontal Gyrus R	784	4	18	48	4	0.018
8	Middle Frontal Gyrus L	656	-42	40	12	3	0.019

L, left hemisphere; R, right hemisphere.

Kitada et al. (2006)

Supplementary table 4. Locations of significant clusters when leaving out Kitada et al. (2006).

Cluster #	Label	Volume (mm^3)	*x*	*y*	*z*	# Experiments	ALE
1	Inferior Frontal Gyrus L	1512	-50	6	24	6	0.017
	Inferior Frontal Gyrus L		-56	6	22		0.016
	Precentral Gyrus L		-58	8	28		0.014
	Precentral Gyrus L		-58	6	14		0.013
	Precentral Gyrus L		-58	2	32		0.012
2	Postcentral Gyrus R	1392	64	-16	22	6	0.021
3	Postcentral Gyrus L	1328	-54	-20	48	7	0.021
4	Insula L	1168	-36	-6	10	5	0.022
5	Postcentral Gyrus L	768	-44	-12	58	4	0.016
	Precentral Gyrus L		-38	-20	52		0.013

L, left hemisphere; R, right hemisphere.

Mueller et al. (2019)

Supplementary table 5. Locations of significant clusters when leaving out Mueller et al. (2019).

Cluster #	Label	Volume (mm^3)	*x*	*y*	*z*	# Experiments	ALE
1	Insula R	1528	58	-20	20	5	0.021
2	Postcentral Gyrus L	1400	-58	-22	46	7	0.019
	Postcentral Gyrus L		-50	-28	56		0.010
3	Insula L	1096	-38	-8	10	5	0.016
	Insula L		-42	-4	2		0.014
4	Precentral Gyrus L	888	-48	6	24	4	0.019
5	Postcentral Gyrus L	832	-56	-20	20	4	0.017

L, left hemisphere; R, right hemisphere.

Podrebarac et al. (2014)

Supplementary table 6. Locations of significant clusters when leaving out Podrebarac et al. (2014).

Cluster #	Label	Volume (mm^3)	*x*	*y*	*z*	# Experiments	ALE
1	Insula R	1760	58	-20	20	7	0.021
	Postcentral Gyrus R		64	-16	22		0.021
2	Postcentral Gyrus L	1648	-54	-20	48	8	0.023
3	Precentral Gyrus L	1432	-48	6	24	7	0.019
	Precentral Gyrus L		-58	8	28		0.014
	Precentral Gyrus L		-58	2	32		0.012
4	Insula L	1240	-36	-6	10	6	0.022
	Insula L		-42	-4	2		0.014
5	Inferior Frontal Gyrus R	984	50	8	24	4	0.025
6	Superior Frontal Gyrus R	832	4	16	48	4	0.018
7	Insula R	824	40	-8	8	5	0.020

L, left hemisphere; R, right hemisphere.

Sathian et al. (2011)

Supplementary table 7. Locations of significant clusters when leaving out Sathian et al. (2011).

Cluster #	Label	Volume (mm^3)	*x*	*y*	*z*	# Experiments	ALE
1	Insula R	1792	58	-20	20	7	0.021
	Postcentral Gyrus R		64	-16	22		0.021
2	Postcentral Gyrus L	1704	-54	-20	48	8	0.023
3	Inferior Frontal Gyrus L	1056	-58	6	22	5	0.016
	Precentral Gyrus L		-58	8	28		0.014
	Precentral Gyrus L		-58	2	32		0.012
4	Inferior Frontal Gyrus R	1008	50	8	24	4	0.025
5	Superior Frontal Gyrus R	864	4	16	48	4	0.018
6	Insula L	760	-38	-6	8	4	0.015
	Insula L		-42	-4	2		0.014
7	Postcentral Gyrus L	656	-44	-12	58	4	0.016
	Precentral Gyrus L		-38	-20	52		0.013
8	Postcentral Gyrus L	632	-56	-20	20	4	0.017

L, left hemisphere; R, right hemisphere.

Simões-Franklin et al. (2011)

Supplementary table 8. Locations of significant clusters when leaving out Simões-Franklin et al. (2011).

Cluster #	Label	Volume (mm^3)	*x*	*y*	*z*	# Experiments	ALE
1	Postcentral Gyrus L	1560	-54	-20	48	6	0.023
2	Precentral Gyrus L	1360	-48	6	24	6	0.019
	Precentral Gyrus L		-58	6	14		0.013
3	Insula R	1328	54	-22	20	6	0.018
	Inferior Parietal Lobule R		64	-16	24		0.017
4	Inferior Frontal Gyrus R	992	50	8	24	4	0.025
5	Insula R	872	40	-8	8	5	0.020
6	Insula L	864	-36	-6	10	4	0.021
7	Postcentral Gyrus L	760	-56	-20	20	4	0.017
8	Postcentral Gyrus L	744	-44	-12	58	4	0.016
	Precentral Gyrus L		-38	-20	52		0.013

L, left hemisphere; R, right hemisphere.

Stilla and Sathian (2008)

Supplementary table 9. Locations of significant clusters when leaving out Stilla and Sathian (2008).

Cluster #	Label	Volume (mm^3)	*x*	*y*	*z*	# Experiments	ALE
1	Insula R	1704	58	-20	20	7	0.021
	Postcentral Gyrus R		64	-16	22		0.021
2	Postcentral Gyrus L	1640	-54	-20	48	8	0.023
3	Precentral Gyrus L	1424	-48	6	24	7	0.019
	Precentral Gyrus L		-58	8	28		0.014
	Precentral Gyrus L		-58	2	32		0.012
4	Inferior Frontal Gyrus R	984	50	8	24	4	0.025
5	Insula L	960	-38	-6	10	5	0.019
	Insula L		-42	-4	2		0.014
6	Superior Frontal Gyrus R	832	4	16	48	4	0.018

L, left hemisphere; R, right hemisphere.

Tang et al. (2021)

Supplementary table 10. Locations of significant clusters when leaving out Tang et al. (2021).

Cluster #	Label	Volume (mm^3)	*x*	*y*	*z*	# Experiments	ALE
1	Precentral Gyrus L	1440	-48	6	24	7	0.019
	Precentral Gyrus L		-58	8	28		0.014
	Precentral Gyrus L		-58	2	32		0.012
2	Insula R	1400	58	-20	20	5	0.021
3	Insula L	1248	-36	-6	10	6	0.022
	Insula L		-42	-4	2		0.014
4	Inferior Parietal Lobule L	1224	-54	-22	48	6	0.019
5	Inferior Frontal Gyrus R	984	50	8	24	4	0.025
6	Insula R	840	40	-8	8	5	0.020
7	Superior Frontal Gyrus R	840	4	16	48	4	0.018

L, left hemisphere; R, right hemisphere.

Wang et al. (2016)

Supplementary table 11. Locations of significant clusters when leaving out Wang et al. (2016).

Cluster #	Label	Volume (mm^3)	*x*	*y*	*z*	# Experiments	ALE
1	Insula R	1408	58	-20	20	6	0.021
2	Insula L	1272	-36	-6	10	6	0.022
	Insula L		-42	-4	2		0.014
3	Postcentral Gyrus L	1248	-54	-20	48	6	0.023
4	Precentral Gyrus L	1040	-48	6	24	5	0.019
	Precentral Gyrus L		-58	8	30		0.013
	Precentral Gyrus L		-58	2	32		0.012
5	Inferior Frontal Gyrus R	968	50	8	24	4	0.025
6	Superior Frontal Gyrus R	864	4	16	48	4	0.018
7	Insula R	848	40	-8	8	5	0.020
8	Postcentral Gyrus L	664	-56	-20	20	4	0.017

L, left hemisphere; R, right hemisphere.

Yang et al. (2017)

Supplementary table 12. Locations of significant clusters when leaving out Yang et al. (2017).

Cluster #	Label	Volume (mm^3)	*x*	*y*	*z*	# Experiments	ALE
1	Postcentral Gyrus R	1440	64	-16	22	6	0.020
2	Postcentral Gyrus L	1400	-54	-20	50	6	0.021
3	Insula R	992	40	-8	8	5	0.020
4	Postcentral Gyrus L	872	-44	-12	58	4	0.016
	Precentral Gyrus L		-38	-20	52		0.013
5	Inferior Frontal Gyrus R	856	48	8	26	3	0.018
	Inferior Frontal Gyrus R		62	10	22		0.011

L, left hemisphere; R, right hemisphere.

Yang et al. (2021)

Supplementary table 13. Locations of significant clusters when leaving out Yang et al. (2021).

Cluster #	Label	Volume (mm^3)	*x*	*y*	*z*	# Experiments	ALE
1	Insula R	1784	58	-20	20	7	0.021
	Postcentral Gyrus R		64	-16	22		0.021
2	Postcentral Gyrus L	1736	-54	-20	48	8	0.023
3	Insula L	1144	-36	-6	10	5	0.021
	Insula L		-42	-4	2		0.014
4	Superior Frontal Gyrus R	888	4	16	48	4	0.018
5	Inferior Frontal Gyrus L	840	-58	6	22	4	0.016
	Precentral Gyrus L		-58	8	30		0.013
	Precentral Gyrus L		-58	2	32		0.012
	Precentral Gyrus L		-46	6	26		0.011
6	Inferior Frontal Gyrus R	696	50	8	24	3	0.019
7	Postcentral Gyrus L	680	-56	-20	20	4	0.017
8	Insula R	664	40	-8	8	4	0.019
9	Postcentral Gyrus L	656	-44	-12	58	4	0.016
	Precentral Gyrus L		-38	-20	52		0.013
10	Middle Frontal Gyrus L	624	-42	40	12	3	0.019

L, left hemisphere; R, right hemisphere.

Supplementary material 2

An exploratory analysis was conducted to assess the differences between studies delivering tactile stimulation either through passive or active touch. Below are the results from the primary analysis of texture perception > control each, with the exception of Simões-Franklin et al. (2011) as the coordinates extracted were from activation via both active and passive touch combined.

Primary analysis

Pooled analysis

Supplementary table 14. Locations of significant clusters for both active and passive stimulation, with the exception of Simões-Franklin et al. (2011).

Cluster #	Label	Volume(mm^3)	*x*	*y*	*z*	# Experiments	ALE
1	Postcentral Gyrus L	1560	-54	-20	48	6	0.023
2	Precentral Gyrus L	1360	-48	6	24	6	0.019
	Precentral Gyrus L		-58	6	14		0.013
3	Insula R	1328	54	-22	20	6	0.018
	Inferior Parietal Lobule R		64	-16	24		0.017
4	Inferior Frontal Gyrus R	992	50	8	24	4	0.025
5	Insula R	872	40	-8	8	5	0.020
6	Insula L	864	-36	-6	10	4	0.021
7	Postcentral Gyrus L	760	-56	-20	20	4	0.017
8	Postcentral Gyrus L	744	-44	-12	58	4	0.016
	Precentral Gyrus L		-38	-20	52		0.013

L, left hemisphere; R, right hemisphere.

Active touch

Supplementary table 15. Locations of significant clusters for active stimulation.

Cluster #	Label	Volume(mm^3)	*x*	*y*	*z*	# Experiments	ALE
1	Insula L	936	-36	-6	12	4	0.017
2	Insula R	920	40	-6	10	4	0.016
3	Precentral Gyrus L	832	-48	6	24	4	0.015
	Precentral Gyrus L		-60	6	22		0.012
4	Postcentral Gyrus L	792	-42	-12	56	3	0.011
	Precentral Gyrus L		-30	-20	62		0.011
	Precentral Gyrus L		-34	-18	60		0.010
	Precentral Gyrus L		-36	-18	56		0.009
	Precentral Gyrus L		-36	-14	64		0.008

L, left hemisphere; R, right hemisphere.

Passive touch

Supplementary table 16. Locations of significant clusters for passive stimulation.

Cluster #	Label	Volume(mm^3)	*x*	*y*	*z*	# Experiments	ALE
1	Postcentral Gyrus L	992	-58	-22	46	4	0.018
	Postcentral Gyrus L		-50	-28	58		0.009
2	Insula R	936	56	-22	20	3	0.018
3	Postcentral Gyrus L	664	-56	-22	20	3	0.014

L, left hemisphere; R, right hemisphere.

Secondary analysis

The contrast and conjunction analysis comparing the ALE maps of concordant activations for active and passive touch types did not reveal any significant differences between the two types of stimulation.

Supplementary material 3

PsychoPy instructions

During this task, you will be exploring textures with your index finger and evaluating them.

At the start of a trial, you will see a white cross indicating you should rest with your index finger stationary on the texture.

A shape will then appear, which will correspond to one of three conditions previously outlined.

A green fixation cross will appear, indicating you should start exploring the texture. Think about the texture properties which correspond to the condition shape during your exploration.

Stop touching the texture when the green cross disappears and keep your finger stationary.

You will rate the texture after sensory and hedonic trials using a slide bar, use your left hand and the mouse to submit your rating.

There will be four blocks, halfway through the block you will be asked to remove your finger from the current texture and switch to the other texture.

Verbal instructions

After EEG fitting

On the screen you can see the measurements from the EEG cap. There are 129 channels, and each of them records the electrical activity on your scalp. EEG records any electrical activities, including signals from your brain, as well as other activities like muscle movements. For example, please perform a series of blinks. You will notice that each blink results in a spike in the EEG recording. Now, clench your teeth. You can observe that doing so creates a noisy black period in the EEG recording. This demonstrates the importance of remaining as still as possible during the task. During the task, it is important to focus on the

computer screen in front of you and try not to look around the room or move your head. Please try to remain as relaxed as possible, particularly in your shoulders, neck, and jaw. Do you need me to make any adjustments to make you more comfortable?

You will have a short break halfway through each block and a longer break at the end of each block, during which you can move freely. If you need to move during the task, please try to limit your movement to the rating period. If you feel uncomfortable at any time, please inform me by either calling for me or knocking on this wall.

Do you have any questions?

Before tactile exploration task

During this task, you will be exploring textures within your index finger. You will complete four blocks, each lasting approximately 18 minutes. In each block, you will be instructed to explore either texture A or texture B. Texture A refers to the texture on your left, while texture B refers to the texture on your right.

Halfway through each block, you will be asked to remove your finger from the texture. It is important that you do not touch the force plate during this time, as it will be calibrated by the researcher. After the calibration, the task will prompt you to place your finger back down, this time on the alternative texture.

During each trial, you will see a white cross, which indicates that you should keep your finger still on the texture. Following the white cross, a condition indicator will appear on the screen, providing instructions on what feature to attend to during the exploration period or whether no specific feature requires attention.

For you, the triangle indicates a sensory trial. During these trials, you should focus on the sensory features of the texture. Pay attention to how the texture feels - is it soft, hard, smooth, or rough?

If you see the square, it indicates a hedonic trial. During these trials, you should focus on how the exploration of the texture feels. Consider whether it is pleasant, unpleasant, comfortable, or uncomfortable.

Lastly, if the circle appears, it indicates a trial with no estimation. You do not need to attend to any specific feature.

A green cross will subsequently appear on the screen, indicating that you should begin the exploration task. You are free to explore the texture with your index finger in any way you like. It is important to pay attention to the condition indicator and think about the outlined feature while performing your exploration.

After the exploration period for sensory and hedonic trials, you will be asked to rate your experience on a sliding scale. Please use your left hand and the mouse to submit your rating without removing your right index finger from the texture. You will not be asked to make a rating after no estimation trials.

During the task ensure that only your right intext finger is touching the force plate. Please do not rest your hand or other fingers on the texture.

First, you will complete some practice trials to ensure you are comfortable with the trial setup.

Do you have any questions?

VAS

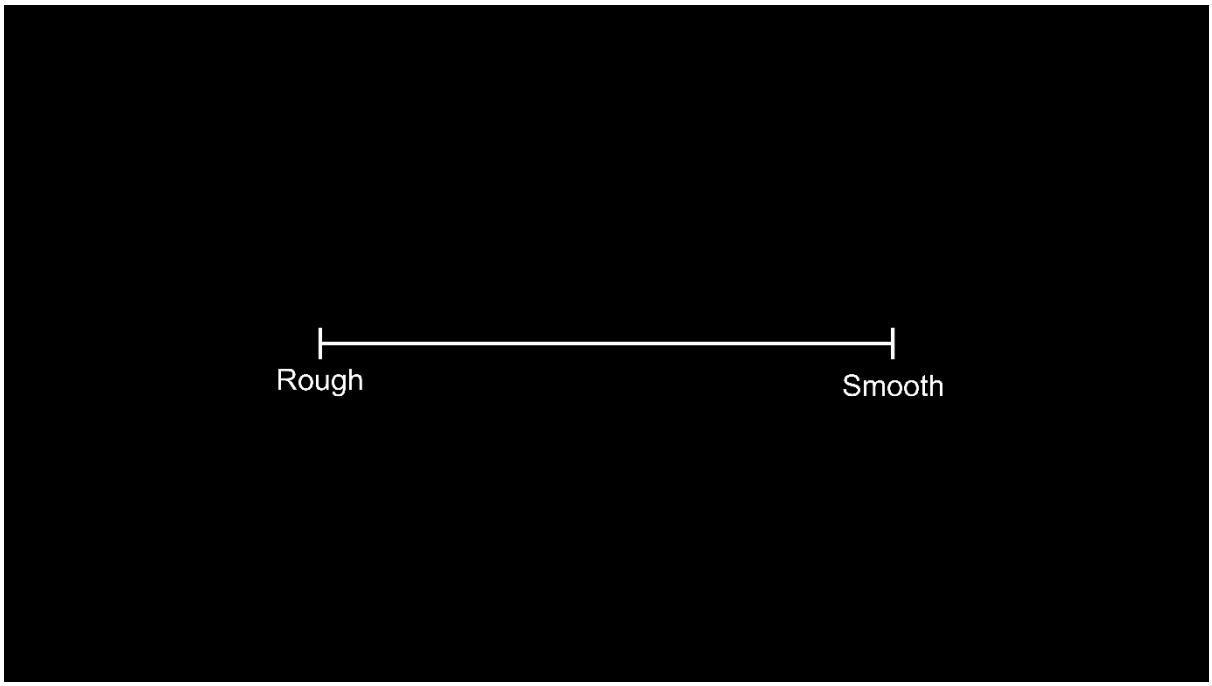

Supplementary figure 1 Example of a VAS for a sensory estimation trial.

Supplementary material 4

The statistical design implemented in SPM12 for a single-subject GLM analysis. The design matrix consists of binary variables specifying the condition of the trials and covariates.

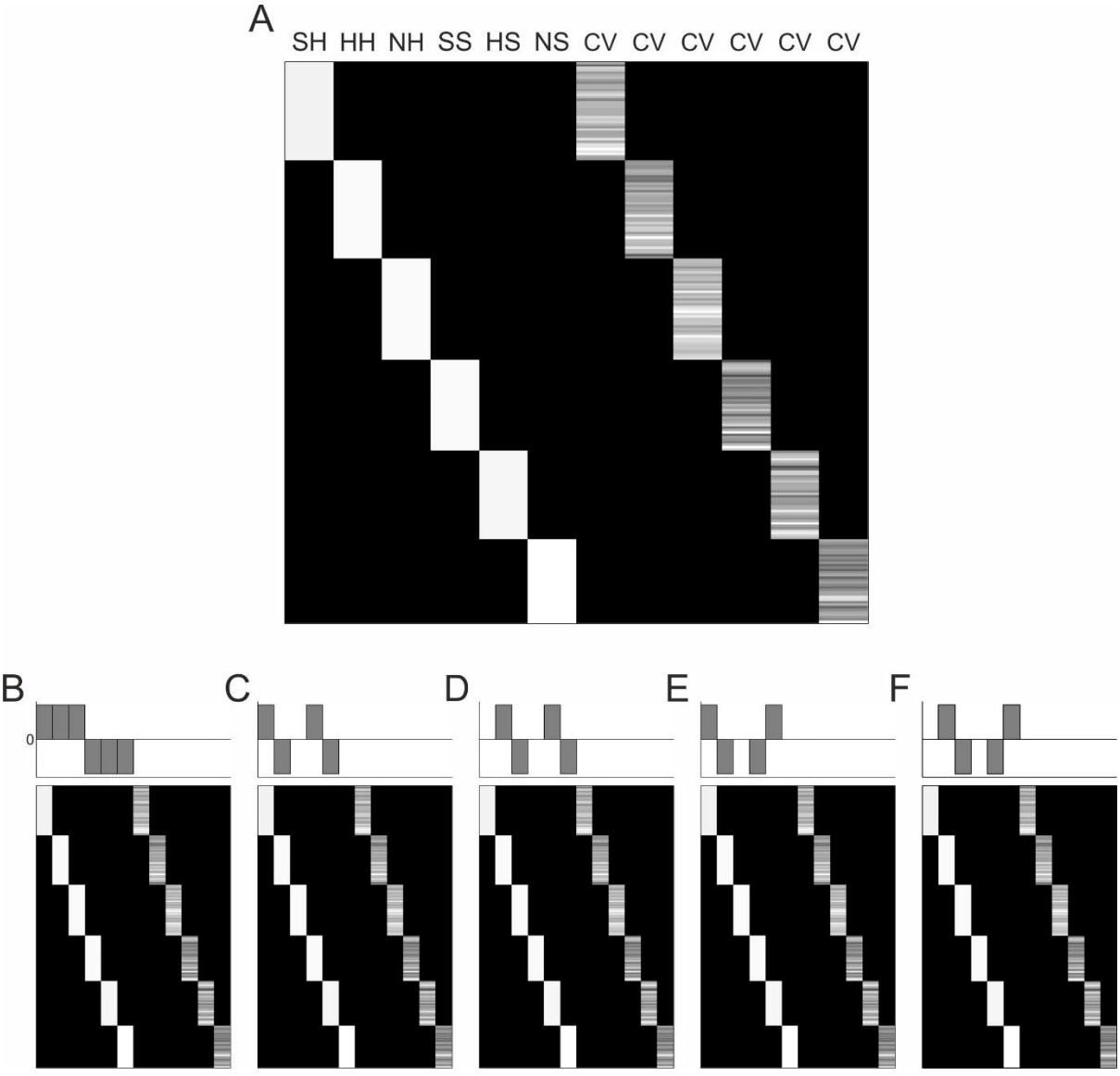

Supplementary figure 2 The statistical design as implemented in SPM12. ***(A)*** *Exemplary GLM design matrix for a single subject. Each column represents a model regressor; trials are listed in rows, sorted according to texture and estimation condition. The first six regressors represent binary variables specifying the trials' condition; hedonic hessian (HH), sensory hessian (SH), no estimation hessian (NH), hedonic silk (HS), sensory silk (SS), and no estimation silk (NS). The remaining six regressors were entered as covariates (CV). (B-F) Exemplary contrast weights to produce contract images to test of the effect of texture;* ***(B)*** *the difference of hessian (SH, HH and NH) vs. silk (SS, HS, and NS). To test the effect of estimation;* ***(C)*** *the difference of sensory (SH and SS) vs. hedonic (HH and HS), and* ***(D)*** *the difference of hedonic (HH and HS) vs no estimation (NH and NS). To test the interaction effect;* ***(E)*** *the difference of sensory hessian and hedonic silk (SH and HS) vs. hedonic hessian and sensory silk (HH and SS), and* ***(F)*** *hedonic hessian and no estimation silk (HH and NS) vs no estimation hessian and hedonic silk (NH and HS).*